THE ROLE OF *CRYPTOCOCCUS NEOFORMANS* DERIVED PHOSPHOLIPASE B1 DURING HOST INFECTION

BY:

ROBERT J. EVANS

A thesis submitted to the University of Birmingham for the degree of DOCTOR OF PHILOSOPHY

Institute of Microbiology and Infection
School of Biosciences
College of Life and Environmental Sciences
University of Birmingham
March 2016

UNIVERSITY OF BIRMINGHAM

Abstract

Cryptococcus neoformans is an opportunistic fungal pathogen and a leading cause of fungal infection related fatalities in immunocompromised hosts. Compared to well-studied *Cryptococcus neoformans* virulence factors like the polysaccharide capsule and melanin synthesis, very little is known about phospholipase B1 (Plb1). Plb1 is a phospholipid modifying enzyme that is implicated in multiple stages of cryptococcal pathogenesis. Herein I demonstrate that a Plb1 deficient strain of *C. neoformans* has a profound defect in intracellular growth within macrophages. In addition I show that the *Δplb1* strain undergoes a novel morphological change during *in vitro* and *in vivo* infection, resulting in a sub-population of very large 'titan cells' that may arise as a result of the mutant's inability to cope within the macrophage. I go on to test whether these phenotypes are due to a reduction in eicosanoid production caused by Plb1 deficiency. Finally I present an additional project where I optimise a *C. neoformans* intracellular proliferation assay for high throughput analysis via flow cytometry. This work provides a new insight into the function of this unappreciated virulence factor and helps to lay the foundation for new treatment strategies to combat cryptococcosis.

Acknowledgements

'You have been told that science grows like an organism. You have been told that, if we today see further than our predecessors, it is only because we stand on their shoulders. But this is an occasion on which I should prefer to remember, not the giants upon whose shoulders we stood, but the friends with whom we stood arm in arm.'

− Peter Medawar, Nobel Prize acceptance speech.

I would be lying if I said that my PhD has been easy. Luckily I have enjoyed huge support from both family and friends which has made it possible. These past four years I have been in Birmingham have been some of the best of my life.

To Robin and Andy my PhD supervisors. Both of you have put your trust in me and have given me so much in the way of support, advice and opportunity. I am extremely grateful for everything you have done for me. I consider you both dear friends.

To avoid this becoming a huge list, thank you to everyone in the HAPI lab. You became a family when I was living away from my own, I will always cherish that. It's OK to admit it - we're just great. Stay awesome, stay HAPI.

Finally, I'd like to thank my other family - my real one. Past, present and departed. If a person is a sum of their parts – the multiplying factor is surely the support of those who shaped them. I love you all.

Thank you.

I dedicate this thesis to all of you.

Robbie

Table of Contents

List of Illustrations

List of Tables

List of Abbreviations

15-d-PGJ$_2$ - 15-Deoxy-Delta-12, 14-prostaglandin J2

AA - Arachidonic acid

AIDS – Acquired immune deficiency syndrome

ANOVA – Analysis of variance

APO - Apochromatic

App1 – Anti-phagocytic protein 1

Arg – Arginine

Asp – Asparagine

BAL – Bronchoalveolar lavage

BBB – Blood brain barrier

BLAST – Basic Local Alignment Search Tool

CA - California

CCL2 – C-C chemokine ligand 2

CCR2 – C-C chemokine receptor type 2

CD4 – Cluster of differentiation 4

CD8 – Cluster of differentiation 8

CD11b – Cluster of differentiation 11b

CD11c – Cluster of differentiation 11c

CD107b – Cluster of differentiation 107b

CD204 – Cluster of differentiation 204

CD40 – Cluster of differentiation 40

CD44 – Cluster of differentiation 44

CD80 – Cluster of differentiation 86

CFS – Cerebrospinal fluid

CFU – Colony forming unit

CFW – Calcofluor White

CNS – Central nervous system

COX - Cyclooxygenase

CR3 – Complement receptor 3

CysLT - Cysteninyl-leukotriene

dH_2O – Deionised water

DOPC - 1, 2-Dioleoyl-sn-glycero-3-phosphocholine

DMEM – Dulbecco's modified Eagle media

DMSO – Dimethyl sulfoxide

DPPC – Dipalmitoyl phosphatidylcholine

EIA – Enzyme Immunoassay

ELISA – Enzyme-linked immunosorbent assay

EP1, EP2, EP3, EP4 – Prostaglandin E_2 receptor 1,2,3,4

EPA - Eicosapentaenoic acid

EX - Epoxide

FasL – FAS receptor ligand

FBS – Fetal bovine serum

FITC - Fluorescein isothiocyanate

FSC – Forward scatter

GXMGal - galactoxylomannan

GATA – Globulin transcription factor

GFP – Green fluorescent protein

GPI - glycosylphosphatidylinositol

GXM – glucuronoxylomannan

H_2O_2 – Hydrogen peroxide

HAART – Highly active antiretroviral therapy

HEPES- 4-(2-hydroxyethyl)-1-piperazineethanesulfonic acid

HETE - hydroxyeicosatetraenoic acid

HIV – Human immune deficiency virus

HPLC – High performance liquid chromatography

IACUC – Institutional Animal Care and Use Committee

IFN-γ – Interferon gamma

IgG – Immunoglobulin G

IgM – Immunoglobulin M

IL-1 – Interleukin 1

IL-4 – Interleukin 4

IL-6 – Interleukin 6

IL-10 – Interleukin 10

IL-12 – Interleukin 12

IL-23 – Interleukin 23

IPR – Intracellular proliferation rate

IRIS – Immune reconstitution inflammatory syndrome

LAMP-1 - Lysosomal-associated membrane protein 1

$_L$-dopa – L-3, 4-dihydroxyphenylalanine

LOX - Lipoxygenase

LPL – Lysophospholipase enzyme activity

LPTA – Lysophospholipase transacetylase enzyme activity

LT - Leukotriene

Lyc-6C – Lymphocyte antigen 6C

LysoPC - Lysophosphatidylcholine

mAb – Monoclonal antibody

MAC – Membrane attack complex

MCP-1 – Macrophage chemotactic protein 1

ME - Minnesota

MHC II – Major histocompatibility complex II

MO - Missouri

MOI – Multiplicity of infection

MR – Mannose receptor

NaCl – Sodium chloride

NADPH – Nicotinamide adenine dinucleotide phosphate (reduced)

NET – Neutrophil extracellular trap

PAMP – Pathogen associated molecular pattern

PA – Phosphatidic acid

PBS – Phosphate buffered saline

PC – Phosphatidylcholine

PCR – Polymerase chain reaction

PE - Phosphatidylethanolamine

PG – Phosphoglyceride

PGD_2 – Prostaglandin D_2

PGE_2 – Prostaglandin E_2

PGF_2 – Prostaglandin F_2

PGG_2 – Prostaglandin G_2

PGH_2 – Prostaglandin H_2

PGI_2 – Prostaglandin I_2

PI – Propidium iodide

PLA_2 - Phospholipase A_2

PLB – Phospholipase B enzyme activity

Plb1 – Phospholipase B1

PRR – pathogen recognition receptor

PS – Phosphatidylserine

Rac1 – Ras-related C3 botulinum toxin substrate 1

SDS – Sodium dodecyl sulphate

Ser – Serine

SPH – Sphingomyelin

SSC – Side scatter

Th1 – T helper cell type 1

Th2 – T helper cell type 2

TNF-α – Tumour necrosis factor alpha

TX - Thromboxane

USA – United States of America

UV – ultra violet

VTPase – Vacuolar-type H^+ - ATPase

WHO – World Health Organisation

YPD – Yeast extract / peptone / dextrose media

CHAPTER 1 – INTRODUCTION

Parts of this chapter have been adapted from already published work (Robert Evans and <u>Robin May</u> 2013. The Mycota XII, pages 97 - 106; ISBN: 978-3-642-39431-7)

1. *Cryptococcus neoformans* and the *Cryptococcus* genus.

1.1 Cryptococcus neoformans

Cryptococcus neoformans is an encapsulated, pathogenic fungus that can cause disease in humans and other animals. The first recorded case of human *C. neoformans* infection was in a subcutaneous skin lesion (Mitchell and Perfect, 1995), but infection more commonly occurs in the lungs following inhalation. Although infection begins in the lungs, *C. neoformans* can disseminate to the central nervous system (CNS) where it can cause fungal meningitis. Dissemination occurs almost exclusively in individuals with pre-existing immune deficiencies. In the decades following the discovery of *C. neoformans*, cases of cryptococcal meningitis were rare because immune deficiency syndromes were uncommon. Medical advances in the 21st century such as organ transplantation and cancer treatment (that require or result in immune deficiency) led to increased cryptococcosis rates; however it was not until the spread of HIV in the 1980s that *C. neoformans* truly emerged as a major global pathogen (Antinori, 2013).

Cryptococcosis currently afflicts around a million people around the world annually - mainly within HIV infected populations. In sub-Saharan Africa, where the HIV epidemic has hit hardest, complications caused by cryptococcosis account for up to 44% of HIV related deaths (Park et al., 2009). Ominously, the rise of cryptococcosis within immune

suppressed populations may foreshadow a wider emergence of disease amongst healthy populations. Of particular note is an ongoing outbreak of cryptococcosis amongst immunocompetent residents of Pacific Northwest Canada and the USA. This outbreak has been caused by a particularly virulent lineage of *Cryptococcus gattii* - a *Cryptococcus* species closely related to *C. neoformans.* The outbreak began in the Vancouver Island area of British Columbia, Canada, in 1999. As of 2009 there were 263 human cases of *C. gattii* infection (Hoang et al., 2011). The outbreak has since spread from Vancouver Island and infections related to the outbreak have been reported across North West Canada as well as many North Western US states (Bartlett et al., 2008; Byrnes et al., 2009; Byrnes,Edmond J., I.,II et al., 2010; Harris et al., 2012; Hoang et al., 2011; MacDougall et al., 2007).

1.2 Pathogenic species within the *Cryptococcus* genus.

Cryptococcus neoformans and *C. gattii* produce a number of virulence factors that help them infect the host; these include a polysaccharide capsule (Bose et al., 2003) (quite unique among fungi), melanin (Casadevall et al., 2000), phospholipase B (Chen et al., 1997a; Wright et al., 2002) and urease (Olszewski et al., 2004; Osterholzer et al., 2009c; Singh et al., 2013).The genus *Cryptococcus* denotes a group of at least 40 basidiomycete fungal species, almost all cases of human infection however are caused by a small group of species within the genus. Until recently it was thought that there were two disease causing species - *C. neoformans* and *C. gatti.* These two species have been further classified according to variations in capsule polysaccharide (Ikeda et al., 1982). Variants are split into five serotypes - serotype A, otherwise known as *C. neoformans var. grubii* or VNI/VNII/VNB; serotype D, otherwise known as *C. neoformans var. neoformans* or genotype VNIV; serotypes B and C, which collectively made up the *C. gattii* species

(Kwon-Chung et al., 2002; Kwon-Chung and Varma, 2006). Serotypes B and C have been further divided into five genotypes (VGI, VGII, VGIII, VGIV and VGIV/VGIIIc). Finally there is serotype AD which is a hybrid of serotypes A and D (Lengeler et al., 2001), in addition to the AD hybrid, there are also reported occurrences of *C. neoformans* / *C. gattii* hybrids in the literature (Aminnejad et al., 2012; Bovers et al., 2006; Bovers et al., 2008). Recently, phylogenetic re-analysis of *C. neoformans* and *C. gattii* genotyping has provided a convincing argument that each genotype is a species in its own right (Hagen et al., 2015). The proposed new species names are given in Table 1.

Existing species name	Serotype	Genotype(s)	Species name as proposed by Hagen et al. 2015 (Hagen et al., 2015)
Cryptococcus neoformans var. grubii	A	VNI / VNII / VNB	*Cryptococcus neoformans*
Cryptococcus neoformans var. neoformans	D	VNIV	*Cryptococcus deneoformans*
Cryptococcus inter-variety hybrid	AD	VNIII	*Cryptococcus neoformans x Cryptococcus deneoformans hybrid*
Cryptococcus gattii	B and C	VGI	*Cryptococcus gattii*
		VGII	*Cryptococcus deuterogattii*
		VGIII	*Cryptococcus bacillisporus*
		VGIV	*Cryptococcus tetragattii*
		VGIV/VGIIIc	*Cryptococcus decagattii*

IMPORTANT NOTE

The species names above represent the vegetative budding forms of *Cryptococcus* that replicate asexually. *Cryptococcus* species can also reproduce sexually via a teleomorph form (Kwon-Chung, 1976a; Kwon-Chung, 1976b) and, as is typically the case for fungal taxonomy, the teleomorph is given a different species name. Thus *C. neoformans* and *C. gattii* have the telomorph forms *Filobasidiella neoformans* and *Filobasidiella bacillispora* respectively. It is still not clear how these teleomorph names will be changed to fit with the new seven species naming system.

Table 1 – Overview of *C. neoformans* and *C. gattii* species nomenclature.

For the remainder of this thesis (unless otherwise stated) *C. neoformans* VNI/VNII/VNB and *C. deneoformans* VNIV will be referred to collectively as '*Cryptococcus neoformans*' whereas *C. gattii* VGI, *C. deuterogattii* VGII, *C. bacillisporus* VGIII , *C. tetragattii* VGIV and *C. decagattii* VGIV/VGIIIc will be referred to collectively as '*Cryptococcus gattii*'. This is due to the similarity in biology between members within each group in terms of pathogenesis and host macrophage interactions - if a distinction between species within each group is made the new species name and the genotype will be given e.g. *Cryptococcus neoformans* VNI/VII (Hagen et al., 2015).

2. The epidemiology and aetiology of cryptococcosis

2.1 Aetiology

C. neoformans and *C. gattii* are primarily environmental organisms, in the literature their environmental niches are often said to be bird guano and rotting wood respectively however additional niches such as the soil are also populated by these fungi (Del Poeta and Casadevall, 2012; Kronstad et al., 2011). The host range for each organism is wide; it includes many different types of birds (e.g. pigeons, parrots and cockatoos), mammals (e.g. koalas, ferrets, dogs, cats, horses, dolphins, bats, humans and bandicoots) and plants (e.g. *Eucalyptus*, pine, mopane tree) (Cogliati, 2013). Interestingly as well as being an environmental niche for cryptococcal survival, plants may also be a host for *Cryptococcus* infection (Warpeha et al., 2013)

There is little evidence to suggest that either *Cryptococcus* species can be spread between animal hosts, thus all cases of infection are presumed to be due to infection from environmental sources. Geographical modelling of the Vancouver Island *C. gattii* outbreak

supports the role of environmental exposure – in a 2010 paper Mak et al. modelled the greater Vancouver Island area to predict environmental habitats most amenable to *C. gattii* colonisation. The habitats that were identified clustered around the South Eastern tip of Vancouver Island and an area on mainland British Columbia across the Strait of Georgia. These areas demarcated almost exactly the geographical spread of the human and veterinary cases reported during the outbreak (Mak et al., 2010).

It is still unclear whether the spore form or the (desiccated) yeast form of *Cryptococcus* is the causative agent of infection. Both spores and desiccated yeast cells have been shown to induce infection experimentally but the relative contribution of each vector to disease aetiology is unclear (Giles et al., 2009). *Cryptococcus* species can sporulate in two ways - sexually when *Cryptococcus* 'a' and 'α' mating type strains reproduce (Kwon-Chung, 1976a; Kwon-Chung, 1976b) and asexually via a process known as monokaryotic fruiting – however only mating type α strains can sporulate via monokaryotic fruiting (Wickes et al., 1996).

Cryptococcus spores possess a number of attributes that make them the likelier candidate for an infectious vector. Firstly, *Cryptococcus* spores are smaller than desiccated yeast cells with a diameter of 1 – 3 µm compared to 3 µm – 8 µm for yeast cells (Botts et al., 2009). At this size, all spores and yeast cells in the lower size range should be able to be inhaled into the alveolar space, but the smaller size range of *Cryptococcus* spores may give them an advantage. Secondly *Cryptococcus* spores are surrounded by a thick outer coating that makes them more resistant to environmental stresses compared to yeast cells (Botts et al., 2009). Persistence in the environment is important because cryptococcosis results almost exclusively from environmental exposure. Finally the process of sporulation leads

to the development of vertical hyphae tipped with basidia, in which the spores grow and are eventually released (Botts and Hull, 2010). These aerial structures should allow spores to become airborne much easier than yeast cells and subsequently more readily inhaled (Velagapudi et al., 2009). For these reasons it is therefore likely that *Cryptococcus* spores are the main causative agent of infection.

2.2 The global distribution of *C. neoformans* and *C. gattii* species

All seven pathogenic *Cryptococcus neoformans* and *Cryptococcus gattii* species (Hagen et al., 2015) can be found across Europe, Asia, North and South America and Oceania (Figure 1). Of these seven *Cryptococcus* species, *Cryptococcus neoformans* VNI is the most prevalent worldwide. Globally *C. neoformans* isolates are about eight times more prevalent that *C. gattii* - Oceania (Australia, New Zealand and Papua New Guinea) is the only continent where *Cryptococcus gattii* is more prevalent than *Cryptococcus neoformans*. *C. neoformans* VNI is also the most clinically important *Cryptococcus* species as it causes the majority of cryptococcosis cases worldwide (Cogliati, 2013). Although *C. neoformans* VNI predominates, a highly virulent *Cryptococcus neoformans* strain called VNB (Beale et al., 2015) also exists. *C. neoformans* VNB is found endemic in a few southern African countries – primarily Botswana; this country is believed to be the geographical point of origin of VNB (Cogliati, 2013; Litvintseva et al., 2006).

Among the *C. gattii* species, *C. deuterogattii* VGII is the most clinically important. *C. deuterogattii* VGII was responsible for the 1999 to present day Vancouver Island outbreak previously discussed (Harris et al., 2012; Hoang et al., 2011). Before the Vancouver Island outbreak, it was thought that *Cryptococcus gattii* species were confined to tropical locales such as Oceania and South America. Analysis of VGII isolates collected during this

7

outbreak revealed two disease causing strains; these two strains were subsequently called VGIIa and VGIIb. VGIIa was found to have caused more infections than VGIIb, the VGIIa strain was also found to be more virulent than VGIIb in mice (Bartlett et al., 2012). It is likely that the VGII outbreak strains originated from Australia or South America and spread to the Pacific Northwest area (Cogliati, 2013).
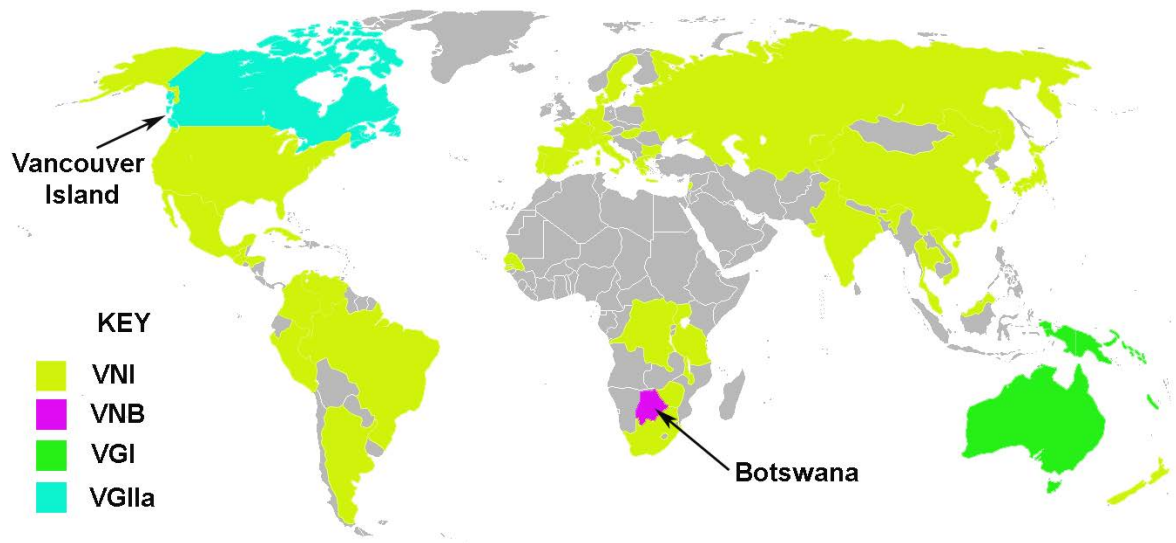
Figure 1:

Map of the world showing the most common *Cryptococcus* genotype found in each country surveyed. Each colour (see 'KEY') represents the most common *Cryptococcus* genotype found in that country according to analysis by Cogliati *et al.* (Cogliati, 2013). Greyed out countries were not included in the analysis by Congliati *et al.* Two locations of interest have been highlighted – Vancouver Island where a recent *C. gattii* outbreak occurred and Botswana where the geographically isolated VNB genotype is found most often (some elements of this figure have been taken from http://commons.wikimedia.org).

2.3 Risk factors for *Cryptococcus neoformans* infection

Most of the world's population are exposed to *Cryptococcus neoformans* at a young age but do not develop cryptococcosis (Abadi and Pirofski, 1999; Goldman et al., 2001; Houpt et al., 1994a). This is because *Cryptococcus neoformans* is primarily an opportunistic pathogen, and, as such, it only causes serious infection in conjunction with pre-existing immune deficiencies. Following inhalation, *C. neoformans* first grows within the alveolar spaces of the lung. *C. neoformans* eventually disseminates from the lungs into the blood stream, unless it is contained and cleared from the lungs by an effective immune response. From the bloodstream *C. neoformans* disseminates to many organs of the body, the CNS is the most common site. This could be due to the fungus's propensity to grow in cerebrospinal fluid (CSF) (Casadevall et al., 2000). Growth of *C. neoformans* in the CNS leads to cryptococcal meningitis (meningoencephalitis) – a complication of infection that can be deadly.

HIV and AIDS

The major risk factor for *C. neoformans* infection, and the subsequent development of cryptococcal meningitis, is HIV infection. Uncontrolled HIV infection can dramatically decrease an individual's $CD4^+$ T cell count, resulting in the development of AIDS (Acquired Immune Deficiency Syndrome). This immunocompromised state leaves individuals highly susceptible to opportunistic pathogens such as *C. neoformans* (Grant et al., 1997).

Cryptococcal meningitis is classified as an AIDS defining illness; in a clinical setting it is often used as an initial diagnosis of HIV positive status. Before the HIV epidemic *C.*

neoformans infection was rare; however as HIV spread, reported cases of cryptococcal meningitis increased dramatically. In the USA during the 1980s (1981 – 1990) when HIV spread globally, cryptococcal meningitis cases rose 1500 % over the previous decade (1965 - 1977) (Antinori, 2013). In developed countries the use of Highly Active Anti-Retroviral therapy (HAART) has brought the HIV epidemic under control; it has done this by preventing the spread of the virus, and also by improving the life expectancy of those infected. Concordant with the introduction of HAART, the prevalence of cryptococcal meningitis in the developed world has also decreased (Dromer et al., 2004; Kaplan et al., 2000; Mirza et al., 2003). Unfortunately, due to its expense, HAART has only recently begun to become available in developing countries.

The impact of cryptococcal meningitis as a co-morbidity of HIV AIDS is still large in the developing world. WHO figures state that in 2013, 35 million individuals worldwide were living with HIV AIDS – in the same year 1.5 million infected individuals died of an AIDS related illness (World Health Organisation, 2015). Around 70 to 90 % of HIV AIDS sufferers develop a neuropathological condition with cryptococcal meningitis being the 3rd leading cause (Del Valle and Pina-Oviedo, 2006). The majority of cryptococcal meningitis cases today occur in Sub-Saharan Africa where the rate of HIV infection is highest. Estimates of infection and mortality rates for cryptococcal meningitis in Sub Saharan Africa vary; this is probably due to poor disease reporting mechanisms in these countries. In the year 2006, an estimated 720,000 (median) cases of cryptococcal meningitis occurred in Sub-Saharan Africa - this figure represents 75 % of the estimated 957,900 (median) cases worldwide that same year. In the same study, the mortality rate following infection was estimated to be 70% i.e. 504,000 deaths out of 720,000 infected (Park et al., 2009).

Some estimates put the mortality rate lower than Park *et al.* - for instance, a Ugandan study by Kambugu *et al.* has estimated a mortality rate of 20 – 42 % for cryptococcal meningitis (Kambugu et al., 2008) whilst in South Africa Bicanic *et al.* estimated a similar mortality rate of 17 – 37 % (Bicanic et al., 2007), although mortality rates of 88% - 100 % have also been reported (Mayanja-Kizza et al., 1998; Mwaba et al., 2001). Overall the cryptococcal burden in Sub-Saharan Africa is hard to judge – this is not likely to change unless diagnosis and medical case reporting is improved in affected countries.

Although the statistics vary, it is likely that unless the HIV epidemic can be controlled cryptococcal meningitis will continue to be a leading cause of AIDS related death in developing countries (Park et al., 2009). The use of HAART in developing countries is slowly becoming more common - especially in Sub-Saharan Africa where large efforts are being made to control the epidemic (Fox and Rosen, 2010). A study from Jarvis *et al.* worryingly shows however that although the use of HAART in a Cape Town hospital increased substantially over a 5 year period (660 patients on HAART in 2003 vs. 13,985 in 2008), the rate of cryptococcal meningitis did not decrease (Jarvis et al., 2009).. Taken together this suggests that although HAART has helped control cryptococcal meningitis in the developed world, further medical advances in developing countries - such as effective diagnosis and treatment - may be needed to obtain a similar effect.

Solid organ transplant

Figures show that around 100,000 solid organ transplants are performed worldwide per year (2007 figure) (Chinen and Buckley, 2010). Solid organ transplant is a risk factor for *C. neoformans* infection due to the long courses of immune suppressive drugs such as cyclosporine and corticosteroid that are prescribed to prevent organ rejection (Patel and

Paya, 1997). On average 3 % of solid organ transplant recipients will develop an opportunistic fungal infection within the first year of transplant. *C. neoformans* causes 7-8% of these fungal infections (Shoham and Marr, 2012); this makes it the third leading cause of infection behind *Candida* and *Aspergillus* species. The median time from transplantation to the development of *Cryptococcus* infection is 2 – 5 years and the mortality rate 1-year post infection is 27 %. Most *Cryptococcus* infections in these patients are similar to those observed in the HIV/AIDS risk group i.e. the fungus disseminates from the lungs to the CNS resulting in cryptococcal meningitis (Shoham and Marr, 2012).

The relatively long gap in time between transplant and infection (2-5 years) suggests that *Cryptococcus* infection usually develops following environmental exposure post transplant. This said infection can sometimes develop much sooner after the transplant. Faster developing infections may be due to the reactivation of a latent *Cryptococcus* infection that the patient already has (this will be discussed in the next section) or (in rare cases), the transplanted organ might have harboured a reservoir of *Cryptococcus* that subsequently infects the recipient (Baddley et al., 2011).

Cancer

Until the HIV epidemic of the 1980s, most cases of cryptococcosis were seen in patients with cancer. The malignancies linked to *Cryptococcus* infection are unsurprisingly those that involve immune cells (or tissues where immune cells develop) such as leukaemia, lymphoma and myeloma. As these cancers progress the immune system becomes depleted of properly functioning white blood cells creating an immune deficient state. The severity

of *C. neoformans* infection in cancer patients is extenuated by the under-lying malignancy which is often at a very late stage when opportunistic infection occurs (Perfect, 2012a).

Other conditions

In addition to the major risk factors described above, there are a number of less common risk factors that may increase an individual's susceptibility to *C. neoformans* infection. These include sarcoidosis (Baughman and Lower, 2005), cirrhosis (Singh et al., 2004) and methamphetamine use (Patel et al., 2013; Talloczy et al., 2008).

Cryptococcosis in immune competent hosts

There are occasionally case reports of cryptococcal meningitis caused by *C. neoformans* in immunocompetent individuals (Chen et al., 2008b; Zhu et al., 2010). This is especially the case in China where it has been estimated that 17 % of individuals presenting with Cryptococcosis have no underlying immune deficiency (Yuchong et al., 2012).Two theories try to explain these cases. The first posits that these infections have been caused by *C. neoformans* strains that have mutated to become more virulent and able to infect healthy individuals. The second that the individuals infected have an undiagnosed genetic immune deficiency that pre-disposes them to *C. neoformans* infection. Recent data suggest that the latter theory i.e. host susceptibility is most likely. In this respect a 2011 study by Ou et al. found that susceptibility to *C. neoformans* in a cohort of non HIV infected patients with cryptococcosis correlated to a number of genetic alleles related to mannose binding lectin protein (Ou et al., 2011).

3. Treatment of *C. neoformans* infection

3.1 Treatment of cryptococcal meningitis

The treatment of cryptococcosis is complicated by the fact that infection usually occurs alongside serious medical conditions such as HIV AIDS or cancer. Additionally, the majority of cryptococcal infections occur in poor countries where effective diagnostics and treatments are not always readily available. Even with access to treatment, cryptococcal meningitis has an unacceptably high mortality rate (Ma and May, 2009).

Aggressive treatment is vital to control cryptococcal meningitis (the most serious manifestation of cryptococcal disease), a three stage therapeutic strategy is used to combat infection – initially antifungal drugs are given intravenously at high doses for about 2 weeks, this clears the CSF of infection and stabilises the patient's meningitis. During the second stage antifungal drug treatment is maintained for a further 8 weeks at a reduced dosage to continue fungal clearance. The third stage involves long-term low dose antifungal drug treatment to prevent relapses of infection. Relapse of infection is a big risk for patients, especially if their underlying immune deficiency still persists (Perfect and Bicanic, 2015).

The best available treatment for cryptococcal meningitis is a combination of intravenous amphotericin B (0.7 – 1.0 mg/kg/day) and flucytosine (100 mg/kg/day) for 2 weeks followed by a long course of oral fluconazole (400 mg/day) to maintain fungal clearance (Jackson and Hosseinipour, 2010). Unfortunately, when given in high doses both amphotericin B and flucytosine are harmful – amphotericin B damages kidney functions

15

while flucytosine can elicit toxic reactions within the body. Liposomal amphotericin B (an improved preparation of amphotericin B) has greatly reduced kidney toxicity, but it is expensive and thus not available in many developing countries (Jarvis et al., 2014). It is now recommended to create a tailored drug regimen for each patient – the relative dosages of each drug should be manipulated to achieve maximum efficacy while constantly monitoring kidney health and flucytosine levels in the blood to avoid unwanted side effects (Jackson and Hosseinipour, 2010; Perfect et al., 2010).

Intravenous Amphotericin B and flucytosine combination therapy can be effective at curing cryptococcal meningitis if used correctly. However, in the developing world where the majority of *C. neoformans* infections are found these drugs are not always available due to cost. In the developing world the less effective but cheaper azole family of drugs are sometimes all that are available. In this setting the azole drug fluconazole commonly used, not only due to its low cost but also as it is one of the most soluble azoles which it an advantage when treating neurological infections. Fluconazole is often given orally at a dose around 400 mg per day (Jackson and Hosseinipour, 2010). The efficacy of fluconazole when administered in this way is poor and has lead to the development of fluconazole resistant *C. neoformans* strains (Bicanic et al., 2006; Sionov et al., 2013; Smith et al., 2015a).

Due to the inefficacy of standard fluconazole treatment there has been a big push in clinical cryptococcal research to find a better alternate for the developing world. Fluconazole appears to have lower toxicity at higher doses compared to amphotericin B or flucytosine. Administering fluconazole at much higher doses – up to 2g/day – has been trialled and has shown better efficacy over lower, standard dosages (Milefchik et al.,

2008). Other trials have experimented with using different doses (Bicanic et al., 2008) or shorter courses (Bicanic et al., 2007) of amphotericin B (to reduce the cost required per patient) in combination with fluconazole with some promising results.

3.2 Treatment of pulmonary and cutaneous infection

The pulmonary stage or cutaneous stages of cryptococcosis is treated less aggressively than disseminated disease – oral fluconazole, itraconazole, voriconazole or posaconazole are recommended. In severe cases pulmonary infection can be treated with intravenous flucytosine and amphotericin B similar to disseminated disease. When infection cannot be cleared pharmacologically, surgical resection can be used to remove infected tissue (Perfect et al., 2010).

3.3 Treatment complications - Cryptococcal IRIS

In the case of HIV associated cryptococcal infection, the introduction of HAART has reduced the requirement for lifelong antifungal drug therapy. However, HAART treatment produces complications of its own for cryptococcosis patients. As HAART reduces HIV viral load the patients' $CD4^+$ T cell count increases, for individuals with opportunistic co infections such as *C. neoformans* or *Mycobacterium tuberculosis,* their rejuvenated immune systems sometimes become dysregulated. As a result of this dysregulation an excessive immune response is generated against pathogen derived antigen circulating in the body leading to dangerous levels of inflammation – this condition is called Immune Reconstitution Inflammatory Syndrome (IRIS) (Murdoch et al., 2007). IRIS has been estimated to affect around 30 % of *Cryptococcus* infected individuals who are also receiving HAART (Shelburne et al., 2005).

4. The Pathogenesis of *Cryptococcus neoformans* infection

Cryptococcosis initiates in the lungs following inhalation of either spores or desiccated yeast cells (Giles et al., 2009). *C. neoformans* first colonises the alveolar space of the lungs where it interacts with cells of the host immune system – most notably with macrophages (Alanio et al., 2011; Charlier et al., 2009; Feldmesser et al., 2000; Ma , 2009) (Figure 2). Most of the world's population are exposed to *C. neoformans* from a young age (Deshaw and Pirofski, 1995b; Houpt et al., 1994b), however life threatening disseminative infection usually only occurs when individuals have an existing immune deficiency. Without an effective immune response to control it, *C. neoformans* grows rapidly within the lungs both extracellularly and within infected macrophages (Feldmesser et al., 2000; Ma , 2009). Pulmonary cryptococcal infection leads to pneumonia like symptoms; without containment the fungus can disseminate from the lungs, into the blood and subsequently to the CNS (Sabiiti and May, 2012). Cryptococcal meningitis occurs as a result of fungal growth in the brain and spinal column; symptoms include - headaches, fever, deafness, blindness, dementia and coma (Ma and May, 2009). Cryptococcal meningitis is a common co-morbidity of HIV AIDS (Chuck and Sande, 1989; Lin et al., 2015; Park et al., 2009); this indicates the requirement of a T-cell mediated adaptive immune response to control and clear infection before it can disseminate (Jarvis et al., 2013; Lindell et al., 2006; Uicker et al., 2006; Wozniak et al., 2011).

4.1 Pulmonary infection

Initial pulmonary infection is an important stage of *C. neoformans* pathogenesis. If *C. neoformans* is not contained within the lungs by the immune system then life threatening cryptococcal meningitis can develop (Sabiiti and May, 2012). During pulmonary infection *C. neoformans* grows within the alveolar space (Garcia-Rodas and Zaragoza, 2012) where it encounters the innate arm of the host immune system. The cellular component of the innate immune response to pulmonary infection includes macrophages, neutrophils and dendritic cells (Wozniak et al., 2006). During early stages of pulmonary infection the innate immune response is the body's only protection against *C. neoformans* until an adaptive immune response can be generated – typically 14 days after the initial inflammatory signals generated by the innate immune system (Cauley and Murphy, 1979).

By inoculating mice with fluorescently tagged *C. neoformans* strains Wozniak *et al.* have found that within 2 hours of infection all three innate phagocytic cell types (macrophages, neutrophils and dendritic cells) can phagocytose *C. neoformans* cells (Wozniak et al., 2006). The early interaction between *C. neoformans* and innate immune cells (with the exception of macrophages) is generally protective for the host (Osterholzer et al., 2009b). Dendritic cells (Hole et al., 2012) and neutrophils (Miller and Kohl, 1983; Miller and Mitchell, 1991) are more fungicidal towards *C. neoformans* than macrophages, this is because macrophages require activation by the adaptive immune system in order to be fully effective at killing *C. neoformans* (Kawakami et al., 1995; Voelz et al., 2009) while dendritic cells and neutrophils are intrinsically fungicidal (Hole et al., 2012; Lehrer and

Ladra, 1977). If macrophages are not appropriately activated *C. neoformans* can become an intracellular parasite (Feldmesser et al., 2000).

4.2 Neutrophils

Neutrophils are able to kill both internalised and extracellular cryptococci (Qureshi et al., 2010; Qureshi et al., 2011). The neutrophil cytoplasm contains a number of cytotoxic granules that are loaded with anti-microbial agents such as myeloperoxidase, serine proteases and cathepsins (Mambula et al., 2000; Segal, 2005). After phagocytosis of C. *neoformans* cells, these cytoplasmic granules fuse with the phagosome and disgorge their contents – at the same time neutrophils generate an intense oxidative burst mediated by the enzyme NADPH oxidase. These two mechanisms combine to kill phagocytosed *C. neoformans* cells (Diamond et al., 1972). Extracellular killing by neutrophils also involves cytoplasmic granules; however in this situation, the contents of the granules are released into the extracellular space rather than into the phagosome (Qureshi et al., 2010). A second killing mechanism called NETosis is also used by neutrophils. During NETosis apoptotic neutrophils release their nuclear contents into the extracellular environment producing cytotoxic effects (Remijsen et al., 2011). Evidence suggests however that the *C. neoformans* capsule is able to inhibit NET formation by neutrophils (Rocha et al., 2015).

Neutrophils are more fungicidal towards *C. neoformans* than macrophages (Miller and Kohl, 1983; Miller and Mitchell, 1991); crucially the anti-fungal activity of neutrophils is intrinsic (Alcouloumre et al., 1993; Ganz et al., 1985; Lehrer and Ladra, 1977), whereas macrophages require classical activation by $CD4^+$ T cells to effectively kill *C. neoformans* (Kawakami et al., 1995; Voelz et al., 2009). Notably however, the *Cryptococcus* polysaccharide capsule offers protection from the antimicrobial activities of neutrophils

(Del Poeta, 2004; Rocha et al., 2015). Environmental cryptococci do not possess large capsules as capsule induction is triggered by growth conditions within the host, suggesting that neutrophils may play an important role in the early defence against *C. neoformans* before capsule growth is induced. It is clear however that careful regulation of the neutrophil response by macrophages and dendritic cells is required to balance their anti-cryptococcal activity with detrimental damage to the lungs (Osterholzer et al., 2009b).

4.3 Macrophages

Resident macrophages within the alveolar space can kill phagocytosed *C. neoformans* cells (Kawakami et al., 1995) by producing free radical oxygen species within the phagosome and lowering phagosomal pH leading to activation of phagosomal digestive enzymes (Amer and Swanson, 2002; Russell et al., 2009). The efficacy of this killing mechanism is dependent on the macrophage's activation state (Kawakami et al., 1995; Voelz et al., 2009).

During infection, macrophages become either 'classically' (M1) or 'alternatively' (M2) activated depending on the cytokine milieu at the site of infection (Classen et al., 2009). Although 'classical' and 'alternative' activation is often used to describe macrophage activation it is becoming increasing clear that the polarisation is not binary – depending on stimulation macrophages can have attributes of both classical and alternative activation at any given time. The use of 'classical' and 'alternative' herein implies to an overall shift towards either extreme on a scale of activation (Martinez and Gordon, 2014).

Classical macrophage activation is protective against *C. neoformans* pulmonary infection whereas alternatively activated macrophages cannot control intracellular infection

(Kawakami et al., 1995; Voelz et al., 2009). Classically activated macrophages kill phagocytosed *C. neoformans* cells (Kawakami et al., 1995; Voelz et al., 2009); classical activation induces the macrophage oxidative burst, required during phagosome maturation, it also increases the amount of pro-inflammatory cytokines such as IL-1, IL-6 and IL-23 that are produced by macrophages during inflammation. The classical activation of macrophages is induced largely by two cytokines – IFN-γ and TNF-α. IFN-γ is produced mainly by Th1 CD4^{+} T helper cells following activation of adaptive immunity (Schoenborn and Wilson, 2007) whereas TNF-α is produced by macrophages following toll like receptor recognition of pathogen associated molecular patterns (PAMPs) (Parameswaran and Patial, 2010). Alternative macrophage activation is induced by the cytokine IL-4 which is a product of Th2 CD4^{+} T helper cells, basophils and mast cells. Alternatively activated macrophages produce lower levels of pro-inflammatory cytokines and are also poor activators of intracellular killing mechanisms (Classen et al., 2009).

The alveolar spaces of the lungs are protected by alveolar macrophages. Each tissue has a tissue specific subset of macrophages that are specially adapted to protect it. Macrophages originate in the bone marrow as monocytes and circulate in the vascular and lymphatic systems, monocytes differentiate into macrophages after they have migrated into a specific tissue. Macrophage specialisation is achieved via tissue specific signalling factors that alter the differentiation phenotype of monocytes upon migration (Hussell and Bell, 2014). Resident alveolar macrophages (CD11c^{+}, CD11b^{-}) initially interact with *C. neoformans*, however evidence from infections of mice indicates that a phenotypically distinct subset of macrophages termed 'exudate macrophages' (CD11c^{+}, CD11b^{+}, Lyc-6C^{high}) migrate into the alveolar space once inflammation begins (Osterholzer et al., 2011). Osterholzer *et al.*

identified these exudate macrophages in 2011 (Osterholzer et al., 2011) however it is likely that they were first identified in 2009 (Osterholzer et al., 2009b) (Pulmonary CD11c$^+$, CD11b$^+$ leukocyte numbers increased significantly in *C. neoformans* infected mice by day 7 post infection), however they were misidentified as dendritic cells (dendritic cells are also CD11c$^+$ and CD11b$^+$). In a second 2009 study Osterholzer *et al.* reported that the source of these 'dendritic cells' were Lyc-6C^{high} monocytes which had migrated to the lungs before differentiating (Osterholzer et al., 2009a). Only in 2011 did Osterholzer *et al.* find that the migratory CD11c$^+$ CD11b$^+$ cell population was composed of macrophages as well as dendritic cells. By 14 days post infection Osterholzer *et al.* found that the exudate macrophage population in the lungs was ~ 2.5 times larger than the original alveolar macrophage population. Exudate macrophages were found to have higher expression levels of phagocytic receptors such as CD107b and CD204, costimulatory molecules such as CD40 and CD86 and the antigen presentation complex MHC II compared to resident alveolar macrophages. Furthermore non-resident exudate macrophages were found to be significantly more fungicidal towards *C. neoformans* than resident alveolar macrophages (Osterholzer et al., 2011). The accumulation of exudate macrophages at the site of infection was found to require expression of CCR2 by monocytes – a chemokine receptor with the ligand known as macrophage chemotactic protein 1 (MCP-1) or C-C motif ligand 2 (CCL2). Previous studies have found that pulmonary levels of CCL2 increase during cryptococcal infection, that CCL2 is required for monocyte and CD4$^+$ T cell migration to the lungs (Huffnagle et al., 1995c; Huffnagle et al., 1997) and that CCL2 levels influence the generation of adaptive immunity (Traynor et al., 2000). Alveolar macrophages as well as lung epithelial cells are known to produce CCL2 (Brieland et al., 1992; Deshmane et al., 2009; Standiford et al., 1991; Yoshimura et al., 1989). Alveolar macrophages therefore

presumably still have an important role during early cryptococcal pulmonary infection by triggering dendritic cell and exudate macrophage accumulation.

The inflammatory response of macrophages to early cryptococcal infection in the lung is vital to generate and coordinate a protective inflammatory response (Wozniak et al., 2006). Paradoxically however some studies have found that the presence of macrophages in the lung can actually aid the fungus. A recent study by Sabiiti *et al.* selected a group of *C. neoformans* strains isolated from HIV[+] patients and exposed them to macrophages *in vitro* (Sabiiti et al., 2014). The phagocytic efficiency and intracellular proliferation of each strain was assessed and then correlated to the clinical outcome for each patient. Sabiiti *et al.* found a positive correlation between improved efficiency of phagocytosis of each strains *in vitro* and fungal burden *in vivo* within the CNS. A similar study by Alanio *et al.* reported a similar correlation (Alanio et al., 2011). These studies indicate that parasitism of host macrophages (under certain conditions) is beneficial to *C. neoformans.* If macrophages are unable to kill phagocytosed cryptococci*,* the macrophages can act as a protective niche for fungal growth (Diamond and Bennett, 1973; Feldmesser et al., 2000; Garcia-Rodas and Zaragoza, 2012; Goldman et al., 2000a; Levitz et al., 1999a) and also potentially also as vehicles for dissemination (Charlier et al., 2009).

A study by Shao *et al.* illustrates the protective versus deleterious paradox that the macrophage poses during cryptococcal infection (Shao et al., 2005). Shao *et al.* assessed the effect of macrophage depletion on pulmonary cryptococcosis in two animal models; mice – which are susceptible to pulmonary *C. neoformans* infection, and rats – which are more resistant to infection than mice. Shao *et al.* found that depletion of macrophages in rats increased fungal burden in the lungs. In contrast, depleting mice of macrophages

decreased fungal burden in the lungs. This study shows how in susceptible hosts, macrophages can aid cryptococcal pathogenesis by providing a protective niche for growth (Diamond and Bennett, 1973; Feldmesser et al., 2000; Garcia-Rodas and Zaragoza, 2012; Goldman et al., 2000a; Levitz et al., 1999a; Shao et al., 2005). In resistant hosts however appropriately activated macrophages are able to kill intracellular *C. neoformans* cells (Kawakami et al., 1995; Voelz et al., 2009).

The requirement for adaptive immunity to activate macrophages before they are able to control *C. neoformans* infection is likely why individuals with AIDS (which causes a CD4$^+$ T cell deficiency) are susceptible to disease (Park et al., 2009). Adaptive immunity takes longer to activate than innate immunity – about 14 days. To activate adaptive immunity professional antigen presenting cells, mainly dendritic cells, carry antigen from the site of infection to lymph nodes where naive T and B cells are found (Savina and Amigorena, 2007).

4.4 Eosinophils

Eosinophils are another class of innate immune cell that are associated with *Cryptococcosis* infection, especially during pulmonary infection. Eosinophilia at the site of an infection is normally associated with parasitic infections however it also occurs during fungal infection and has been reported during pulmonary *Cryptococcus* infection of mice and rats (Huffnagle et al., 1994; Huffnagle et al., 1995a). The recruitment of eosinophils during cryptococcal infection has been shown to be CD4$^+$ T cell and IL-5 dependant (Huffnagle et al., 1994). There is some evidence for eosinophilia during human *Cryptococcus* infection but it is not as well documented as in rodents (Watanabe et al., 1995). This may be because in human *C. neoformans* infection often occurs alongside

CD4$^+$ T cell depletion due to HIV infection and this phenotype that is not commonly replicated in mouse or rat models of infection.

4.5 Adaptive immune response

Cytokine production by CD4$^+$ T cells - as well as antibody production by B cells - can augment the ability of innate immune macrophages and neutrophils to clear *C. neoformans* infection (Voelz and May, 2010). Furthermore CD4$^+$ T cells also exhibit direct anti microbial activity against *C. neoformans* by releasing granulysin (Zheng et al., 2007). The generation of a Th1 adaptive immune response – characterised by the production of IFN-γ and IL-12 by CD4$^+$ T cells – is protective against cryptococcal pulmonary infection, whereas a Th2 adaptive immune response – characterised by the production of IL-4 and IL-10 by CD4$^+$ T cells – is non protective (Chen et al., 2008a).

As has previously been discussed, a Th1 adaptive immune response leads to 'classical' activation of macrophages. 'Classically' activated macrophages are more fungicidal towards *C. neoformans* compared to Th2 'alternatively' activated macrophages (Voelz et al., 2009). In a 2009 study, Voelz *et al.* elucidated the basis for this observation (Voelz et al., 2009). *In vitro* treatment of macrophages with Th1 associated cytokines (IFN-γ and TNF-α) increased macrophage phagocytosis of *C. neoformans* and *C. gattii* cells whereas Th2 associated cytokines (IL-4 and IL-13) did not – this is in agreement with a previous study from Kawakami *et al.* (Kawakami et al., 1995). Interestingly Voelz *et al.* found that Th1 cytokine treatment of macrophages did not alter their ability to control intracellular proliferation of the fungus as one might expect, however Th2 cytokine treatment made macrophages less effective at controlling infection (Voelz et al., 2009).

It is known that *C. neoformans* actively promotes the development of Th2 biased immunity during infection (Voelz and May, 2010). One of the ways that *C. neoformans* promotes Th2 immunity is by manipulating dendritic cell function via expression of the *Cryptococcus* virulence factor urease (Osterholzer et al., 2009c). Mice infected with a urease deficient *C. neoformans* mutant were found to have stronger Th1 immune responses compared to those infected with the wild type strain, this resulted in better fungal clearance. Urease expression by *C. neoformans* during pulmonary infection was found to increase the number of phenotypically immature dendritic cells at the site of infection. Furthermore greater numbers of immature dendritic cells were found in lymph nodes associated with the mouse lung. Antigen presentation by immature dendritic cells poorly induces Th1 induction and promotes Th2 immunity during *C. neoformans* infection (Chen et al., 2008a; Osterholzer et al., 2009c). As well as urease, additional virulence factors have been found to affect dendritic cell function. In this respect it has been observed that dendritic cells exposed to encapsulated *C. neoformans* strains develop different gene expression patterns to cryptococci exposed to un-encapsulated strains (Lupo et al., 2008). Additionally it has recently been shown that prostaglandin E_2 (PGE_2) signalling in the lung during *C. neoformans* infection promotes alternative macrophage activation (Shen and Liu, 2015) – host immune cells such as macrophages (Park et al., 2006) and also *C. neoformans* itself (Noverr et al., 2003a) produce PGE_2 but Shen et al. do not address the source in their study.
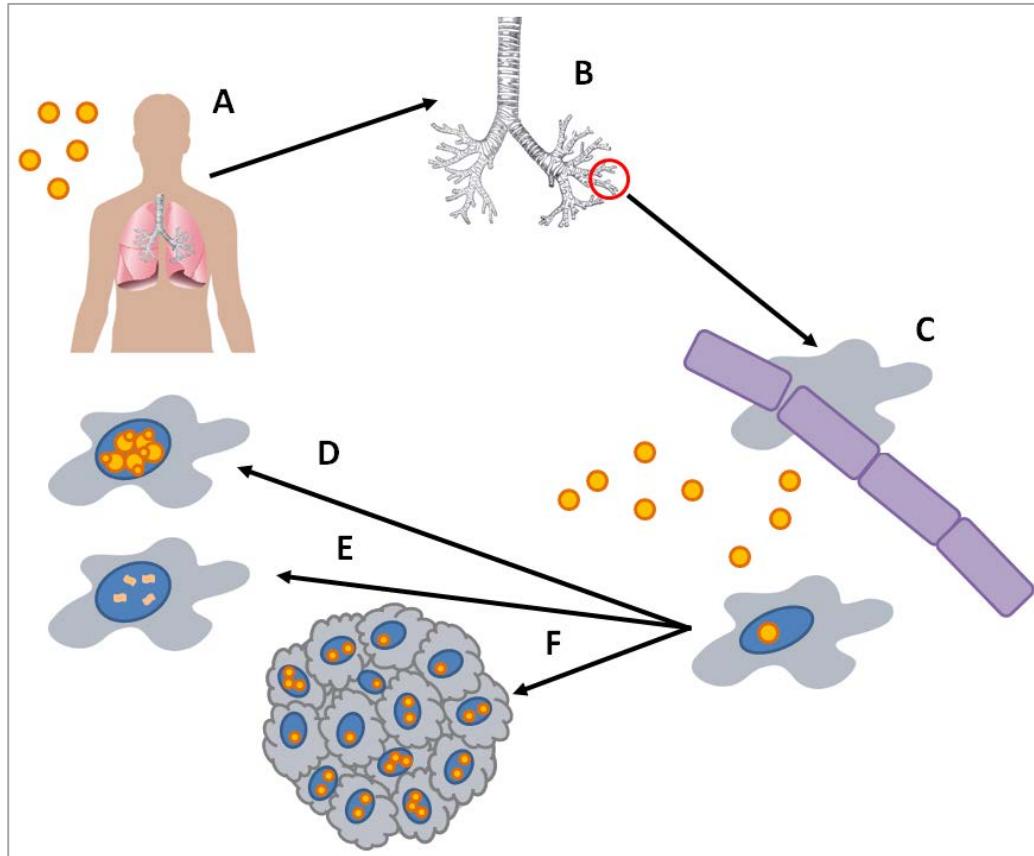
Figure 2 –

The pathogenesis of Cryptococcosis. **A.** *Cryptococcus neoformans* infection begins when desiccated yeast cells, or infectious spores, are inhaled into the respiratory tract. **B.** Inhaled *Cryptococcus* cells reach the alveolar spaces of the respiratory tract where they germinate and grow. **C.** As part of the host innate immune response against *C. neoformans*, professional phagocytes such as macrophages and neutrophils migrate to the site of infection in the alveolar space. These cells phagocytose extracellular *C. neoformans* cells. Following phagocytosis there are three possible outcomes for *C. neoformans* and the macrophage. **D.** The macrophage is improperly activation and as a result cannot control the intracellular growth of *C. neoformans*, growth within the macrophage phagosome, escape from the macrophage and subsequent dissemination to the central nervous system is

possible. **E.** The macrophage is properly activated; it can kill the intracellular *C. neoformans* cells. F. The macrophage cannot kill phagocytosed *C. neoformans* cells but instead is able to contain them within a granuloma. For *C. neoformans* infection, fatal disseminative disease (**D)** occurs almost exclusively in individuals with pre-existing immune deficiencies whereas total clearance (**E)** and latent disease (**F**) can manifest in individuals who are immune competent (some elements of this figure have been taken from http://commons.wikimedia.org).

4.6 Disease latency

Latent infection develops when a balance is reached between the host's immune defence and the pathogen's virulence. There is evidence to suggest that pulmonary *C. neoformans* infection can enter a latent stage (Garcia-Hermoso et al., 1999). Latent *C. neoformans* infection is characterised by the formation of granuloma like structures in the lungs. *Cryptococcus* cells remain viable within these structures, additionally if the host immune response weakens sufficiently (e.g. an individual with latent infection develops an immune deficiency) then the fungus can emerge from the granuloma and re-establish infection potentially leading to disseminative disease (Garcia-Hermoso et al., 1999; Goldman et al., 2000b).

Cryptococcal granulomas develop in the alveolar space and are composed of aggregates of infected macrophages. Macrophages within these cryptococcal granulomas have 'giant cell' and 'multinuclear' morphologies that are also seen in Tuberculosis granulomas. *C. neoformans* is contained intracellularly inside macrophages within the granuloma - this is different to Tuberculosis granulomas where mycobacterium cells reside in a necrotic pocket formed at the centre of the granuloma (Shibuya et al., 2005).

Epidemiologically, it is hard to estimate the global prevalence of latent *C. neoformans* infection. For healthy populations the majority of *Cryptococcus* infections are asymptomatic and go unreported, thus the presence of latent infection is never suspected. Studies that have measured the level of anti-cryptococcal immunoglobulin titres within immune competent populations conclude that cryptococcal infection is inevitable by adulthood (Deshaw and Pirofski, 1995a; Goldman et al., 2001; Houpt et al., 1994b) and most individuals are first exposed to the fungus during childhood (Abadi and Pirofski,

1999; Goldman et al., 2000b; Houpt et al., 1994a). These conclusions seem reasonable considering the ubiquity of *C. neoformans* within the natural environment, thus it is likely that an individual encounters *C. neoformans* many times during a single lifetime - it is not known however how often these encounters lead to the development of latent infection.

Studies suggest that latent pulmonary cryptococcal infection may re-emerge if the host develops an immune deficiency. In this respect it has been found *in vivo* that latent *Cryptococcus* infection of rats can be induced to reactivate following immune suppressive glucocorticoid treatment (Goldman et al., 2000b). Additional evidence for latent infection can be found in a clinical study from Garcia-Hermoso *et al.* In this study Garcia-Hermoso *et al.* determined the genetic origin of clinical *C. neoformans* isolates taken from a cohort of cryptococcosis sufferers in France. Their analysis found that a number of immunocompromised African immigrants in the study (who had lived in France for many years before developing immune deficiency) were infected with *C. neoformans* strains originating in Africa. Garcia-Hermoso *et al.* concluded that these patients may have developed a latent form of cryptococcosis before moving to France and that the infection re-emerged when immune deficiency later developed (Garcia-Hermoso et al., 1999).

4.7 Extrapulmonary infection

If pulmonary *Cryptococcus* infection cannot be controlled there is a good chance that the fungus will disseminate from the lungs to other organs in the body via the blood stream. Dissemination from the lungs to the CNS is a crucial escalation point for *Cryptococcus* infection; this is because growth of *C. neoformans* in the brain and CSF causes cryptococcal meningitis - the most fatal complication of *C. neoformans* infection (Sabiiti and May, 2012). *C. neoformans* infection begins in the lungs. In order to reach the CNS,

31

the fungus must disseminate from the lungs into the blood stream and then subsequently across the blood brain barrier (BBB) into the CNS. The BBB is a highly specialised barrier that separates the CNS from the rest of the body. The brain is especially sensitive to tissue damage due to its slow rate of regeneration; to prevent damage blood brain barriers restricts movement of potentially harmful cells, proteins and large molecules from the blood into the CNS (Ballabh et al., 2004) .

4.8 Exit from the lungs

For *C. neoformans* to disseminate to the CNS it must first exit the lung by crossing the epithelial and endothelial cells layers that separate the alveolar space from the blood stream. It has been observed that *C. neoformans* can bind to alveolar epithelial cells and subsequently invade into the intracellular space. The initial adhesion of *C. neoformans* to epithelial cells appears to be mediated via the binding of glucuronoxylomannan (GXM) – one of the two major constituent polysaccharides in the cryptococcal capsule (Bose et al., 2003). Although GXM was found to mediate initial adhesion to lung epithelial cells, intracellular invasion required active processes by the fungus (Barbosa et al., 2006). The virulence factor phospholipase B1 (Plb1) has been identified as a potential mediator of the lung epithelium invasion. In a study by Santangelo *et al.* it was found that in a mouse model of infection, Plb1 was required for dissemination from the lungs into the bloodstream but not from the bloodstream to the brain (Santangelo et al., 2004). Using a Plb1 deficient *C. neoformans* mutant strain (*Δplb1)* Santangelo *et al.* observed a lower rate of fungal dissemination for *Δplb1* compared to the wild type strain when mice were infected intratracheally. Interestingly when Santangelo *et al.* took *Δplb1* infected macrophages from the lungs of mice and injected them directly into the blood stream of

uninfected mice they found that *Δplb1* no longer showed a difference in CNS dissemination. Taken together the data from this study suggests that Plb1 is required for dissemination from the lungs into the blood stream but is expendable for subsequent invasion of the blood brain barrier (Santangelo et al., 2004). Plb1 is a lipid modifying enzyme that is capable of hydrolysing phospholipids (key constituents of cell plasma membranes); this function may explain its role in dissemination as this activity could potentially disrupt the integrity of lung epithelium. Interestingly, one of the preferred substrates of Plb1 is dipalmitoyl phosphatidylcholine (DPPC) which is one of the most abundant lipids found in lung surfactant, this could indicate an additional target for Plb1 during pulmonary infection (Wright et al., 2007).

4.9 Penetration of the blood brain barrier

The blood brain barrier is composed of the endothelial cells; these cells line all of the capillaries which supply the CNS with blood. The endothelial cells that make up the blood brain barrier have a greater number of tight junctions between adjacent cells and less pinocytotic activity than normal endothelium – these properties make the BBB less permissive to transcellular and paracellular movement (Ballabh et al., 2004).

It is known that *C. neoformans* is able to cross the BBB; however, the mechanism it uses to do this is still unclear. There are currently three theories for how *C. neoformans* crosses the BBB (Figure 3). The first theory dictates that *Cryptococcus* yeast cells that are circulating in the blood during fungemia interact with endothelial cells in brain capillaries, and cross the BBB transcellularly (through endothelial cells) (Chang et al., 2004). Secondly cryptococci may pass paracellularly (between adjacent endothelial cells) following disruption of the BBB (Chen et al., 2003; Olszewski et al., 2004). The third theory is called

the 'Trojan Horse' hypothesis, this theory posits that macrophages infected with *C. neoformans* cross the BBB and release their fungal cargo into the CNS. Evidence to support all three theories of dissemination can be found in the literature suggesting that the mechanisms may not be mutually exclusive and in fact may co-exist. In this respect a study that examined disseminative cryptococcosis in an *in vivo* mouse model found that cryptococcal cells could be found within the brain both extracellulary or associated with monocytes and endothelial cells (Chrétien et al., 2002).

In order for *C. neoformans* to transcytose across the BBB, it must first bind to an endothelial cell. After binding to the endothelium, the fungus facilitates its entry by rearranging the cytoskeleton of the endothelial cell (Chen et al., 2003). In order to interact for a sufficient time with host endothelial cells for transcytosis to occur *C. neoformans* must stop itself in the blood flow. Intravital imaging of *C. neoformans* in mouse brain capillaries has found that arrest of movement in the capillary lumen appears to be purely via mechanic trapping when the size of *Cryptococcus* cells exceeds that of the capillary. Once stopped *C. neoformans* binds to the endothelium and crosses the blood brain barrier. While stopping in the blood vessel was found to be passive, crossing of the endothelial layer was found to be an active process requiring viable cryptococcal cells (Shi et al., 2010a). The active mediation of uptake by *C. neoformans* is indicated by additional studies which show that the cryptococcal virulence factors urease (Shi et al., 2010b; Singh et al., 2013) and Plb1 (Maruvada et al., 2012) play a role in fungal uptake by endothelial cells. A further, well defined, active invasion mechanism has also been identified whereby *C. neoformans* incorporates hyaluronic acid into its capsule (Jong et al., 2007; Liu et al., 2013) that is likely derived from metabolism of host inisitol by *C. neoformans*. Hyaluronic

34

acid in the *C. neoformans* capsule is able to bind to CD44 expressed on endothelial cells, facilitating transcytosis of *Cryptococcus* cells through the endothelium (Jong et al., 2008).
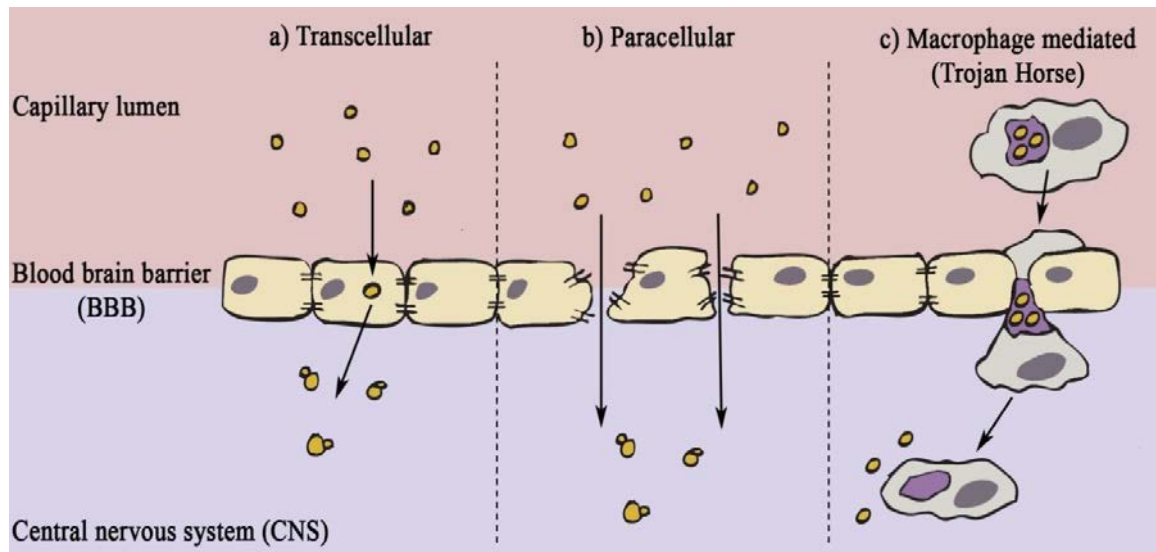
Figure 3 - Possible routes of dissemination across the blood brain barrier (BBB) for *C. neoformans*. There are three routes that *C. neoformans* is thought to use to cross the blood brain barrier (BBB): **A** - fungal cells may pass directly through endothelial cells lining capilliaries in the brain, cells are taken up at the apical side and exit on the basal side – this is termed the transcellular route; **B -** fungal cells pass betweeen endothelial cells following disruption of cell to cell contacts, this disruption could be due to factors produced by the fungi or inflammation – this is called the paracellular route; **C-** macrophages that are infected with *C. neoformans* cells could pass from the circulation through the blood brain barrier via diapedesis, the fungi within the macrophage then escape into the extracellular space- this is called 'Trojan Horse' dissemination.

4.10 'Trojan Horse' dissemination

The 'Trojan Horse' theory of dissemination posits that *C. neoformans* infected macrophages migrate from the lungs to the CNS where upon they release their infective cargo. It is possible that *C. neoformans* could disseminate into the blood unaided and then are engulfed by macrophages and transported to the brain. In this respect it has been shown that *Cryptococcus* infected macrophages injected directly into the blood lead to increased fungal burden in the brain (Charlier et al., 2009).

Once an infected macrophage has migrated to the CNS, *Cryptococcus* cells within must escape in order to grow freely within the brain tissue. One of the most interesting aspects of cryptococcal pathogenesis is the fungus's cellular escape mechanism called 'vomocytosis' (also known as non-lytic expulsion). Vomocytosis is a mechanism first observed in 2006 by two groups independently (Alvarez and Casadevall, 2006; Ma et al., 2006). This mechanism allows *C. neoformans* to escape from infected macrophages without causing host cell lysis. Exiting without host cell lysis is likely to be beneficial to *C. neoformans* as it would result in lower levels of inflammation. Vomocytosis was first discovered and is largely studied *in vitro* however there is good evidence to show that the process also occurs *in vivo* (Nicola et al., 2011). Vomocytosis is also reported to occur in other fungi such as *Candida albicans* (Bain et al., 2012) and *Candida krusei* (Garcia-Rodas et al., 2011).

4.11 Growth within the CNS

Following dissemination, *Cryptococcus neoformans* proliferates within the CNS. Cryptococcal meningitis is associated with high levels of fungal burden in the CNS –

primarily in the CSF where the fungus readily grows. Due to the rapid growth of *C. neoformans* within CSF, dissemination of only a few cryptococci into the CNS can precipitate cryptococcal meningitis. A 1994 study by Hill *et al.* illustrates this phenomenon - following intravenous infection of mice with *C. neoformans* Hill *et al.* estimated that as few as 10 cells or 0.1 % of their original inoculum (10^4 cells) disseminated to the brain. By day 7 post infection Hill *et al.* found that the *Cryptococcal* burden in the CNS was 10^6 cells, surpassing the total original inoculum by a factor of 100 (Hill and Aguirre, 1994). One of the reasons why *C. neoformans* grows so well in the CNS could be because *C. neoformans* metabolises neurotransmitters such as dopamine to produce melanin which is a known cryptococcal virulence factor (Casadevall et al., 2000).

The growth of *C. neoformans* within the CNS triggers an immune response that is partly effective at decreasing the proliferation of the fungus. Protective immunity against CNS infection is dependent on $CD4^+$ T cells (Buchanan and Doyle, 2000; Hill and Aguirre, 1994; Uicker et al., 2006) however the accumulation of $CD8^+$ T cells, macrophages and neutrophils during CNS infection has also been observed (Buchanan and Doyle, 2000). Furthermore, the efficacy of this immune response is dependent on IFN- γ and TNF-α; this suggests that, as with pulmonary infection, Th1 cell mediated immunity is required for immunity following dissemination to the CNS (Buchanan and Doyle, 2000; Hill and Aguirre, 1994; Uicker et al., 2006)

To summarise this section, protective immunity against pulmonary *C. neoformans* infection requires a robust innate immune response in the form of neutrophils, macrophages and dendritic cells (Wozniak et al., 2006). When *Cryptococcus* infection is recognised, host cells are able to phagocytose and kill the fungus; furthermore, recognition

of *C. neoformans* leads to immune cell activation and the release of pro-inflammatory cytokines that shape the future adaptive immune response. The adaptive immune response is important because unless macrophages are 'classically' activated by a Th1 adaptive immune response, *C. neoformans* is able to survive within them intracellularly (Diamond and Bennett, 1973; Feldmesser et al., 2000; Garcia-Rodas and Zaragoza, 2012; Goldman et al., 2000a; Levitz et al., 1999a). Dendritic cells that become activated by the presence of fungal cells in the lungs are required to trigger the development this adaptive immune response (Wozniak et al., 2006). Antigen presentation by dendritic cells in the lymph nodes can activate $CD4^+$ T helper cells, these cells then migrate to the site of infection where they promote either a protective Th1 immune response or a non protective Th2 immune response (Voelz and May, 2010). The response that these $CD4^+$ T cells induce depends on conditions at the time of their activation e.g. the phenotype of antigen presenting cells and composition of the cytokine milieu at the site of infection.

There are broadly three potential outcomes to *C. neoformans* infection. The first outcome is seen in healthy hosts - *Cryptococcus* spores or yeast cells in the alveolar space are phagocytosed by host innate immune cells. A robust Th1 adaptive immune response leads to 'classical' macrophage activation. 'Classically' activated macrophages are able to kill the fungus resulting in total clearance of infection (Kawakami et al., 1995; Voelz et al., 2009). The second outcome is usually seen in hosts who have a pre-existing immune deficiency. Host macrophages phagocytose cryptococci; however in the absence of a protective Th1 response – and perhaps in the presence of a non protective Th2 response – macrophages are unable to control their intracellular burden (Feldmesser et al., 2000; Voelz et al., 2009). Cryptococci subsequently replicate inside of macrophages (Feldmesser

et al., 2000). Uncontrolled pulmonary infection then leads to dissemination to the CNS (Sabiiti and May, 2012). The third outcome - disease latency - is the least studied of the three outcomes. In this scenario a healthy host experiences pulmonary infection however their immune system is unable to completely clear the fungus from the lungs. Cryptococci remain in the lungs in a latent state contained within granulomatous structures formed by infected macrophages (Shibuya et al., 2005). Cryptococcal infection may reactivate from this latent state at a future date if the host develops an immune deficiency (Garcia-Hermoso et al., 1999).

5. *Cryptococcus* virulence factors during infection

The interaction between *C. neoformans* and host macrophages during pulmonary *C. neoformans* infection is an important stage of pathogenesis for both the pathogen and the host. Macrophages can phagocytose and kill *C. neoformans* however they do not become fully effective at controlling infection until they are 'classically' activated by Th1 CD4$^+$ T cells (Kawakami et al., 1995; Voelz et al., 2009), whereas 'Alternatively' activated macrophages are susceptible to intracellular parasitism by *C. neoformans* (Voelz et al., 2009). The fungus is able to survive within the macrophage's phagosome and proliferate (Feldmesser et al., 2000; Garcia-Rodas and Zaragoza, 2012); additionally *C. neoformans* may use the macrophage as a vehicle for dissemination from the lungs to the CNS (Charlier et al., 2009).

The outcome of cryptococcosis is determined by the host's ability to defend against infection and also the ability of a particular *C. neoformans* strain to cause infection (Perfect, 2012b). Host factors (such as the strength and polarisation of the immune response) do significantly influence the outcome of *C. neoformans* infection; however,

virulence factors produced by the fungus also play a role. During infection *C. neoformans* utilises a number of virulence factors to help it survive within the host, these include the cryptococcal polysaccharide capsule (Bose et al., 2003), melanin production (Casadevall et al., 2000), the ability to grow at mammalian body temperature (Perfect, 2006), Titan cell morphology changes (Crabtree et al., 2012; Zaragoza et al., 2010) and secreted enzymes such as Plb1 (Cox et al., 2001; Djordjevic, 2010).

5.1 The *Cryptococcus* polysaccharide capsule

A characteristic feature of *C. neoformans* is the polysaccharide capsule that surrounds its cell wall. The capsule is composed of two key polysaccharide components: glucuronoxylomannan (GXM) and glucuronoxylomannogalactan (GXMGal) (Bose et al., 2003; Heiss et al., 2009) (Figure 5), with a ratio of approximately 9:1 by mass in favour of GXM (Idnurm et al., 2005). Capsule growth can be stimulated *in vitro* by high CO_2, neutral pH, low levels of available iron, high mannitol levels or low nutrient conditions. These conditions are similar in many ways to those found during host infection (Granger et al., 1985; Guimaraes et al., 2010; Vartivarian et al., 1993; Zaragoza et al., 2003a; Zaragoza and Casadevall, 2004) and concurrently, capsule growth has also been observed to occur *in vivo* (Rivera et al., 1998). Synthesis of the capsule is controlled by at least four genes, designated *CAP64, CAP59, CAP10 and CAP60* (Buchanan and Murphy, 1998; Ma and May, 2009). In a series of studies Chang *et al.* found that deletion of each CAP gene produced an acapsular mutant (Chang and Kwon-Chung, 1994; Chang et al., 1996; Chang and Kwon-Chung, 1998; Chang and Kwon-Chung, 1999). Acapsular *C. neoformans* mutants have been found to be avirulent during infection indicating that the capsule is required for host infection (Chang and Kwon-Chung, 1994; Fromtling et al., 1982). The

41

capsule has a number of properties that contribute to virulence during infection but the most important seems to be its anti-phagocytic properties as acapsular strains can be phagocytosed more readily than capsular strains by macrophages (Cross and Bancroft, 1995; Kozel and Gotschlich, 1982).
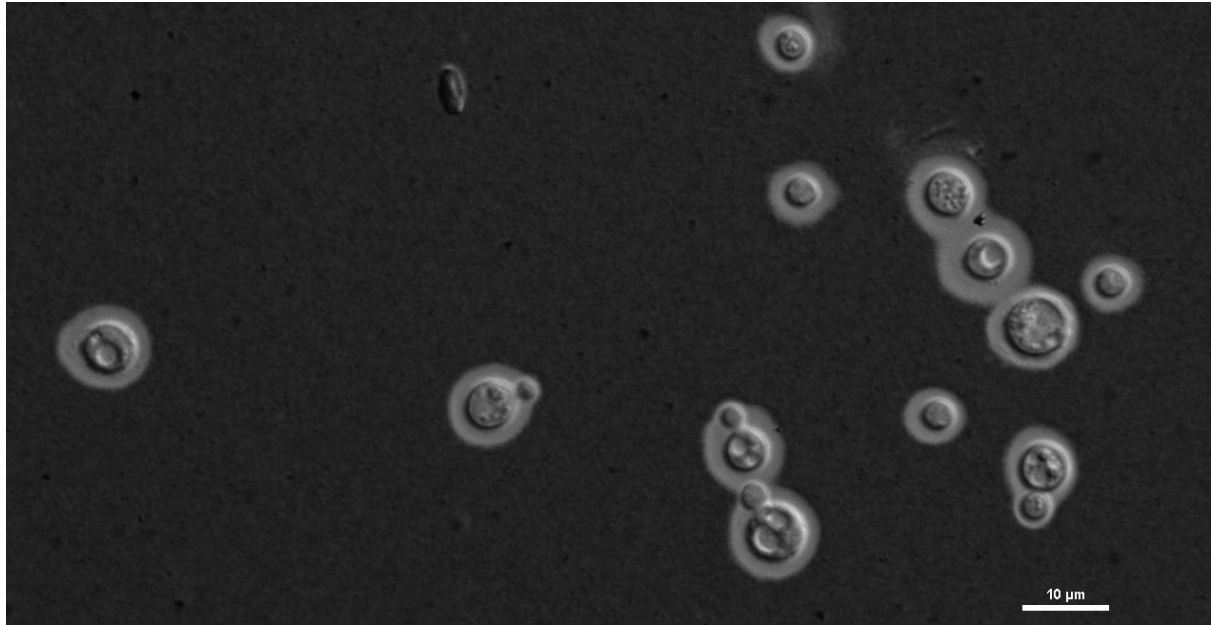
Figure 4 – India ink stain of *C. neoformans* var. grubii strain H99, India ink staining reveals the characteristic polysaccharide capsule surrounding *Cryptococcus* cells as a white halo.

5.2 Anti-phagocytic properties of the *Cryptococcus* capsule

Macrophages must detect the presence of foreign organisms before they can phagocytose them. To detect foreign organisms, macrophages express a number of phagocytic receptors on their cell surface; these receptors detect ligands that are found on foreign cells but not host cells. Phagocytic receptors are categorised according to the nature of their ligands. Non opsonic phagocytic receptors or 'pathogen recognition receptors' (PRRs) bind to 'pathogen associated molecular patterns' or PAMPs - such as polysaccharide residues or lipid species found on the surface of foreign cells. Meanwhile opsonic receptors bind to opsonising proteins, such as antibodies or complement proteins that coat foreign cells following activation of the humoral immune system. One of the main ways that the capsule protects *C. neoformans* against phagocytosis is by providing a shroud around the cell that interferes with macrophage detection. This shrouding effect blocks uptake via both opsonic and non-opsonic phagocytic receptors although it appears to have a greater inhibitory effect on non-opsonic uptake, since non-opsonised *C. neoformans* cells are almost completely protected from phagocytosis (Mukherjee et al., 1996).

Phagocytosis of yeast-like fungi that do not produce a polysaccharide capsule, such as *Candida albicans* and *Saccharomyces cerevisiae* has been found to occur via non-opsonic phagocytic receptors such as Dectin-1 and Mannose receptor (MR) (Brown and Gordon, 2001; Gantner et al., 2005; Giaimis et al., 1993; Porcaro et al., 2003). Both of these phagocytic receptors bind to cell wall constituents found in the cell wall of fungi ; Dectin-1 binds to β-1, 3 and β-1, 6 linked glucan residues (Brown and Gordon, 2003) while MR binds to mannoproteins (Mansour et al., 2006). Macrophages can easily phagocytose acapsular *C. neoformans* mutants via Dectin-1 or MR ligation but they struggle to

44

phagocytose encapsulated cells (Cross and Bancroft, 1995). In wild type capsular strains, the ligands for each receptor are obscured by the overlying capsule, thus it is thought that non-opsonic phagocytic receptors such as Dectin-1 and MR may contribute to the phagocytosis of recently inhaled cryptococcal cells (which have a minimal capsule), but once conditions within the host stimulate capsule growth non-opsonic uptake becomes redundant.

Opsonisation is more effective at facilitating the detection and phagocytosis of *C. neoformans* because opsonins bind to capsular components and thus are more accessible to macrophage phagocytic receptors than the non-opsonic receptor ligands. Two main classes of opsonic phagocytic receptors are expressed by macrophages: complement receptors, which recognise activated complement proteins deposited on the surface of foreign cells during infection, and Fc receptors, which recognise the Fc regions of immunoglobulin (antibody) molecules bound to specific antigens.

The complement cascade is an important component of the innate immune system. Complement proteins are found circulating in blood serum and also in tissues. Upon detection of infection, the complement cascade is activated. Activation of the complement cascade results in the sequential cleavage of complement proteins – the end products of the cascade opsonise foreign cells and trigger further inflammation; in some cases they can also induce apoptosis of foreign cells such as bacteria (Sarma and Ward, 2011).

Complement can be activated via three pathways – the classical pathway, the alternative pathway (these are different from macrophage classical and alternative activation pathways) and also the lectin pathway. Classical complement activation requires the presence of immunoglobulin – either IgM or IgG - bound to the surface of the foreign cell.

Alternative activation and lectin activation are triggered by PAMPs on the surface of foreign cells and as such do not require antigen specific immunoglobulin to be bound to the cell prior to activation. Regardless of activated route the end result of each cascade is the generation of complement protein fragments which are deposited on foreign cell surfaces. The fragments produced are C3b, C3a, C5a and C5bC6C7C8(C9)$_n$ - also known as the 'membrane attack complex' (MAC). C3b is opsonising protein that can be recognised by phagocytes, C3a and C5a are pro-inflammatory agents that can stimulate chemotaxis and activation of immune cells at the site of infection and the MAC is able to form pores in foreign cell membranes potentially leading to cell death (Sarma and Ward, 2011). Antibody produced during cryptococcal infection is thought to be ineffective at activating classical complement cascades (Houpt et al., 1994a) and thus the alternative complement and lectin cascades are likely more important during *C. neoformans* infection.

As previously mentioned, *C. neoformans* is phagocytosed poorly by macrophages unless cryptococci are opsonised (Mukherjee et al., 1996). In terms of phagocytosis of *C. neoformans* therefore, C3b is the most important product of the complement cascade as it is an opsonising protein. Furthermore it has been shown that C3 deficiency leads to increased susceptibility to *C. neoformans* infection (Diamond et al., 1973). Macrophages are able to recognise C3b via the phagocytic receptor 'complement receptor 3' (CR3) however there is evidence that the capsule can obscure C3b on *C. neoformans* cells. *Cryptococcus* cells that have thicker capsules (Zaragoza et al., 2003b) or a capsule that is less dense (Gates and Kozel, 2006) have increased protection against complement mediated phagocytosis by macrophages. By increasing the thickness of the capsule or by decreasing its density *C. neoformans* is able to reduce the efficacy of C3b opsonisation.

This is thought to be because a thicker, more permeable capsule is able to hide C3b below its surface thus obscuring C3b from recognition by CR3.

Host production of antibodies against newly encountered antigens requires activation of the adaptive immune response - secondary exposure to an antigen however evokes a quicker response due to the persistence of immunological memory. Antibody opsonisation improves the phagocytic uptake of foreign cells in two ways. Firstly they amplify complement opsonisation by activating the classical complement pathway (Sarma and Ward, 2011), secondly antibodies directly promote phagocytosis via ligation of macrophage Fc receptors which bind to the non variable region of antigen bound antibodies (Nimmerjahn and Ravetch, 2007).

In healthy individuals, anti-capsular GXM antibody titres are often used as markers of acquired immunity to *C. neoformans* (Deshaw and Pirofski, 1995a; Goldman et al., 2001; Houpt et al., 1994a). The protective role of anti GXM antibodies during infection however is debateable. For example a 1994 study by Houpt *et al.* found that the sera of healthy subjects contained IgG and IgM antibodies reactive against cryptococcal GXM, but that these antibodies were ineffective at activating the classical complement cascade (Houpt et al., 1994a). Interestingly antibodies which cannot bind to Fc receptors such as IgM have been found to be opsonic against *C. neoformans*. It is thought that the binding of these antibodies to the fungus results in alteration of the capsule (Taborda and Casadevall, 2002).

Another potential source of opsonins during pulmonary *Cryptococcus* infection is surfactant proteins. Surfactant proteins are a key component of lung surfactant – a protective mixture of lipids and proteins that lines the lungs. During pulmonary infection,

surfactant proteins bind to pathogens, clump them together and induce uptake by professional phagocytes. Studies that examine the interaction between *C. neoformans* and surfactant proteins have found that the binding of surfactant protein SP-D can enhance the uptake of *C. neoformans* by macrophages, however it was observed that the presence of capsule does effectively block this binding. In addition to this it was found that following phagocytosis SP-D protects *C. neoformans* from fungicidal conditions within the macrophage (Geunes-Boyer et al., 2009), this finding is in agreement with additional studies that have found that the presence of surfactant proteins facilitates *Cryptococcus* infection (Geunes-Boyer et al., 2012; Holmer et al., 2014).

5.3 Other capsule virulence mechanisms

During infection *C. neoformans* sheds capsule polysaccharide into the surrounding environment (Eng et al., 1986; Zaragoza et al., 2009). Shed capsule is called exopolysaccharide. Exopolysaccharide can be detected during infection in the extracellular space within infected tissues (Eng et al., 1986) but also intracellularly within macrophages (Tucker and Casadevall, 2002). Comparison of polysaccharide residues obtained from capsule associated and exopolysaccharide pools reveal structural differences, this suggests that exopolysaccharide may be produced specifically for secretion as opposed to simply diffusing out from the capsule (Frases et al., 2008).

During macrophage infection exopolysaccharide accumulates within the macrophage (Tucker and Casadevall, 2002), due both to accumulation from phagocytosed *Cryptococcus* cells and also from the direct engulfment of exopolysaccharide (Chang et al., 2006; Monari et al., 2003). This means that both infected and uninfected macrophages can become loaded with exopolysaccharide during *C. neoformans* infection. GXM has a

number of effects on macrophages and other host immune cells. Interactions with GXM can modulate macrophage expression of co-stimulatory molecules required for activation and also cytokine production (Monari et al., 2005a). Additionally GXM has been found to upregulate macrophage expression of FAS ligand (FasL) (Monari et al., 2005b; Villena et al., 2008) – a ligand via which macrophages can induce apoptosis of T cells (Monari et al., 2005b) as well as other macrophages (Villena et al., 2008) during *C. neoformans* infection.

5.4 Capsule independent antiphagocytic factors

C. neoformans also has capsule independent antiphagocytic mechanisms. A study by Liu *et al.* has identified a GATA family transcription factor called Gat201 that appears to control such a mechanism (Liu et al., 2008). Knockout of the *GAT201* gene affected the transcription of ~1,100 genes in *C. neoformans* although only 62 of these genes are thought to be regulated by direct binding of Gat201. Phenotypic analysis of the *GAT201* knockout strain showed reduced capsule size and increased uptake by macrophages. The susceptibility to phagocytosis observed was greater than that of acapsular mutants alone suggesting that capsule independent antiphagocytic mechanisms are also controlled by Gat201 potentially via two downstream genes – *BLP1* and *GAT204* (Chun et al., 2011). Another capsule independent antiphagocytic mechanism is the secreted protein App1. This protein is expressed by *C. neoformans* during infection. App1 reduces complement dependent phagocytosis by blocking macrophage CR3 receptors (Luberto et al., 2003).

5.5 Melanin production

Melanin is a dark coloured pigment that is produced by *C. neoformans* under certain growth conditions. *Cryptococcus* synthesis of melanin requires an external substrate

meaning that melanisation only occurs under growth conditions where a suitable phenolic or indolic precursor substrate is available (Casadevall et al., 2000). The synthesis of melanin by *C. neoformans* is catalysed by the cryptococcal enzyme laccase (Williamson et al., 1998).

Melanisation is another mechanism used by *C. neoformans* to promote virulence. Clinical *C. neoformans* isolates that produce high levels of melanin have been found to be more virulent than lower melanin producing strains (Huffnagle et al., 1995b) as well as melanin deficient mutants (Kwon-Chung and Rhodes, 1986; Kwon-Chung et al., 1982; Salas et al., 1996). Production of melanin has been shown to occur *in vivo* by a number of studies (Nosanchuk et al., 1998; Nosanchuk et al., 1999; Rosas et al., 2000). As previously mentioned, to produce melanin *C. neoformans* requires an external substrate. Interestingly the CNS contains a number of catecholamine molecules such as dopamine, and epinephrine which are produced by the host as neurotransmitters but are also ideal compounds for *C. neoformans* to produce melanin (melanisation of *C. neoformans* is often induced experimentally using growth media supplemented with $_L$-dopa (a catecholamine precursor), this may partly explain why *C. neoformans* has a preference for growth in the CNS following dissemination (Casadevall et al., 2000).

Melanin is known to have a number of different functions during host infection. Firstly it appears to be an immune modulator – it was observed that mice infected with high melanin producing strains produced lower levels of TNF- α during pulmonary infection and had lower levels of lymphocyte proliferation (Huffnagle et al., 1995b). Additionally one of melanin's properties is that it is an antioxidant and as such it has been observed that melanised *C. neoformans* are more resistant to free radical oxygen and nitrosative species

produced by immune cells such as macrophages and neutrophils during inflammation (Wang et al., 1995). Finally, because melanin is a negatively charged molecule, melanised cells are more repulsive towards other cells which usually have an inherent negative charge, thus melanisation may interfere with phagocytic cells while they are attempting to engulf *C. neoformans* (Casadevall et al., 2000).

It has been already been discussed that in a recent study by Sabiiti *et al.* it was found that *C. neoformans* isolates with higher laccase activity were more virulent clinically (Sabiiti et al., 2014). Although a correlation between laccase activity and clinical outcome was identified there was no correlation between melanisation and clinical outcome with the same strains. This suggests that laccase has virulence attributes that are independent of melanin production. In this respect laccase has also been linked to the production of immune modulatory eicosanoids by *C. neoformans* (Erb-Downward et al., 2008) and may also have a secondary role during CNS infection as the catecholamine molecules that laccase turns into melanin are also potentially toxic to the fungus (Casadevall et al., 2000).

5.6 Growth at mammalian body temperatures

C. neoformans is primarily an environmental organism and as such it grows well at ambient temperatures e.g. around 25°C or room temperature. This said the range of temperatures that *C. neoformans* can grow at is relatively broad, this is important as the ability to grow at 37°C makes *C. neoformans* a viable pathogen of humans and other mammals. Mammals are endothermic or 'warm blooded' animals; this means that they expend energy in order to warm themselves and maintain a constant body temperature. Ectothermic or 'cold blooded' animals on the other hand have an internal body temperature that is the same as their environment. Ectothermic animals are susceptible to colonisation

51

by environmental microorganisms such as fungi because their body temperature provides optimal growing conditions. By maintaining a body temperature above the ambient temperature of the environment, mammals preclude colonisation by many environmental microorganisms that could otherwise be potential pathogens.

A good demonstration of this paradigm is seen with Chytridiomycosis – a disease of amphibians caused by the fungus *Batrachochytrium dendrobatidis* that has in recent years caused the extinction of a number of frog species and threatens many more. Amphibians are ectothermic or 'cold blooded' and as a result their body temperature is roughly the same as the ambient temperature of their immediate environment. This makes frogs susceptible to infection by *B. dendrobatidis* which also grows well at ambient temperatures e.g. $17^{o}C$ to $25^{o}C$. Interestingly it has been found that infected frogs can be cured of Chytridiomycosis by raising their body temperature with a heat lamp to $30^{o}C$ - a temperature outside *B. dendrobatidis'* acceptable growth range (Chatfield and Richards-Zawacki, 2011).

It is noteworthy that out of the 50 plus *Cryptococcus* species in the *Cryptococcus* genus, *C. neoformans* and *C. gattii* are the only *Cryptococcus* species that regularly cause infection in humans – concurrently these two species are the only *Cryptococcus* species that are able to grow at human body temperature of $37^{o}C$. Additionally, rabbits have been observed to be more resistant to *C. neoformans* infection than many mammals. One of the reasons for this resistance could be because rabbits have a slightly higher body temperature, $\sim 39^{o}C$ (Perfect, 2006). These points highlight the importance of optimal and maximum temperatures of growth for a pathogen such as *C. neoformans* during infection.

A number of genes that help *C. neoformans* grow at mammalian body temperature have been identified. Many of these genes are involved in either metabolism or protein synthesis which presumably reflects the kinds of denaturing stress that above optimal temperatures can have on cells (Perfect, 2006). For instance, cryptococcal growth at high temperatures induces up regulation of the *TPS* and *TPS2* genes. Increased expression of these two genes leads to higher levels cellular levels of the polysaccharide trehalose which protects cellular proteins from denaturation (Petzold et al., 2006). Another *Cryptococcus* gene involved in temperature dependant growth is *CPA1* - this gene is required for growth by *C. neoformans* at the very top of its temperature range (39°C) however at 37°C the gene is dispensable, this indicates that there is a stratification in genes required for temperature growth (Wang et al., 2001).

5.7 Titan cell morphology

Several studies have reported the presence of abnormally large *Cryptococcus* cells in the lungs during *in vivo* infection (Cruickshank et al., 1973; Feldmesser et al., 2001; Love et al., 1985; Zaragoza et al., 2010), these 'giant' or 'Titan' cells appear to be resistant to phagocytosis (Okagaki et al., 2010). The diameter of Titan Cells differs between studies, with ranges from around 25 μm to 100 μm, making their volume up to 900 times greater than that of normal cryptococci (Zaragoza et al., 2010). The underlying mechanism or stimuli behind Titan Cell development is not known although the presence of macrophages, or at least spent media used to grow macrophages, can induce the morphology suggesting that interactions with the macrophage play at least some role in the process (Okagaki et al., 2010).

Titan Cells appear to be more resistant to phagocytosis than normally sized cells. The most obvious defence a Titan Cell has against a macrophage is its physical size. However recent work has suggested that the presence of Titan Cells during infection may also protect neighbouring wild type cells from phagocytosis, suggesting the presence of a secreted inhibitory factor (Okagaki et al., 2010; Okagaki and Nielsen, 2012). The presence of Titan cells during infection also appears to shift the host immune response from Th1 towards Th2, again the mechanism behind this observation is unknown but it could also be due to a secreted factor produced by Titan cells (Crabtree et al., 2012; Garcia-Barbazan et al., 2015).

5.8 Phospholipase B1

Phospholipase B1 (Plb1) is a phospholipid modifying enzyme with multiple enzymatic activities (Chen et al., 1997b). In cryptococcal cells a significant proportion of Plb1 enzymatic activity is cell wall associated, although secretion of Plb1 from *Cryptococcus* is known to occur *in vitro* (Wright et al., 2002). Plb1 is secreted following cleavage of a GPI anchor motif that anchors the enzyme to the cell wall (Djordjevic et al., 2005b; Siafakas et al., 2007) and export of Plb1 to the cell wall is facilitated by Sec14-1 – part of *C. neoformans'* protein export system (Chayakulkeeree et al., 2011). Plb1 has optimal activity in acidic conditions at around pH 4.0 to 5.0 (conditions similar to that of the phagosome) and is active at 37°C (Chen et al., 2000).

In line with this putative role in pathogenesis, deletion of *PLB1* strongly attenuates virulence in *C. neoformans* (Chayakulkeeree et al., 2011; Cox et al., 2001; Noverr et al., 2003a; Santangelo et al., 2004). Mice infected with a *PLB1* deletion *C. neoformans* strain (*Δplb1)* show reduced fungal burden in the lungs (Chayakulkeeree et al., 2011). In

addition, during murine infection Plb1 appears to be required for cryptococcal dissemination from the lungs into the blood stream (Santangelo et al., 2004), and additionally may be involved in translocation of cryptococcal cells across the blood brain barrier into the brain (Maruvada et al., 2012). Plb1 will be discussed with greater detail in the introduction to Chapter 2.

5.9 Evolution of *C. neoformans* virulence

Cryptococcus neoformans is primarily an environmental fungus that grows in the soil and rotting wood; it does not need to infect a host to complete its life cycle and has not evolved to do so. It is thought that the virulence factors that allow *C. neoformans* to infect the host evolved due to completely different evolutionary pressures. A widely accepted theory to explain this 'accidental virulence' (Casadevall and Pirofski, 2007) is that *C. neoformans'* virulence mechanisms were actually evolved as a result of a predator/prey relationship between the *C. neoformans* and soil amoeba. Within the soil there are species of amoeba that are quite similar to macrophages in that they ingest prey cells via phagocytosis and digest cells within a structure similar to the phagosome. Many of the mechanisms that allow *C. neoformans* to survive within macrophages also help the fungus avoid predation by amoeba such as *Acanthamoeba castellani* (Steenbergen et al., 2001).

Experimentally it has been shown that *Acanthamoeba castellani* is able to phagocytose and eat *C. neoformans* cells, additionally many aspects of the *Cryptococcus* / macrophage relationship – e.g. intracellular proliferation, exopolysaccharide accumulation and vomocytosis have been shown to also occur when *C. neoformans* is eaten by *A. castellani* (Chrisman et al., 2010; Steenbergen et al., 2001). Furthermore, virulence factors required by *C. neoformans* to cause macrophage infection such as Plb1 and the presence of the

polysaccharide capsule also help the fungus survive within *Acanthamoeba castellani* after it is eaten (Steenbergen et al., 2001; Steenbergen and Casadevall, 2003).

Conventionally evolved pathogens (i.e. pathogens that have specially evolved to cause infection such as the fungal pathogen *Pneumocystis jirovecii*) possess virulence factors that have evolved under selective pressure in their respective hosts. Evolutionary pressure means that these virulence factors usually benefit the pathogen and as a result are often detrimental to the host. Due to the fact that *C. neoformans* has not evolved as part of a host/pathogen relationship its virulence factors are often paradoxical in function.

An example of *C. neoformans'* paradoxical virulence during infection is its phagocytosis by host macrophages. During infection *C. neoformans* attempts to prevent phagocytosis by host macrophages, even though parasitism of macrophages can be beneficial to the fungus. In this respect it has already been discussed that unactivated macrophages during the early stages of infection are possibly detrimental to the host (Shao et al., 2005) due to the fact that *C. neoformans* cells are able to survive and grow within the phagosome (Feldmesser et al., 2000). If *C. neoformans* were a conventional pathogen one would posit that the fungus would have evolved a mechanism to actively induce uptake by macrophages rather than avoid it. Even though *C. neoformans* cells benefit from macrophage phagocytosis they actively attempt to avoid it by producing antiphagocytic defences such as the polysaccharide capsule (Mukherjee et al., 1996) and proteins such as APP1 (Luberto et al., 2003). In the context of a conventionally evolved host/pathogen relationship these two mechanisms are at odds, however when seen against the evolutionary context of a predator/prey relationship it begins to make more sense. As an environmental fungus, *Cryptococcus* has evolved mechanisms to avoid being eaten by soil dwelling amoeba

because being predated produces evolutionary pressure. Inevitably however in a predator/prey relationship the amoeba can also evolve to become more efficient at eating *Cryptococcus*, therefore as well as actively trying to avoid being eaten by the amoeba, *C. neoformans* also evolves mechanisms to survive within amoeba in the event that the initial anti phagocytic defences fail. Thus in the context of host infection it is not *C. neoformans'* 'intention' to infect macrophages but if it is phagocytosed it can employ survival mechanisms to cope with its situation.

A

Polysaccharide capsule

Cell wall

Budding daughter cell

Cytoplasm

Bud scar

B

Caspule
- Glucuronoxylomannan (GXM)
- Glucuronoxylomannogalactan (GXMGal)

Cell wall
- Mannoproteins
- β 1,6 Glucan
- β 1,3 Glucan
- Chitin
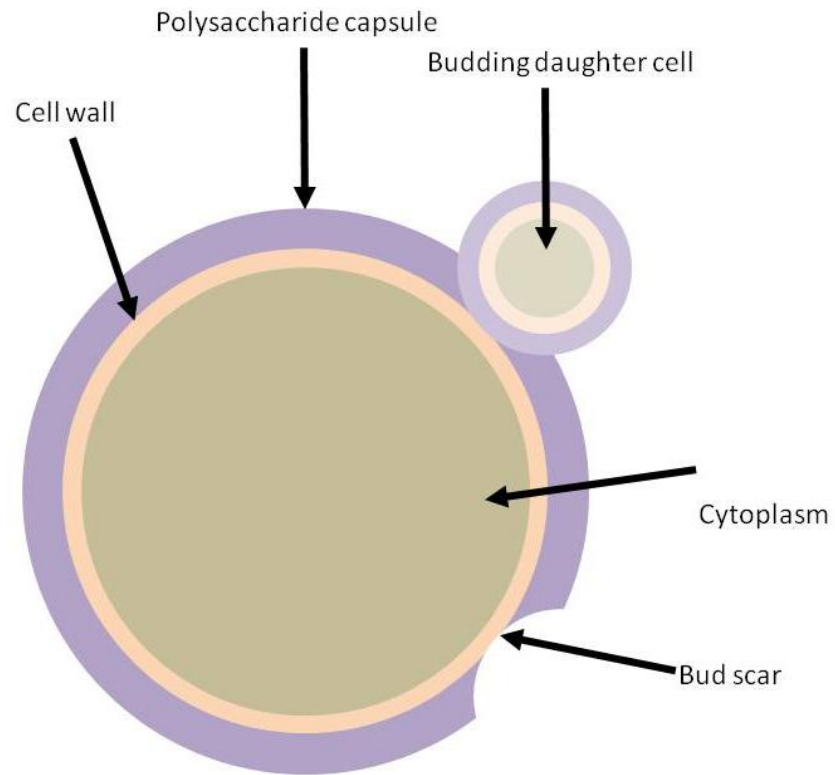
Figure 5

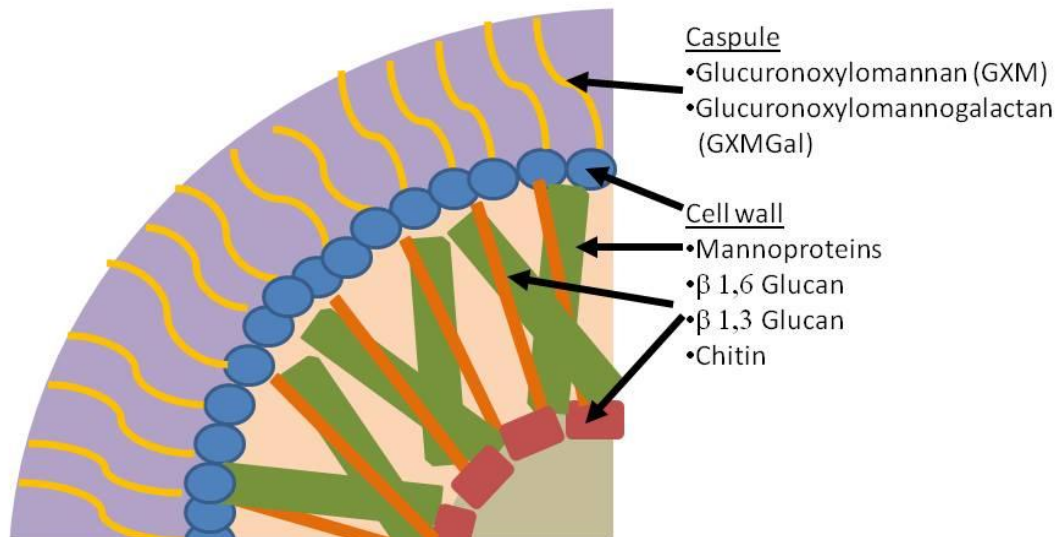**A.** Schematic showing the general structure of a *Cryptococcus* cells with the capsule and cell wall layer marked in addition to a budding daughter cell and a 'bud scar' – the impression left by a recently departed daughter cell. **B.** A zoomed in schematic showing the cryptococcal capsule and cell wall with the major constituents of each structure marked showing their relative position.

6. *Cryptococcus neoformans* / macrophage interactions

6.1 Survival within the phagosome

During macrophage infection *C. neoformans* is contained within the phagosome. In order to survive and proliferate within the phagosome *C. neoformans* must endure and/or subvert the fungicidal conditions generated during phagosomal maturation. Phagosomes that contain *C. neoformans* do mature (at least to some degree) meaning that the fungus must resist the deadly conditions within the phagosome. Increasingly, however, there is also evidence to suggest *C. neoformans* is able to attenuate the full extent of phagosome maturation.

C. neoformans uses a number of strategies to survive within the phagosome. The production of melanin by *C. neoformans* has been shown to protect the fungus against free radical oxygen species produced during the macrophage oxidative burst (Wang et al., 1995). In addition to melanin, capsule enlargement during macrophage infection may also be protective against oxygen free radicals as it creates a barrier between the cell body and phagosomal contents. Additionally GXM within the *Cryptococcus* capsule may act as an antioxidant (Feldmesser et al., 2000; Garcia-Rodas and Zaragoza, 2012; Monari et al., 2006; Vecchiarelli et al., 1996).

Although *C. neoformans* is resistant to fungicidal conditions within the phagosome it does also appear to manipulate phagosome maturation, in doing so it is likely that *C. neoformans* blunts the full killing effects of phagosome maturation. In this respect *C. neoformans* is able to increase the permeability of the phagosome membrane (Tucker and Casadevall, 2002); increased permeability would allow leakage of phagosome components

resulting in lower concentrations of digestive enzymes but also lower acidification due to proton leakage.

During phagosome maturation the activity of the V-ATPase proton pump increases the acidity of the phagosome; low acidic pH is damaging in itself to living organisms however the low pH also helps activate digestive enzymes contained within the phagosome. It is generally thought that *C. neoformans* does not hinder the acidification of the phagosome (Levitz et al., 1999a); however a recent study by Smith *et al.* has found evidence to the contrary – in this study Smith et al. found that acidification of the phagosome, as measured using LysoTracker Red pH dye, did not occur in ~ 90% of phagosomes containing live *C. neoformans* cells, when heat or UV killed *Cryptococcus* cells were used however acidification occurred in almost 100% of phagosomes. Due to the fact that *C. neoformans* does not inhibit V-ATPase activity the aforementioned increase in phagosomal permeability could be an explanation for the lack of acidification. Increased phagosome permeability (Tucker and Casadevall, 2002) would likely result in a leakage of H^+ protons from the phagosome and as a result a higher phagosomal pH. Paradoxically although *C. neoformans* may reduce phagosomal acidification during macrophage infection as it has been found that the phagosomal acidification may actually be beneficial to *C. neoformans,* since neutralising phagosomal pH can block intracellular replication (Levitz et al., 1999a). This discrepancy is probably another carry over from the predator/prey vs. host/pathogen evolution paradigm that was discussed in the previous section.

6.2 Replication within the phagosome

A number of studies have examined the correlation between *Cryptococcus* replication and overall virulence. For *C. gattii* a positive correlation can be observed between a strain's

ability to replicate within the macrophage and *in vivo* virulence (Ma et al., 2009). For *C. neoformans* the same correlation cannot be seen (Sabiiti et al., 2014). This difference may be due to the differences in pathogenesis between the two species. For *C. gattii,* disseminative infection is not as common as for *C. neoformans* – *C. gattii* stays within the lungs and death usually occurs from overwhelming pulmonary infection. With this in mind, intracellular proliferation of *C. gattii* within alveolar macrophages likely has a much greater impact on pathogenesis than *C. neoformans*. This is because the additional factor of *C. neoformans'* need to disseminate to the brain also determines to its virulence. Although intracellular proliferation might not have as direct an impact on *C. neoformans* virulence as it does with *C. gattii,* replication within macrophages is still an important survival mechanism prior to dissemination.

6.3 Escape from the macrophage

Proliferation within macrophages is beneficial to *C. neoformans* however escape from the macrophage and dissemination from the lungs determines the outcome of infection. As previously mentioned *C. neoformans* possesses a specialised macrophage escape mechanism termed vomocytosis (Ma et al., 2006), or non-lytic expulsion (Alvarez and Casadevall, 2006; Nicola et al., 2011). This mechanism may help *C. neoformans* disseminate to the CNS within infected macrophages via the 'Trojan Horse' route of dissemination.

Vomocytosis is a relatively rare macrophage interaction, it occurs in about 10% - 20% of macrophages *in vitro* (Ma et al., 2006). Vomocytosis rates *in vivo* are thought to be higher, although the methodology to measure vomocytosis *in vivo* is potentially not as definitive as *in vitro* methods (Nicola et al., 2011). Prior to vomocytosis the macrophage phagosome

has been found to permeablise (Johnston and May, 2010). During vomocytosis a *Cryptococcus* containing phagosome moves to the edge of the macrophage, the phagosome then fuses with the macrophage plasma membrane and the *Cryptococcus* cell is expelled.

Vomocytosis is sometimes termed non-lytic expulsion due to the observation that both the macrophage and *Cryptococcus* appear to remain viable following expulsion. This said there is some evidence to suggest that the process of vomocytosis may affect the macrophage – in this respect it has been reported that following vomocytosis many macrophages develop enlarged vesicles within the cytoplasm. The contents and purpose of these vesicles is unknown and as such it is not known whether they represent cellular stress or are themselves detrimental to macrophage physiology (Alvarez and Casadevall, 2007). Additionally the macrophage appears to detect and subsequently try to block vomocytosis from occurring (Johnston and May, 2010).

The cellular events driving vomocytosis are not fully understood. Interestingly, host cells appear to attempt to block vomocytosis by initiating repeated actin polymerisation / depolymerisation cycles (actin flashing) around the phagosome following permeabilisation (Johnston and May, 2010). Vomocytosis only occurs from phagosomes containing live yeast indicating that vomocytosis is at least in part yeast mediated (Ma et al., 2006; Smith et al., 2015b), additionally the secreted virulence factor Plb1 has been shown to be involved in the process (Chayakulkeeree et al., 2011).

A distinct but related cellular event to vomocytosis occurs during cryptococcal infection of macrophages, this event is called 'lateral transfer' (Alvarez and Casadevall, 2007; Ma et al., 2007). During lateral transfer a *Cryptococcus* cell is able to pass between two adjacent macrophages seemingly without leaving the intracellular compartment. Lateral transfer

occurs when two macrophages move together so that there is contact between plasma membranes – it is still not clear whether the coming together of two macrophages is an active process driven by the fungus or the host cell or whether lateral transfer only occurs when two macrophages stochastically touch. As with vomocytosis, lateral transfer was first described *in vitro* although it is also thought to occur *in vivo*. Its role during cryptococcal pathogenesis is also unclear. Speculatively it could be a way for macrophages unable to cope with intracellular infection to pass off their burden to surrounding cells that may be able to help. Alternatively, it is possible that *Cryptococcus* triggers the event for the opposite reason i.e. to escape from a macrophage that is beginning to kill it into one that might be more amenable to intracellular parasitism.

To summarise this section, the role of the macrophage during antifungal immune responses is of central importance (Figure 6). Not only is the macrophage responsible for detecting infection and shaping subsequent immune responses, it is also required to directly kill and clear fungal cells. The behaviour of the macrophage during *C. neoformans* infection is of even greater importance than most fungal infections because while the macrophage seeks to clear infection, the fungus itself relies on the macrophage as safe niche for intracellular proliferation and possibly as a vehicle for CNS dissemination. During macrophage infection *C. neoformans* employs a number of virulence factors that allow it survive and replicate within the macrophage and also to escape once intracellular parasitism no longer beneficial. Many of the virulence factors produced by *C. neoformans* seem perfectly adapted to survival in the host. This is at odds with the fact that *C. neoformans* evolved as an environmental pathogen, thus it is likely that many of these virulence mechanisms were

evolved by *C. neoformans* as a result of interactions between the fungus and soil dwelling

phagocytic amoeba.
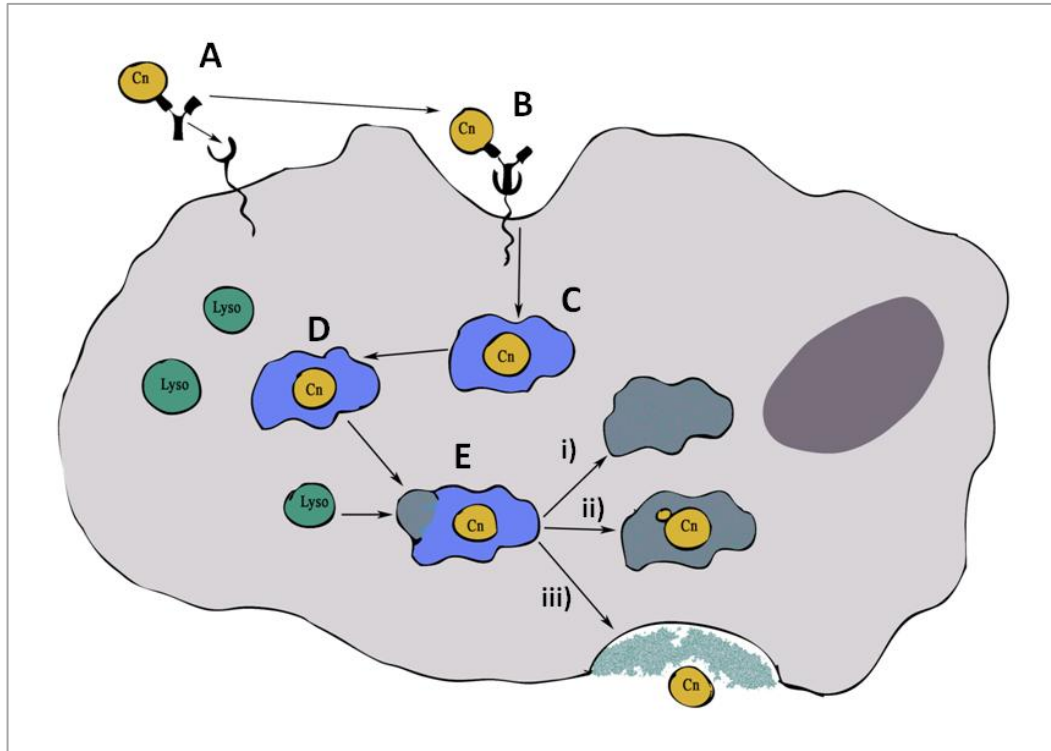
Figure 6.

The possible outcomes following *C. neoformans* infection of macrophages. **A.** Opsonised *C. neoformans* (in this case opsonised with antibody) binds to phagocytic receptors on the cell surface of the macrophage. **B.** Ligation of phagocytic receptors induces cytoskeletal rearrangements within the macrophage resulting in invagination of the membrane and the formation of phagocytic pseudopodia around the bound cell. **C.** *C. neoformans* is contained inside the macrophage within a membrane bound compartment called the phagosome. **D.** Overtime the phagosome matures, maturation begins with the recruitment of V-ATPase, NADPH oxidase and NOS to the phagosome membrane resulting in the lowering of pH and the production of reactive oxygen species within the phagosome. **E.** Phagosomal maturation culminates when lysosomes fuse with the phagosome, this releases digestive proteolytic enzymes into the phagosome (which is now termed the phagolysosome). There

are three possible outcomes for *C. neoformans* following formation of the phagolysosome i) fungicidal conditions within the phagosome destroy the fungus which is then digested. ii) *C. neoformans* resists the conditions within the phagolysosome and begins to replicate. iii) *C. neoformans* escapes from the macrophage via a process called vomocytosis - N.B. outcome iii) can happen after replication e.g. outcome ii).

7. Project summary

The following sections will detail the experimental work that I have undertaken during my PhD study. Each chapter discusses a different aspect of project, each chapter has been written as if it were a standalone publication e.g. introduction, materials and methods and discussion (albeit more in-depth). The chapters are as follows.

CHAPTER 2 - THE ROLE OF CRYPTOCOCCAL PHOSPHOLIPASE B1 DURING MACROPHAGE INFECTION

An abridged version of this chapter has already been published (Evans et al., 2015). This chapter deals with the main focus of my PhD research. In this chapter I explore how expression of the *C. neoformans* virulence factor Phospholipase B1 (Plb1) influences the outcome of macrophage infection. To do this I use a *C. neoformans* mutant strain deficient in Plb1 called *Δplb1* and characterise some of the phenotypes that arise during *in vitro* infection of J774 murine macrophages.

In this study I demonstrate that *Δplb1* deficiency results in lower replication of *C. neoformans* within macrophages, as well as increased susceptibility to macrophage killing and phagocytosis. I also a describe a novel morphological phenotype for *Δplb1* that develops during macrophage infection – this morphology appears to be closely related to Titan Cell morphologies but, in contrast to classical Titan morphology, occurs intracellularly. These findings suggest that Plb1 might have a previously unknown function in the control of the Titan Cell morphology.

CHAPTER 3 – THE ROLE OF EICOSANOIDS DURING CRYPTOCOCCAL INFECTION OF MACROPHAGES

This chapter continues from my published research (Evans et al., 2015), the research in this chapter is based upon a hypothesis that eicosanoids produced by *C. neoformans* influence the outcome of macrophage infection – potentially by mimicking and interfering with host eicosanoid signalling pathways.

This chapter details work I have conducted to this point to address this hypothesis. First I examine whether co-infected macrophages that contain *Δplb1* Plb1 deficient cells and wild type Plb1 producing H99 cells show any difference in phenotype to singly infection *Δplb1* cells, in order to test whether a secreted factor produced by the wild type cells can rescue Plb1 deficient cryptococci within the same cell. Next I attempt to reverse some of the phenotypic observations I have previously published (Evans et al., 2015) by adding exogenous eicosanoids or eicosanoids precursors to infected macrophages in culture.

CHAPTER 4 – DEVELOPMENT OF A HIGH THROUGHPUT FLOW CYTOMETRY METHOD FOR THE DETERMINATION OF *CRYPTOCOCCUS* INTRACELLULAR PROLIFERATION

This chapter represents research I have performed as part of a side project to develop a high throughput flow cytometry based protocol to accurately measure the intracellular proliferation of *C. neoformans* within *in vitro* cultured macrophages. The benefits of this protocol over other available protocols is that it does not require the use of antibody labelling or genetic modification of *C. neoformans*, instead it makes use of readily available cell staining reagents (Calcofluor white and propidium iodide) thus the protocol is quick and easy to perform. It is hoped that this protocol will open up the study of *C. neoformans* intracellular proliferation such that large gene knockout libraries and clinical isolate collections can be quickly and accurately examined.

This chapter details how the methodology was developed and also includes a proof of principle experiment using a selection of clinical isolates and comparing the flow cytometry results to the standard haemocytometer based method of counting.

CHAPTER 2 – THE ROLE OF CRYPTOCOCCAL PHOSPHOLIPASE B1 DURING MACROPHAGE INFECTION

Parts of this chapter have been adapted from work already published work. (Evans et al., Infection and Immunity 2015 Apr;83(4):1296-304. doi: 10.1128/IAI.03104-1).

The Titan cell data (Figure 7) was a result of collaboration with Kirsten Nielsen and Zhongming Li, Department of Microbiology, University of Minnesota, MN 55455, USA.

1. Introduction

During infection, *C. neoformans* produces a number of secreted enzymes that can influence pathogenesis; phospholipase B1 (Plb1) is one such enzyme (Cox et al., 2001). Plb1 is a lipid modifying enzyme that has multiple enzymatic activities; it is secreted by *C. neoformans* during growth and is known to be expressed during infection (Himmelreich et al., 2003; Santangelo et al., 2005). Plb1 is member of a family of phospholipase enzymes - phospholipase enzymes are found in some form in most eukaryotic cells; their function is to modify phospholipid molecules and their constituents. Generally, phospholipases cleave lipids but some variants of the enzyme (such as Plb1) have a number of complex enzymatic activities that allow them to both cleave and also form new phospholipid molecules (Djordjevic, 2010).

1.1 Phospholipase enzyme classification.

Phospholipids are an important group of lipids within living cells. All phospholipids share a similar structure – a glycerol backbone attached by ester linkages at one end to two fatty acid chains, and at the other, to a phosphate head group. The types of fatty acids and

phosphate head groups attached to the glycerol backbone determine each class of phospholipid. Phospholipids are major constituents of lipid bi-layers found in cell membranes; they are able to form these bi-layers due to their dual hydrophobic and hydrophilic properties in aqueous solution. In addition to forming cell membranes, phospholipids and their constituents have roles in cell signalling processes, cell growth and cellular metabolism (van Meer et al., 2008).

Phospholipases are grouped into a number of classes – A, B, C and D. Each class of phospholipase cleaves phospholipid molecules at a different location to produce different products. Phospholipase A_1 or A_2 activities hydrolyse the ester linkage between the fatty acid tail and the glycerol back bone of the phospholipid to produce a free fatty acid and a lysophospholipid (Figure 1). Phospholipase A_1 enzymes cleave at the Sn1 position while phospholipase A_2 enzymes cleave at the Sn1 position – phospholipase enzymes that cleave at either the Sn1 or Sn2 position are classed as phospholipase B enzymes. Phospholipase C enzymes cleave the phosphate head group from phospholipids producing diacylglycerol and a free phosphate head group while phospholipase D cleaves within the phosphate head group producing phosphatidic acid and a free head group in the form of an alcohol (Shea et al., 2006).
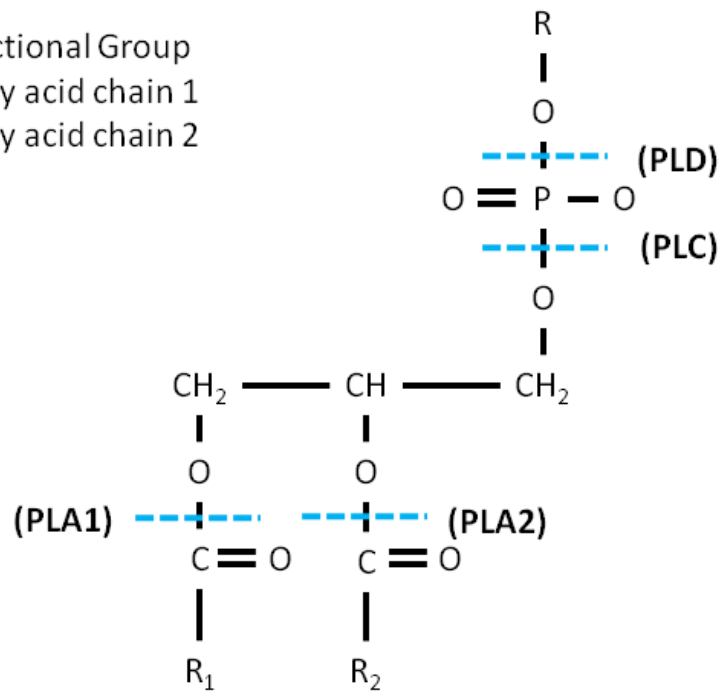
Figure 1 – A Diagram showing the cleavage sites for the enzymes Phospholipase A1 (PLA1), Phospholipase A2 (PLA2), Phospholipase C (PLC) and Phospholipase D (PLD) within the chemical structure of a phospholipid.
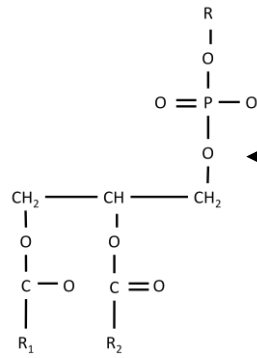
1.2 Cryptococcal phospholipase B1 (Plb1).

Plb1 is encoded by the gene *PLB1*. This gene is encoded on *C. neoformans*'s third largest chromosome as a single copy. The *PLB1* gene is 2218 base pairs long and contains six introns (Cox et al., 2001). Once expressed Plb1 is 637 amino acids in length; native Plb1 is about 75 kDa in size however the protein has a number of N-linked glycosylation sites that increase the size of the protein to 120 kDa (Chen et al., 2000; Turner et al., 2006). Plb1 has 17 predicted N-linked (Asn-X-Ser/Thr) (Chen et al., 2000) and 3 predicted O-linked (Ser-Thr) glycosylation sites (Latouche et al., 2002) in its amino acid sequence however it is possible that not all of these sites are utilised. Full Plb1 glycosylation is required for enzymatic activity (Chen et al., 2000) and also for secretion (Turner et al., 2006). Other key features of Plb1 include a 19 amino acid N-terminal leader peptide secretion motif that targets Plb1 for secretion from *Cryptococcus* and a 22 amino acid C-terminal glycosylphosphatidylinositol (GPI) anchor motif that anchors the Plb1 to the cryptococcal membrane prior to secretion (Djordjevic et al., 2005a). Deletion of these motifs leads to Plb1 hyposecretion and Plb1 hypersecretion respectively; these phenotypes indicate the role of each motif in regulating Plb1 secretion (Djordjevic et al., 2005b). Additionally Plb1 possesses lipase (GLSGGS) and phospholipase (AGGGXRAML) motifs (Latouche et al., 2002).

1.3 Plb1 enzymatic activities.

Plb1 is generally referred to in the literature by its generic name 'Phospholipase B1' (denoting its A_1 and A_2 activities); this name can be misleading because Plb1 has additional enzymatic activities not addressed by standard phospholipase nomenclature. In addition to phospholipase B (PLB) activity, Plb1 also has lysophospholipase (LPL) and

lysophospholipase transacetylase (LPTA) activities (Figure 2). These additional enzymatic activities allow Plb1 to degrade and also remodel phospholipids. LPL activity allows Plb1 to hydrolyse lysophospholipid species produced by prior PLB activity to form a phosphoglycerol species and a free fatty acid. This is achieved by hydrolysing the remaining fatty acid chain from the lysophospholipid. LPTA activity meanwhile takes the lysophospholipid produced by prior PLB activity and reattaches a free fatty acid at either the Sn1 or Sn2 position forming a complete phospholipid (Djordjevic, 2010).

(Phospholipid)

R
$|$
O
$|$
$O = P - O$
$|$

CH_2 — CH — CH_2
$|$ $|$
O O
$|$ $|$
$C - O$ $C = O$
$|$ $|$
R_1 R_2

PLB Activity

(Lysophospholipid)

R
$|$
O
$|$
$O = P - O$
$|$
O
$|$
CH_2 — CH — CH_2
O O
$|$
$C = O$
$|$
R_2

OR

R
$|$
O
$|$
$O = P - O$
$|$
O
$|$
CH_2 — CH — CH_2
O O
$|$
$C - O$
$|$
R_1
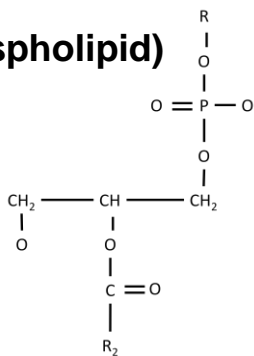
LPTA Activity

LPL Activity

(Glycerophospholipid)

R
$|$
O
$|$
$O = P - O$
$|$
O
$|$
CH_2 — CH — CH_2
$|$ $|$
O O
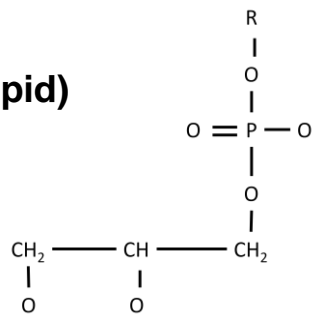
Figure 2 -

Schematic diagram showing the different enzymatic actions of Plb1. Phospholipid molecules are broken down by the enzyme's phospholipase B (PLB) activity producing a free fatty acid and a lysophospholipid. The lysophospholipids produced by PLB activity can be further degraded by the enzyme's lysophospholipase (LPL) activity to give a glycerophospholipid and a second free fatty acid. Finally, Plb1's lysophospholipase transactylase (LPTA) activity can produce new phospholipid molecules by combining intermediate lysophospholipid species and free fatty acids.

Initially it was believed that *C. neoformans* produced three separate enzymes with PLB, LPL or LPTA activities (Santangelo et al., 1999). It was soon discovered however that a single enzyme, Plb1, possessed all three activities (Chen et al., 2000). Interestingly all three Plb1 enzymatic activities are facilitated by a single active site. Knockout of three key amino acids – Arg108, Ser146 and Asp392 - within this active site has been shown to abrogate all three enzymatic activities simultaneously (Jones et al., 2007). All three Plb1 activities have optimal activity at acidic pHs – PLB activity has an optimal pH of 4.0 while LPL and LPTA activities have an optimal pH range of 4.0 – 5.0 (Chen et al., 2000). As each enzymatic activity has a different set of optimal conditions, the relative dominance of each activity changes depending on the physiological location of Plb1 within the *Cryptococcus* cell. In this respect it has been shown that PLB activity dominates when Plb1 is secreted while LPL and LPTA activities dominate cytosolically and when the enzyme is cell wall/membrane associated (Ganendren et al., 2004).

The substrate specificity of Plb1 is broad; its preferred substrates are Dipalmitoylphosphatidylcholine (DPPC) and 1, 2-Dioleoyl-sn-glycero-3-phosphocholine (DOPC) however it can also hydrolyse many other phospholipid species found in cell membranes such as Phosphatidylinositol (PI), Phosphoglyceride (PG) and Phosphatidylserine (PS). It has been found that Plb1's PLB activity cannot hydrolyse Phosphatidic acid (PA), Sphingomyelin (SPH), Trioleoylglycerol or Palmitoylcarnitine (Chen et al., 2000). Analysis of Plb1's LPL activity has found that 1-Palmitoyl lyso-PC and 1-Oleoyl lyso-PC are the preferred substrates and that Lyso-PI, 1-Palmitoyl lyso-PE while 1-Palmitoyl lyso-PS can also be hydrolysed.

1.4 Phospholipase B1 enzymes from other species of fungi.

Many species of fungi – both pathogenic and non-pathogenic – produce enzymes similar to Plb1. Non pathogenic fungi that produce similar enzymes include *Saccharomyces cerevisiae* (Lee et al., 1994)*, Penicillium notatum* (Sugatani et al., 1978) and *Schizosaccharomyces pombe* (Oishi et al., 1996). Pathogenic species that produce enzymes similar to Plb1 include *Candida albicans* (Leidich et al., 1998; Sugiyama et al., 1999)*, Aspergillus fumigatus* (Shen et al., 2004) and *Cryptococcus gattii* (Latouche et al., 2002; Wright et al., 2004). Phospholipase B enzymes from non-pathogenic fungi and pathogenic fungi differ in a number of ways. Phospholipase B enzymes from pathogenic fungi have between 10 and 100 times greater PLB activity than non pathogenic species, additionally the substrate preferences of the pathogenic phospholipase B enzymes include lipids such as DPPC which are found in host lung surfactant. This suggests that these pathogenic phospholipase B enzymes are capable of attacking host lipids in the periphery. Non-pathogenic phospholipase B enzymes meanwhile prefer lipids more commonly found on the inner leaflet of cell membranes suggesting a role in fungal homeostasis (Djordjevic, 2010).

As mentioned, *C. neoformans* and the more virulent *Cryptococcus* species *Cryptococcus gattii* both produce very similar Phospholipase B1 enzymes (91.7% peptide sequence homology) (Latouche et al., 2002). Interestingly the ratio of PLB to LPL activity for *C. gattii* derived phospholipase B1 is higher than that seen with *C. neoformans* derived phospholipase B1. Additionally, the substrate specificity of *C. gattii* phospholipase B1 is much narrower than *C. neoformans* phospholipase B1. For *C. gattii* phospholipase B1, the only substrates hydrolysed in significant amounts by the enzyme's PLB and LPL activities

are DPPC and 1-palmitoyl lyso-PC respectively. The higher PLB: LPL ratio observed for *C. gattii* phospholipase B1 and its preference for lipids found in lung surfactant may, at least in part, explain why *C. gattii* infection typically involves more pulmonary activity and less disseminative disease than *C. neoformans* infection (Wright et al., 2004).

1.5 Plb1 secretion.

Following translation, Plb1 moves into the endoplasmic reticulum where it is glycosylated. Plb1 is then exported from the endoplasmic reticulum to the cryptococcal cell surface where it is secreted (Djordjevic, 2010). Transport of Plb1 to the cryptococcal cell surface is dependent on the protein Sec14. *C. neoformans* has two Sec14 homologs – Sec14-1 and Sec14-2. Sec14-1 (and to a lesser extent Sec14-2) facilitates the export of Plb1 to the cryptococcal cell wall before secretion. A *C. neoformans* mutant deficient in Sec14-1 (*Δsec14-1*) still expresses Plb1 however cell wall associated, and secreted, activity of Plb1 is almost completely abrogated (Chayakulkeeree et al., 2011). At the *Cryptococcus* cell surface, Plb1 localises to the cell membrane and also to the fungal cell wall. Plb1's C-terminal GPI anchor motif allows it to anchor to the *Cryptococcus* cell membrane where it appears to concentrate in lipid rafts (Siafakas et al., 2006). In the cell wall meanwhile Plb1 is thought to crosslink with β-1, 6-glucan moieties (Djordjevic, 2010). Secretion of Plb1 occurs when the GPI anchor is cleaved by proteases, phospholipases (C and D) or glucanases. It has been observed that the majority (>85%) of phospholipase B activity in *C. neoformans* is associated with the cellular fraction of *C. neoformans* - as opposed to supernatant (Santangelo et al., 1999). Interestingly however experiments with the *Δsec14-1* mutants indicate that many of the virulence mechanisms facilitated by Plb1 are dependent on secreted enzymatic activity (Chayakulkeeree et al., 2011).

1.6 Evidence that Plb1 is a virulence factor during host infection.

Plb1 was first identified as a cryptococcal virulence factor by Chen et al. in 1997. Chen *et al.* assessed the relative phospholipase activity of fifty *C. neoformans* isolates from both environmental and clinical sources. Once they had identified strains with high, medium and low phospholipase activities they infected a representation selection of isolates into BALB/c mice and identified a correlation between high phospholipase activity and increased fungal virulence (Chen et al., 1997a). In 2001 a *PLB1* deletion mutant (*Δplb1)* was produced by Cox *et al.* in the *C. neoformans* H99 genetic background. Cox *et al.* found that that mice infected with this mutant had a significantly increased time of survival compared to those with wild type infection, while in a rabbit meningitis model *Δplb1* had poorer survival in CSF (Cox et al., 2001). A subsequent study using a similar mouse pulmonary infection model found that the poor virulence of *Δplb1* is linked to both reduced fungal burden in the lungs and also reduced dissemination to the CNS (Chayakulkeeree et al., 2011).

Reduced fungal burden in the lungs during host infection may occur because *Δplb1* cannot grow properly within host macrophages. In this respect it has been reported that the *Δplb1* mutant has a number of growth and survival deficiencies in a variety of experimental macrophage infection models (Cox et al., 2001; Noverr et al., 2003a; Wright et al., 2007). It has also been observed that *Δplb1* mutant cells have reduced cell wall and cell membrane stability leading to increased susceptibility to the membrane stressor SDS (Chayakulkeeree et al., 2011; Siafakas et al., 2007). This decreased stress resistance may explain why *Δplb1* does not grow well within the macrophage phagosome. In addition to decreased stress resistance it has been observed that Plb1 helps *C. neoformans* to acquire, metabolise and

detoxify host lipids during macrophage infection. In this respect Wright *et al*. have shown that *C. neoformans* cells can scavenge host derived fatty acids such as arachidonic acid via a Plb1 dependant process, during *in vitro* infection of THP1 macrophages. In this same study it was found that *C. neoformans* could metabolise host associated lipids such as DPPC and DOPC as an alternative energy source if glucose was omitted from growth media − importantly this metabolism was also Plb1 dependant. Finally, *Δplb1 C. neoformans* cells were found to be unable to detoxify the lipid LysoPC (a lipid species derived from DPPC metabolism that can be toxic to eukaryotic cells) under glucose poor conditions. Interestingly both wild type and *Δplb1* cells could cope with LysoPC when glucose was added to the growth media. Wright *et al.* concluded that Plb1 LPTA activity provides a glucose independent way to detoxify LysoPC to PC under low energy poor conditions, however in the presence of glucose Plb1 is made redundant by the ATP dependant Coenzyme A pathway that can also detoxify LysoPC (Djordjevic, 2010; Wright et al., 2007).

As well as promoting fungal lung burden, it has been observed that Plb1 also helps to facilitate the dissemination of *C. neoformans* from the lungs to the CNS (Chayakulkeeree et al., 2011; Cox et al., 2001; Santangelo et al., 2004). In this respect it has been observed that during *in vivo* mouse infection, Plb1 is required for dissemination from the lungs into the bloodstream but not for dissemination from the blood into the CNS (Santangelo et al., 2004). To disseminate from the lungs *C. neoformans* presumably needs to interact with lung epithelial cells in order to either to trigger translocation or to damage the epithelial layer sufficiently to breach it. As previously discussed one of the preferred substrates of Plb1 is Dipalmitoylphosphatidylcholine (DPPC), a key constituent of lung surfactant that

coats and protects that lung epithelium (Chen et al., 2000). Additionally it has also been observed that the *Δplb1* strain adheres to lung epithelial cells poorly *in vitro* suggesting that Plb1 may help *C. neoformans* bind to lung epithelium prior to dissemination (Ganendren et al., 2006).

In vivo data suggests that Plb1 facilitates dissemination from the lungs into the bloodstream but not from the blood stream into the CNS (Santangelo et al., 2004); this said *in vitro* data has been published that implicates Plb1 in various aspects of CNS dissemination. For instance it has been reported that *C. neoformans* facilitates translocation across human endothelial cell monolayers via the activation of Rac1 (Maruvada et al., 2012). Additionally it has been found that *Δplb1* cells have a lower rate of vomocytosis from macrophages (Chayakulkeeree et al., 2011) *in vitro* which could hinder dissemination to the CNS via the 'Trojan Horse' mechanism.

In addition to Plb1 which has PLB, LPL and LPTA enzymatic activities, *C. neoformans* and *C. gattii* also produce lysophospholipase enzymes that have just LPL and LPTA activities. It has been suggested that these lysophospholipase enzymes may contribute a significant proportion of the LPL and LPTA activities observed during fungal growth. Analysis of the purified *C. gattii* enzyme indicates that the optimum pH range of LPL and LPTA activities is pH 7.0, much higher than the corresponding acidic optimal pH for LPL and LPTA activities from Plb1 (Coe et al., 2003).

To summarise, Plb1 is a virulence factor required by *C. neoformans* during host infection. It has been observed that the Plb1 deficient *C. neoformans* mutant strain *Δplb1* has attenuated virulence during *in vivo infection* (Cox et al., 2001). During infection this strain displays lower fungal burden in the lungs (Chayakulkeeree et al., 2011), and reduced

dissemination to the CNS (Chayakulkeeree et al., 2011; Cox et al., 2001; Santangelo et al., 2004). A number of studies have also reported that *Δplb1* may be attenuated within macrophages, therefore it is possible that Plb1 mediated virulence during *in vivo* infection may be due to Plb1 influencing the outcome of macrophage intracellular parasitism (Cox et al., 2001; Noverr et al., 2003a; Wright et al., 2007).

The main aim of my PhD research was to explore how expression of Plb1 contributes to the outcome of the interaction between *C. neoformans* and the macrophage. To do this I used the previously constructed *Δplb1* strain (Cox et al., 2001) *w*hich is deficient in Plb1 and examined how deficiency of this protein changed the well characterised interaction between *C. neoformans* and *in vitro* murine macrophage J774 cell line. In this chapter I will detail my findings. Herein I report that Plb1 is critical for both proliferation and survival within J774 macrophages. In addition, I show that the *Δplb1* strain responds to macrophage infection by significantly increasing both capsular thickness and overall cell size within the phagosome and in the murine lung. This novel morphology is reminiscent of, and closely related to, the previously published titan cell morphology (Crabtree et al., 2012; Okagaki et al., 2010; Zaragoza et al., 2010). This interesting finds and suggests that control of cryptococcal Titan cell morphology during by Plb1 may play a vital role in the outcome of host macrophage infection.

2. Materials and methods

2.1 Ethics statement

A total of fourteen mice were handled in strict accordance with good animal practice, as defined by the relevant national and/or local animal welfare bodies. All animal work was approved by the University of Minnesota Institutional Animal Care and Use Committee (IACUC) under protocol no. 1308A30852.

2.2 Strains, media and cell lines

Strains used in this work are listed in the Appendix (Appendix Table 1, page 188). Strains were stored long-term in MicroBank vials at -80°C. Strains were rescued onto YPD agar (YPD 50 g/L Sigma Aldrich, 2 % Agar – Melford) for 48 hours at 25°C and then stored until needed at 4°C. Before experimentation, liquid cultures were grown from these stock plates in 2 ml YPD growth medium (50 g/L) for 24 hours at 25°C under constant rotation.

The J774 murine macrophage cell line was used for all *in vitro* infection assays. Cells were passaged in DMEM culture media with serum (Dulbecco's Modified Eagle medium, low glucose, Sigma Aldrich, 10 % FBS - Invitrogen, 1% 10,000 units Penicillin / 10 mg streptomycin – Sigma Aldrich, 1 % 200 mM L – glutamine – Sigma Aldrich). Assays were performed with J774 cells between passages 4 and 15. Assays were performed in serum-free DMEM (DMEM high glucose, 1% P/S, 1% L-glutamine) unless otherwise stated.

2.3 Intracellular proliferation assay

The Intracellular proliferation assay was performed as previously described (Ma et al., 2009). Briefly, 24 hours before infection, 1×10^5 J774 macrophages were seeded into 24

well plastic plates (Greiner Bio One Cell Star) in 1 ml culture media with serum and incubated for 24 hours at 37°C 5% CO_2. Before infection, J774 cells were activated with 150 ng/ml phorbol 12-myristate 13-acetate in DMSO (PMA) Sigma), in 1 ml serum free culture medium for 45 minutes. This media was then replaced with serum-free media alone. Simultaneously, overnight *C. neoformans* cultures grown at 25°C in YPD were washed three times in sterile 1x PBS, counted and adjusted to 1 x10^{7} cells per ml in PBS before opsonisation for 1 hour with 10 µg/ml anti capsular 18B7 antibody (a kind gift from Arturo Casadevall, Albert Einstein College of Medicine, New York USA). The activated J774 cells were then infected with 100 µl opsonised *C. neoformans* to give an MOI of 10 (e.g. 1x10^{5} J774 / 1x10^{6} *C. neoformans*) in un-supplemented serum-free DMEM (e.g. no PMA) and incubated for 2 hours at 37°C 5% CO_2. After two hours (time point 0) infected wells were washed at least 3 times with warm 1x PBS until all non-phagocytosed *C. neoformans* cells were removed from the wells.

For calculation of the intracellular proliferation rate the number of internal cryptococci was counted at time points 0, 18 and 24 (t.p. 0 + 18 hr, + 24 hr respectively). At each time point each well to be counted was washed three times with 1x PBS to remove any extracellular yeast. The macrophages in the well were then lysed in 200 µl deionised water (dH_2O) for 30 minutes. To remove lysed macrophages and cryptococci a pipette tip was used to scrape the surface of the well, the 200 µl of lysate was then removed to a clean Eppendorf and a further 200 µl dH_2O added to the well to wash any remaining cells, this 200 µl was also added to the Eppendorf to give a final sample volume of 400 µl.

C. neoformans cells in the lysate were quantified at each time point with a cell counting chamber and the intracellular proliferation rate (IPR) calculated by dividing the count at

which intracellular burden peaked by the count at time point 0. Viability testing of the recovered cells was achieved by diluting the lysate to give a concentration of 200 yeast cells per 100 μl, and then plated onto YPD agar at $25^{\circ}C$ for 48 hours prior to counting colony forming units.

2.4 Phagocytosis assay

24 hours before assaying, J774 macrophages were seeded onto 13 mm glass cover slips (nitric acid treated) inside 2 cm^2 24 well plates at a concentration of $1x10^5$ cells per ml in 1ml DMEM culture media with serum and incubated at $37^{\circ}C$ and 5% CO_2. Activation and infection of the macrophages with opsonised *C. neoformans* cells followed the same protocol as described above for the intracellular proliferation assay. After a 2-hour incubation the cells were washed 3 times with 1x PBS to remove un-phagocytosed cells and then fixed for 10 minutes with 250 μl 4% paraformaldehyde in PBS at $37^{\circ}C$. Following fixation, coverslips were washed with 1x PBS and sterile deionised water and mounted on glass slides using Mowiol mountant (100 mM Tris-HCl, pH 8.5, 9% Mowiol, 25% glycerol). Mounted coverslips were analysed on a Nikon Ti – S inverted microscope fitted with a plan APO 60x1.40 DIC oil immersion objective.

2.5 Cell size assay

J774 cells were plated into 24 well plates, activated and infected with opsonised *C. neoformans* strains as described above for the IPR assay. Two hours post infection each well was washed at least 3 times with warm 1x PBS until all non-phagocytosed *C. neoformans* cells were removed from the wells, 1 ml serum free DMEM media was then added to each well.

The 24-well plate was placed into an environmentally controlled stage (Okolabs) set to 37°C, 5 % CO_2. The cells were imaged using a Nikon TE2000 microscope fitted with a Digital Sight DS-Qi1MC camera and a Plan APO Ph1 20 x dry objective. Images were recorded every 4 minutes for 20 hours. Image acquisition and analysis was performed using the Nikon NIS Elements software package (Nikon).

Cell size was measured using the ellipse area tool, measuring from the centre of each *Cryptococcus* cell to edge, to obtain the diameter of each cell.

2.6 *In vivo* titan cell and phagocytosis assay

**The Titan cell experiments (Figure 8) were kindly performed by Kirsten Nielsen and Zhongming Li, Department of Microbiology, University of Minnesota, MN 55455, USA. **

Cryptococcus neoformans cells were grown in YPD broth overnight. Cells were pelleted and resuspended in sterile phosphate-buffered saline (PBS) at a concentration of 1×10^7 cells/ml based on haemocytometer count. Groups of 6- to 8-week-old female A/J mice (Jackson Laboratory, Bar Harbor, ME) were anesthetized by intraperitoneal pentobarbital injection. Four to five mice per treatment were infected intranasally with 5×10^5 cells in 50 µl PBS. At 3 days post-infection, mice were sacrificed by CO_2 inhalation. Lungs were lavaged with 1.5 ml sterile PBS three times using an 18.5-gauge needle placed in the trachea. Cells in the lavage fluid were pelleted and fixed in 3.7% formaldehyde at room temperature for 30 min. Cells were washed once with PBS, and >500 cells per animal were analyzed for size by microscopy (AxioImager, Carl Zeiss, Inc.). Cell body sizes were measured with cells classified as small cells (<15µm in cell body diameter) or titan cells (>15 µm in cell body diameter).

2.7 Titan cell flow cytometry

H99 was cultured in YPD broth overnight. Cells were pelleted, washed three times in PBS and fixed in 3% paraformaldehyde at room temperature for 10 min. Bronchoalveolar lavage (BAL) samples were washed once in 0.05% sodium dodecyl sulfate (SDS) to lyse mammalian cells and then washed three times in sterile water. Cells were pelleted and fixed in 3% paraformaldehyde at room temperature for 10 min. Following fixation, samples were washed with PBS, stained with 0.5 µg/ml Hoechst (Sigma, St. Louis, MO) at room temperature for 10 min, washed again with PBS and then resuspended in PBS. Approximately 10,000 cells were examined for cell size by forward scatter (FSC) and for DNA content by Hoechst staining using an LSRII flow cytometer with FACSDiva software (BD Biosciences, San Jose, CA). Graphs were generated using Flowjo software (Tree Star, Inc., Ashland, OR). T-test was used to analyze the differences in titan cell formation and phagocytosis, and P-values of < 0.05 were considered significant.

2.8 Cell stress

Overnight *C. neoformans* cultures in 2 ml YPD were grown at 25°C. Cultures were diluted 1:1000 into 500 µl buffered YPD (pH 7.0, 15mM HEPES) in plastic bottomed 48 well plates (Greiner) with the following concentrations of SDS: 0, 0.01, 0.05, 0.1, 0.25, 0.5 mM, H_2O_2:0, 0.125, 0.25, 0.5, 1, 3, 6, 14 mM or NaCl: 0, 125, 250, 500, 1000 mM. The plate was then sealed with a breathable membrane (Breath Easy®, Sigma Aldrich) and growth curve assays performed for 24 hours at 30°C in a Fluostar Omega plate reader using a custom script that took 600 nm absorbance readings from the bottom of the plate every 30 minutes. Between reads the plate was shaken at 200 RPM with a linear shaking pattern.

2.9 Statistics

Figure 3:

Figure 3A, infection rate data was analysed using Chi-square on the raw count (.e.g. total uninfected macrophages vs. total infected macrophages), three pair wise tests were made comparing H99 to *Δplb1*, *Δplb1* to *Δplb1:PLB1* and *Δplb1* to *Δplb1:PLB1*. Bonferroni correction was used to correct for multiple comparions. * p ≤ 0.05, ** p ≤ 0.01, *** p ≤ 0.001 and **** p ≤ 0.0001. The corrected α value was 0.017.

Figure 3B, Phagocytic uptake data determined to be normally distributed using the Shaprio-Wilk normality test (p-value < 0.05 reject null hypothesis that data is not normally distributed) (See appendix Table 2, page 188). Unpaired two tailed T tests were performed, comparing each strain to the H99 wild type. Bonferroni correction was used to correct for multiple comparions. * p ≤ 0.05, ** p ≤ 0.01, *** p ≤ 0.001 and **** p ≤ 0.0001. The corrected α value was 0.025

Figure 4:

4A - Intracellular proliferation rate (IPR) data was determined to be normally distributed using the Shaprio-Wilk normality test (p-value < 0.05 reject null hypothesis that data is not normally distributed) (See appendix Table 3, page 189). Unpaired two tailed T tests were performed, comparing each strain to the H99 wild type. Bonferroni correction was used to correct for multiple comparisons. * p ≤ 0.05, ** p ≤ 0.01, *** p ≤ 0.001 and **** p ≤ 0.0001. The corrected α value was 0.0125.

4B - CFU viability data was determined to be normally distributed using the Shaprio-Wilk normality test (p-value < 0.05 reject null hypothesis that data is not normally distributed) (See appendix Table 4, page 187). A two way ANOVA with Tukey post test was used to compare 0hr, 18hr and 24hr time points for each strain. P values under 0.05 were taken to be statistically significant * p ≤ 0.05, ** p ≤ 0.01, *** p ≤ 0.001 and **** p ≤ 0.0001.

4 C-E - Phagocytic uptake data (4C i, 4D i and 4E i) was determined to be normally distributed using the Shaprio-Wilk normality test (p-value < 0.05 reject null hypothesis that data is not normally distributed) (See appendix table 2, page 188). Unpaired two tailed T tests were performed, comparing each strain to the H99 wild type. Bonferroni correction was used to correct for multiple comparions. * p ≤ 0.05, ** p ≤ 0.01, *** p ≤ 0.001 and **** p ≤ 0.0001. The corrected α value was 0.025. Intracellular proliferation rate (IPR) data (Figures 4C ii, 4D ii and 4E ii), was determined to be normally distributed using the Shaprio-Wilk normality test (p-value < 0.05 reject null hypothesis that data is not normally distributed) (See appendix table 3, page 189). Unpaired two tailed T tests were performed, comparing each strain to the H99 wild type. Bonferroni correction was used to correct for multiple comparisons. * p ≤ 0.05, ** p ≤ 0.01, *** p ≤ 0.001 and **** p ≤ 0.0001. The corrected α value was 0.025.

Figure 6:

6 A-D - Cell size measurement data (A-D) was found to be not normally distributed using the Shapiro-Wilk normality test (p-value < 0.05 reject null hypothesis that data is not normally distributed) (See appendix tables 5 to 12, page 190 to 192). Comparison between time points was made using a Mann Whitney U test (e.g. StrainX 0 hour vs. StrainX 18

hour). A p-value below 0.05 was taken as significant. * p ≤ 0.05, ** p ≤ 0.01, *** p ≤ 0.001 and **** p ≤ 0.0001.

Figure 8:

A. i) – iii) Data is displayed as % however statistical analysis was performed on raw count data, three pair wise chi-squared tests were made comparing H99 to *Δplb1*, *Δplb1* to *Δplb1:PLB1* and *Δplb1* to *Δplb1:PLB1*. Bonferroni correction was used to correct for multiple comparisons (3). The corrected α value was 0.017. **** H99 vs. *Δplb1* p = >0.0001. ** H99 vs. *Δplb1:PLB1 p = 0.0014 **** Δplb1 vs. Δplb1:PLB1 p = >0.0001*.

3. Results

3.1 Plb1 deficiency leads to increased uptake of *C. neoformans* cells by J774 macrophages

I first assessed to what extent the *PLB1* knockout strain, *Δplb1*, was phagocytosed by macrophages in comparison to the wild type parent H99 strain and a genetic reconstitution strain *Δplb1:PLB1*. I found that following two hours of infection, the percentage of J774 murine macrophages with at least one internalised *C. neoformans* cell was significantly greater for *Δplb1* compared to H99 or *Δplb1:PLB1* (Figure 3. A). Quantification of the fungal burden per macrophage also revealed a two-fold increase in the number of *Δplb1* cells phagocytosed per host cell (Figure 3. B). This suggests that Plb1 activity contributes significantly to the well-known antiphagocytic phenotype of *C. neoformans*.
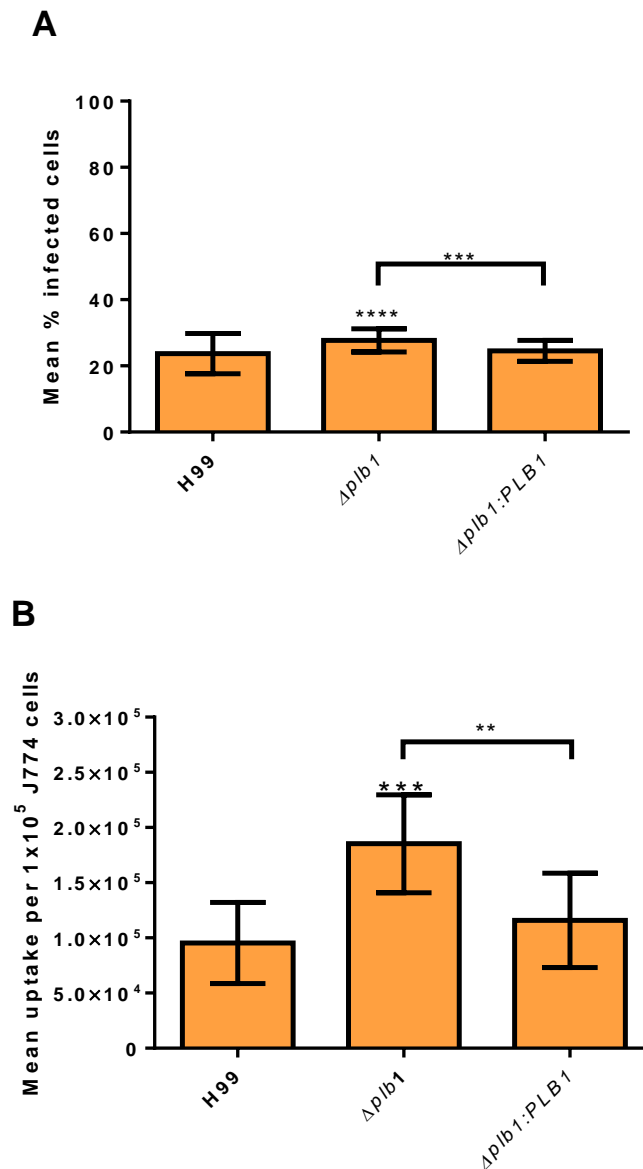
A

B

Figure 3 A. Analysis of phagocytic uptake of *C. neoformans* strains by J774 macrophages - Percentage of macrophages within a population that show *C. neoformans* infection following 2 hours incubation with opsonised cryptococci at a MOI of 1:10. N= 4, a minimum of 500 macrophages were counted for each condition. (Data displayed as % however statistical analysis was performed on infection rate data was analysed using the raw count (.e.g. total uninfected macrophages vs. total infected macrophages), three pair

94

wise chi-squared tests were made comparing H99 to *Δplb1*, *Δplb1* to *Δplb1:PLB1* and *Δplb1* to *Δplb1:PLB1*. Bonferroni correction was used to correct for multiple comparisons (3). The corrected α value was 0.017. **** H99 vs. *Δplb1 p = 0.00004,* *** *Δplb1 vs. Δplb1:PLB1* p = 0.005) **B.** Total burden of infection within a fixed population of J774 cells ($1x10^5$) following 2 hours incubation with opsonised cryptococci at a MOI of 1:10. N=9. *** H99 vs. *Δplb1* p = 0.0003. ** *Δplb1 vs. Δplb1:PLB1* p = 0.0038 (Unpaired two tailed T test performed comparing each strain, α corrected for multiple comparisons (3) using Bonferroni correction. Corrected α = 0.017).

3.2 Plb1 is required for intracellular proliferation of *C. neoformans* within J774 macrophages

PLB1 knockout leads to reduced fungal lung burden during murine infection; in addition it abrogates dissemination to the brain (Chayakulkeeree et al., 2011; Maruvada et al., 2012) and reduces the budding of *Cryptococcus* cells within macrophages (Cox et al., 2001). To investigate this phenotype further I performed an intracellular proliferation rate (IPR) assay. I observed an intracellular proliferation defect for the *Δplb1* strain vs. wild type H99 (IPR=*1.12,* versus *2.42* for *H99.* p = 0.023*),* a defect that was fully restored in the *Δplb1:PLB1* reconstitute strain (Figure 4. A). Interestingly, no intracellular proliferation defect was observed when I tested the *Δsec14-1* strain (Figure 4. A). Since Sec14-1 is required for efficient secretion of Plb1 (Chayakulkeeree et al., 2011), it appears that intracellular, but not secreted, Plb1 is important for proliferation within host cells.

Due to the increased efficiency of *Δplb1* uptake observed, I wondered whether the reduced proliferation I saw for *Δplb1* simply reflected initial overcrowding within the host macrophage as this phenotype has been described previously (Alanio et al., 2011). To test this, I reduced the uptake of *Δplb1* by omitting the opsonisation step before infection. Infecting with unopsonised *Cryptococcus* reduced uptake for all three strains (Figure 4. E - i) – un-opsonised *Cryptococcus* can still be phagocytosed by macrophages but at a lower rate (Guerra et al., 2014; Ma , 2009). Omitting opsonisation did not alter the growth defect observed (Figure 4. E - ii). To test a different type of opsonisation I also tried opsonising with pooled serum instead of antibody. At the concentration used (5% pooled human serum) I did not see significant differences in uptake, as compared to antibody opsonisation (Figure 4. C - i), and the proliferation defect remained (Figure 4. C - ii).

Taken together, these data suggest that Plb1 plays a direct role in regulating intracellular proliferation in *C. neoformans* regardless of the fungal intracellular burden.
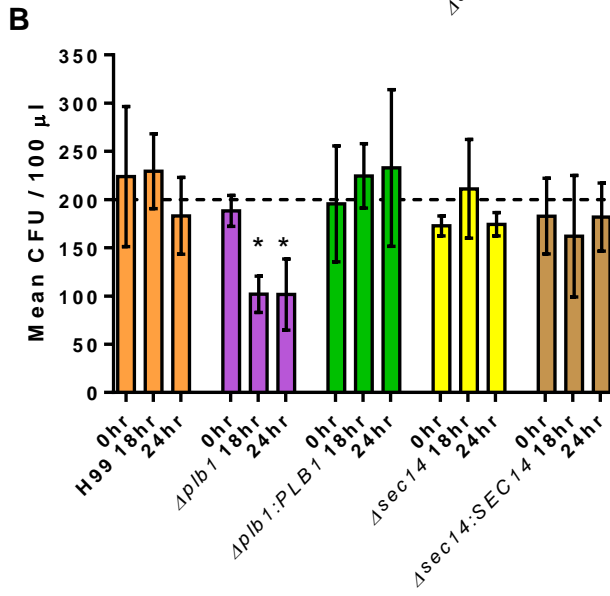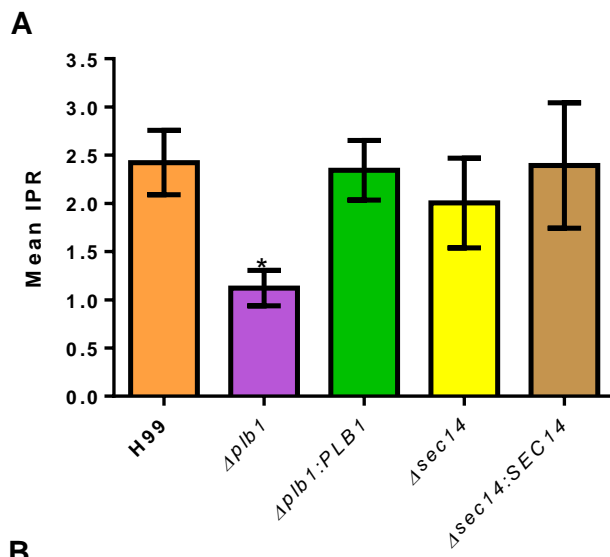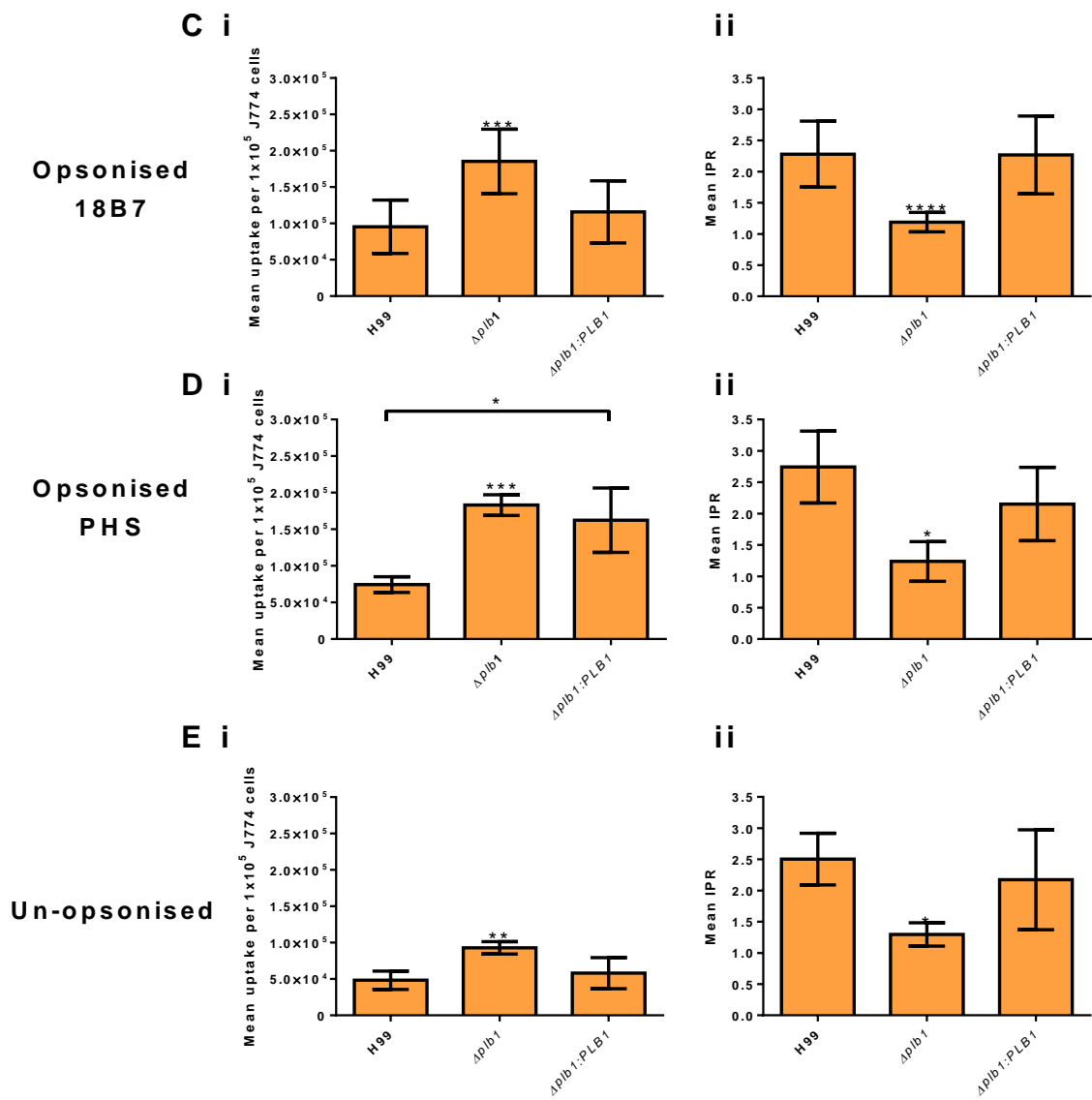
Figure 4 – Analysis of intracellular proliferation and viability of *C. neoformans* within J774 macrophages. A. Mean IPR for each *C. neoformans* strain within murine J774 macrophages. N = 3. * H99 vs. *Δplb1* p= 0.004, (Two tailed unpaired T tests used, each strain was compared to H99 wild type, knockouts strains were also compared to reconstitute strains α corrected for multiple comparisons (6) using Bonferroni correction. Corrected α = 0.008). **B.** Viability of *C. neoformans* cells recovered from J774 macrophages following IPR assay. Cells recovered following macrophage lysis were counted and diluted to give an expected plated inoculum of 200 cells. N = 4. * *Δplb1 0hr* vs. *Δplb1 18hr* p= 0.0422, *Δplb1 0hr* vs. *Δplb1 24hr* p= 0.0415 *(*Two-way ANOVA + Tukey post test comparing time points for each strain). Note –Figure 4 **C** - i is reproduced from Figure 3 B; it has been reproduced for ease of comparison. **C. - i** Total burden of infection within a fixed population of J774 cells ($1x10^5$) following 2 hours incubation with anti-capsule antibody (18B7) opsonised cryptococci at a MOI of 1:10. N=9. *** H99 vs. *Δplb1* p = 0.0003 (Two tailed unpaired T test, each strain compared, α corrected for multiple comparisons (3) using Bonferroni correction. Corrected α = 0.017*).* **C. - ii** Mean IPR for anti-capsule antibody (18B7) opsonised H99, *Δplb1 and Δplb1:PLB1* within murine J774 macrophages. N= 8. **** H99 vs. *Δplb1* p = <0.0001 (Two tailed unpaired T test, each strain compared, α corrected for multiple comparisons (3) using Bonferroni correction. Corrected α = 0.017). **D. - i** Total burden of infection within a fixed population of J774 cells ($1x10^5$) following 2 hours incubation with pooled human serum opsonised cryptococci at a MOI of 1:10. N = 3. *** H99 vs. *Δplb1* p = 0.0004,* *H99 vs. Δplb1:PLB1* p = 0.028 (Two tailed unpaired T test, each strain compared, α corrected for multiple comparisons (3) using Bonferroni correction. Corrected α = 0.025*)* **D. - ii** Mean

intracellular proliferation rate for pooled human serum opsonised H99, *Δplb1 and*

Δplb1:PLB1 within murine J774 macrophages. N= 3. H99 vs. *Δplb1* p = 0.016 (Two tailed

unpaired T test, each strain compared, α corrected for multiple comparisons (3) using

Bonferroni correction. Corrected α = 0.017). **E. - i** Total burden of infection within a fixed

population of J774 cells ($1x10^5$) following 2 hours incubation with unopsonised

cryptococci at a MOI of 1:10. N=3. ** H99 vs. *Δplb1* p = 0.0073 (Two tailed unpaired T

test, each strain compared, α corrected for multiple comparisons (3) using Bonferroni

correction. Corrected α = 0.017). **E. - ii** Mean intracellular proliferation rate for

unopsonised H99, *Δplb1* and *Δplb1:PLB1* within murine J774 macrophages. N=3. * H99

vs. *Δplb1 p= 0.010* (Two tailed unpaired T test, each strain compared, α corrected for

multiple comparisons (3) using Bonferroni correction. Corrected α = 0.017*).*

3.3 Plb1 contributes to *C. neoformans* cell survival during infection

The low intracellular proliferation defect observed for *Δplb1* could be due to slower *Cryptococcus* proliferation and/or increased intracellular killing by the macrophage. To address the second possibility, I plated *C. neoformans* cells recovered from macrophages at 18 and 24 hours post infection on YPD agar to enumerate CFU. No significant difference in CFUs among any of the five strains was seen at time point 0 (2 hours post infection) however at time point 18 (20 hours post-infection) the viability of *Δplb1*, but not *Δsec14-1*, had dropped significantly (Figure 4. B) compared to H99. Taken together these data suggest that both growth and survival of *Δplb1* is impaired within the phagosome during macrophage infection.

3.4 Plb1 deficiency does not significantly affect cryptococcal stress responses

I hypothesised that low IPR in the macrophage may be a result of stressful conditions during macrophage infection – possibly because *Δplb1* is unable to control or resist cellular stresses within the macrophage. I tested this hypothesis using three stress factors that may be found within the phagosome – SDS (membrane attack), NaCl (osmotic stress) and hydrogen peroxide (H_2O_2 – reactive oxygen species). I found a noticeable defect in the *Δplb1* mutant ability to grow when challenged with SDS; this defect has been previously published (Chayakulkeeree et al., 2011). In addition to SDS susceptibility I also found that *Δplb1* also appears to have a growth defect at high (1000 mM) concentrations of NaCl (Figure 5).
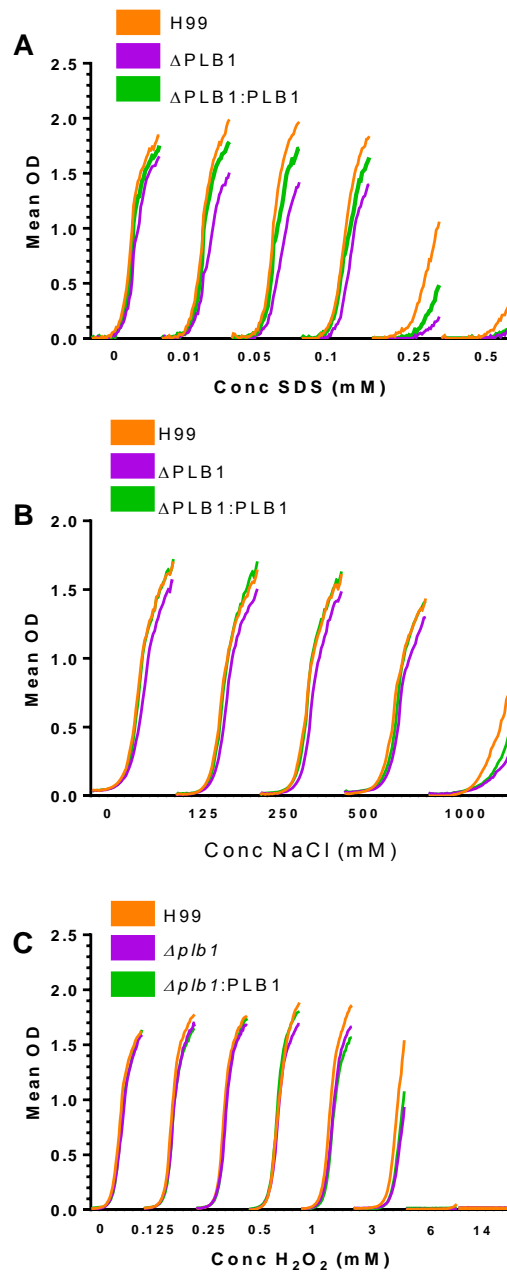
Figure 5: Growth curve testing of *C. neoformans* strains to stresses similar to those found in the macrophage phagosome. Overlaid growth curves with increasing concentrations of stress factors which partly mimic stresses in the phagosome – **A** SDS (membrane attack), **B** NaCl (Osmotic stress) and **C** H_2O_2 (Reactive oxygen species). n = 3

**3.5 PLB1 knockout leads to changes in cryptococcal cell body morphology**

During the course of this work I noticed that some *Δplb1* cells showed a marked increase in cell body diameter within infected macrophages, a morphology that was not observed for H99 or *Δplb1:PLB1* (Figure 6. E-F). Quantification of this phenomenon (Figure 6.) showed that the diameter of the cell body and capsule thickness of *Δplb1* cells increased significantly during an 18 hour macrophage infection (Figure 6. A-E). Interestingly, I observed a significant decrease in cell diameter for H99 and *Δplb1:PLB1* over the same incubation period (Appendix tables 13 and 14 pages 193 and 194 respectively), this is probably due to active cell budding occurring within the macrophage, leading to a drop in mean diameter for the overall population. Extending the period of live cell imaging to 48 hrs I found that the enlarged *Δplb1* cells did not noticeably increase in size after 18 hours post infection.

Changes in *Cryptococcus* cell size during *in vivo* infection have been previously documented, ultimately resulting in the production of very large titan cells (Crabtree et al., 2012; Feldmesser et al., 2001; Zaragoza et al., 2010). To my knowledge, though, this is the first published observation of a similar (albeit less dramatic) process occurring within a macrophage (rather than extracellulary) and the first time that Plb1 has been implicated in this pathway. Previous studies have reported that the size increase observed in titan cells is accompanied by increased nuclear content due to polyploidy (Okagaki et al., 2010; Zaragoza et al., 2010). In agreement with this, flow cytometry analysis of *Δplb1* cells following macrophage infection revealed a population of cells (Figure 7A Q3) that are either polyploidy or likely on the verge of ploidy (Figure 7).
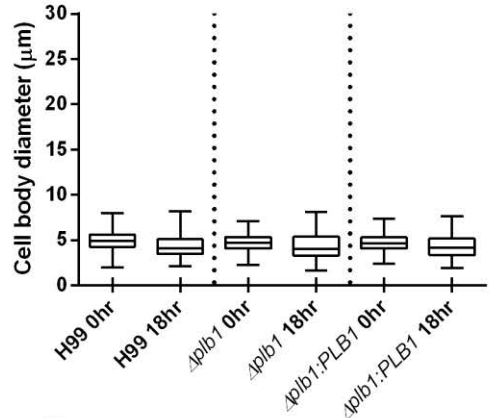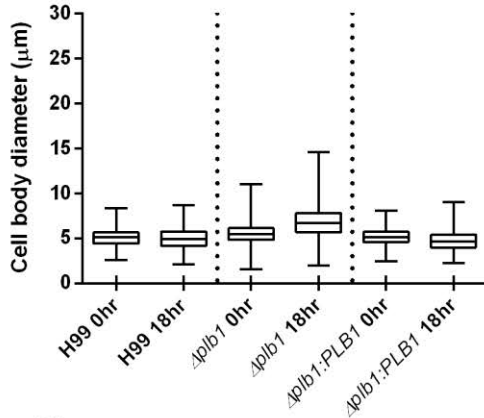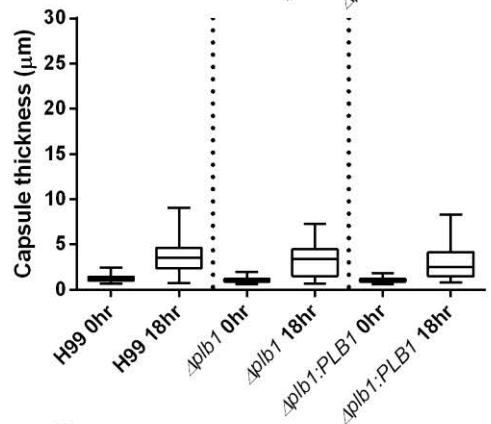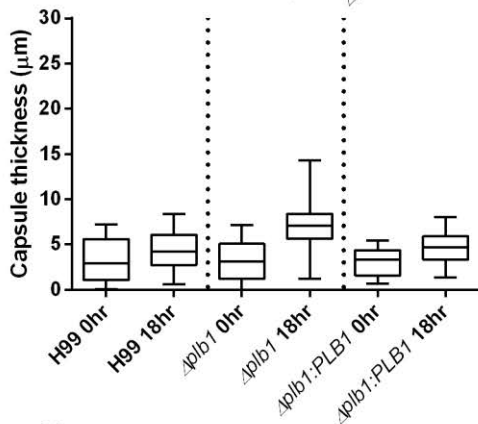
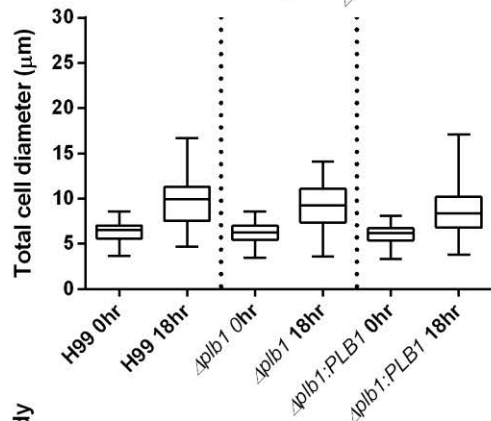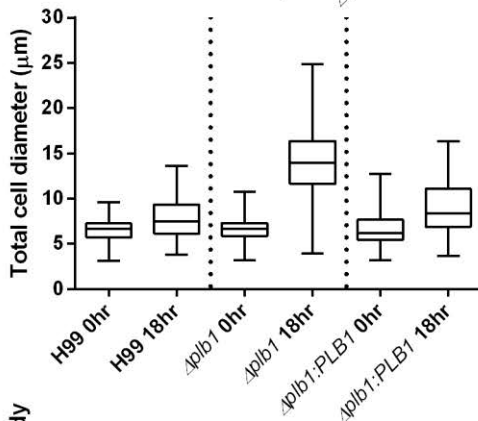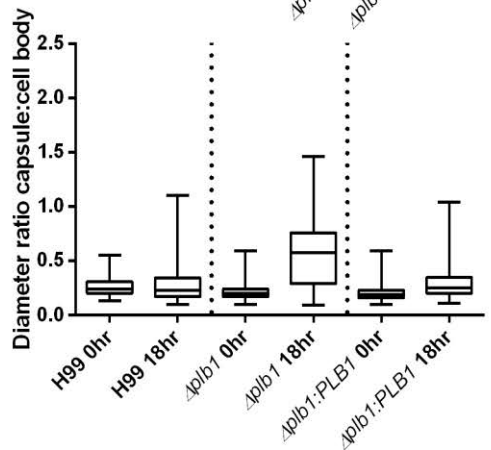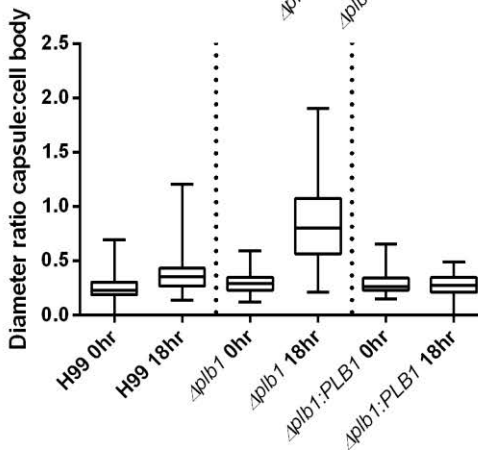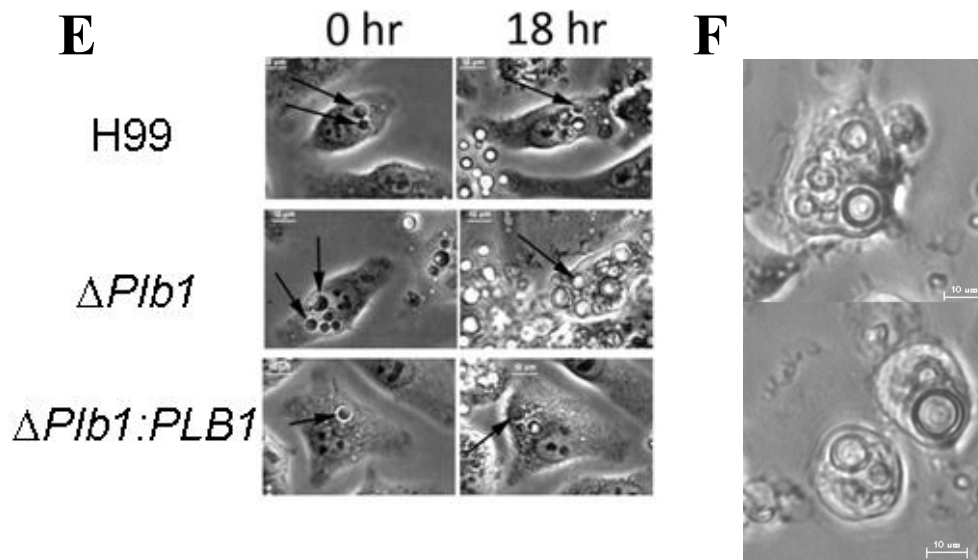**Figure 6. Analysis of the change in cell body size and capsule thickness of *C. neoformans* strains during the course of J774 macrophage infection. A-D** Dimensions of *C. neoformans* cells were measured after either 18 hours inside J774 macrophages or 18 hours in serum free DMEM media **B.** Capsule thickness was calculated by subtracting cell body diameter from total diameter including capsule. **D** The ratio of cell body to capsule was calculated by dividing cell body diameter by capsule thickness. **A-D** The top and bottom of the box mark the 75th and 25th percentiles respectively, the bisecting line in the box marks the median and the two whiskers mark the maximum and minimum range. Mann Whitney U tests were performed on each time point pair. Full statistical results are given in supplementary table 13 and 14 (see appendix, tables 13 and 14 pages 193 and 194 respectively). **E** Still bright field images from live cell microscopy following the same macrophage over 18 hours for H99, *Δplb1* and *Δplb1:PLB1*. Black arrows indicate the location of single *C. neoformans* cells within the macrophage. **F** Still bright field images from live cell microscopy following viable *Δplb1* infected macrophages – images taken at 40 hours post infection, scale bar = 10 μm.

3.6 *Δplb1* cells have a higher rate of titan cell formation *than wild type during in vivo murine infection*

The Titan cell data (Figure 8) was the result of collaboration with Kirsten Nielsen and Zhongming Li, Department of Microbiology, University of Minnesota, MN 55455, USA.

My *in vitro* observation of *Δ*plb1 cell enlargement was reminiscent of the titan cell morphology observed during *in vivo* murine pulmonary infection (Feldmesser et al., 2001; Okagaki et al., 2010; Zaragoza et al., 2010). To test whether this phenotype was recapitulated *in vivo*, pulmonary infections were conducted in mice and then cryptococcal cell body diameter was quantified for following bronchoalveolar lavage (BAL) at 3 days post infection. As with my *in vitro* data, *in vivo* infection with *Δplb1* produced about 2.5 times more titan cells (cryptococci with a cell body diameter greater than 15 μm) than H99 or *Δplb1:PLB1* (Figure 8 Ai). Flow cytometry of lavaged, Hoechst stained *Δplb1* titan cells indicate that there is a large population of cell which are either polyploidy, or on their way to becoming polyploidy. This in agreement with previously published characterisation of titan cells (Okagaki et al., 2010; Zaragoza et al., 2010) as well as my *in vitro* observation of *Δplb1* cells (Figure 8 A). Taken together these findings suggest the morphological changes I observed during *in vitro* macrophage infection with *Δplb1* are consistent with an increase in the production of titan cells by this strain *in vivo*.
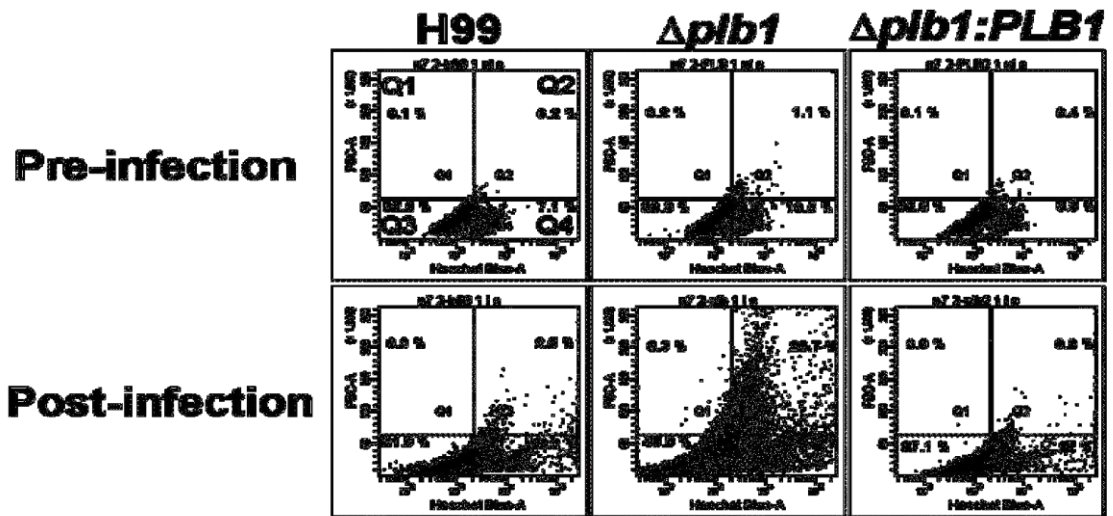
Figure 7 – Flow cytometry analysis of *C. neoformans* samples pre and post incubation with J774 macrophages (18 hours). Samples were stained with Hoechst to quantify DNA content, FSC-A (forward scatter area) indicates relative cell size across the samples. Cells were gated based on size and nuclear content with cells in Q3 consistent with small cells in G1, Q4 indicative of small cells in G2, and Q2 indicative of polyploidy titan cells with both large size and increased DNA content.

3.7 *In vivo Δ*plb1 Titan cell formation is not associated with phagocytosed cells.

In addition to quantifying overall Titan cell formation in BAL samples, the number of *Cryptococcus* cells within host phagocytes following BAL was also counted, as well as the cell body diameter of each *Cryptococcus* within each lavaged host cell.

Counting revealed there were significantly fewer lavaged host cells containing *Cryptococcus* for *Δplb1* infected mice compared to H99 or *Δplb1:PLB1* (Figure 8 A. - ii). Very few of these internalised *Cryptococcus* cells were above 10 μm in diameter and those that were above 10 μm could be found in similar numbers for H99, *Δplb1* and *Δplb1:PLB1* (Figure 8 A. - iii). No cells greater than 15 μm were found inside phagocytes in either the control or *Δplb1* infections (data not shown). This leads me to conclude that *in vivo Δplb1* Titan cell formation potentially occurs initially within host cells (as observed *in vitro)* but these large *Cryptococcus* are released from host cells either by host cell lysis *in vivo* or due to the physical process of lavage prior to the time point examined.

A i

ii

iii

B

H99 (YPD)   H99 (*In vivo*)   ▲*plb1* (*In vivo*)

C

H99   ΔPlb1   ΔPlb1:PLB1
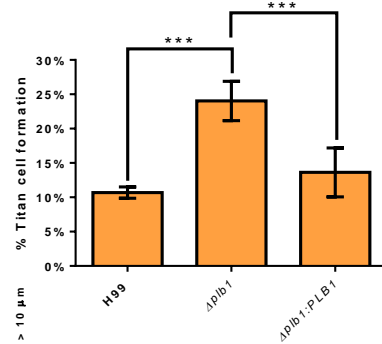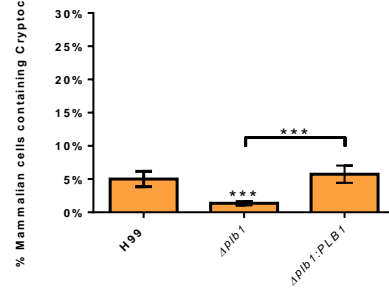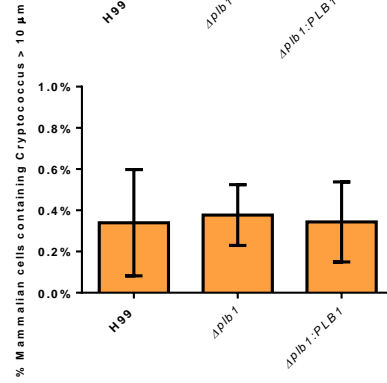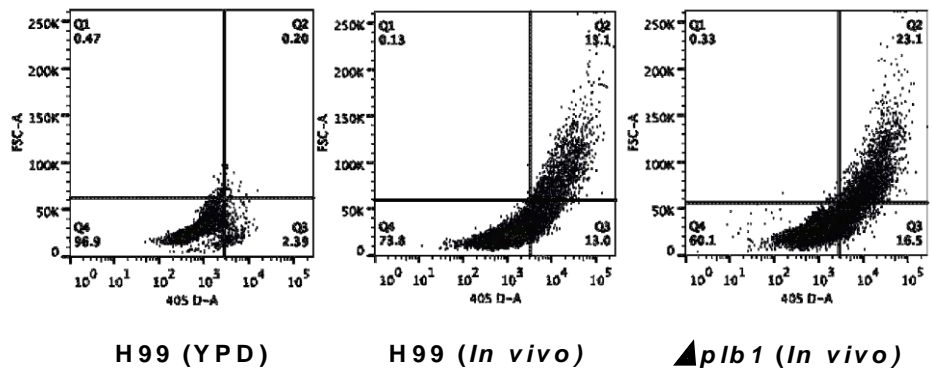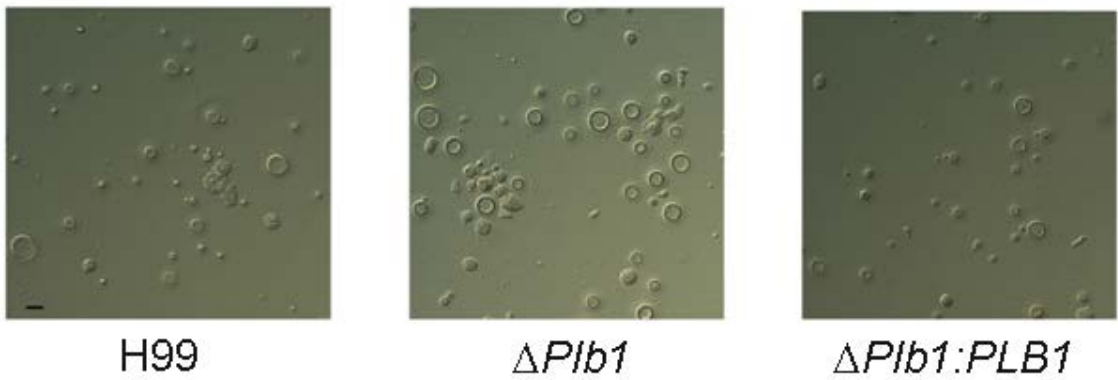
Figure 8 – *In vivo* **titan cell assay on** *Cryptococcus* **cells lavaged from mouse lungs 3 days post infection. A. - i** A minimum of 500 cells per animal were analysed to quantify cell body diameter, *Cryptococcus* cells >15 μm in diameter were considered titan cells. Data displayed as % however statistical analysis was performed using raw count data (.e.g. total titan cells vs. total non titan cells), three pair wise chi-squared tests were made comparing H99 to *Δplb1*, *Δplb1* to *Δplb1:PLB1* and *Δplb1* to *Δplb1:PLB1*. Bonferroni correction was used to correct for multiple comparisons (3). The corrected α value was 0.017. **** H99 vs. *Δplb1* p = >0.0001. ** H99 vs. *Δplb1:PLB1 p = 0.0014 **** Δplb1 vs. Δplb1:PLB1* p = >0.0001. **A. - ii** Host cells lavaged from the lungs were examined for phagocytosed *Cryptococcus* cells. Data displayed as % however statistical analysis was performed on raw count data (.e.g. total *Cryptococcus* inside mammalian cells vs. total *Cryptococcus* outside mammalian cells), three pair wise chi-squared tests were made comparing H99 to *Δplb1*, *Δplb1* to *Δplb1:PLB1* and *Δplb1* to *Δplb1:PLB1*. Bonferroni correction was used to correct for multiple comparisons (3). The corrected α value was 0.017 **** H99 vs. *Δplb1* p = <0.0001. **** *Δplb1 vs. Δplb1:PLB1* p = <0.0001 **A. - iii** The cell body diameter of phagocytosed *Cryptococcus* cells within lavaged host macrophages was quantified, data for phagocytosed cells > 10 μm are given. Data displayed as % however statistical analysis was performed raw count data (.e.g. total *Cryptococcus* cells > 10 μm inside mammalian cells vs. total *Cryptococcus* 10 μm outside mammalian cells), three pair wise chi-squared tests were made comparing H99 to *Δplb1*, *Δplb1* to *Δplb1:PLB1* and *Δplb1* to *Δplb1:PLB1*. Bonferroni correction was used to correct for multiple comparisons (3). The corrected α value was 0.017. No significance found. **B.** *Cryptococcus* from H99 and *Δplb1* bronchoalveolar lavage samples were stained with Hoechst and analysed for size and nuclear content. Cells were gated based on size and

nuclear content with cells in Q3 consistent with small cells in G1, Q4 indicative of small cells in G2, and Q2 indicative of polyploidy titan cells with both large size and increased DNA content. **C** Bright field images of lavaged cells from H99, *Δplb1* or *Δplb1:PLB1* infected lungs. Scale bar = 15 μm.

4. Discussion

During cryptococcal pathogenesis, *C. neoformans* interacts with professional phagocytes in the alveolar space (Feldmesser et al., 2000) and in the blood stream and other tissues following dissemination. The outcome of this interaction appears to be vital for disease progression, as the macrophage provides a protective niche for replication (Ma et al., 2009) and a potential 'Trojan horse' for dissemination to the CNS (Charlier et al., 2009; Chrétien et al., 2002). Together with previous studies, my findings strongly suggest that expression of Plb1 is critical in regulating cryptococcal/macrophage interactions.

Firstly, I show that *PLB1* deletion leads to enhanced uptake by phagocytes *in vitro* (Figure 3. B). Since Plb1 is a GPI-linked, cell wall associated protein (Djordjevic et al., 2005b), it is likely that loss of this enzyme affects the cryptococcal cell surface and, presumably, this change facilitates more efficient binding of phagocyte receptors. Examination of different opsonisation methods (Figure 4. C – i, D – i, E - i) suggests that increased uptake is due to a combination of antibody, complement and non-opsonic ligands. Cryptococcal cell wall instability following *PLB1* deletion has been published previously (Siafakas et al., 2007) and thus this instability could lead to increased ligand exposure on the *Cryptococcus* cell surface. In light of these observations, a detailed chemical analysis of the cell surface composition in this strain would be of considerable future interest.

Following phagocytosis, I found that *C. neoformans* requires the expression of Plb1 to proliferate and survive normally within the macrophage (Figure 4). This finding provides a mechanism to explain previous reports of reduced fungal burdens following infection with *Δplb1* (Chayakulkeeree et al., 2011). Interestingly, however, the *Δsec14-1* strain shows no such defect in intracellular proliferation (Figure 4A). Since this strain shows strongly

reduced Plb1 secretion (Chayakulkeeree et al., 2011), the most likely explanation is that the primary role of Plb1 in driving intracellular proliferation is in the metabolism of fungal phospholipids within the cryptococcal cell, rather than in acting directly upon host phospholipids. However, secreted Plb1 appears to have additional roles in virulence, since the *Δsec14-1* strain is attenuated in animal models (Chayakulkeeree et al., 2011). It is tempting to speculate that the documented involvement of *SEC14* in regulating vomocytosis (Chayakulkeeree et al., 2011) may be one such role. It is also possible that the expression of Plb1 by *Cryptococcus* within infected macrophages changes how the macrophage responds to infection – to explore this possibility further it will be essential in the future to determine whether the expression of Plb1 can alter the maturation state of macrophages and their subsequent cytokine production profile.

A striking morphological observation arising from my macrophage infection experiments was that *Δplb1* showed a marked increase in both cell body diameter and capsule thickness during infection, with a maximum measured diameter (including capsule) of almost 25 μm (Figure 6. C). That this size change was not seen in the wild type or *Δplb1:PLB1* reconstituted strains suggests that this morphology results from the loss of Plb1. Previously reported titan cells grown *in vivo* range in diameter from 15 - 100 μm, excluding capsule (Okagaki et al., 2010; Zaragoza et al., 2010). Therefore, the size increase observed is smaller than that of previously reported titan cells, but significantly larger than the normal cryptococcal size range. Interestingly, previous reports of titan cells induced *in vitro* also noted the cells tended to be smaller than those generated *in vivo* (Okagaki et al., 2010). Flow cytometry analysis of *Δplb1* cells following macrophage infection (Figure 7) indicates a mixed population of large cells with high DNA content but also a group of

normal sized cells with high DNA content which may be on the verge of becoming giant cells (Okagaki et al., 2010).Thus it is likely these cells may represent individual yeast that are "en route" to becoming titan cells, or have somehow been constrained by the macrophage, or that the *in vitro* conditions do not provide the necessary stimulus to produce the largest titan cells.

From my *in vitro* data I conclude that *Δplb1* forms large cells within macrophages; similar to the Titan cell morphology seen *in vivo*. Titan cell formation has previously been induced *in vitro* using macrophage conditioned media (Okagaki et al., 2010), however titan cell formation induced inside an infected macrophage has, to my knowledge, not previously been reported. Although I have not identified the trigger for this morphology it is evidently linked to Plb1 deficiency. The development of this morphology within the macrophage may be a response to increased stress experienced by *Δplb1* as indicated by the decreased viability of this strain within the phagosome. As well as confirming a previously published susceptibility to SDS (Chayakulkeeree et al., 2011) (Figure 5) I also noticed that the *Δplb1* strain was susceptible to high concentrations of NaCl indicating that this strain may be vulnerable to osmotic stress and membrane attack. The phagosome exposes Cryptococci to a diverse repertoire of additional stresses and it is likely that these complex conditions limit growth of this mutant. One possible source of stress within the phagosome that links my observed phenotypes is the observation that in wild type cryptococci, Plb1 concentrates at the neck of newly forming buds (Lev et al., 2014). This suggests that Plb1 may have a role in bud development and thus it is conceivable that modification of membrane phospholipids by Plb1 during budding could be required for membrane curvature at the newly formed bud site or release of the daughter cell. The inability of the *Δplb1* strain to

properly bud would explain the proliferation defect observed and could generate sufficient cellular stress to reduce cryptococcal viability and trigger the development of titan like cells.

A strong link between my *in vitro* observations and previously published *in vivo* development of titan cells is supported by the finding that the *Δplb1* strain forms greater numbers of 'classical' titan cells (i.e. cell body diameter above 15 μm and high nuclear content indicative of polyploidy) *in vivo* compared to the wild type and reconstituted strains (Figure 8 A. i). These data suggest that Plb1 activity is involved in the repression of titan cell formation during infection. In addition, the fact that the *Δsec14-1* strain does not manifest similar cell size increases during *in vitro* infection (unpublished data) indicates that intracellular rather than extracellular Plb1 activity regulates the titan cell morphology. Interestingly, titan cell development may be linked to phospholipid availability (Chrisman et al., 2011), suggesting a potential link to Plb1 activity. Titan cell formation *in vivo* has been reported to increase the pathogenicity of *C. neoformans* (Crabtree et al., 2012; Okagaki et al., 2010), my conclusion that *Δplb1* has increased Titan cell formation therefore seems at odds with *in vitro* data presented in figure 3 and 4 showing that the *Δplb1* is attenuated in macrophages. It is therefore possible that the large *Δplb1* cells may not exhibit all the features of titan cells (for instance, in conferring "cross-protection" on non-titan cells in the same host). Alternatively, it may be that full pathogenicity requires only a minor titan cell population and hence the enhanced titan cell frequency seen in *Δplb1* actually reduces overall virulence.

In summary, my data indicate that Plb1 plays a key role both in intracellular survival within host phagocytes and in driving cryptococcal cell size changes both *in vitro* and *in vivo*.

CHAPTER 3 – THE ROLE OF EICOSANOIDS DURING CRYPTOCOCCAL INFECTION OF MACROPHAGES

1. Introduction

My own work, and that of others, has show that the *C. neoformans* virulence factor Phospholipase B1 (Plb1) helps the fungus survive within macrophages during infection (Cox et al., 2001; Evans et al., 2015; Noverr et al., 2003a). I have found that the *C. neoformans* Plb1 deficient strain *Δplb1* is phagocytosed more efficiently by macrophages (Chapter 2. Figure 3), proliferates less within the phagosome (Chapter 2. Figure 4 - A) and is more susceptible to macrophage killing (Chapter 2. Figure 4 – B). Additionally, I have described a cryptococcal morphology that Plb1 deficient cells develop during macrophage infection (Chapter 2. Figure 6) which is closely related to Titan cell morphology seen during *in vivo* infection (Chapter 2. Figure 8) (Evans et al., 2015).

Although a number of studies – including my own (Evans et al., 2015) - report phenotypes observed during macrophage infection with the Plb1 deficient mutant *Δplb1*, the mechanisms behind these observations has yet to be fully elucidated. Theories for how Plb1 causes virulence include the enzyme's ability to attack host membranes and also to scavenge, metabolise and detoxify host derived lipids during infection (Djordjevic, 2010). This chapter describes work I have done to explore another theory. The theory is that Plb1 allows *C. neoformans* to produce eicosanoid species during infection that closely resemble those produced by the host. The link between Plb1 and eicosanoid synthesis by *C. neoformans* is well known (Noverr et al., 2001; Noverr et al., 2003a). The effects these

eicosanoids have on the outcome of host infection though have not been well explored and, it is possible that *Cryptococcus* derived eicosanoids could mimic and interfere with host eicosanoid signalling in such a way as to influence the outcome of the host pathogen interaction between organisms.

Eicosanoids are a class of lipid molecules; the prefix eicosa- (the number 20 in Greek) signifies their common origin as oxidised derivatives of 20 carbon fatty acids. The three 20 carbon fatty acids that give rise to eicosanoids are eicosapentaenoic acid (EPA), arachidonic acid (AA) and di-homo-γ-linolenic acid (Harizi et al., 2008). It has been found that *C. neoformans* produces a number of eicosanoid species that are similar to those produced by mammalian cells, as can other fungi such *Candida albicans* (Noverr et al., 2001). The eicosanoid synthesis pathway has been well characterised in mammalian cells but in fungi there is still much that is not known – one thing that is clear, however, is that the pathway is not analogous to that of mammalian cells.

1.1 Mammalian eicosanoid production

The main pool of stored AA in mammalian cells is located in cell membranes where this fatty acid (among other fatty acids) is found incorporated into the lipid bi-layer of cell membranes. Phospholipids are composed of three main subunit, a central glycerol backbone that is attached at one end to a phosphate head group and at the other end to two fatty acids via the Sn1 and Sn2 ester linkages (van Meer et al., 2008). In mammalian cells, AA is liberated from membrane phospholipids by the enzyme phospholipase A_2 (PLA_2). PLA_2 activity specifically hydrolyses phospholipid Sn2 ester linkages; hydrolysis of this ester linkage cleaves the Sn2 fatty acid tail from the phospholipid producing a free fatty acid and a lysophospholipid (see chapter 3, figure 1). The enzymatic action of PLA_2 on

phospholipids that contain AA at their Sn2 position results in the accumulation of free AA within the cell. PLA$_2$ activity is often triggered as a result of cellular damage or inflammatory signalling (Harizi et al., 2008).

In mammalian cells, AA is oxidised by three different enzymes that each produce different classes of eicosanoids. The three enzymes are cyclooxygenase (COX) of which there are two isotypes – COX-1 and COX-2, lipoxygenases (LOX) of which there are three isotypes – LO-1, LO-2 and LO-3 and finally P450 epoxygenase. Oxidation of AA by the COX enzymes produces prostaglandins, prostacyclins and thromboxanes (TXs) – eicosanoid species that are known collectively as prostanoids. Oxidation of AA by the LOX enzymes produces leukotrienes (LT), cysteninyl-leukotrienes (CysLTs) and lipoxins (LXs). Finally P450 epoxygenase produces hydroxyeicosatetraenoic acids (HETEs) and epoxides (EXs) as end products (Harizi et al., 2008).
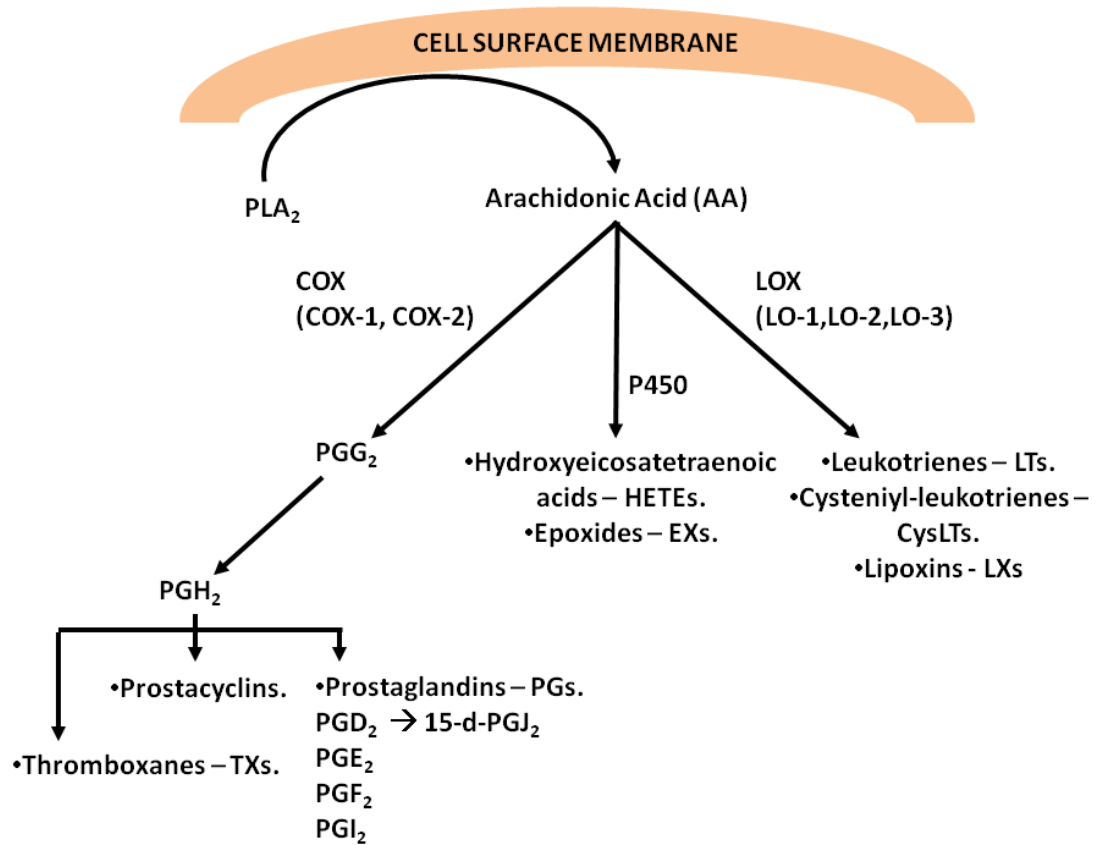
Figure 1 – Diagram showing the different eicosanoids products of arachidonic acid (AA) metabolism by the COX, LOX and P450 enzymes.

1.2 Mammalian prostaglandins

In mammalian cells, AA that has been liberated from cell membrane phospholipids is converted into the prostanoid species by the enzymes COX-1 and COX-2. Generally, COX-1 is constitutively expressed within mammalian cells at low levels and is involved with the production of prostanoids for homeostatic functions. COX-2 expression in contrast is induced as a result of cell signalling events such as those seen during inflammation and tissue injury (Simmons et al., 2004). COX mediated oxidation of AA produces PGG_2. PGG_2 is a volatile lipid species that is quickly converted to the more stable species PGH_2. PGH_2 is the universal precursor to all prostanoid species. The conversion of PGH_2 to each prostanoid is catalysed by specific enzymes. In the case of prostaglandins the conversion of PGH_2 to the end product is catalysed by prostaglandin synthase enzymes – each prostaglandin species has a specific synthase enzyme (Harizi et al., 2008).

Mammalian cells produce a number of prostaglandins - PGE_2, PGD_2, PGI_2, PGF_2 and 15-d-PGJ_2. The prostaglandins PGE_2, PGD_2, PGI_2 and PGF_2 are all produced from PGH_2 by end product specific prostaglandin synthase enzymes e.g. prostaglandin E synthase, prostaglandin D synthase etc. 15-d-PGJ_2 is the exception as it formed via the spontaneous dehydration of PGD_2 (Harizi et al., 2008).

Following synthesis, prostaglandins are exported from mammalian cells into the extracellular space. In multi cellular organisms, prostaglandins act as potent signalling molecules; they are known to regulate a number of physiological processes including inflammatory cell activation, smooth muscle contraction / relaxation, and blood clotting via the activation of platelets. The effective distance of prostaglandin signalling is small; prostaglandin signalling is mostly autocrine e.g. they act on the cells that produces them,

however they may also signal to very closely neighbouring cells via paracrine signalling (Harizi et al., 2008; Ricciotti and FitzGerald, 2011).

Prostaglandin signalling is facilitated by G-protein coupled prostaglandin receptors that are found expressed on the surface of cells. Each prostaglandin e.g. PGE_2, PGD_2 etc. signals via a separate group of receptors. PGE_2 for example signals via EP receptors of which four are found in humans (EP1, EP2, EP3 and EP4). The cellular response that prostaglandin signalling triggers depends on the pattern of prostaglandin receptors expressed on the cell surface and the cell type and tissue where the signalling occurs. In terms of inflammation the signalling of a prostaglandin such as PGE_2 can result in anti-inflammatory or pro-inflammatory effects depending on which of the EP receptors are expressed on the surface of a cell. Thus it is hard to ascribe specific effects to each prostaglandin as their action varies so greatly throughout the body (Harizi et al., 2008; Ricciotti and FitzGerald, 2011).

1.3 Eicosanoid production by *C. neoformans*

Although fungi are known to produce eicosanoids, the pathways that lead to their synthesis are still largely uncharacterised. Much of the research done in this area to date has focussed on trying to identify fungal enzymes that are analogous to enzymes in higher organisms such as cyclooxygenase and prostaglandin synthase homologs. The conclusions from these investigations so far, are that direct homologs do not exist, or at least not enough of them to constitute a completely analogous fungal pathway of synthesis. In this respect the only analogous enzymatic activity that can be identified across many fungal species is phospholipase A_2 activity – possessed by enzymes such as Plb1 from *C. neoformans* – that presumably liberates AA from membrane phospholipids (Chen et al., 2000). Concurrently in *C. neoformans* Plb1 is one of only two enzymes that is conclusively linked to eicosanoid

123

synthesis by the fungus (Erb-Downward et al., 2008; Noverr et al., 2003a). Noverr *et al* found that the Plb1 deficient *C. neoformans* strain *Δplb1* produced lower levels of eicosanoids when grown in standard media; however, when exogenous AA was substituted into the media eicosanoid production returned to wild type levels. This suggests that Plb1 fulfils the role of mammalian PLA$_2$ for *C. neoformans* (Noverr et al., 2003a).

Further down the eicosanoid pathway a couple of studies in *C. neoformans* have attempted to determine whether eicosanoid synthesis relies on the expression of an enzyme similar to COX. Attempts to disrupt *Cryptococcus* eicosanoids synthesis using pharmacological COX inhibition have proved inconclusive. In this respect, in a 2001 study Noverr *et al.* observed that COX inhibitors such as indomethacin significantly decreased prostaglandin production by *C. neoformans* (Noverr et al., 2001) but a later 2007 study by Erb-Downward *et al.* found that *C. neoformans* prostaglandin production was not affected by indomethacin (Erb-Downward and Huffnagle, 2007). Additionally, homology searches using BLAST do not reveal any proteins with a direct homology to mammalian COX (personal observation, unpublished). Similarly poor results occur when BLAST searches are used to identify homologous prostaglandin synthase enzymes and prostaglandin receptors in *C. neoformans* (personal observation, unpublished) however in a 2003 review Noverr *et al.* do mention finding a *Cryptococcus* gene homologous to a PGF synthase found in *Trypanosoma bruceii* (Noverr et al., 2003b) .

Although fungi and other lower eukaryotes such as protozoa do not seem to possess COX enzymes analogous to those found in higher eukaryotes these organisms still produce eicosanoids. Therefore, alternative COX independent pathways of production must exist. To explain this, two potential routes of synthesis have been proposed. The first involves

the action of lipoxygenases; these enzymes can form lipid species that have similar structural properties to eicosanoids via the addition of dioxygen molecules to carbon chains, but, prefer linoleic acid to AA (Noverr et al., 2003b); to date, however homologs have not been identified in *C. neoformans* (Erb-Downward et al., 2008). The second possibility is that arachidonic acid may be oxidised in a non enzymatic reaction by oxygen free radicals (Noverr et al., 2003b).

In *C. neoformans* the only other protein known to be linked to prostaglandin production other than Plb1 is Laccase (Erb-Downward et al., 2008). This enzyme is a known virulence factor in *C. neoformans* however until recently this was solely thought to be due to its involvement in the production of melanin (Casadevall et al., 2000). *Cryptococcus neoformans* has two genes that code for laccase enzymes *LAC1* and *LAC2*. DNA microarray analysis has found that cryptococcal expression of *LAC1* and *LAC2* is induced when *C. neoformans* cells are phagocytosed by macrophages - *LAC1* and *LAC2* were found to be induced 3.8 fold and 3.0 fold respectively 2 hours after phagocytosis by J774 murine like macrophages *in vitro* (Fan et al., 2005).

Laccase's role in the production of eicosanoids highlights a previously unknown aspect of this virulence factor. Analysis shows that laccase cannot convert AA to prostaglandins species although it can convert PGG_2 to PGE_2, suggesting that in *C. neoformans* laccase may fulfil the role of prostaglandin E_2 synthase (Erb-Downward et al., 2008). Interestingly in a recent study Sabiiti *et al.* found that high *Cryptococcus* laccase activity of clinical isolates *in vitro* correlated to poor clinical outcome when compared against patient medical records. Although laccase activity correlated to poor patient outcome the relative amount of melanin produced by a representative selection of these strains did not (Sabiiti et al.,

2014). This suggests that laccase has virulence attributes independent of melanin production and perhaps laccase's involvement in prostaglandin synthesis could be this attribute.

1.4 Potential functions of *C. neoformans* derived eicosanoids during infection

C. neoformans is known to produce a number of eicosanoids during infection (Noverr et al., 2003a) – PGE_2, PGD_2, $PGF_{2\alpha}$, TXB_2 and 5-HETE are among those detected (Noverr et al., 2001). Some of the eicosanoid species produced by *C. neoformans* such as PGE_2 and PGD_2 have been found to have a remarkable similarity to their respective mammalian prostaglandin standards (Erb-Downward et al., 2008). Due to this similarity, is it likely that fungal derived prostaglandins can mimic and interfere with host signalling during infection. Due to the fact that prostaglandins are involved in the control of the inflammatory response (Harizi et al., 2008) it is therefore likely that fungal eicosanoids could influence the host immune response against *C. neoformans*.

In this respect a very recent study has found compelling evidence suggesting that PGE_2 produced during *C. neoformans* pulmonary infection is beneficial to the fungus and detrimental to the host. During murine infection, blockage of the PGE_2 receptors EP2 and EP4 led to increased survival of treated mice. Additionally, PGE_2 signalling in the lung via EP2 and EP4 was shown to be correlated to increased alternative macrophage activation and decreased classical activation (Shen and Liu, 2015). It has already been discussed in previous chapters that in order to effectively control *C. neoformans* infection, host macrophages must be classically activated (Kawakami et al., 1995; Voelz et al., 2009). This suggests that eicosanoid production in the lung may influence the macrophage response to infection; in agreement with this are findings that eicosanoids derived from *C.*

neoformans can reduce TNF-α and increase IL-10 cytokine production by murine splenocytes (Noverr et al., 2001).

In addition to influencing macrophage biology, fungal eicosanoids may be able to manipulate the immune response at a wider level. PGE_2, which is one of the most ubiquitous prostaglandins during inflammation, can produce a Th2 $CD4^+$ biased immune response by down regulating IL-12 release from macrophages (van der Pouw Kraan et al., 1995). With this in mind it has been observed that the development of Th1 adaptive immune responses is protective against *C. neoformans* infection whereas the Th2 adaptive immune response is not (Hoag et al., 1997; Voelz et al., 2009; Wormley et al., 2007).

In chapter 2 of this thesis, and the associated published work (Evans et al., 2015), I report a number of phenotypes that develop during J774 macrophage infection if *C. neoformans* is deficient in Plb1. Using a Plb1 deficient *C. neoformans* strain, *Δplb1,* I have shown that Plb1 deficiency increases phagocytosis of *C. neoformans* by macrophages (Chapter 2. Figure 3), reduces intracellular proliferation and viability within the phagosome (Chapter 2. Figure 4) and also triggers a novel intracellular cell morphology switch (Chapter 2. Figure 6) that is linked to extracellular Titan Cell formation (Chapter 2. Figure 8) (Evans et al., 2015).

The *Δplb1* strain has been found to have almost completely abrogated eicosanoid production unless exogenous AA is present (Noverr et al., 2003a). With this in mind the data I present in this chapter was aimed at determining whether *C. neoformans* derived eicosanoids − or the lack thereof − can account for the observed phenotypes during macrophage infection.

I show that the addition of exogenous AA and PGE_2 – but not PGD_2 – increases the intracellular proliferation of *Δplb1* within J774 macrophages; but does not reach statistical significance. In the discussion, I discuss how this hypothesis can be better addressed with future work.

2. Materials and methods

2.1 Strains, media and cell lines

Strains used in this work are listed in the Appendix (Appendix Table 1, page 188). All *C. neoformans* strains used were stored long-term in MicroBank vials at -80°C. Strains were recovered onto YPD agar (YPD 50 g/L Sigma Aldrich, 2 % Agar – Melford) for 48 hours at 25°C and then stored until needed at 4°C. Before experimentation, liquid cultures were grown from these stock plates in 2 ml YPD growth medium (50 g/L) for 24 hours at 25°C under constant rotation.

The J774 murine macrophage cell line was used for all *in vitro* infection assays. Cells were passaged in DMEM culture media with serum (Dulbecco's Modified Eagle medium, low glucose, Sigma Aldrich, 10 % FBS - Invitrogen, 1% 10,000 units Penicillin / 10 mg streptomycin – Sigma Aldrich, 1 % 200 mM L – glutamine – Sigma Aldrich). Assays were performed with J774 cells between passages 4 and 15. Assays were performed in serum-free DMEM (DMEM high glucose, 1% P/S, 1% L-glutamine) unless otherwise stated.

2.2 *Cryptococcus* preparation for assays

Overnight *C. neoformans* cultures grown at 25 ^{o}C in YPD were washed three times in sterile 1x PBS, counted and adjusted to 1 x10^7 cells per ml in PBS before opsonisation for 1 hour with 10 μg/ml anti capsular 18B7 antibody (a kind gift from Arturo Casadevall, Albert Einstein College of Medicine, New York USA). The opsonisation step was timed so that the incubation time finished at the same time as the macrophage activation step described below.

2.3 Macrophage activation for assays

24 hours before infection, 1×10^5 J774 macrophages were seeded into 24 well plastic plates (Greiner Bio One Cell Star) in 1 ml culture media with serum and incubated for 24 hours at 37 °C 5% CO_2. Before infection, J774 cells were activated with 150 ng/ml phorbol 12-myristate 13-acetate (PMA) dissolved in DMSO (Sigma) in 1 ml serum free culture medium for 45 minutes. This media was then replaced with serum-free media alone. The activation step was timed so that the incubation ended at the same time as the *Cryptococcus* opsonisation step described above.

2.4 Eicosanoid treatment

Treatment with the exogenous eicosanoids PGE_2 and PGD_2 or the eicosanoid precursor AA was performed after the macrophage activation step of the macrophage infection protocol described above. The SF DMEM macrophage activation media was removed and replaced with 1 ml SF DMEM supplemented with PGE2, PGD_2, or AA at the desired concentration, untreated and vehicle infection controls were also performed for each experiment.

Activated and treated J774 cells were then infected with 100 μl opsonised *C. neoformans* to give an MOI of 10 (e.g. 1×10^5 J774 / 1×10^6 *C. neoformans*) and incubated for 2 hours at 37°C 5% CO_2. After two hours, infected wells were washed at least 3 times with warm 1x PBS until all non-phagocytosed *C. neoformans* cells were removed from the wells. Following washing the PBS was removed and replaced with 1 ml SF DMEM containing PGE2, PGD_2, or AA at the same concentration as used initially. Infected macrophages were then incubated at 37°C until the appropriate time point for the assay.

2.5 Intracellular proliferation assay

For calculation of the intracellular proliferation rate the number of internal cryptococci was counted at time points 0 (time point 0 = 0 hr after non phagocytosed cells washed away) and 18 hours (Time point 18 = 18 hr after time point 0). At each time point each well to be counted was washed three times with 1x PBS to remove any extracellular yeast. The macrophages in the well were then lysed in 200 µl deionised water (dH_2O) for 30 minutes. To remove lysed macrophages and cryptococci a pipette tip was used to scrape the surface of the well, the 200 µl of lysate was then removed to a clean Eppendorf and a further 200 µl dH_2O added to the well to wash any remaining cells, this 200 µl was also added to the Eppendorf to give a final sample volume of 400 µl.

C. neoformans cells in the lysate were quantified at each time point with a cell counting chamber and the intracellular proliferation rate (IPR) calculated by dividing the count at which intracellular burden peaked by the count at time point 0.

Viability testing of the recovered cells was achieved by diluting the lysate to give a concentration of 200 yeast cells per 100 µl, and then plating onto YPD agar at $25^{o}C$ for 48 hours prior to counting colony forming units.

2.6 Co-infection assay

Subsequent to the washing away of non-phagocytosed *Cryptococcus* cells and replacement of the eicosanoid treatment media, the 24-well plate was placed into an environmentally controlled stage (Okolabs) set to $37^{o}C$, 5 % CO_2. The cells were imaged using a Nikon TE2000 microscope fitted with a Digital Sight DS-Qi1MC camera and a Plan APO Ph1 20

x dry objective. Images were recorded every 4 minutes for 20 hours. Image acquisition and analysis was performed using the Nikon NIS Elements software package (Nikon).

Movies were scored manually, First co-infected macrophages (i.e. those that contained at least one fluorescent H99-GFP *Cryptococcus* cell and at least one non-fluorescent *Δplb1* *Cryptococcus* cells were identified at the start of the movie (0 hr) and fungal burden (total number of each strain) scored. Each co-infected macrophage was followed over 18 hr. At the 18 hr time point the fungal burden within each macrophage was re-scored. The IPR was calculated by totalling the fungal burdens of co-infected macrophages and dividing the 0 hr burden by the 18 hr burden. Singly infected H99-GFP and *Δplb1* controls were scored in the same way. Around 120 co-infected macrophages were scored per experimental replicate.

2.7 PGE$_2$ EIA ELISA

Culture supernatant from eicosanoid infected macrophages infected with *C. neoformans* as described above were collected at 0 hour and 18 hour time points. Supernatants were analysed as per the PGE$_2$ EIA ELISA kit instructions (Cayman Chemical, Item Number 514010).

2.8 Statistics

Figure 2: Two independent, *two* tailed, unpaired T tests performed for H99-GFP vs. *Δplb1* and H99-GFP (co-infection) vs. *Δplb1* (Co-infection).

Figure 3:

Figure 3A: Intracellular proliferation rate (IPR) data was determined to be normally distributed using the Shaprio-Wilk normality test (p-value < 0.05 reject null hypothesis that data is not normally distributed) (see appendix table 15, page 195). Bonferroni correction was used to correct for multiple comparisons. The Bonferroni correction was used to correct for multiple comparisons (3) the corrected α value was 0.016.

Figure 3B: CFU viability data was determined to be normally distributed using the Shaprio-Wilk normality test (p-value < 0.05 reject null hypothesis that data is not normally distributed) (See appendix table 16, page 195). A two-way ANOVA with Tukey post test was used to compare 0hr, 18hr and 24hr time points for each strain. P values under 0.05 were taken to be statistically significant * $p \leq 0.05$, ** $p \leq 0.01$, *** $p \leq 0.001$ and **** $p \leq 0.0001$.

Figure 4: PGE_2 EIA ELISA data was determined to be normally distributed using the Shaprio-Wilk normality test (p-value < 0.05 reject null hypothesis that data is not normally distributed) (See appendix table 16). (See appendix table 17, page 196). Two-way ANOVA with Tukey post test performed to compare concentrations within treatment groups – no significance found within respective treatment group.

Figure 5:

Figure 5 A: Intracellular proliferation rate (IPR) data was determined to be normally distributed using the Shaprio-Wilk normality test (p-value < 0.05 reject null hypothesis that data is not normally distributed) (See appendix table 15, page 195). Unpaired two tailed T tests were performed, comparing each strain to the H99 wild type. The Bonferroni

correction was used to correct for multiple comparisons (3) the corrected α value was 0.016.

Figure 5 B: Intracellular proliferation rate (IPR) data was determined to be normally distributed using the Shaprio-Wilk normality test (p-value < 0.05 reject null hypothesis that data is not normally distributed) (see appendix table 15, page 195). Unpaired two tailed T tests were performed, comparing each strain to the H99 wild type. The Bonferroni correction was used to correct for multiple comparisons (3) the corrected α value was 0.016.

Figure 5 C: Two-way ANOVA with Tukey post test performed to compare time points and treatment for each strain.

3. Results

I have previously described how the *Δplb1* mutant (a mutant *C. neoformans* strain with abrogated Plb1 expression) has decreased proliferation (Chapter 2, Figure 4A) and viability (Chapter 2, Figure 4B) within macrophages as well as a novel intracellular morphology (Chapter 2, Figure 7). The aim of my work in this chapter was to begin to determine why these phenotypes occur. One reason for these phenotypes may be because the *Δplb1* mutant is deficient in eicosanoid production unless exogenous AA is provided (Noverr et al., 2003a). It is possible that eicosanoids such as PGE_2 and PGD_2 produced by *C. neoformans* during macrophage infection may interfere with normal macrophage eicosanoid signalling and as a result influence the outcome of macrophage infection.

3.1 The IPR defect of *Δplb1* may be dependent on a secretory factor (but additional replicates needed).

A number of published studies conclude that secreted Plb1 enzyme activity (as opposed to intrinsic Plb1 activity) contributes to cryptococcal virulence during infection (Chayakulkeeree et al., 2011; Santangelo et al., 2004). In the previous chapter however I found that for *Δplb1's* intracellular proliferation and viability phenotypes this is not the case (Chapter 2. Figure 4). In this respect I found that the *Δsec14-1* strain, which still expresses Plb1 but has almost completely abrogated Plb1 secretion (Chayakulkeeree et al., 2011), did not have a significantly different growth or viability phenotype to the H99 wild type strain.

To further investigate whether a secretory factor produced by *C. neoformans* during macrophage infection influences cryptococcal growth within macrophages I co-infected

macrophages with both H99 and *Δplb1* strains then calculated an IPR value for each strain. If Plb1, or a Plb1 related secretory factor such as an eicosanoid, did influence cryptococcal growth within macrophages then it was hoped that the *Δplb1* mutant cells would grow at wild type levels if wild type H99 cells were present inside the same macrophage.

To test this co-infection hypothesis, I co-infected J774 macrophages with two strains of *C. neoformans* simultaneously – I used the *Δplb1* mutant strain and a GFP-tagged H99 strain (H99-GFP). The H99-GFP strain was chosen because it is a fluorescently tagged *Cryptococcus* strain made in the same genetic background as *Δplb1*. It was hoped that the fluorescence of H99-GFP would differentiate it from *Δplb1* during macrophage infection and thus allow me calculate an IPR for each co-infecting strain.

To produce co-infected macrophages I inoculated a 1×10^5 J774 murine macrophage monolayer seeded into a 24 well plate with a 50:50 mix of antibody opsonised H99-GFP and *Δplb1* at an MOI of 1:10 (i.e. 5×10^5 H99-GFP and 5×10^5 *Δplb1*). I found that this inoculum mixture gave me a co-infection rate of about 5 % (i.e. macrophages that contained at least one H99-GFP cell and at least one *Δplb1* cell when viewed with microscopy). To calculate the co-infection IPR, an 18 hour live cell microscopy movie was made. Co-infected macrophages at 0 hr (the movie start time) were scored manually for their initial fungal burden, followed for 18 hours and re-scored for final fungal burden. The IPR of each co-infected strain was calculated by totalling the total fungal burden for each strain at 0 hr and 18 hr and dividing the final net burden at 18 hr by the initial net burden at 0 hr. For control and comparison singly infected H99-GFP and *Δplb1* J774 monolayers were also scored in the same way.

The data appears to show that the intracellular proliferation defect of *Δplb1 is* slightly but significantly rescued within co-infected macrophages that have H99-GFP cells within them (Figure 2 (p = 0.017). Unfortunately, with an experimental replicate number of only two there is insufficient power to support this conclusion with statistical testing. Taken together this suggests that further work will need to be performed in order elucidate the effects of co-infection.
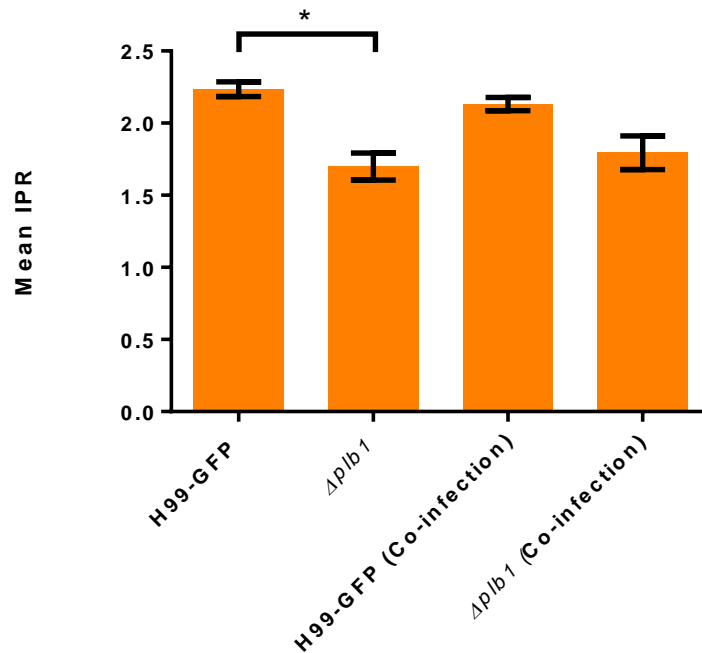
Figure 2 – A Co-infection experiment between *Δplb1* and H99-GFP to determine if secreted Plb1 affects cryptococcal growth within the macrophage. Co-infected macrophages (i.e. those that contained both H99-GFP and *Δplb1*) at 0 hr were scored for fungal burden and then followed and scored again at 18 hr. The IPR was calculated by totalling the number of cryptococci at both time points and dividing the fungal burden at 18 hr by the fungal burden at 0 hr. The 'H99-GFP' and 'Δplb1' conditions represent singly infected controls. n = 2, error bars = Standard deviation. Independent two tailed, unpaired T tests performed for H99-GFP vs. Δplb1 and H99-GFP (co-infection) vs. *Δplb1* (Co-infection). * H99-GFP vs. *Δplb1* p = 0.019.

3.2 Treatment of *Δplb1* infected macrophages with exogenous AA appears to reverse its defective IPR phenotype

Although my co-infection experiment was not conclusive, it has been published that eicosanoids such as PGE_2 and PGF_2 are secreted by *C. neoformans* and furthermore their production is dependent on Plb1 expression. In this respect it has been observed that the *Δplb1* mutant strain cannot produce eicosanoids unless exogenous arachidonic acid (AA) is added its growth medium (Noverr et al., 2003a). This finding suggests that Plb1 is required to produce a pool of AA that is then metabolised into eicosanoid species such as PGE_2.. This finding could fit with data from another study which implicates that Plb1 facilitates the metabolism of host macrophage derived AA (Wright et al., 2007). With this in mind *C. neoformans* may use AA derived from host cells during infection to produce eicosanoids that can influence the outcome of infection.

To examine this possibility I infected J774 macrophages with H99, *Δplb1 and Δplb1:PLB1* and treated infected cells with 30 μg/ ml AA. If eicosanoids do help *Cryptococcus* grow within macrophages, then it was hoped that by adding exogenous AA to infected cells the IPR and viability of the *Δplb1* strain would be raised. Interestingly I did find that the IPR of *Δplb1* could be increased via the addition of exogenous AA (Figure 3. A). In untreated macrophages the IPR of *Δplb1* is significantly reduced compared to the wild type strain H99 (p = <0.001) however when exogenous AA is added the mean IPR of *Δplb1* increases to a point where it is no longer significantly different from H99 – this data suggests that exogenous AA can in fact boost the IPR of *Δplb1* during macrophage infection – this indicates that eicosanoids such as PGE_2 may drive *C. neoformans* intracellular proliferation and that additionally this process may be Plb1 dependant. Although I observed an increase

in IPR for *Δplb1* upon addition of exogenous AA I did not see an increase in intracellular

viability (Figure 3. B*). This suggests that although AA can boost *Δplb1* intracellular

proliferation it does not affect *Δplb1*'s underlying susceptibility to macrophage killing.
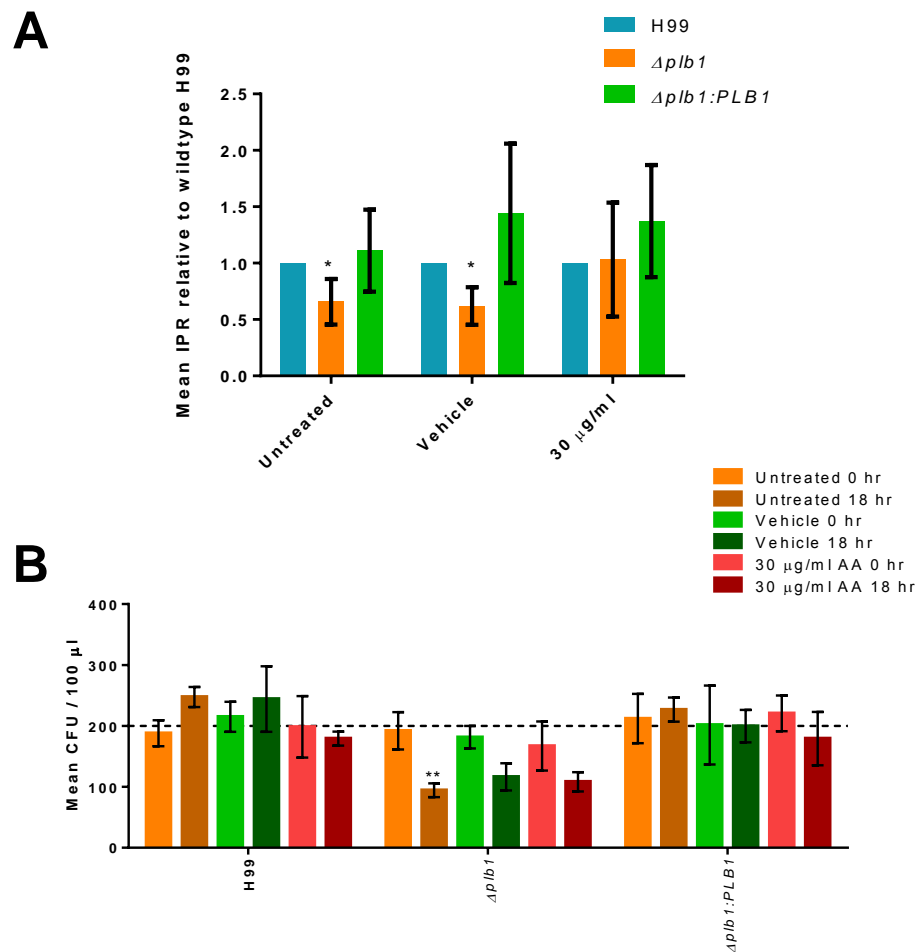
Figure 3 - A. Intracellular proliferation of *C. neoformans* strains H99, *Δplb1* and *Δplb1:PLB1* following treatment with 30 μg/ml Arachidonic Acid (AA). Untreated and vehicle controls (AA solvent – 100% ethanol) were also performed. IPR is given relative to the H99 wild type strain for each condition. n = 6, error bars = standard deviation. Multiple unpaired T tests performed for each treatment group vs. H99. H99 untreated vs. *Δplb1* * p = < 0.001, *H99* vehicle vs. *Δplb1* * p = <0.001, *Δplb1* untreated vs. *Δplb1* + 30 μg/ml AA ns p = 0.122. The Bonferroni correction was used to correct for multiple comparisons (3) the corrected α value was 0.016. **B.** Viability of *C. neoformans* cells

recovered from J774 macrophages following IPR assay. Cells recovered following macrophage lysis were counted and diluted give an expected plated inoculum of 200 cells. n = 4, error bars = standard deviation. Two-way ANOVA with Tukey post test performed to compare time points and treatment for each strain. Untreated 0 hr vs. Untreated 18 hr ** $p = 0.001$.

3.3 Treatment of infected macrophages with exogenous AA leads to increased PGE$_2$ production

The fact that adding exogenous AA to infected macrophages increases the IPR of the *Δplb1* strain suggests that *C. neoformans* IPR may be boosted by increased eicosanoid levels within the macrophage. It has been shown in another study that PGE$_2$ signalling during pulmonary cryptococcosis in mice can produce favourable conditions for cryptococcal growth in the lung. In the same study it was observed that alveolar macrophages from infected lung tissue were alternatively rather than classically activated. This suggests that PGE$_2$ signalling during infection may alter macrophage activation and help *C. neoformans* to survive (Shen and Liu, 2015). The next step after observing that exogenous AA could significantly increase the IPR of *Δplb1* therefore was to determine which eicosanoid was responsible.

Noverr *et al.* described how the *Δplb1* mutant could only produce eicosanoids if exogenous AA was present. Noverr et al. tested this phenomenon in liquid growth media (Sabourand dextrose broth), but they did not examine whether eicosanoids were produced during macrophage infection (Noverr et al., 2003a). In this study Noverr et al. showed that the widely studied prostaglandin PGE$_2$ is produced in a Plb1 dependant manner. The next step of this research therefore was to determine whether the addition of exogenous AA increased the amount of PGE$_2$ produced by *C. neoformans* infected macrophages. Additionally, I also wanted to determine whether *C. neoformans* infected macrophages produce PGE$_2$ in a Plb1 dependant manner. If this were the case then one might expect *Δplb1* infected macrophages to produce less PGE$_2$ compared to H99 and *Δplb1:PLB1*

infected macrophages, furthermore one might observe that when exogenous AA is available this deficiency would be restored.

In order to test this idea I infected J774 macrophages with either H99, *Δplb1* or the genetic reconstituted strain *Δplb1:PLB1* and after 18 hours of infection measured the levels of PGE$_2$ in the cell culture supernatant using a PGE$_2$ specific ELISA. In addition to measuring the base level of PGE$_2$ production during infection I also measured PGE$_2$ levels when infected macrophages were treated with exogenous AA at a concentration of 30 μg/ml – the same concentration used in my IPR experiment (Figure 3).

ELISA analysis revealed that *C. neoformans* infected macrophages do produce detectable levels of PGE$_2$ (Figure 4) - for non arachidonic acid treated, H99 infected macrophages the mean PGE$_2$ concentration in the supernatant was determined to be 482 pg/ml. Importantly however *Δplb1* infected macrophages (also untreated) did not produce significantly different levels of PGE$_2$ (Mean = 445 pg/ml), additionally uninfected macrophages also produced similar levels of PGE$_2$ (Mean = 491 pg/ml). Interestingly however I did find that treatment of infected macrophages with exogenous AA did increase the amount of detectable PGE$_2$ in the supernatant about 4 fold – for AA treated, H99 infected macrophages the mean PGE$_2$ concentration in the supernatant was determined to be 1908 pg/ml – however as before there was no significant difference in PGE$_2$ produced by H99 infected macrophages, *Δplb1* infected macrophages or even uninfected macrophages. Taken together these findings suggest that *C. neoformans* infection does not significantly increase PGE$_2$ levels within macrophage supernatants and that the PGE$_2$ that is produced is macrophage derived. However because PGE$_2$ levels still increased when exogenous AA is

added to macrophages, this suggests the boost in IPR observed for *Δplb1* when AA is added may be due to increased PGE_2 levels within infected macrophages.
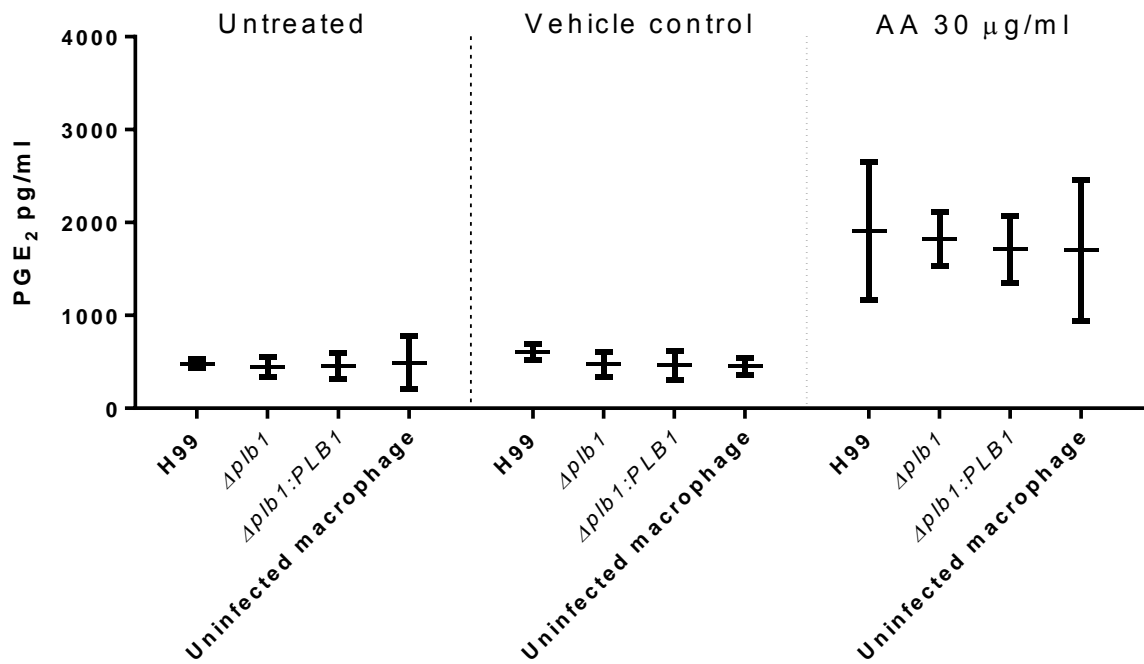
Figure 4 – PGE$_2$ monoclonal EIA ELISA performed on supernatants from *C. neoformans* infected macrophages collected at 18 hr time point of infection (i.e. 18 hours after non-phagocytosed cryptococci were washed away). Mean concentration (pg/ml) of PGE$_2$ plotted with SD. n = 4. Two-way ANOVA with Tukey post test performed to compare concentrations within treatment groups – no significance found.

3.4 Efforts to determine whether increased PGE$_2$ levels due to exogenous AA treatment increase the IPR of *Δplb1* remain inconclusive

In order to determine whether the increased IPR for *Δplb1* observed when exogenous AA was added to infected macrophages (Figure 3. A) was due to increased PGE$_2$ as indicated by the subsequent ELISA experiment (Figure 4), the next step in the project was to perform an IPR experiment with exogenous PGE$_2$. It is likely however that addition of AA to macrophages increases a number of prostaglandins as well as PGE$_2$, therefore to see if the IPR increase seen for *Δplb1* was PGE$_2$ specific or a result of other prostaglandins I also chose to test an addition prostaglandin – PGD$_2$.

Unfortunately, IPR analysis of *Δplb1 i*nfected macrophages after the addition of either PGE$_2$ or PGD$_2$ did not provide conclusive evidence that either prostaglandin can promote *C. neoformans* IPR. The reason for this was because the IPRs for either treatment condition were too variable to accurately determine if any effect was occurring (Figure 5. A and Figure 5. B). Similarly variable results were also seen for viability testing (Figure 5. C). In order to determine if either prostaglandin does influence *C. neoformans* growth within the macrophage optimisation of the experiment or alternatively a new experimental approach is needed.

In conclusion I have found that although co-infection of *Δplb1* with H99 may rescue *Δplb1's* IPR (Figure 2), the addition of exogenous AA can significantly increase the IPR of *Δplb1, but* not intracellular viability (Figure 3). Additionally, I show that *C. neoformans* infected macrophages treated with exogenous AA produce significantly higher levels of PGE$_2$ (Figure 4) indicating that prostaglandin levels may mediate this IPR increase. Taken together this data suggests that eicosanoid levels within infected macrophages do affect *C.*

neoformans IPR in a *Δplb1* dependant manner, however the main source of these eicosanoids is likely to be the macrophage. Although exogenous AA increases the IPR of *Δplb1,* experiments to determine whether this increase is a specific effect of PGE_2 remain inconclusive.
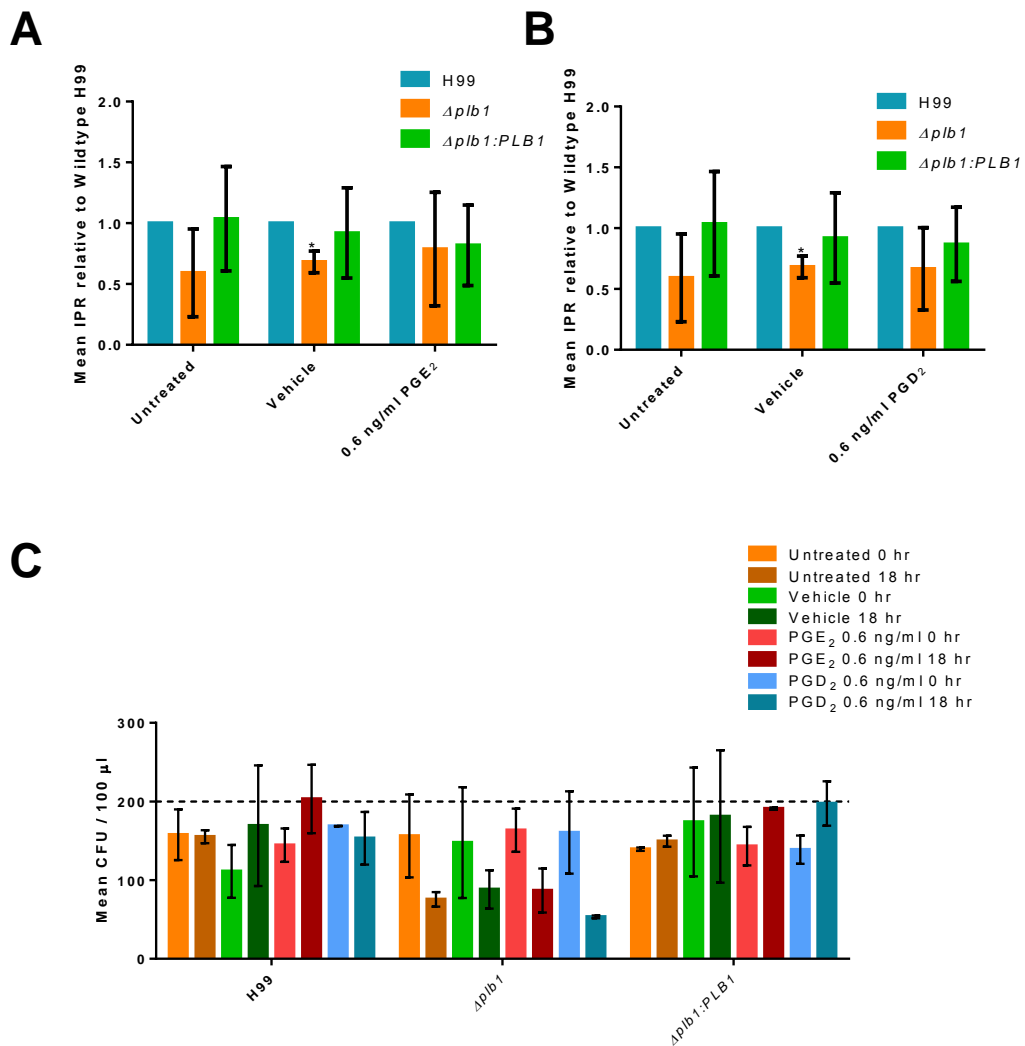
Figure 5 – A Intracellular proliferation of *C. neoformans* strains H99, *Δplb1* and *Δplb1:PLB1* following treatment with 0.6 ng/ml Prostaglandin E₂ (PGE₂). Untreated and vehicle controls (PGE₂ solvent – 100% ethanol) were also performed. IPR is given relative to the H99 wild type strain for each condition. n = 3, error bars = standard deviation. Multiple unpaired T tests performed for each treatment group vs. H99. H99 vehicle control vs. *Δplb1* vehicle control * p= 0.003 **B** Intracellular proliferation of *C. neoformans* strains

H99, *Δplb1* and *Δplb1:PLB1* following treatment with 0.6 ng/ml Prostaglandin D_2 (PGD_2). Untreated and vehicle controls (PGD_2 solvent – 100% ethanol) were also performed. IPR is given relative to the H99 wild type strain for each condition. n = 3, error bars = standard deviation. Multiple unpaired T tests performed for each treatment group vs. H99 vehicle control vs. *Δplb1* vehicle control * p= 0.003. *C.* Viability of *C. neoformans* cells recovered from J774 macrophages following IPR assay. Cells recovered following macrophage lysis were counted and diluted give an expected plated inoculum of 200 cells. n = 2, error bars = standard deviation. Two-way ANOVA with Tukey post test performed to compare time points and treatment for each strain. No significance found.

4. Discussion

I have previously found that Plb1 is required by *C. neoformans* for intracellular proliferation and viability within macrophages (Chapter 2. Figure 4). The purpose of the work described in this chapter was to begin to determine how Plb1 mediates these effects. Within this in mind the theory that I wanted to test was that Plb1 allows *C. neoformans* to produce eicosanoids (Noverr et al., 2003a) which may mimic and interfere with macrophage function during infection.

In Chapter 2, I show that the proliferative and viability defects of the *Δplb1* mutant within macrophages are due to a deficiency in intrinsic *Cryptococcus* Plb1 activity as opposed to secreted Plb1 activity (Chapter 2. Figure 4). To confirm this observation, I designed a co-infection experiment to determine whether the intracellular proliferation defect of the *Δplb1* mutant could be reversed by the presence of H99-GFP within the same macrophage.

I found that co-infection does appear to slightly but significantly rescue the IPR defect of the *Δplb1* mutant (Figure 2), however this experiment had a low number of experimental repeats (n=2) so statistical testing of this effect was not powerful enough to offer firm conclusions. There are also a few caveats to this experiment. Firstly, macrophages were determined to be 'co-infected' if they contained both H99-GFP and *Δplb1* however there was no way to determine if the *Cryptococcus* strains shared the same phagosome. This experimental limitation meant that secreted factors may have gone undetected if they were unable to move between phagosomes. The best way to address this problem in future experiments would be to visualise the phagosome membrane using fluorescent antibodies against a phagosomal marker such as LAMP-1 (Levitz et al., 1999b) and con-focal microscopy. Demarcating the phagosome membrane will allow co-infected *Cryptococcus*

151

strains within the same phagosome to be identified and scored appropriately. The second caveat to the co-infection experiment is that the wild type H99-GFP strain I used was not technically wild type as it has been modified to express a fluorescent tag. Although it is assumed that the H99-GFP strain expresses and secretes normal levels of Plb1 this has not been experimentally determined. It is worth noting that this strain's stress responses and also some key virulence characteristics within macrophages such as intracellular proliferation and phagocytosis have been found to-be very similar to wild type H99, however this said the expression of Plb1 was not a parameter that was tested. It is therefore possible that the genetic manipulation performed on this strain could have affected the expression of Plb1. For proper verification of the data therefore, radiometric analysis of the H99-GFP strain is needed to confirm that it possesses wild type Plb1 activity. If the H99-GFP does have reduced Plb1 activity, then the wild type H99 strain could be used instead with a suitable differentiating stain such as calcofluor white instead of the GFP tag.

Due to the limitations of the co-infection experiment I decided to directly test whether eicosanoids produced during macrophage infection may influence IPR. It has been previously shown that *C. neoformans* produces immune modulatory eicosanoids (Noverr et al., 2001) and that their production is Plb1 dependant unless exogenous AA is provided (Noverr et al., 2003a). This suggests that the role of Plb1 in eicosanoid production is the liberation of AA from cell membranes prior to eicosanoid synthesis.

Interestingly I found that treating *Δplb1* infected macrophages with exogenous AA (30 *µg/ml)* increased *Δplb1's* IPR (Figure 3. A). This indicates that *Δplb1's* intracellular proliferation deficiency may be due to eicosanoid deficiency (Noverr et al., 2003a). Although exogenous AA increases the IPR of *Δplb1,* it does not appear to improve the

reduced viability of the *Δplb1* strain (Chapter 2. Figure 4- B). This is intriguing as it suggests that although the IPR and viability phenotypes observed in the *Δplb1* mutant are both linked to Plb1 they may occur due to divergent aspects of Plb1 deficiency.

C. neoformans produces a number of eicosanoid species (Noverr et al., 2001) however some of the most abundant species produced by the fungus are prostaglandins such as PGE$_2$, PGD$_2$ and PGF$_2$. Although *C. neoformans* produces its own eicosanoids, the macrophages they infect are also key producers during inflammation – especially when exogenous AA is provided (Stenson et al., 1981). For this reason, it was important for me to determine firstly whether the IPR boosting effect of adding AA to infected macrophages was due to increased eicosanoid levels, and secondly to determine whether these eicosanoids were macrophage or *Cryptococcus* derived.

To do this I took the supernatant from *Δplb1* infected macrophages and measured the amount of PGE$_2$ produced after 18 hours of infection with and without exogenous AA treatment (30 *μg/ml)*. Through ELISA analysis of macrophage supernatants, I found that there was no significant difference in the amount of PGE$_2$ produced by H99 or *Δplb1* infected macrophages, and additionally, that uninfected macrophages produced similar amounts of PGE$_2$. Taken together the data suggest that neither Plb1 nor *C. neoformans* infection itself significantly affects the amount of PGE$_2$ produced by infected macrophages. I did find however that treating *C. neoformans* infected macrophages with AA does significantly increase the amount of PGE$_2$ they produce, these findings indicate that the increased IPR of *Δplb1* I observed following AA treatment (Figure 3. A) may have been due to increased amounts of PGE$_2$ within treated macrophages.

The ELISA I used could only determine the amount of PGE$_2$ produced by macrophages; however, it is likely that macrophages produce a range of eicosanoids following exogenous AA treatment. For this reason, addition work must be done to determine which eicosanoids are produced. To do this I could use an ELISA with a much broader specificity – for instance I could use an ELISA which is reactive against all prostaglandin species. This broader approach could then be supplemented by performing additional ELISAs, each specific to a different eicosanoid species in order to pinpoint important species. An alternative method to multiple ELISAs would be to analyse culture supernatants with HPLC – by using [^{3}H]-AA and appropriate standards, multiple radiolabelled eicosanoid species and their relative abundance can be identified in a single experiment (Noverr et al., 2001). Additionally, using HPLC, the type and amount of eicosanoids produced by either *Cryptococcus* or the macrophage during infection could be determined by pre-incubating *C. neoformans* cultures and/ or macrophage monolayers with [^{3}H]-AA before infection.

Finally, to determine whether the increase in IPR seen for *Δplb1* following exogenous AA treatment (Figure 3) was a result of increased PGE$_2$ levels detected by the ELISA (Figure 4). I performed a series of IPR and viability assays as before but instead of treating with exogenous AA, I used exogenous PGE$_2$ (0.6 ng/ml) or PGD$_2$ (0.6 ng/ml). Unfortunately, I found that the IPR and viability data generated was too variable to determine whether these exogenous prostaglandins modulated the IPR of *Δplb1* in the same way that I saw with AA. The reason for this variability is likely to be because prostaglandins are highly volatile molecules and as such it is likely that following addition to tissue culture media they were quickly degraded. This degradation could result in a highly variable amount of prostaglandin actually reaching infected macrophages during each experimental replicate.

154

The simplest way to decrease the variability of this assay would be to perform a greater number of experimental repeats. If this approach does not work, then the assay may need to be adapted to reduce the variability. One solution to this problem might be to use alternative prostaglandin derivatives that are more stable than their natural counterparts. In this respect a more stable PGE_2 derivative called 16, 16-dimethyl prostaglandin E_2 exists. If the breakdown of PGE_2 could be reduced then the concentration of the prostaglandin reaching infected macrophages, and the duration of its effect, could be increased; potentially increasing the efficacy of this treatment. Another alternative could be to selectively target specific prostaglandin receptors with pharmacological receptor agonists. In the case of PGE_2 the EP2 and EP4 have recently been shown to promote *C. neoformans* infection (Shen and Liu, 2015), selective agonists to both of these receptors have been identified and could be used instead of PGE_2 itself (Billot et al., 2003; Paralkar et al., 2003).

In conclusion, thus far experiments with *Δsec14-1* (Chapter 2. Figure 4. A) as well as tentative co-infection data (Figure 2) indicate that a secreted IPR inducing factor is not produced by *C. neoformans* (and specifically it is not likely to be Plb1). I have shown that the IPR deficiency of the *Δplb1* strain can be reversed by treating infected macrophages with exogenous AA (Figure 3 A) which is known to be linked to *C. neoformans* eicosanoid production (Noverr et al., 2003a). ELISA analysis of *C. neoformans* macrophages revealed that exogenous AA treatment increases the levels of PGE_2; however, this $PGE2_2$ is likely to be largely macrophage derived as opposed to being produced by *C. neoformans*. Nonetheless these results indicate that PGE_2 or a related eicosanoid induced by exogenous AA treatment is able to increase the proliferation of *C. neoformans* within macrophages.

Future work must focus on determining which eicosanoids are involved in these effects and additionally how *C. neoformans* and Plb1 fit into this puzzle.

CHAPTER 4 – DEVELOPMENT OF A HIGH THROUGHPUT FLOW CYTOMETRY METHOD FOR THE DETERMINATION OF *CRYPTOCOCCUS* INTRACELLULAR PROLIFERATION

1 - Introduction

During pulmonary cryptococcosis, *Cryptococcus neoformans* is phagocytosed by alveolar macrophages. The function of phagocytosis is to destroy pathogenic organisms, however *Cryptococcus* is able to survive within the macrophage phagosome and proliferate (Feldmesser et al., 2000). Survival and proliferation of *C. neoformans* within macrophages is important to disease pathogenesis, in this respect it has been shown that *C. neoformans* strains which proliferate well inside macrophages have a higher overall virulence compared to strains that proliferate poorly within macrophages (Alanio et al., 2011; Mansour et al., 2011).

1.1 Why a new method for measuring intracellular proliferation is needed.

The study of cryptococcal virulence is currently being revolutionised by the creation of systematic gene knockout libraries (Liu et al., 2008). The library produced by Liu *et al.* (which consists ~1200 gene knockout mutants) represents the first part of a much larger project by the Madhani and Noble groups that aims to create a signature tagged knockout mutant for every expressed gene within the *C. neoformans* genome (with the *C. neoformans var. grubii* serotype A H99 strain as the wild type genetic background). The completion of this library and its subsequent release to the wider scientific community will

provide a powerful resource for researchers as it will allow systematic analysis of all virulence associated genes within the *Cryptococcus* genome. The first 1,201 gene knockout mutants (Liu et al., 2008) are available for purchase as 13 separate 96 well plates; *C. neoformans* is estimated to have ~6500 genes (Loftus et al., 2005) meaning that once finished the completed genome knockout library will be spread over at least 67 plates (assuming the 96 well plate format is maintained).

In order to fully utilise genomic knockout libraries, high throughput protocols must be developed to quickly and accurately interrogate the huge number of mutants involved. Established assays designed to quantify the proliferative capacity of *C. neoformans* strains within macrophages are generally slow and laborious as they require manual quantification of macrophage burden using microscopy analysis. Therefore, there is a need to develop faster protocols for sample preparation and analysis before high throughput analyses can be performed.

1.2 A discussion of existing methodologies

In their 2008 study Liu *et al.* assessed the proliferative capacity for each of their 1,201 mutants by placing them into groups of 48 (where each mutant had a distinct signature tag) and inoculating each group into mice. After the end point of infection, the relative abundance of each mutant within the lungs was determined using quantitative PCR. Using this method Liu *et al.* were able to correlate the virulence of a mutant with its ability to grow within the lung; however with this assay it is difficult to determine whether a mutant's proliferation was intracellular or extracellular during infection (Liu et al., 2008). Additionally, to assay all 1,201 mutants Liu *et al.* used around 75 mice (25 groups of 48, 3 mice per group). To do a similar assay with the full genomic library at least 407 mice

would be needed (136 groups of 48, 3 mice per group). With this in mind it is quite reasonable in terms of ethics, expense and logistics to suggest an alternative *in vitro* screen using a macrophage cell line before *in vivo* work is attempted.

The aim of this project was to optimise the existing intracellular proliferation rate (IPR) assay used by our group (Evans et al., 2015; Ma et al., 2009; Voelz et al., 2009) so that sample analysis could be completed faster. To accomplish this, I adapted the assay so that a flow cytometer could be used to quantify *Cryptococcus* as an alternative to manual counting by haemocytometer.

The IPR assay I adapted is described fully in the materials and methods section of Chapter 2. Briefly J774 murine macrophages are seeded into 24 well plates and infected with antibody opsonised *C. neoformans* cells at an MOI of 1:10 (1×10^5 J774 cells, 1×10^6) *C. neoformans* cells. After two hours of phagocytosis the macrophage monolayer is washed with PBS to remove non phagocytosed cryptococci. Macrophages are then lysed with deionised water (dH_2O) at several time points and the number of *Cryptococcus* cells within each lysate sample quantified. A baseline count is always taken 2 hours after infection (i.e. as soon as non-phagocytosed cryptococci are removed); subsequent time points are usually taken at 18 hours and 24 hours after the baseline time point. The IPR of a strain is calculated by dividing the maximal fungal burden (usually the 18 hour time point) by the baseline - e.g. a baseline count of 2×10^6 cryptococci per ml and an 18 hours count of 4×10^6 cryptococci per ml would give an IPR of 2 ($4 \times 10^6 / 2 \times 10^6 = 2$). The counting of IPR assay samples is normally performed manually using a light microscope and a haemocytometer counting chamber. Depending on the concentration of cryptococci in the cell lysate this counting process can take up to 2 minutes per sample and as such is a rate limiting step in

the assay. By developing a faster method to count each sample, the IPR assay should be more amenable to high throughput analyses of genomic knockout libraries as well as large clinical isolate collections.

The flow cytometer used for this project was a two laser Attune© bench top flow cytometer (Life Technologies – Thermo Fisher Scientific, USA). The advantage of this instrument for the project was that it had been designed for day to day use by a single lab (as opposed to a much more complex central facility flow cytometer). Due to the relative simplicity of the instrument it is possible for lab members to use it with very little experience. An additional advantage of this instrument is the availability of a plate 'autoloader'; this add-on allows an entire 96 or 384 well plate to be analysed automatically using software commands.

Our lab has shown that an IPR assay can be performed using flow cytometry (Voelz et al., 2010). To visualise and count cryptococci within macrophages this assay used a GFP-tagged *C. neoformans* strain. The drawback to this protocol was that the creation of GFP-tagged *C. neoformans* strains was laborious and unfeasible for high throughput screening unless a library is constructed in a fluorescent background. As well as our own group, other groups have also used flow cytometry to measure *Cryptococcus* intracellular proliferation (Alanio et al., 2011). In this study Alanio *et al.* negated the need for GFP - tagged strains by employing calcofluor white (CFW - a chitin specific stain) to stain *C. neoformans* cells and fluorescently conjugated antibodies to differentiate between phagocytosed and non-phagocytosed cryptococci. In their study Alanio *et al.* assayed 54 *C. neoformans* clinical isolates, the need for antibody staining adds additional labour and expense to sample preparation which might make a larger high throughput screen (e.g. 6,500 strains, or even 1,201 strains) difficult to perform in the same way. Another aim of

this project therefore was to ensure that minimal sample preparation was required in order to make the protocol quick, cost effective and compatible with a high throughput 96 well plate format.

Herein I report that that a mixture of two cell dyes - propidium iodide (PI) and CFW – can be used to stain and count *C. neoformans* cells within assay samples using flow cytometry. This staining protocol is quick and easy to perform; additionally I present evidence that the data produced is comparable to manual haemocytometer counting of IPR samples.

2. Materials and methods

2.1 Strains, media and cell lines

Strains used in this work are listed in the Appendix (Appendix Table 1 page 186). *C. neoformans* strains were stored long-term in MicroBank vials at -80°C. Strains were rescued onto YPD agar (YPD 50 g/L Sigma Aldrich, 2 % Agar – Melford) for 48 hours at 25°C and then stored until needed at 4°C. Before experimentation, liquid cultures were grown from these stock plates in 2 ml YPD growth medium (50 g/L) for 24 hours at 25°C under constant rotation.

The J774 murine macrophage cell line used was passaged in DMEM culture media with serum (Dulbecco's Modified Eagle medium, low glucose, Sigma Aldrich, 10 % FBS - Invitrogen, 1% 10,000 units Penicillin / 10 mg streptomycin – Sigma Aldrich, 1 % 200 mM L– glutamine – Sigma Aldrich). Assays were performed with J774 cells between passages 4 and 15. Assays were performed in serum-free DMEM (DMEM high glucose, 1% P/S, 1% L-glutamine) unless otherwise stated.

2.2 Macrophage infection

Briefly, 24 hours before infection, 1×10^5 J774 macrophages were seeded into 24 well plastic plates (Greiner Bio One Cell Star) in 1 ml culture media with serum and incubated for 24 hours at 37°C 5% CO_2. Before infection, J774 cells were activated with 150 ng/ml phorbol 12-myristate 13-acetate in DMSO (Sigma), in 1 ml serum free culture medium for 45 minutes. This media was then replaced with serum-free media alone. Simultaneously, overnight *C. neoformans* cultures grown at 25°C in YPD were washed three times in sterile 1x PBS, counted and adjusted to 1×10^7 cells per ml in PBS before opsonisation for 1 hour

with 10 μg/ml anti capsular 18B7 antibody (a kind gift from Arturo Casadevall, Albert Einstein College of Medicine, New York USA). The activated J774 cells were then infected with 100 μl opsonised *C. neoformans* to give an MOI of 10 (e.g. $1x10^5$ J774 / $1x10^6$ *C. neoformans*) in un-supplemented serum-free DMEM and incubated for 2 hours at 37^oC 5% CO_2. After two hours (time point 0) infected wells were washed at least 3 times with warm 1x PBS until all non-phagocytosed *C. neoformans* cells were removed from the wells.

For calculation of the intracellular proliferation rate the number of internal cryptococci were counted at time point 0 hr and time point 18 (18 hours after time point 0). At each time point each well to be counted was washed three times with 1x PBS to remove any extracellular yeast. The macrophages in the well were then lysed in 200 μl deionised water (dH_2O) for 30 minutes. To remove lysed macrophages and cryptococci a pipette tip was used to scrape the surface of the well, the 200 μl of lysate was then removed to a clean Eppendorf and a further 200 μl dH_2O added to the well to wash any remaining cells, this 200 μl was also added to the Eppendorf to give a final sample volume of 400 μl.

2.3 Manual counting

C. neoformans cells in the lysate were quantified at time points 0 and 18 with a haemocytometer counting chamber and the intracellular proliferation rate (IPR) calculated by dividing the number of cryptococci per 0.1 μl at time point 18 by the same count made at time point 0.

2.4 Flow cytometry counting

IPR lysate samples (macrophage debris and cryptococci washed from infected wells, 400 µl in dH$_2$) were stained with Calcofluor White (CFW - 2 µg/ml final concentration) and Propidium Iodide (PI - 5 µg/ml final concentration), mixed well and incubated for 10 minutes at room temperature before analysis.

Flow cytometry analysis was performed using the Attune blue / violet bench top flow cytometer (Life Technologies, Thermo Fisher Scientific USA). Samples were first visualised using FSC-H (Forward scatter) and SSC-H (side scatter) channels to ensure that events of the correct size and complexity were analysed. The VL1-H channel (430 nm – 470 nm emission wavelength) was used to detect CFW fluorescence, the BL3-H channel (640 nm 'long pass' emission wavelength) was used to detect PI fluorescence and the BL1-H channel (515 nm – 545 nm emission wavelength) was used to detect GFP fluorescence. Baseline PMT sensitivities were set using an unstained sample control before experiments with the unstained signal set to 10^2 relative fluorescence (the recommended baseline for the Attune). Data was acquired at a flow rate of 100 µl/ min; 10,000 events were collected for each sample.

To count each sample, the Attune flow cytometer software was used. Dot plots of BL3-H vs. VL1-H were produced for each sample. First using a macrophage alone sample (macrophage debris, no *Cryptococcus*) a gate was drawn to the bottom right of the macrophage debris population (Figure 5 A), next a sample infected with GFP-tagged *Cryptococcus neoformans* H99 strain was used to confirm the position of the gate in relation to the *Cryptococcus* population (Figure 5 B) (as defined by a GFP positive signal).

Once the position of the gate was verified PI/CFW stain IPR samples could be analysed and counted (Figure 5 C).

To quantify the number of cryptococci within each sample the Attune software was able to output a statistic of 'events per µl' in a defined gate; this output was used for all counts. To calculate the IPR the 'number of events per µl' at 18 hr was divided by the 'number of events per µl' at 0 hr count.

2.5 Statistics

Figure 5:

Figure 5A: Two tailed, unpaired T test performed, comparing methodologies for each strain (e.g. flow cytometry vs. haemocytometer).

Figure 5B: Data was tested for normality using the Shapiro Wilk test (see appendix table 18 page 196). Two tailed, unpaired T test performed, comparing methodologies for each clinical isolate (e.g. flow cytometry vs. haemocytometer).

Figure 6: Two-way ANOVA performed for each sample ('Tube' versus 'Plate' versus 'Haemocytometer' for each sample, no significant differences).

3. Results

It has been already been demonstrated that *Cryptococcus* intracellular proliferation can be quantified using flow cytometry (Alanio et al., 2011; Voelz et al., 2010), however new methodologies must be developed if flow cytometry is to be used as a high throughput screen.

3.1 Flow cytometry analysis of unstained lysate samples revealed that staining was needed to differentiate macrophage debris for *Cryptococcus* cells.

Flow cytometry analysis of unstained IPR samples via forward scatter (FSC - used to express a cell's physical size) and side scatter (SSC – used to express a cell's internal complexity) revealed that all events within the sample clustered into a single homogenous population (Figure 1- A) – this population contained *Cryptococcus* cells as well as partially lysed macrophages and macrophage debris. Thus to accurately quantify the number of *Cryptococcus* cells within the lysate, fluorescent staining was required so that the *Cryptococcus* population could be gated and the macrophage debris discarded.

3.2 The use of a GFP tagged *Cryptococcus* strain confirmed the existence of the *Cryptococcus* population within the lysate.

To confirm where on this dot plot the *Cryptococcus* population resided I used a GFP tagged *C. neoformans* strain (H99-GFP) that could easily be gated using its GFP positive signal (Voelz et al., 2010). By back-gating this GFP positive signal (Figure 1- Bi) to the original FSC/SSC scatter plot, the *Cryptococcus* population could easily be identified within the sample (Figure 1- Bi and Figure 1- Bii).

In order to quantify the *Cryptococcus* population identified using the H99-GFP control for non GFP strains, I needed to design a protocol that would allow me to specifically stain either the macrophage or the *Cryptococcus* populations. By doing so I would be able to produce a fluorescent signal that could be detected by the flow cytometer and gated around to separate each population.
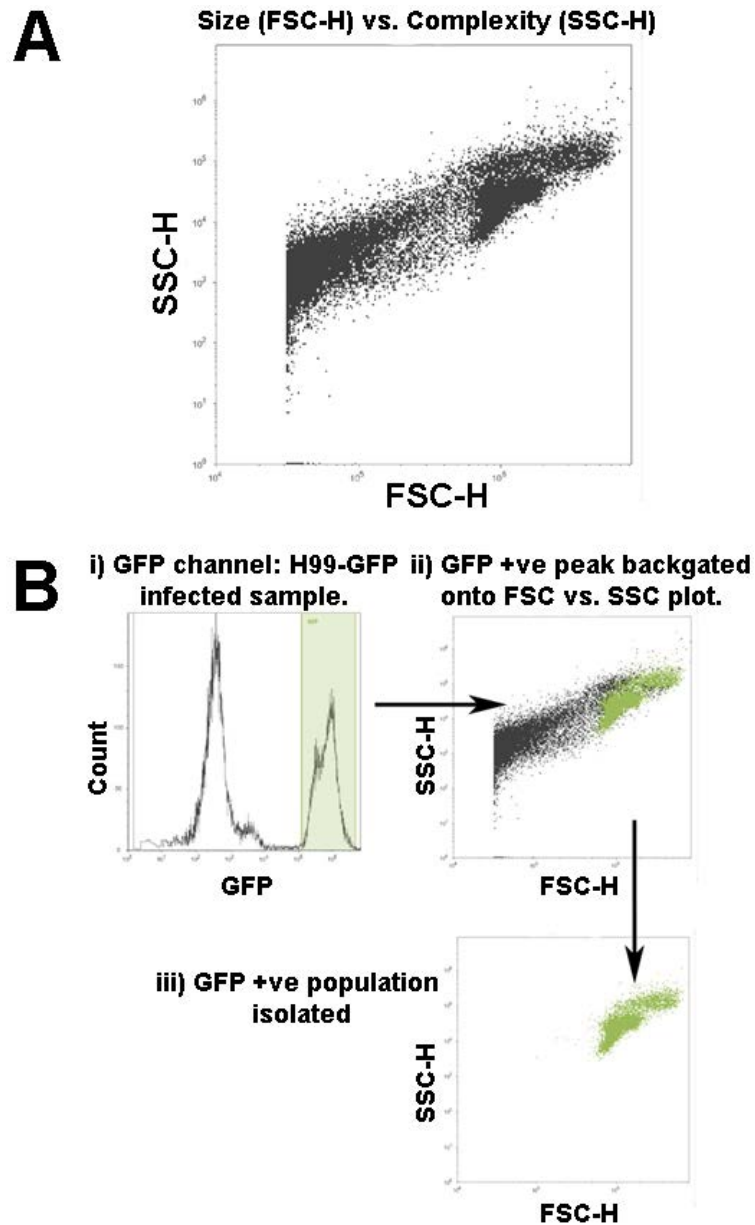
Figure 1: **Flow cytometry method for detecting *C. neoformans* using the H99-GFP strain. A.** Dot plot (FSC-H vs. SSC-H) unstained IPR sample (X axis minimum = 10^4, Y axis minimum 10^2). **B i.** Histogram BL1-H channel (515-545 nm emission wavelength), gated for GFP positive macrophage around 10^6 intensity. **B ii**. GFP positive gate from Bi back gated onto FSC-H vs. SSC-H scatter plot for the same sample. **B iii.** Scatter plot FSC-H vs. SSC-H displaying GFP positive population only.

3.3 Attempts to differentiate the *Cryptococcus* population from macrophage debris using anti-capsular antibody staining indicated that an alternative might be more efficient

My first approach to specifically stain *Cryptococcus* cells within the IPR samples, was to use the 18B7 anti-capsular antibody (a kind gift from Arturo Casadevall) because in theory this antibody should bind only to *C. neoformans* cells, I then used a FITC conjugated anti mouse IgG secondary antibody to allow visualisation using the flow cytometer's BL-1 channel (515nm -545 nm emission wavelength).

Antibody staining of the lysate (primary stain - 1 hour with 10 μg/ml anti capsular 18B7) did reveal a similar population (in terms of position and shape on the dot plot) to the *Cryptococcus* population I had previously identified with GFP H99 (Figure 1- Biii and Figure 2- C). Although the GFP positive *Cryptococcus* population was identifiable, it could not be well resolved from the non-fluorescent signal (Figure 2- B) suggesting that the antibody was staining macrophage debris as well as *Cryptococcus* cells (Figure 2- D). I felt that the overlap between the two populations would make gating too subjective to give an accurate count; additionally, the staining protocol itself was too complicated for high throughput screening of large numbers of samples. For these reasons I decided to try another approach that did not require antibody staining.
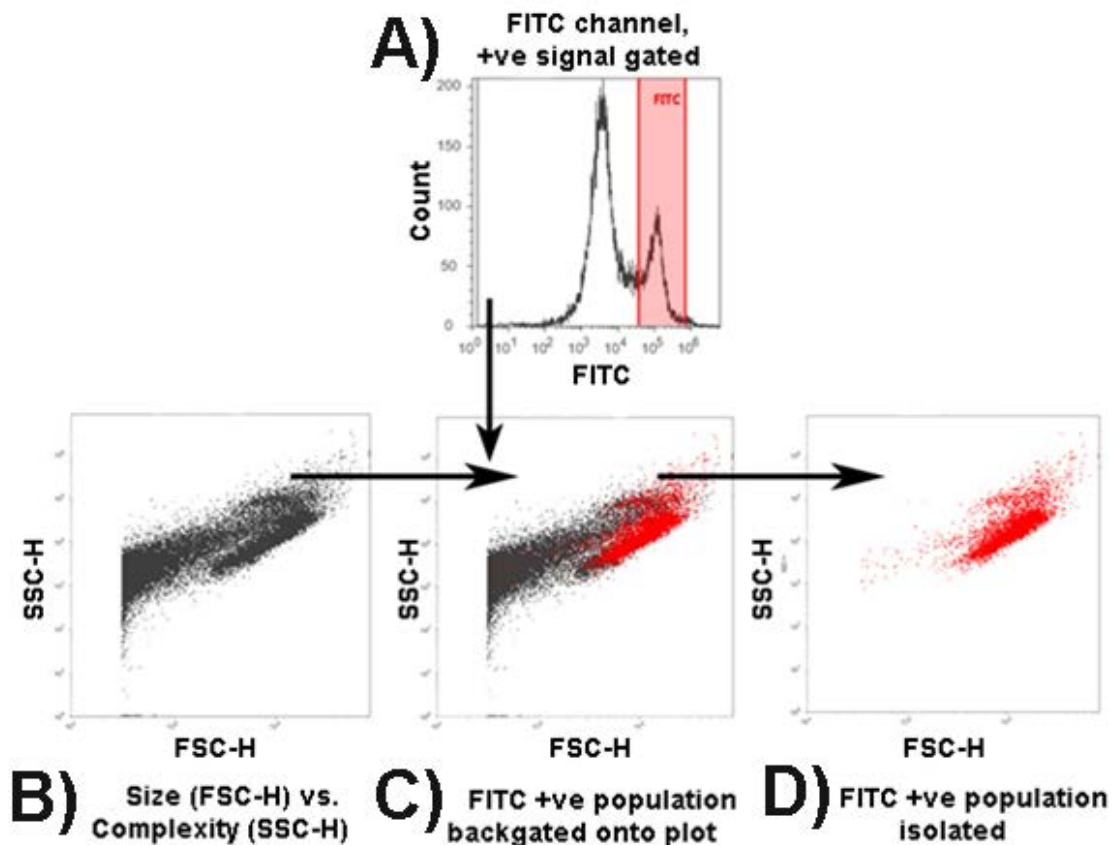
Figure 2: Flow cytometry method for detecting *C. neoformans* using anti capsular antibody staining. A. Histogram BL1-H (FITC channel – 515nm – 545 nm emission wavelength), gate "FITC" shows FITC positive peak. **B.** FSC-H vs. SSC-H scatter plot IPR sample stained with primary anti-capsular antibody and secondary FITC. **C.** FITC positive population back-gated onto FSC-H vs. SSC-H dot plot. **D.** FSC-H vs. SSC-H scatter plot, FITC positive population isolated. Cells stained for 1 hour with 10 μg/ml anti capsular 18B7 antibody (a kind gift from Arturo Casadevall, Albert Einstein College of Medicine, New York USA) and a further 30 minutes with an a rabbit anti mouse IgG FITC conjugated secondary (1:500 dilution, Life Technologies).

3.4 A staining protocol using propidium iodide and calcofluor white proved to be effective at separating *Cryptococcus* and macrophage debris populations during analysis

The poor resolution of populations I observed when I used the anti-capsular antibody led me to me to develop a protocol that used two cell dyes, with different fluorescent signals, to specifically stain both the macrophage and the *Cryptococcus* populations within the sample. The two dyes I selected to do this were Calcofluor white (CFW) and propidium iodide (PI). The reason these two dyes were selected is because CFW stains chitin, which is found in the fungal cell wall but not in mammalian cells, and PI can stain dead cells due its ability to bind to nucleic acids released during cell lysis. I hypothesised therefore that *Cryptococcus* cells would stain PI low and CFW high while the macrophage debris would stain PI high and CFW low.

Flow cytometry analysis of samples stained with PI and CFW revealed two distinct populations (Figure 3- B) – PI was detected using the BL3 channel (640 nm plus emission wavelength) and CFW was detected using the VL-1 channel (430 nm – 470 nm emission wavelength). By running a mock infection control (Figure 3- Cii) (e.g. only macrophage debris) and a H99- GFP control sample (Figure 3- Ciii) the smaller population to the right of the plot was confirmed to be the *C. neoformans* cell population – the GFP signal was detected using the BL-1 channel (515 nm – 545 nm emission wavelength). These data show that using PI and CFW in combination allows *Cryptococcus* cells to be reliably separated from macrophage debris.

The H99-GFP tagged control did reveal that there were detectable GFP signals within the macrophage debris population (Figure 3- Ciii) suggesting that the populations may not be

completely resolved – some of these signals are likely due to auto-fluorescence however it is possible that macrophages that have not completely lysed may still contain some *Cryptococcus* cells.
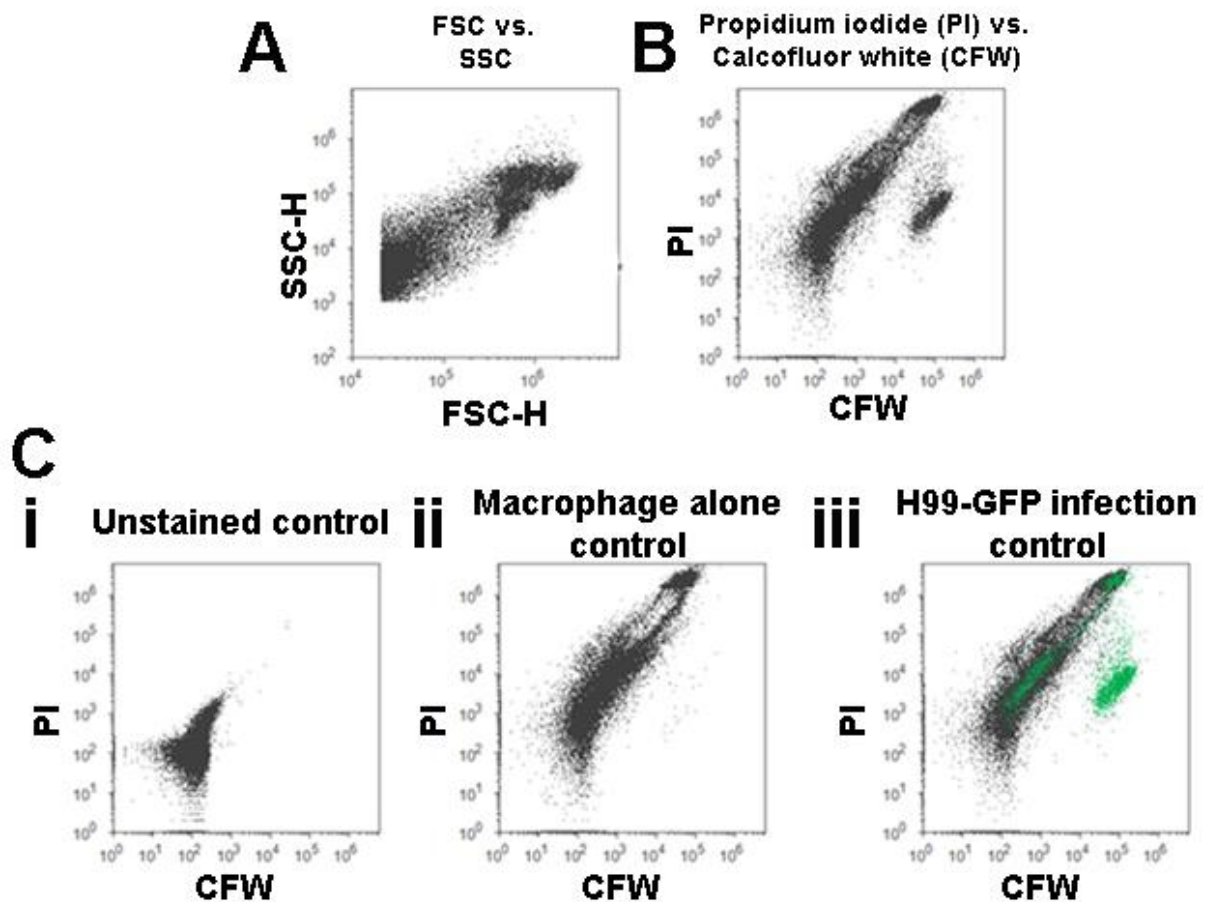
Figure 3: Flow cytometry method for detecting *C. neoformans* using calcofluor white (CFW) and propidium iodide (PI) A. FSC-H vs. SSC-H scatter plot IPR sample stained with CFW and PI **B.** Dot plot (PI vs. CFW) IPR sample stained with Propidium Iodide (PI) and Calcofluor White (CFW), (PI – BL3-H 640 nm plus emission wavelength, CFW – VL1-H 530nm – 570 nm emission wavelength). **C i.** Dot plot (PI vs. CFW) unstained IPR sample (PI – BL3-H 640 nm plus emission wavelength, CFW – VL1-H 530 nm – 570 nm emission wavelength). **ii.** Dot plot (PI vs. CFW) 'macrophage alone' control sample (PI – BL3-H 640 plus emission wavelength, CFW – VL1-H 530 nm – 570 nm emission wavelength). **iii.** Dot plot (PI vs. CFW) H99-GFP infection control sample (PI – BL3-H

173

640 nm plus emission wavelength, CFW – VL1-H 530 nm – 570 nm emission wavelength), GFP positive cells are shown in green.

To count each sample, the Attune flow cytometer software was used. A Dot plot of BL3-H vs. VL1-H was produced to analyse each sample. First using a 'macrophage alone' control (macrophage debris, no *Cryptococcus*) a gate was drawn to the bottom right of the macrophage debris population (Figure 4 - A), next a sample infected with GFP-tagged *Cryptococcus neoformans* H99 strain was used to confirm the position of the gate in relation to the *Cryptococcus* population (Figure 4 - B) (as defined by a GFP positive signal). Once the position of the gate was verified PI/CFW stain IPR samples could be analysed and counted (Figure 4 - C). To quantify the number of cryptococci within each sample the Attune software was able to output a statistic of 'events per µl' in a defined gate; this output was used for all counts. To calculate the IPR the 'number of events per µl' at 18 hr was divided by the 'number of events per µl' at 0 hr count.
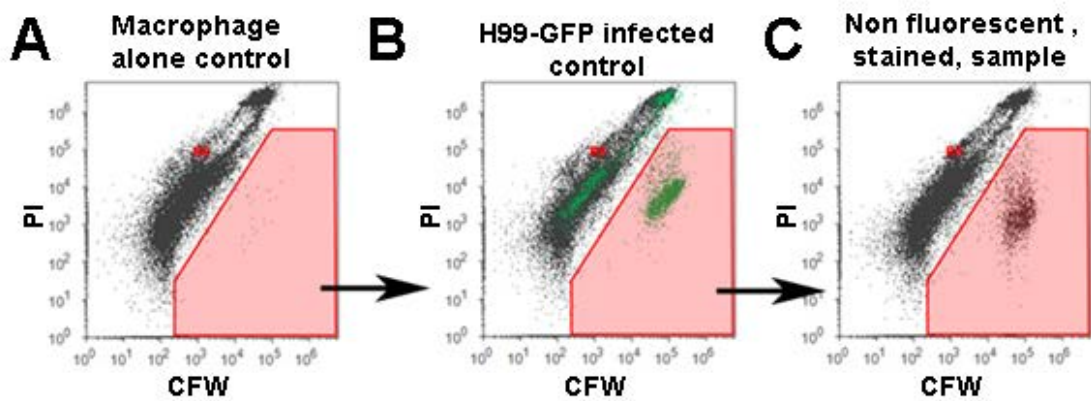
Figure 4 – An example of how an IPR sample is gated and analysed using my new assay. A. First a 'Macrophage alone' control sample is used to determine the boundaries of the macrophage debris; a gate (red box) is drawn where the *Cryptococcus* population is anticipated to be **B.** Next a H99-GFP infected control sample is used to confirm the position of the *Cryptococcus* population and the gate (red box), the GFP positive signal is detected using the BL-1 channel (515 nm – 545 nm wavelength emission) and back-gated onto the dot pot. **C.** Finally, the PI/CFW stained sample(s) are analysed using the drawn gate (red box). The 'number of events per µl' in the drawn gate (red box) is used to quantify the number of cryptococci in the sample.

3.5 Comparing the new flow cytometry based counting protocol against existing haemocytometer counting methods indicates that the new method gives comparable results

To confirm that flow cytometry analysis of IPR samples gave similar results to haemocytometer counting I first analysed three strains that I have used extensively during this research – H99, *Δplb1* and *Δplb1:PLB1*. This set of strains is a useful test for the assay because the *Δplb1* strain (a knockout strain deficient in a *C. neoformans* virulence factor Phospholipase B1) is a *Cryptococcus* mutant that has been previously shown to have a proliferation defect in macrophages. Comparison of analysis methods for these three strains show that flow cytometry counting gives very similar results to the established haemocytometer counting method (Figure 5- A), furthermore a two tailed T test revealed no significant difference between the two methods. To further verify my assay, I tested 6 *C. neoformans* clinical isolates (coded CL1 – CL6) in the same way comparing the haemocytometer count and flow cytometry count of identical samples (Figure 5- B). Once again I found no significant difference between the quantification methods. The fact that the flow cytometry counts are consistent with the haemocytometer counts and that the flow cytometer can detect an intracellular proliferation defect resulting from gene knockout suggesting that my flow cytometry based assay should work with the analysis of gene knockout libraries.
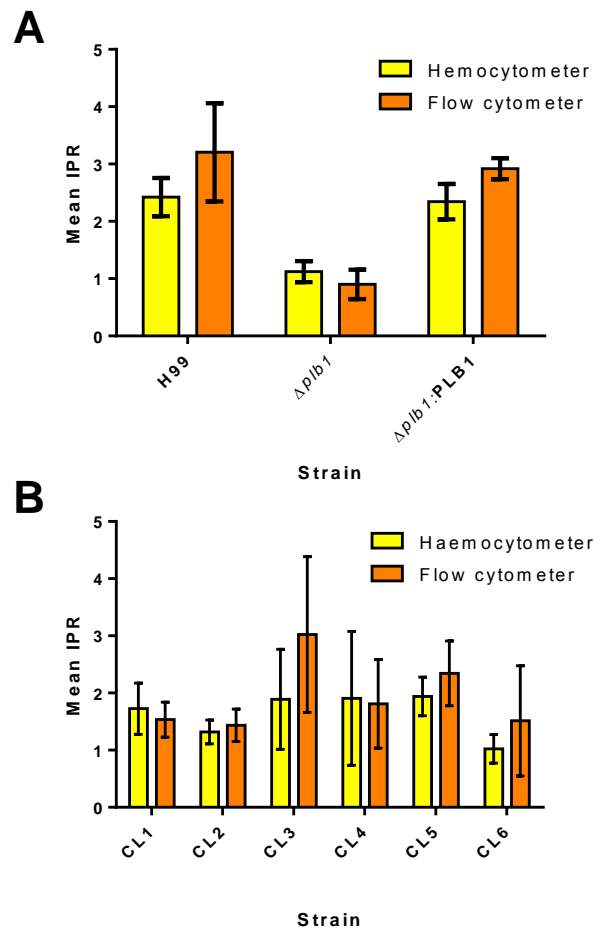
Figure 5 Comparison of identical IPR samples counted with a haemocytometer and the now flow cytometry assay. A. The *Δplb1* strain has been previously shown by myself to have a growth defect compared to its wild type background H99 and a genetic reconstitute *ΔPlb1:PLB1* (Haemocytometer count n = 2, Flow cytometry count n = 3, error bars = standard deviation) Two tailed, unpaired T test performed for each sample (Haemocytometer versus Flow cytometry, no significant differences). **B.** Comparison of identical IPR samples counted with a haemocytometer and the new flow cytometry assay. Six clinical isolates (coded CL1 – CL6) were chosen to represent the real world application of the assay. (n = 3, error bars = Standard deviation). Two tailed, unpaired T test

performed for each sample (Haemocytometer versus Flow cytometry, no significant differences).

In addition to validating the assay versus established counting methods I also began the process of optimising the protocol for high throughput analysis of 96 well plates. In this respect I wanted to test how the assay would work if samples were stained and analysed in a 96 well plates. Up to this point in the project I had stained and analysed IPR samples in 0.5 ml Eppendorf tubes – a potentially huge time and labour saver for high throughput analysis would be if the 'autoloader' add on that is available for the Attune flow cytometer could be used instead.

Comparison of the counts given by the flow cytometer when the same IPR samples were loaded manually in Eppendorf tubes for analysis and also automatically by using a 96 well plate shows that samples can be analysed with the flow cytometer's 'auto loader' add-on with comparable counts to both manual tube loading and also haemocytometer counting (Figure 6).

In conclusion I present a flow cytometry based IPR assay that can significantly increase the speed of determining the intracellular proliferation rate of *C. neoformans* (Figure 3 and Figure 4). This technique uses readily available cell dyes (PI); additionally, once stained, the samples should be able to be analysed on almost all models of flow cytometer that have blue and red lasers. This protocol offers a significant improvement over existing protocols and importantly gives comparable results to existing methods (Figure 5). The ability to analyse strains in a 96 well plate format with this protocol should allow the screening of significantly more strains within a single experiment (Figure 6). This development will allow high throughput analyses of *C. neoformans* gene knockout libraries (Liu et al., 2008) as well as large clinical isolate collections.
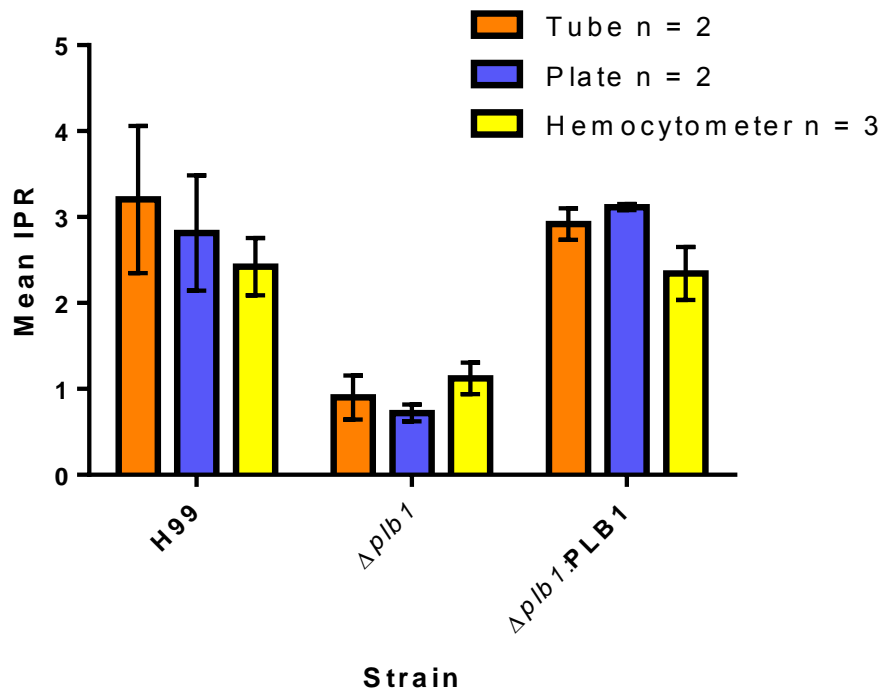
Figure 6 – A comparison between different sample loading methods. The IPR given

when IPR samples were stained and analysed in 0.5 ml Eppendorf tubes (n=2) or a 96 well

plate (n=2, analysed using the Attune 'Auto sampler' add on) were compared to

haemocytometer counts (n=3). Error bars = standard deviation. Two-way ANOVA

performed for each sample ('Tube' versus 'Plate' versus 'Haemocytometer' for each

sample, no significant differences).

4. Discussion

In this project I sought to optimise flow cytometry as a method for determining the intracellular proliferation rate of a *Cryptococcus* strain growing *in vitro* within a macrophage cell line. The assay that I optimised has been widely used by our lab, the rate limiting step of the assay is quantifying the fungal burden of *Cryptococcus* infection macrophages at each time point – currently this is performed manually using a light microscope and a haemocytometer cell counter. The ability to perform this count using a flow cytometer would significantly speed up the assay and mean that many more strains and/or conditions could be analysed within a single experiment. The ability to analyse more samples in a single experiment would make our IPR assay more high throughput and allow analyses of genomic knockout libraries as well as large clinical isolate collections in order to determine genes and factors that help *C. neoformans* replicate within macrophages during host infection.

Our lab has previously used flow cytometry to similar effect however this protocol relied on the creation of GFP tagged *C .neoformans* strains (Voelz et al., 2010). Alanio *et al.* have published an assay that uses flow cytometry to measure the intracellular proliferation of *C. neoformans* however the protocol uses a number of different antibodies to stain cryptococci meaning that the protocol may be too complex for high throughput of whole genome knockout libraries which will likely consist of 6,500 plus mutants (Loftus et al., 2005).

The samples produced by the IPR assay that had to be counted consisted of a mixture of partially lysed macrophages, macrophage debris and *Cryptococcus* cells. The lysis step is required in the assay to release cryptococci from the macrophage so that they can be

182

counted however this step also introduces additional complexity to the count and I found that the physical size (FSC) and complexity (SSC) of the macrophage debris was similar to that of *Cryptococcus* cells (Figure 1- A), this meant that additional staining steps were required in order to resolve the two populations before accurate counts could be made.

The first approach I took to separate the two populations was to stain the *C. neoformans* cells in the lysate with a primary antibody generated against *Cryptococcus* capsule polysaccharide (18B7) and a second FITC conjugated anti mouse IgG antibody. This staining approach did a reasonable job of staining the *Cryptococcus* cells within the lysate; however, there was a high level of unwanted staining within the macrophage population (Figure 2- i). The reason for this was twofold – firstly when using immunohistochemistry there is always the risk of non specific binding of either the primary or secondary antibody. Secondly it has been found that during infection *C. neoformans* sheds capsule polysaccharide into its environment and that this exopolysaccharide can accumulate within macrophages (Eng et al., 1986; Tucker and Casadevall, 2002) – this means that macrophages might have specifically bound 18B7 due to the presence of exopolysaccharide in partially lysed cells. If this were the case it would mean that antibodies against capsule polysaccharide are not a good way to specifically stain *C. neoformans* cells as the polysaccharide is not found exclusively in the *Cryptococcus* capsule during infection.

A second, more successful approach was found to resolve the *Cryptococcus* and macrophage populations in the lysate using two different cell stains – calcofluor white (CFW) and propidium iodide (PI). These two cell stains work in combination to resolve the macrophage and *Cryptococcus* populations within the lysate – CFW specifically stains

Cryptococcus cells by binding to chitin and PI stains lysed macrophages by binding to nucleic acids released during cell lysis. It was anticipated that each stain alone would have background staining and auto-fluorescence issues similar to antibody staining, however in combination it was hoped that resolution would be improved. This proved to be the case as analysis of lysate samples stained with PI and CFW using a dot plot with CFW (VL-1) verses PI (BL-3) revealed two much more distinct populations (Figure 3 – B).

The larger population had variable staining with PI and generally less CFW staining (Figure 3 – B) – this population was identified as the macrophage debris using a control 'macrophage alone' sample that contained lysed macrophages but no cryptococci (Figure 3- Cii). The variability in PI staining is likely due to the heterogeneity of this population as it contains macrophages in varying states of lysis and fragmentation. The second, smaller population stained poorly with PI but stained well with CFW (Figure 3 – B) – by using the H99-GFP tagged *C. neoformans* strain (Voelz et al., 2010) as a control I was able to verify that this population was composed of *Cryptococcus* cells (Figure 3- Ciii).

The H99-GFP tagged control did reveal that there were detectable GFP signals within the macrophage debris population (Figure 3- Ciii) suggesting that the populations may not be completely resolved – some of these signals are likely due to auto-fluorescence however it is possible that macrophages that have not completely lysed may still contain some *Cryptococcus* cells. Optimisation of the lysis step should be able to reduce this from occurring – to optimise I would suggest increasing the lysis time when using dH_2O from what is currently used (30 minutes at $37^{o}C$). Additional lysis efficiency might be achieved by lysing macrophages with a detergent such as Triton X-100 or SDS instead of dH_20. A possibly related observation is that the macrophage debris has at least two different

components − a large proportion of the macrophage debris stains poorly with PI while a smaller part stains well with both PI and CFW (Figure 3 − B). The larger PI^{low} CFW^{low} proportion of the macrophage debris is likely to be well lysed macrophages as well as cellular debris from cell culture and background interference from the PMT detectors, the smaller PI^{high} CFW^{high} proportion is likely to be partially lysed macrophages that may still contain *C. neoformans* cells. While the current analysis is accurate enough to give comparable IPR data to haemocytometer counting, it would be beneficial in the future to examine each of the populations defined by the BL-3/VL-1 dot plot (Figure 3 − B) in order to determine their composition. One way to do this would be to separate each population using FACS and then manually examine each population via microscopy scoring for the occurrence of important observations e.g. extracellular cryptococci/ partially lysed macrophages / partially lysed macrophages containing cryptococci. If the smaller PI^{high} CFW^{high} population did contain partially lysed macrophages with cryptococci inside, then as discussed optimisation of lysis step will be required.

To validate my flow cytometer based assay I have shown that IPR data generated with it is comparable to IPRs calculated using haemocytometer counting (Figure 5). In addition to demonstrating that my flow cytometry assay can detect a known intracellular proliferation defect (Figure 5 −A), I also demonstrate that the assay can be used with a small array of clinical isolates (Figure 5- B). Although the mean IPR result using the flow cytometry method is similar to the haemocytometer result the standard deviation is generally larger, this suggesting that a larger number of replicates may need to be performed when using the flow cytometer assay the get an accurate result − the improved speed of the assay and

subsequently the increased number of conditions that can be tested in a single assay however should hopefully mitigate this requirement.

Finally, I show that the assay can be performed on the Attune$^{©}$ flow cytometer (Life Technologies, Thermo Fisher Scientific) using the 'auto sampler' add on (Figure 6). This add-on allows the user to analyse an entire 96 or 384 well plate automatically. The advantage of analysing samples in this way is two-fold, firstly hands off sample analysis means is a time saver for users as they do not have to load each sample manually. Secondly the ability to analyse a 96 well plate means that the *C. neoformans* genomic knockout library currently under construction (Liu et al., 2008) could be analysed in its supplied 96 well format. By maintaining the same format through macrophage infection, staining and analysis, sample manipulation would be kept to a minimum reducing labour and pipetting error. Keeping to a 96 well format also offers the possibility of using liquid handling robots for sample preparation. With this in mind the next step to optimise the assay for high throughput analysis would be to perform macrophage infection in 96 well plates instead of 24 well plates. Switching plate format is likely to cause increased assay variability as from experience cell seeding densities do not always scale appropriately, additionally the washing steps will become harder as washing efficiency is generally reduced when a smaller well size is used.

In conclusion this chapter reports a successful adaption of an existing IPR assay in order to vastly speed up sample analysis. To do this I have made use of flow cytometry to count *C. neoformans* cells. Experimentation with staining methods revealed that a mix of PI and CFW could consistently separate macrophage debris and *Cryptococcus* components of the sample for counting. Flow cytometry analysis of IPR samples is significantly faster than

the alternative haemocytometer – whereas haemocytometer counting can take up to 3 minutes per sample my flow cytometer method takes about 20 seconds per sample. Importantly this new method of counting gives comparable results to haemocytometer counting (Figure 5); additionally, future optimisation of the protocol should allow the entire assay to be performed in a 96 well plate format (Figure 6). These findings are a significant step towards developing a truly high throughput IPR assay. The development of such as assay will allow researchers to screen large genomic knockout libraries currently being made (Liu et al., 2008) in order to identify every *Cryptococcus* gene associated with intracellular growth within macrophages.

Appendix

1. Supplementary Data

Strain	Description	Reference
H99	*C. neoformans* serotype A mating type α. Wild type parent strain.	
Δplb1	*PLB1* gene knockout	(Cox et al., 2001)
Δplb1:PLB1	*Δplb1* with *PLB1* gene reconstituted	(Cox et al., 2001)
Δsec14	*SEC14-1* gene knockout	(Chayakulkeeree et al., 2011)
Δsec14:SEC14	*Δsec14* with *SEC14-1* gene reconstituted	(Chayakulkeeree et al., 2011)
H99-GFP	H99 strain with GFP under constitutive expression (actin promoter)	(Voelz et al., 2010)

Table 1:

Cryptococcus neoformans strains used in this study

Figure (Chapter 2)	H99 (p value)	*Δplb1* (p value)	*Δplb1:PLB1* (p value)
3B and 4C i)	0.849	0.684	0.409
4D i)	0.694	0.169	0.883
4E i)	0.089	0.764	0.087

Table 2: Shapiro Wilk normality test for phagocytic uptake data (Chapter 2 Figures 3B, 4C i), 4D i) and 4E i). p-value < 0.05 reject null hypothesis that data is not normally distributed

Figure (Chapter 2)	H99 (p value)	Δplb1 (p value)	Δplb1:PLB1 (p value)	Δsec14 (p value)	Δsec14:SEC14 (p value)
4A and 4 Cii	0.214	0.441	0.689	0.731	0.05
4D ii)	0.437	0.871	0.738		
4E ii)	0.323	0.591	0.061		

Table 3: Shapiro Wilk normality test for intracellular proliferation rate data (Chapter 2 Figures 4A, 4C ii), 4D ii) and 4E ii). p-value < 0.05 reject null hypothesis that data is not normally distributed.

Figure (Chapter 2)	H99 (p value)			Δplb1 (p value)			Δplb1:PLB1 (p value)		
	0 hr	18 hr	24 hr	0 hr	18 hr	24 hr	0 hr	18 hr	24 hr
4B	0.163	0.38	0.813	0.896	0.188	0.209	0.611	0.282	0.072
	Δsec14 (p value)			Δsec14:SEC14 (p value)					
	0 hr	18 hr	24 hr	0 hr	18 hr	24 hr			
4B	0.686	0170	0.072	0.153	0.084	0.659			

Table 4: Shapiro Wilk normality test for CFU viability data (Chapter 2 Figure 4B). p-value < 0.05 reject null hypothesis that data is not normally distributed.

Figure (Chapter 2)	H99 (p value)		Δplb1 (p value)		Δplb1:PLB1 (p value)	
	0 hr	18 hr	0 hr	18 hr	0 hr	18 hr
Figure 6 A 'J774 infection'	0.007	< 0.0001	< 0.0001	< 0.0001	0.021	< 0.0001

Table 5: Shapiro Wilk normality test for cell size data (Chapter 2 Figure 6A 'J774 infection'). p-value < 0.05 reject null hypothesis that data is not normally distributed.

Figure (Chapter 2)	H99 (p value)		Δplb1 (p value)		Δplb1:PLB1 (p value)	
	0 hr	18 hr	0 hr	18 hr	0 hr	18 hr
Figure 6 A 'DMEM control'	0.109	< 0.0001	0.071	< 0.0001	0.146	< 0.0001

Table 6: Shapiro Wilk normality test for cell size data (Chapter 2 Figure 6A 'DMEM control'). p-value < 0.05 reject null hypothesis that data is not normally distributed.

Figure (Chapter 2)	H99 (p value)		Δplb1 (p value)		Δplb1:PLB1 (p value)	
	0 hr	18 hr	0 hr	18 hr	0 hr	18 hr
Figure 6 B 'J774 infection'	0.109	< 0.0001	0.072	< 0.0001	0.146	< 0.0001

Table 7: Shapiro Wilk normality test for cell size data (Chapter 2 Figure 6B 'J774 infection'). p-value < 0.05 reject null hypothesis that data is not normally distributed.

Figure (Chapter 2)	H99 (p value)		Δplb1 (p value)		Δplb1:PLB1 (p value)	
	0 hr	18 hr	0 hr	18 hr	0 hr	18 hr
Figure 6 B 'DMEM control'	< 0.0001	0.0001	0.0012	0.0001	< 0.0001	< 0.0001

Table 8: Shapiro Wilk normality test for cell size data (Chapter 2 Figure 6B 'DMEM control'). p-value < 0.05 reject null hypothesis that data is not normally distributed.

Figure (Chapter 2)	H99 (p value)		Δplb1 (p value)		Δplb1:PLB1 (p value)	
	0 hr	18 hr	0 hr	18 hr	0 hr	18 hr
Figure 6 C 'J774 infection'	0.21	0.0010	0.14	0.92	< 0.0001	< 0.0001

Table 9: Shapiro Wilk normality test for cell size data (Chapter 2 Figure 6C 'J774 infection'). p-value < 0.05 reject null hypothesis that data is not normally distributed.

Figure (Chapter 2)	H99 (p value)		Δplb1 (p value)		Δplb1:PLB1 (p value)	
	0 hr	18 hr	0 hr	18 hr	0 hr	18 hr
Figure 6 C 'DMEM control'	< 0.0001	0.0001	0.0012	0.0001	< 0.0001	< 0.0001

Table 10: Shapiro Wilk normality test for cell size data (Chapter 2 Figure 6C 'DMEM control'). p-value < 0.05 reject null hypothesis that data is not normally distributed.

Figure (Chapter 2)	H99 (p value)		Δplb1 (p value)		Δplb1:PLB1 (p value)	
	0 hr	18 hr	0 hr	18 hr	0 hr	18 hr
Figure 6 D 'J774 infection'	< 0.0001	< 0.0001	< 0.0001	0.0001	< 0.0001	0.0001

Table 11: Shapiro Wilk normality test for cell size data (Chapter 2 Figure 6D 'J774 infection'). p-value < 0.05 reject null hypothesis that data is not normally distributed.

Figure (Chapter 2)	H99 (p value)		Δplb1 (p value)		Δplb1:PLB1 (p value)	
	0 hr	18 hr	0 hr	18 hr	0 hr	18 hr
Figure 6 D 'DMEM control'	< 0.0001	< 0.0001	< 0.0001	0.001	< 0.0001	0.0001

Table 12: Shapiro Wilk normality test for cell size data (Chapter 2 Figure 6D 'DMEM control'). p-value < 0.05 reject null hypothesis that data is not normally distributed.

Measurement	Comparison	P value	Mann-Whitney U	Difference between medians (actual)
Cell body diameter (Chapter 2. Figure 7- A)	H99 0hr vs. H99 18hr	0.0001	1.014e+006	-0.2028
	Δplb1 0hr vs. *Δplb1 18hr*	< 0.0001	546491	1.208
	Δplb1:PLB1 0hr vs. *Δplb1:PLB1* 18hr	< 0.0001	1.956e+006	-0.5025
Capsule thickness (Chapter 2. Figure 7 - B)	H99 0hr vs. H99 18hr	< 0.0001	11394	1.280
	Δplb1 0hr vs. *Δplb1 18hr*	< 0.0001	3745	3.959
	Δplb1:PLB1 0hr vs. *Δplb1:PLB1* 18hr	< 0.0001	10367	1.371
Total diameter (Chapter 2. Figure 7 - C)	H99 0hr vs. H99 18hr	< 0.0001	10680	0.8187
	Δplb1 0hr vs. *Δplb1 18hr*	< 0.0001	1216	7.275
	Δplb1:PLB1 0hr vs. *Δplb1:PLB1* 18hr	< 0.0001	11269	2.156
Ratio cell body to capsule (Chapter 2. Figure 7- D)	H99 0hr vs. H99 18hr	< 0.0001	10608	0.1257
	Δplb1 0hr vs. *Δplb1 18hr*	< 0.0001	2504	0.5094
	Δplb1:PLB1 0hr vs. *Δplb1:PLB1* 18hr	0.6907	19736	0.008603

Table 13 – Mann Whitney U test statistical analysis for cell size experiments 'J774 infection' condition – Chapter 2. Figure 6 – A,B,C,D.

Measurement	Comparison	P value	Mann-Whitney U	Difference between medians (actual)
Cell body diameter (Chapter 2. Figure 7- A)	H99 0hr vs. H99 18hr	< 0.0001	132678	-0.8300
	Δplb1 0hr vs. *Δplb1 18hr*	< 0.0001	165572	-0.6700
	Δplb1:PLB1 0hr vs. *Δplb1:PLB1* 18hr	< 0.0001	159019	-0.4900
Capsule thickness (Chapter 2. Figure 7- B)	H99 0hr vs. H99 18hr	< 0.0001	7343	2.340
	Δplb1 0hr vs. *Δplb1 18hr*	< 0.0001	9941	2.330
	Δplb1:PLB1 0hr vs. *Δplb1:PLB1* 18hr	< 0.0001	8137	1.500
Total diameter (Chapter 2. Figure 7- C)	H99 0hr vs. H99 18hr	< 0.0001	12835	3.410
	Δplb1 0hr vs. *Δplb1 18hr*	< 0.0001	11712	2.975
	Δplb1:PLB1 0hr vs. *Δplb1:PLB1* 18hr	< 0.0001	14594	2.200
Ratio cell body to capsule. (Chapter 2. Figure 7- D)	H99 0hr vs. H99 18hr	0.0675	41824	-0.01000
	Δplb1 0hr vs. *Δplb1 18hr*	< 0.0001	13214	0.3750
	Δplb1:PLB1 0hr vs. *Δplb1:PLB1* 18hr	< 0.0001	24158	0.0600

Table 14 – Mann Whitney U test statistical analysis for cell size experiments 'DMEM control' condition – Chapter 2. Figure 6 – A,B,C,D.

Figure (Chapter 3)	H99	Δplb1 (p value)			Δplb1:PLB1 (p value)		
		Untreated	Vehicle	Eicosanoid	Untreated	Vehicle	Eicosanoid
3A (AA)	N/A	0.1114	0.2606	0.7123	0.7168	0.1885	0.8798
5A (PGE$_2$)	N/A	0.72	0.053	0.004	0.618	0.943	0.562
5B (PGD$_2$)	N/A	0.717	0.053	0.937	0.618	0.943	0.479

Table 15: Shapiro Wilk normality test for intracellular proliferation data (Chapter 3 Figures 3A, 5A and 5B).

Figure (Chapter 3)	H99 0hr (p value)			H99 18 hr (p value)			Δplb1 0hr (p value)		
	Un-treated	Vehicle	AA	Un-treated	Vehicle	AA	Un-treated	Vehicle	AA
3B	0.114	0.638	0.252	0.654	0.149	0.659	0.905	0.972	0.413
	Δplb1 18hr (p value)			Δplb1:PLB1 0hr (p value)			Δplb1:PLB1 18hr (p value)		
	Un-treated	Vehicle	AA	Un-treated	Vehicle	AA	Un-treated	Vehicle	AA
3B	0.179	0.799	0.333	0.748	0.301	0.474	0.550	0.465	0.119

Table 16: Shapiro Wilk normality test for CFU viability data (Chapter 3 Figure 3B).

	Untreated	Vehicle control	Arachidonic Acid
H99	0.934	0.1966	0.239
Δplb1	0.704	0.951	0.274
Δplb1:PLB1	0.278	0.512	0.939
Uninfected control	0.153	0.368	0.36

Table 17: Shapiro Wilk normality test for PGE$_2$ EIA ELISA data (Chapter 3 Figure 4).

	Haemocytometer	Flow cytometer
CL1	0.185	0.599
CL2	0.078	0.549
CL3	0.757	0.417
CL4	0.523	0.688
CL5	0.926	0.766
CL6	0.346	0.346

Table 18: Shapiro Wilk normality test for Flow cytometry IPR method comparison data (Chapter 4 Figure 5B).

2. Purification and crystallisation of the *C. neoformans* protein CnLyso1

2.1 Introduction

To date crystallographic study of cryptococcal proteins has been limited. A species search of the RCSB protein databank (http://www.rcsb.org/pdb) for *Cryptococcus neoformans* returns 24 crystal structures representing 15 unique proteins. Only 3 structures have been reported at a resolution smaller than 2 Å.

C. neoformans expresses an independent enzyme to CnPlb1 which only exhibits lysophospholipase and lysophospholipase transacetylase activities. *LYSO1* encodes the 426 amino acid protein CnLyso1 which has a predicted molecular weight of 48.3 kDa, although analysis of secreted fractions suggest the protein may exist as a dimer or trimer with a size of 97 − 140 kDa. Interestingly enzyme activity experiments using a *LYSO1* knockout *C. neoformans* mutant suggests that expression of *LYSO1* is required for wild type levels of CnPlb1 activity. This suggests that CnPlb1 and CnLyso1 may interact post translationally.

I attempted to clone and purify two cryptococcal proteins associated with phospholipid modification – Phospholipase B1 and Lysophospholipase. Lysophospholipase was the first protein I attempted to purify and crystallise; this was because this protein had fewer glycosylation that CnPlb1 and as a result biologically active protein should have been expressible in *E. coli*. In contrast CnPlb1 has glycosylation sites which are needed for full activity. Thus for CnPlb1 a different approach would be needed, it is likely that I would have had to express the protein in a eukaryote such as *Pichia pastoris* in order to obtain active protein.

I attempted to express two versions of CnLyso1; the full length protein and a truncated protein which has had the first 85 amino acids cleaved from the N terminus, the reasoning behind this being that these amino acids are not predicted to contribute to the protein structure and may in fact hinder successful purification. The vector system I used to express CnLyso1 was the pMALx vector – either the pMALc (cytoplasmic) or pMALp (periplasmic variant. Expression of eukaryotic proteins in a prokaryote like *E. coli* can lead to problems in post translational modification and folding. Expression of the protein with a periplasmic transport tag may improve folding efficiency.

Although I managed to construct the clones, preliminary expression experiments indicated that optimisation of expression; purification and crystallisation would take more time than was availible. The results presented below are given as record for future researchers.

2.2 Materials and methods

Primers

All of the Primers used in this project were ordered from MWG-biotech. For cloning the following primers were used: pMALxLongFwd 5'-CAA CAA CCT CGG GAT CGA GGG AAG GAT GCC ACT TCA CAA TCC CAT CTG G-3', pMALxShortFwd 5'-CAA CAA CCT CGG GAT CGA GGG AAG GGA AGA ACT TGA TTC TGG CGC CAA ACG-3' , pMALxRev 5'-GGT TTT CCC AGT CAC GAC GTT GTA AAA CCT AGC ATC GCT GCA CCA GCC ACG AGC G-3'. For sequencing the following primers were used: pMALxSeqFwd 5'-ACT GTC GAT GAA GCC CTG AA-3', pMALxSeqRev 5'-GCG GGC CTC TTC GCT ATT AC-3'. Unless otherwise stated primers were used in the following pairs – PP1 (pMALx:Cn*LYSO1* full length) – pMALxLongFwd and pMALxRev. PP2 (pMALx:Cn*LYSO1* truncated) – pMALxShortFwd and pMALxRev.

Cloning

Amplification of the *LYSO1* from our source plasmid and subsequent transfer into the target plasmids was performed using an adapted restriction free protocol from van den Ent et al. (Van den Ent at al. 2006 J. Biochem. Biophys. Methods 67 (2006) 67 - 74). Restriction free cloning is a method for cloning a gene of interest into a target plasmid without the use of restriction enzymes. The protocol requires two PCR reactions. In the first reaction the gene of interest is amplified from a source plasmid using a pair of ~48 bp primers (ending in a 3' G or C) designed to complement ~24 bp from the gene of interest as well as a ~24 bp flanking region at either the 5' (forward primer) or 3' (reverse primer) of the insertion site. In the second PCR the product from the first reaction is mixed with the

empty target plasmid. Linear (rolling circle) replication of the plasmid occurs however the newly replicated plasmid contains the gene insert. Following the reaction un used template plasmid is degraded with Dpn1 enzyme. The plasmid can then be transformed into suitable *E. coli* strains, firstly DH5a is used for plasmid propagation and confirmation of gene insert using sequencing and the BL-1 for expression.

The source plasmid containing full length cryptococcal *LYSO1* was a kind gift from a collaborator (Julie Djordjevic, Centre for Infectious Diseases and Microbiology, Westmead Millennium Institute, Sydney, Australia). For the first PCR reaction 1 µl source plasmid (1:10 diluted from stock) was mixed with 2.5 µl of each forward and reverse primer (PP1 or PP2 100 pmol/ µl), 4 µl dNTP mix (Bioline, 5 mM stock concentration for each dNTP), 1 µl Phusion polymerase (New England Biolabs), 20 µl 5X Phusion HF buffer, 3 µl DMSO, 2 µl 2.5nM MgCl$_2$. The reaction volume was then made up to 100 µl with sterile deionised water. The PCR program followed the conditions recommended for the Phusion polymerase – an initial denaturation step of 98 ^{o}C for 30 seconds then 35 cycles of denaturation at 98 ^{o}C for 10 seconds, annealing at 57 ^{o}C for 30 seconds and extension at 72 ^{o}C for 40 seconds (15-30 seconds per kb), followed by a final extension step at 72 ^{o}C for 10 minutes.

Following the first PCR reaction, the PCR products were checked for purity on a 2 % agarose gel (100 V ~ 30 minutes). Reactions giving a single clean band at the right size were purified using the QIAquick PCR purification kit (Qiagen) following the instructions provided.

For the second PCR reaction the following mix was used: 4 µl PCR product from the first reaction, 2 µl dNTP mix, 20 µl Phusion 5X HF buffer, 1 µl Phusion polymerase and 1 µl

target plasmid (used at stock concentration or diluted 1:5 or 1:40 in sterile deionised water). The reaction volume was then made up to 100 µl with sterile deionised water. Each 100 µl reaction was then split into three separate tubes (e.g. 33 µl each) marked A, B or C.

The PCR program used had an initial denaturation step at 98 ^{o}C for 30 seconds followed by 35 cycles of the following: denaturation at 98 ^{o}C for 30 seconds for tubes A, B and C. Then an annealing step where a temperature gradient was used, tubes marked A were annealed at 62 ^{o}C, tubes marked B at 55.5 ^{o}C and tubes marked C at 50 ^{o}C all for 30 seconds, then an extension step at 72 ^{o}C for 12 minutes was applied to tubes A, B and C. Finally a extension step at 72 ^{o}C for 10 minutes was used.

Dpn1 digestion

After the second PCR program all unreplicated target plasmid was removed using a Dpn1 digest − newly synthesised copies of the plasmid with *LYSO1* inserted are not methylated whereas any leftover target plasmid is. For each 33 µl PCR reaction the following was added − 1 µl Dpn1 (New England Biolab 20,000 units/ml), 1.1 µl B4 buffer and 14.9 µl sterile deionised water   to give a digestion reaction volume of 50 µl. Tubes were digested at 37 ^{o}C for 5 hours. Tubes A, B and C for each condition were then combined and purified using the QIAquick PCR purification kit.

Transformation

Following purification, the pMALx plasmid with either full length or truncated *LYSO1* inserted was transformed into *E. coli* strain DH5a − 80 µl chemically competent *E. coli* were added to 12 µl of the purified PCR product, mixed and left on ice for 20 minutes. The

cells were then heat shocked at 42 ^{o}C for 90 seconds and then rested on ice for 5 minutes, 700 µl SOC (Super Optimal broth with Catabolite repression) was added then to each tube before incubating at 37 ^{o}C / 200 rpm shaking for one and a half hours. The tubes were then centrifuged at 13g for 1 minute to pellet the cells which were then concentrated by resuspending in 100 µl of the original supernatant. This 100 µl was then streaked onto an LB agar plate with Carbenicillin selection (100 µg/ml) and incubated at 37 ^{o}C overnight to allow transformed colonies to grow.

Colonies which had grown overnight were tested for the presence of the *LYSO1* gene with colony PCR using the primer pairs used in the first round of PCR. Colonies showing positive bands for the colony PCR were grown up in overnight culture with selection and mini-prepped. The purified plasmid was sequenced in the School of Biosciences Central Genomic facility using pMALxShortFwd and pMALxRev – primers to confirm proper insertion of *LYSO1*. For expression the completed plasmid was cloned into *E. coli* BL-1.

IPTG induction small scale

A single colony of each transformant was picked and grown in a 10 ml overnight LB culture with 100 µg/ml carbenicillin. This overnight culture was diluted 1:100 into fresh LB and incubated for 3 hours at 37 ^{o}C with 200 rpm shaking. After 3 hours 1 µl/ml 10mg/ml IPTG was added to induce expression and the culture was incubated for a further 3 hours.

Samples from each culture were taken and checked for OD to equalise protein levels for gel loading. Samples were lysed in SDS loading buffer at 100 ^{o}C for 10 minutes then

centrifuged to clear particular debris. Samples were analysed on a 10 % acrylamide SDS-PAGE gel run at 150 v for hour before coomassie staining.

Auto induction

The autoinduction media had the following composition: 10 g/L tryptone, 5 g/L yeast extract, 25 mM g/L Na_2HPO_4, 25 mM KH_2PO_4, 50 mM NH_4CL, 2 mM $MgCl_2$, 0.5% glycerol, 0.05 % glucose, 0.2 % lactose and 5 ml/L trace metal solution, 100 μg/L carbenicillin [80].

A 10 ml overnight culture grown from a single colony of transformed BL-1 *E. coli* was grown at 37 °C with 200 rpm shaking under selection with 100 μg/ml carbenicillin in half strength LB broth. This culture was diluted 1:100 into 400 ml autoinduction media in a 2L conical flask. The flask was incubated at 37 °C for 4.5 hours with 200 rpm shaking and then incubated at 18 °C overnight with 200 rpm shaking. After overnight incubation cultures were pelleted at 6000 rpm for 8 minutes 4 °C, the supernatant was then discarded, the pellets weighed and frozen at -80 °C.

Protein purification

The frozen pellet was removed from -80 °C and allowed to thaw before being resuspended in 40 ml 'MBP binding buffer' or buffer 'A' (20 mM Tris Hcl pH 7.4, 200 mM NaCl, 1 mM EDTA) and left to mix for 45 minutes before being chilled on ice. Cells were then lysed via sonication at 40 % power for eight 20 second bursts interspaced with chilling on ice.

Cell lysate was clarified in two centrifugation steps. The first centrifugation at 15,000 g for 25 minutes, the second at 50,000 g for one hour, both at 4 $^{\circ}$C. For both steps the supernatant was retained and the pellet discarded.

The clarified lysate (also known as 'onto') was loaded onto a 5 ml MBP column (GE healthcare), the column was then washed with several column volumes of buffer A before protein elution with MBP 'elution buffer' or 'buffer B' (20 mM Tris HCL pH 7.4, 200 mM NaCl, 1 mM EDTA and 10 mM Maltose), eluted fractions were retained and tested for protein concentration with Bradford's reagent and analysed with SDS-PAGE and western blotting.

2.3 Results

The cloning and purification of CnLyso1 in *E. coli* was to be attempted before CnPlb1. To maximise our chances of producing functional, soluble protein we chose to express CnLyso1 using in two different cellular locations – within the cytosol or transported to the periplasmic space. For this we chose to express CnLyso1 using the pMALx vector system as cytoplasmic (pMALc) and periplasmic (pMALp) variants of the vector exist. In addition to varying protein localisation we also attempted to optimise future crystallisation by creating a truncated version of CnLyso1 with the first 85 amino acids cleaved from the N terminal – these amino acids were not predicted to contribute to the overall structure of CnLyso1 and thus might affect successful crystallisation of the protein. Thus we planned to produce four different clones – pMALc: *LYSO1* 'full length', pMALc: *LYSO1* 'truncated', pMALp: *LYSO1* 'full length' and pMAL:*LYSO1* 'truncated'.

To clone *LYSO1* into the pMALx vectors we used restriction free cloning. Full length or truncated copies of the *LYSO1* gene were first amplified from a plasmid containing cryptococcal *LYSO1* (kindly provided by our collaborator Julie Djordjevic). The purify of this amplification was checked on a 4 % agarose gel (Figure 1), for each reaction this revealed clean single bands at the approximate size for each product.
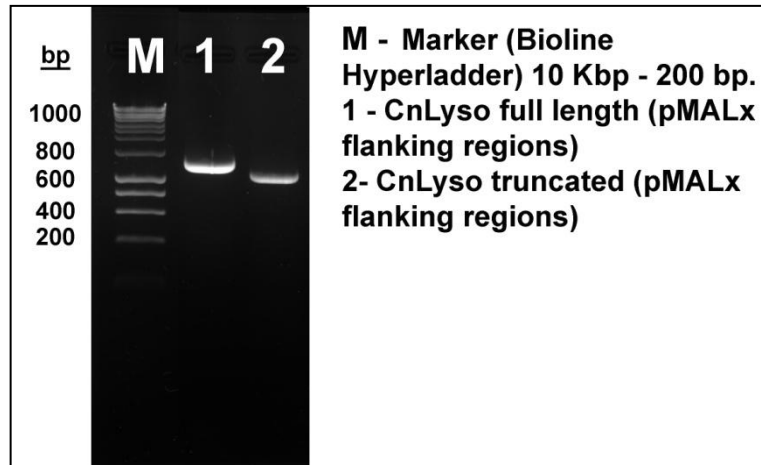
Figure 1 – 4 % agarose gel to check the purity of each primary PCR reaction. Lane 1 – *LYSO1* full length, Lane 2 – *LYSO1* truncated.

The resulting purified fragment from each amplification product were mixed with empty pMALc or pMALp vector in a second PCR reaction where the empty plasmid replicates via rolling circle replication, however when the plasmid replicates there is a chance that the DNA fragment containing the *LYSO1* gene will be incorporated into the plasmid at the appropriate integration site. Following PCR left over empty plasmid (methylated DNA) was removed from the reaction using Dpn1 leaving only newly synthesised plasmid copies (unmethylated). The plasmids were then transformed into DH5a *E. coli*. Resulting colonies were tested for the presence of the insert using colony PCR. Positive colonies were sequenced to confirm *LYSO1* was present and correctly inserted into the plasmid.

Interestingly doing the colony PCR I encountered a high occurrence of false positives – e.g. colonies which appeared positive during colony PCR but when sequenced did not contain *LYSO1* but instead empty vectors. The reason for these false positives was unclear however it may be due to *E. coli* cells becoming coated with empty vector and the *LYSO1* gene fragment during transformation but not internalising the molecules. Modification of

the sequencing step improved the detection rate. Initially I was using the same primers for both sequencing and the initial PCR step; these primers complement sequence in both the gene of interest and the target plasmid. Switching to new sequencing primers one of which only complemented the plasmid and one which only complemented *LYSO1* decreased the number of false positives occurring, hugely improving the efficiency of the protocol.

An initial small scale expression was performed with the first clone to be completed – pMALc: *LYSO1* truncated. Expression of CnLyso1 was tested in three successful *E. coli* BL-1 transformants – A, B and C. A clear band at ~40 kDa is visible for each induced culture (+ve) but not for unindicted cultures (-ve). This band would match the size of truncated CnLyso1, however it does not match the total size of the CnLyso1: MBP fusion protein – therefore if this band does show IPTG dependant expression it is not the complete, tagged protein (Figure 2).
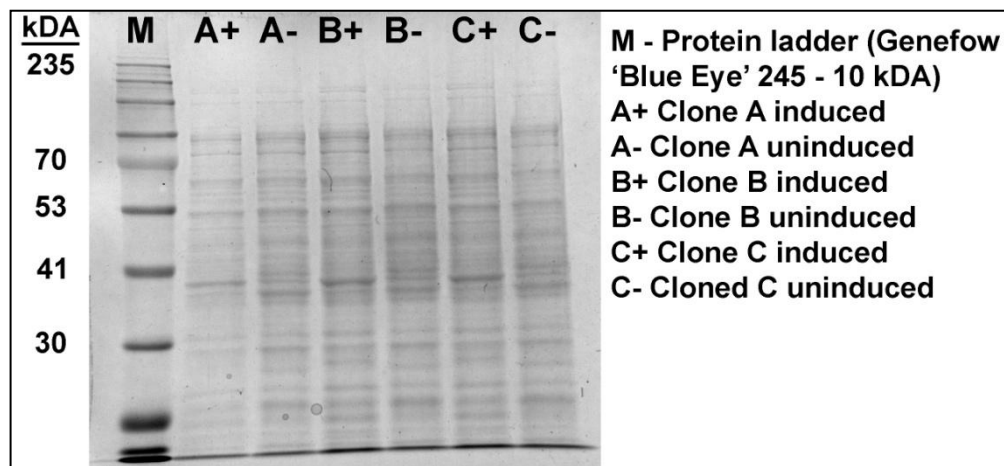
Figure 2 - Small scale expression study with IPTG induction using the pMALc: *LYSO1* construct transformed into *E. coli* BL-1. 10 % acrylamide gel run for 1 hour at 150 V.

Once all four clones were completed it was decided to try auto induction instead of IPTG induction to see if this would improve the yield and stability of the expressed protein. From

experience auto induction generally produces high yields of protein, if this is the case with SDS-PAGE the band containing the tagged protein should be much larger than the background lysate. Following autoinduction a small sample of each culture was taken and lysed in SDS running buffer before running on SDS-PAGE. Examining the gel there are no bands at the expected size for either the full length CnLyso1: MBP (~100 kDa) or fragmented length that stands out from the background of the lysate. This suggests that if the protein is being expressed it is being expressed at low levels (Figure 4)
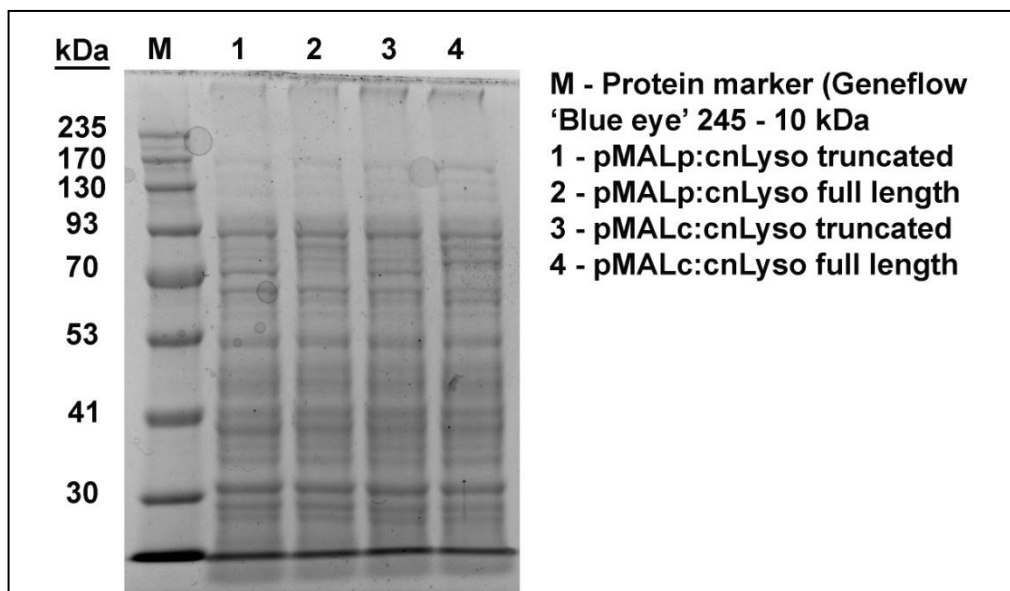
Figure 3 – SDS-PAGE analysis of lysed culture samples following autoinduction. 10 % acrylamide gel, 150 V 1 hour.

Although the yield during autoinduction did not appear to be high I chose to purify the protein from the clarified lysate by passing over a MBP column and performed a Western blot with against MBP just to see if the protein was present at low levels. The Western blot shows that for each clone there are three main bands with MBP present – one at 110 kDa, one at 50 kDa and one at 40 kDa. The band at 110 kDa could represent the full sized

CnLyso1: MBP tagged protein whereas the two smaller bands could be the result of fragmentation for some of the expressed protein.
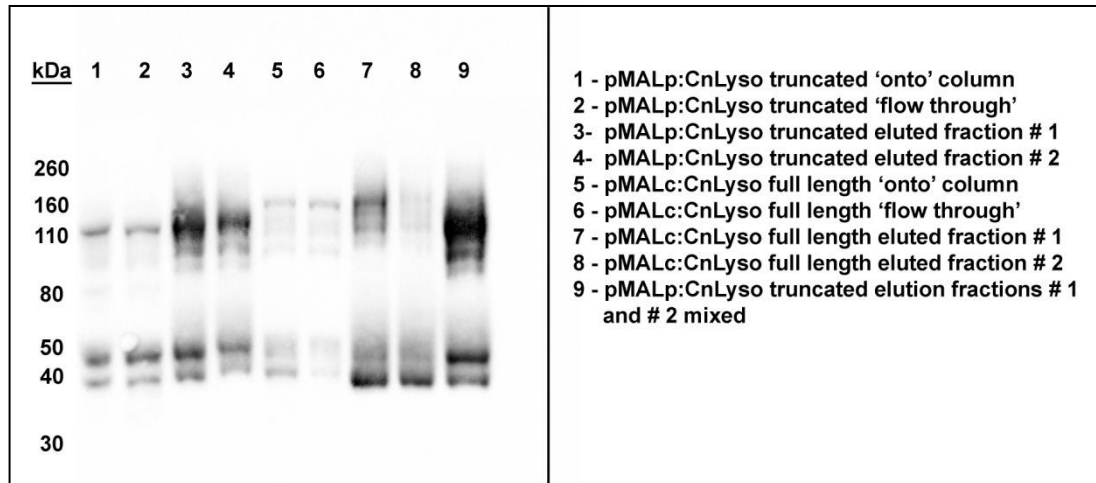
Figure 4 – Western blot analysis following protein purification with MBP columns for each clone. The antibody used is against the MBP tag.

Cryptococcal Phospholipase B1 Is Required for Intracellular Proliferation and Control of Titan Cell Morphology during Macrophage Infection

Robert J. Evans,[a] Zhongming Li,[b] William S. Hughes,[a,c] Julianne T. Djordjevic,[d] Kirsten Nielsen,[b] Robin C. May[a,e]

Institute of Microbiology and Infection and School of Biosciences, University of Birmingham, Birmingham, United Kingdom[a]; Department of Microbiology, University of Minnesota, Minneapolis, Minnesota, USA[b]; University of Warwick, Coventry, United Kingdom[c]; Centre for Infectious Diseases and Microbiology, Westmead Millennium Institute, Westmead, New South Wales, Australia[d]; NIHR Surgical Reconstruction and Microbiology Research Centre, University Hospitals of Birmingham NHS Foundation Trust, Queen Elizabeth Hospital Birmingham, Birmingham, United Kingdom[e]

Cryptococcus neoformans is an opportunistic fungal pathogen and a leading cause of fungal-infection-related fatalities, especially in immunocompromised hosts. Several virulence factors are known to play a major role in the pathogenesis of cryptococcal infections, including the enzyme phospholipase B1 (Plb1). Compared to other well-studied *Cryptococcus neoformans* virulence factors such as the polysaccharide capsule and melanin production, very little is known about the contribution of Plb1 to cryptococcal virulence. Phospholipase B1 is a phospholipid-modifying enzyme that has been implicated in multiple stages of cryptococcal pathogenesis, including initiation and persistence of pulmonary infection and dissemination to the central nervous system, but the underlying reason for these phenotypes remains unknown. Here we demonstrate that a Δ*plb1* knockout strain of *C. neoformans* has a profound defect in intracellular growth within host macrophages. This defect is due to a combination of a 50% decrease in proliferation and a 2-fold increase in cryptococcal killing within the phagosome. In addition, we show for the first time that the Δ*plb1* strain undergoes a morphological change during *in vitro* and *in vivo* intracellular infection, resulting in a subpopulation of very large titan cells, which may arise as a result of the attenuated mutant's inability to cope within the macrophage.

Cryptococcus neoformans is a pathogenic fungus that can cause severe and often fatal meningoencephalitis, especially in immunocompromised hosts. In recent years, *C. neoformans* has become a major emerging pathogen, due largely to the global HIV pandemic. In sub-Saharan Africa, for example, *C. neoformans* likely accounts for up to 44% of fatal HIV-related secondary infections (1). During infection, *C. neoformans* is known to interact closely with host macrophages (2) following inhalation of infectious spores from the environment into the lungs (3). Many virulence factors expressed by *C. neoformans* allow the fungus to evade phagocytosis by macrophages or to improve survival once phagocytosed (4).

One such virulence factor is phospholipase B1 (Plb1), a phospholipid-modifying enzyme with multiple enzymatic activities (5). In cryptococcal cells, a significant proportion of Plb1 enzymatic activity is cell wall associated, although secretion of Plb1 from *Cryptococcus* is known to occur *in vitro* (6). Plb1 is secreted following cleavage of a glycosylphosphatidylinositol (GPI) anchor motif, which anchors the enzyme to the cell wall (7, 8), and export of Plb1 to the cell wall is facilitated by Sec14-1, which is part of *C. neoformans*'s protein export system (9). Plb1 has optimal activity under acidic conditions, at around pH 4.0 to 5.0 (conditions similar to that of the phagosome), and is active at 37°C (10).

In line with this putative role in pathogenesis, deletion of *PLB1* strongly attenuates virulence in *C. neoformans* (9, 11–13). Mice infected with a *PLB1* deletion *C. neoformans* strain (Δ*plb1*) show reduced fungal burden in the lungs (9). In addition, during murine infection Plb1 appears to be required for cryptococcal dissemination from the lungs into the bloodstream (12) and additionally may be involved in the translocation of cryptococcal cells across the blood-brain barrier into the brain (14).

The reason why the Δ*plb1* strain is attenuated during infection has not yet been fully elucidated. In this study, we sought to explore the role of Plb1 during macrophage infection. We report that Plb1 is critical for both proliferation and survival within the macrophage. In addition, we show that the Δ*plb1* strain responds to macrophage infection by significantly increasing both capsular diameter and overall cell size within the phagosome and in the murine lung. This morphology is reminiscent of previously reported titan cells (15–17) and suggests that control of cryptococcal cell size by Plb1 may play a vital role in the outcome of host macrophage infection.

MATERIALS AND METHODS

Ethics statement. A total of 14 mice were handled in strict accordance with good animal practice, as defined by the relevant national and/or local

TABLE 1 Strains used in this study

Strain or genotype	Description	Reference
H99	*C. neoformans* serotype A mating type α; wild-type parent strain	
Δ*plb1*	*PLB1* gene knockout	10
Δ*plb1*::*PLB1*	Δ*plb1* strain with *PLB1* gene reconstituted	10
Δ*sec14*	*SEC14-1* gene knockout	13
Δ*sec14*::*SEC14*	Δ*sec14* strain with *SEC14-1* gene reconstituted	13

animal welfare bodies. All animal work was approved by the University of Minnesota Institutional Animal Care and Use Committee (IACUC) under protocol no. 1308A30852.

Strains, media, and cell lines. The strains used in this work are listed in Table 1. Strains were stored long-term in MicroBank vials at −80°C. Strains were rescued onto yeast extract-peptone-dextrose (YPD) agar (YPD, 50 g/liter [Sigma-Aldrich]; 2% agar [Melford]) for 48 h at 25°C and then stored until needed at 4°C. Before experimentation, liquid cultures were grown from these stock plates in 2 ml YPD growth medium (50 g/liter) for 24 h at 25°C under constant rotation.

The J774 murine macrophage cell line was used for all *in vitro* infection assays. Cells were passaged in Dulbecco's modified Eagle medium (DMEM) culture media with serum (DMEM, low glucose, from Sigma-Aldrich; 10% fetal bovine serum [FBS] from Invitrogen; 1% 10,000 units penicillin–10 mg streptomycin from Sigma-Aldrich; 1% 200 mM L-glutamine from Sigma-Aldrich). Assays were performed with J774 cells between passages 4 and 15. Assays were performed in serum-free DMEM (DMEM [high glucose], 1% penicillin-streptomycin, 1% L-glutamine) unless otherwise stated.

Intracellular proliferation assay. The intracellular proliferation assay was performed as previously described (18). Briefly, 24 h before infection, 1×10^5 J774 macrophages were seeded onto 24-well plastic plates (Greiner Bio One Cell Star) in 1 ml culture medium with serum and incubated for 24 h at 37°C and 5% CO_2. Before infection, J774 cells were activated with 150 ng/ml phorbol 12-myristate 13-acetate in dimethyl sulfoxide (DMSO; Sigma) in 1 ml serum-free culture medium for 45 min. This medium was then replaced with serum-free medium alone. Simultaneously, overnight *C. neoformans* cultures grown at 25°C in YPD were washed three times in sterile 1× phosphate-buffered saline (PBS), quantified, and adjusted to 1×10^7 cells per ml in PBS before opsonization for 1 h with 10 μg/ml anticapsular 18B7 antibody (a kind gift from Arturo Casadevall, Albert Einstein College of Medicine, New York, NY, USA). The activated J774 cells were then infected with 100 μl opsonized *C. neoformans* to give a multiplicity of infection (MOI) of 10 (e.g., 1×10^5 J774 cells for 1×10^6 *C. neoformans* cells) in unsupplemented serum-free DMEM and incubated for 2 h at 37°C, 5% CO_2. After 2 h (time point 0), infected wells were washed at least 3 times with warm 1× PBS until all nonphagocytosed *C. neoformans* cells were removed from the wells.

For calculation of the intracellular proliferation rate, the number of internal cryptococci was determined at time points 0, 18, and 24 (time points 0, 0 + 18 h, and 0 + 24 h, respectively). At each time point, each well to be counted was washed three times with 1× PBS to remove any extracellular yeast. The macrophages in the well were then lysed in distilled water for 30 min. *C. neoformans* cells in the lysate were quantified at each time point with a cell-counting chamber, and the intracellular proliferation rate (IPR) was calculated by dividing the count at which the intracellular burden peaked by the count at time point 0. Viability testing of the recovered cells was achieved by diluting the lysate to give a concentration of 200 yeast cells per 100 μl and then plating onto YPD agar at 25°C for 48 h prior to counting CFU.

Phagocytosis assay. Twenty-four hours before assaying, J774 macrophages were seeded onto 13-mm glass coverslips (nitric acid treated) inside 2-cm² 24-well plates at a concentration of 1×10^5 cells per ml in 1 ml

DMEM culture medium with serum and incubated at 37°C and 5% CO_2. Activation and infection of the macrophages with opsonized *C. neoformans* cells followed the same protocol as described above for the intracellular proliferation assay. After 2 h of incubation, the cells were washed 3 times with 1× PBS to remove unphagocytosed cells and then fixed for 10 min with 250 μl 4% paraformaldehyde in PBS at 37°C. Following fixation, coverslips were washed with 1× PBS and sterile deionized water and mounted on glass slides using Mowiol mountant (100 mM Tris-HCl [pH 8.5], 9% Mowiol, 25% glycerol). Mounted coverslips were analyzed on a Nikon Ti-S inverted microscope fitted with a Plan apochromatic (APO) 60 × 1.40 differential interference contrast (DIC) oil immersion objective.

Cell size assay. J774 cells were plated into 24-well plates, activated, and infected with opsonized *C. neoformans* strains as described above for the IPR assay. Two hours postinfection, each well was washed at least 3 times with warm 1× PBS until all nonphagocytosed *C. neoformans* cells were removed from the wells, and 1 ml serum-free DMEM was then added to each well.

The 24-well plate was placed into an environmentally controlled stage (Okolabs) set to 30°C, 5% CO_2. The cells were imaged using a Nikon TE2000 microscope fitted with a Digital Sight DS-Qi1MC camera and a Plan APO Ph1 20× dry objective. Images were recorded every 4 min for 20 h. Image acquisition and analysis was performed using the Nikon NIS Elements software package (Nikon).

Cell size was measured using the ellipse area tool, measuring from the center of each *Cryptococcus* cell to the edge, to obtain the diameter of each cell.

***In vivo* titan cell and phagocytosis assay.** *Cryptococcus neoformans* cells were grown in YPD broth overnight. Cells were pelleted and resuspended in sterile phosphate-buffered saline at a concentration of 1×10^7 cells/ml based on hemocytometer count. Groups of 6- to 8-week-old female A/J mice (Jackson Laboratory, Bar Harbor, ME) were anesthetized by intraperitoneal pentobarbital injection. Four to five mice per treatment were infected intranasally with 5×10^5 cells in 50 μl PBS. At 3 days postinfection, mice were sacrificed by CO_2 inhalation. Lungs were lavaged with 1.5 ml sterile PBS three times using a 18.5-gauge needle placed in the trachea. Cells in the lavage fluid were pelleted and fixed in 3.7% formaldehyde at room temperature for 30 min. Cells were washed once with PBS, and >500 cells per animal were analyzed for size by microscopy (AxioImager, Carl Zeiss, Inc.). Cell body sizes were measured, and cells were classified as small cells (<15 μm in cell body diameter) or titan cells (>15 μm in cell body diameter).

Titan cell flow cytometry. H99 was cultured in YPD broth overnight. Cells were pelleted, washed three times in PBS, and fixed in 3% paraformaldehyde at room temperature for 10 min. Bronchoalveolar lavage (BAL) samples were washed once in 0.05% sodium dodecyl sulfate (SDS) to lyse mammalian cells and then washed three times in sterile water. Cells were pelleted and fixed in 3% paraformaldehyde at room temperature for 10 min. Following fixation, samples were washed with PBS, stained with 0.5 μg/ml Hoechst (Sigma, St. Louis, MO) at room temperature for 10 min, washed again with PBS, and then resuspended in PBS. Approximately 10,000 cells were examined for cell size by forward scatter (FSC) and for DNA content by Hoechst staining using an LSRII flow cytometer with FACSDiva software (BD Biosciences, San Jose, CA). Graphs were generated using Flowjo software (Tree Star, Inc., Ashland, OR). The *t* test was used to analyze the differences in titan cell formation and phagocytosis, and *P* values of <0.05 were considered significant.

Cell stress. Overnight *C. neoformans* cultures in 2 ml YPD were grown at 25°C. Cultures were diluted 1:1,000 into 500 μl buffered YPD (pH 7.0, 15 mM HEPES) in plastic-bottomed 48-well plates (Greiner) with various concentrations of SDS (0, 0.01, 0.05, 0.1, 0.25, and 0.5 mM), of H_2O_2 (0, 0.125, 0.25, 0.5, 1, 3, 6, and 14 mM), or of NaCl (0, 125, 250, 500, 1,000 mM). The plate was then sealed with a breathable membrane, and growth curve assays were performed for 24 h at 30°C in a Fluostar Omega plate reader using a custom script that took 600-nm absorbance readings from
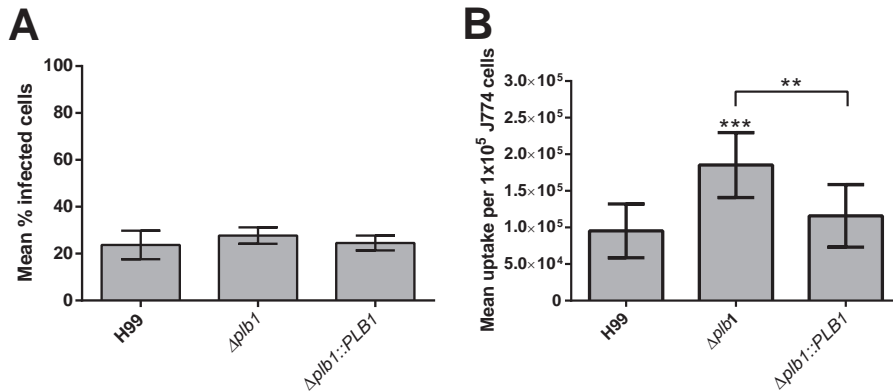
FIG 1 (A) Percentages of macrophages within a population that show *C. neoformans* infection following 2-h incubation with opsonized cryptococci at an MOI of 1:10 ($n = 4$). A minimum of 500 macrophages were counted for each condition. (Unpaired t test was performed, no significance.) (B) Total burden of infection within a fixed population of J774 cells (1×10^5) following 2-h incubation with opsonized cryptococci at an MOI of 1:10 ($n = 9$). ***, H99 versus Δ*plb1* strain, $P = 0.0003$; **, Δ*plb1* versus Δ*plb1::PLB1* strains, $P = 0.0038$ (unpaired t test).

the bottom of the plate every 30 min. Between reads, the plate was shaken at 200 rpm with a linear shaking pattern.

Statistics. Unless otherwise stated, all statistics were performed using Prism Graphpad software. For cell size measurement comparison between time points, a Mann-Whitney U test was performed (e.g., StrainX 0 h versus StrainX 18 h). Unless stated otherwise, a P value below 0.05 was taken as significant. Unless otherwise stated, all figures have error bars representing standard errors. Significance is shown on figures by asterisks as follows: *, $P \leq 0.05$; **, $P \leq 0.01$; ***, $P \leq 0.001$; and ****, $P \leq 0.0001$.

RESULTS

Plb1 deficiency leads to increased uptake of *C. neoformans* cells by J774 macrophages. We first assessed to what extent the *PLB1* knockout strain, Δ*plb1* strain, was phagocytosed by macrophages in comparison to the wild-type parent strain H99 and a genetically reconstituted strain, Δ*plb1::PLB1* strain. We found that, following 2 h of infection, the percentage of J774 murine macrophages with at least one internalized *C. neoformans* cell did not differ significantly between wild-type strain H99, Δ*plb1* strain, and Δ*plb1::PLB1* reconstituted strain (Fig. 1A). Quantification of the fungal burden per macrophage, however, revealed a 2-fold increase in the

number of Δ*plb1* cells phagocytosed per host cell (Fig. 1B, $P = 0.0003$). This suggests that Plb1 activity contributes significantly to the well-known antiphagocytic phenotype of cryptococci.

Plb1 is required for intracellular proliferation of *C. neoformans* within J774 macrophages. *PLB1* knockout leads to a reduced fungal lung burden during murine infection; in addition, it abrogates dissemination to the brain (9, 14) and has previously been shown to reduce budding of *C. neoformans* within macrophages (11). To investigate this phenotype further, we performed an intracellular proliferation rate assay. We observed an intracellular proliferation defect for the Δ*plb1* strain versus the wild-type strain (IPR = 1.12 versus 2.42 for H99; $P = 0.023$), a defect that was fully restored in the Δ*plb1::PLB1* reconstituted strain (Fig. 2A). Interestingly, no intracellular proliferation defect was observed when we tested the Δ*sec14* strain (Fig. 2A). Since Sec14-1 is required for efficient secretion of Plb1 (9), it appears that intracellular, but not secreted, Plb1 is important for proliferation within host cells.

Due to the increased efficiency of Δ*plb1* cell uptake observed, we wondered whether the reduced proliferation we see for Δ*plb1*
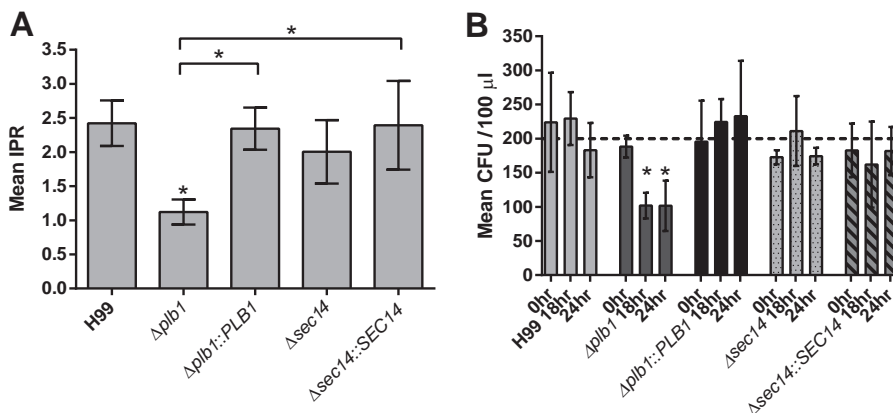
FIG 2 (A) Mean intracellular proliferation rate for each *C. neoformans* strain within murine J774 macrophages ($n = 3$). *, H99 versus Δ*plb1* strain, $P = 0.023$; *, Δ*plb1* versus Δ*plb1::PLB1* strains, $P = 0.033$; *, Δ*plb1* versus Δ*sec14::SEC14* strains, $P = 0.0263$ (one-way analysis of variance [ANOVA] plus Tukey posttest). (B) Viability of *C. neoformans* cells recovered from J774 macrophages following the IPR assay. Cells recovered following macrophage lysis were counted and diluted, giving an expected plated inoculum of 200 cells ($n = 4$). *, Δ*plb1* strain 0 h versus Δ*plb1* strain 18 h, $P = 0.0422$; *, Δ*plb1* strain 0 h versus Δ*plb1* strain 24 h, $P = 0.0415$ (two-way ANOVA plus Tukey posttest comparing time points for each strain).

cells simply reflects initial overcrowding within the host macrophage. To test this, we reduced the uptake of Δ*plb1* cells by omitting the opsonization step before infection. Infecting with unopsonized *Cryptococcus* reduced uptake for all three strains (see Fig. S1Ci in the supplemental material: unopsonized *Cryptococcus* can still be phagocytosed by macrophage but at a lower rate [19, 20]) but did not alter the growth defect observed (see Fig. S1Cii in the supplemental material). To test a different method of opsonization, we also tried opsonizing with pooled serum instead of antibody. At the concentration used (5% pooled human serum), we did not see significant differences in uptake, compared to antibody opsonization (see Fig. S1Bi in the supplemental material), and the proliferation defect remained (see Fig. S1Bii in the supplemental material). Taken together, these data suggest that Plb1 plays a direct role in regulating intracellular proliferation in cryptococci regardless of the fungal intracellular burden.

Plb1 contributes to *C. neoformans* cell survival during infection. The low intracellular proliferation defect observed for Δ*plb1* could be due to slower *Cryptococcus* proliferation and/or increased intracellular killing by the macrophage. To address the second possibility, we plated *C. neoformans* cells recovered from macrophages at 18 and 24 h postinfection on YPD agar to enumerate CFU. No significant difference in CFU among any of the five strains was seen at time point 0 (2 h postinfection); however, at time point 18 (20 h postinfection), the viability of Δ*plb1* strain but not that of the Δ*sec14-1* strain had dropped significantly (P = 0.04) (Fig. 2B) compared to that of H99. Taken together, these data suggest that both growth and survival of the Δ*plb1* strain are impaired within the phagosome during macrophage infection.

Plb1 deficiency does not significantly affect cryptococcal stress responses. We hypothesized that low IPR in the macrophage may be a result of stressful conditions during macrophage infection—possibly because the Δ*plb1* strain is unable to control or resist cellular stresses within the macrophage. However, exposing the Δ*plb1* strain to a variety of stresses showed no significant difference from the wild type other than the previously reported susceptibility to SDS (9) (Fig. 3A and B).

PLB1 knockout leads to changes in cryptococcal cell body morphology. During the course of this work, we noticed that some Δ*plb1* cells showed a marked increase in cell body diameter within infected macrophages, a morphology that was not observed for H99 or the Δ*plb1::PLB1* strain (Fig. 4E and F). Quantification of this phenomenon (Fig. 4) showed that the diameter of both the cell body and the capsule of Δ*plb1* cells increased significantly during an 18-h macrophage infection (Fig. 4A to E). Interestingly, we observed a significant decrease in cell diameter for H99 and Δ*plb1::PLB1* cells over the same incubation period (see Table S1 in the supplemental material), which is probably due to active cell budding occurring within the macrophage, leading to a drop in mean diameter for the overall population. Extending the period of live cell imaging to 48 h, we found that the enlarged Δ*plb1* cells did not noticeably increase in size after 18 h postinfection.

Changes in *Cryptococcus* cell size during *in vivo* infection have been previously documented, ultimately resulting in the production of very large titan cells (15–17, 21). To our knowledge, though, this is the first published observation of a similar (albeit less dramatic) process occurring within a macrophage (rather than extracellularly) and the first time that *PLB1* has been implicated in this pathway. Previous studies have reported that the size
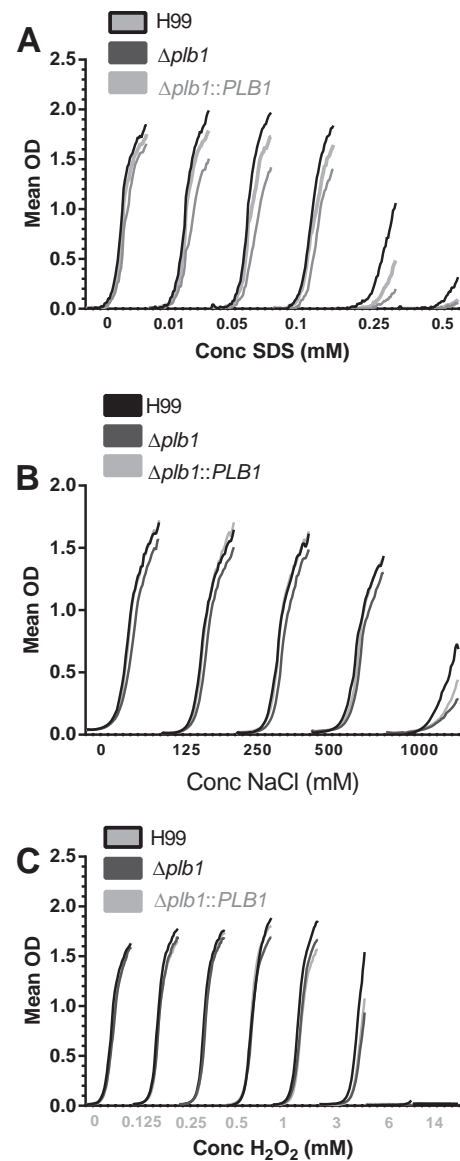
FIG 3 Overlaid growth curves with increasing concentrations of stress factors that partly mimic stresses in the phagosome. (A) SDS (membrane instability); (B) NaCl (osmotic shock); (C) H_2O_2 (reactive oxygen).

increase observed in titan cells is accompanied by increased nuclear content due to polyploidy (15, 16). In agreement with this, flow cytometric analysis of Δ*plb1* cells following macrophage infection demonstrated a positive correlation between cell size and DNA quantity (Fig. 5A), indicating increased nuclear content within these cells.

Δ*plb1* cells have a higher rate of titan cell formation than do wild-type cells during *in vivo* murine infection. Our *in vitro* observation of Δ*plb1* cell enlargement was reminiscent of the titan cell morphology observed during *in vivo* murine pulmonary infection (15, 16, 21). To test whether this phenotype was recapitulated *in vivo*, we conducted pulmonary infections in mice and then quantified cryptococcal size following bronchoalveolar lavage (BAL) at 3 days postinfection. As with our *in vitro* data, *in vivo* infection with Δ*plb1* cells produced about 2.5 times more titan
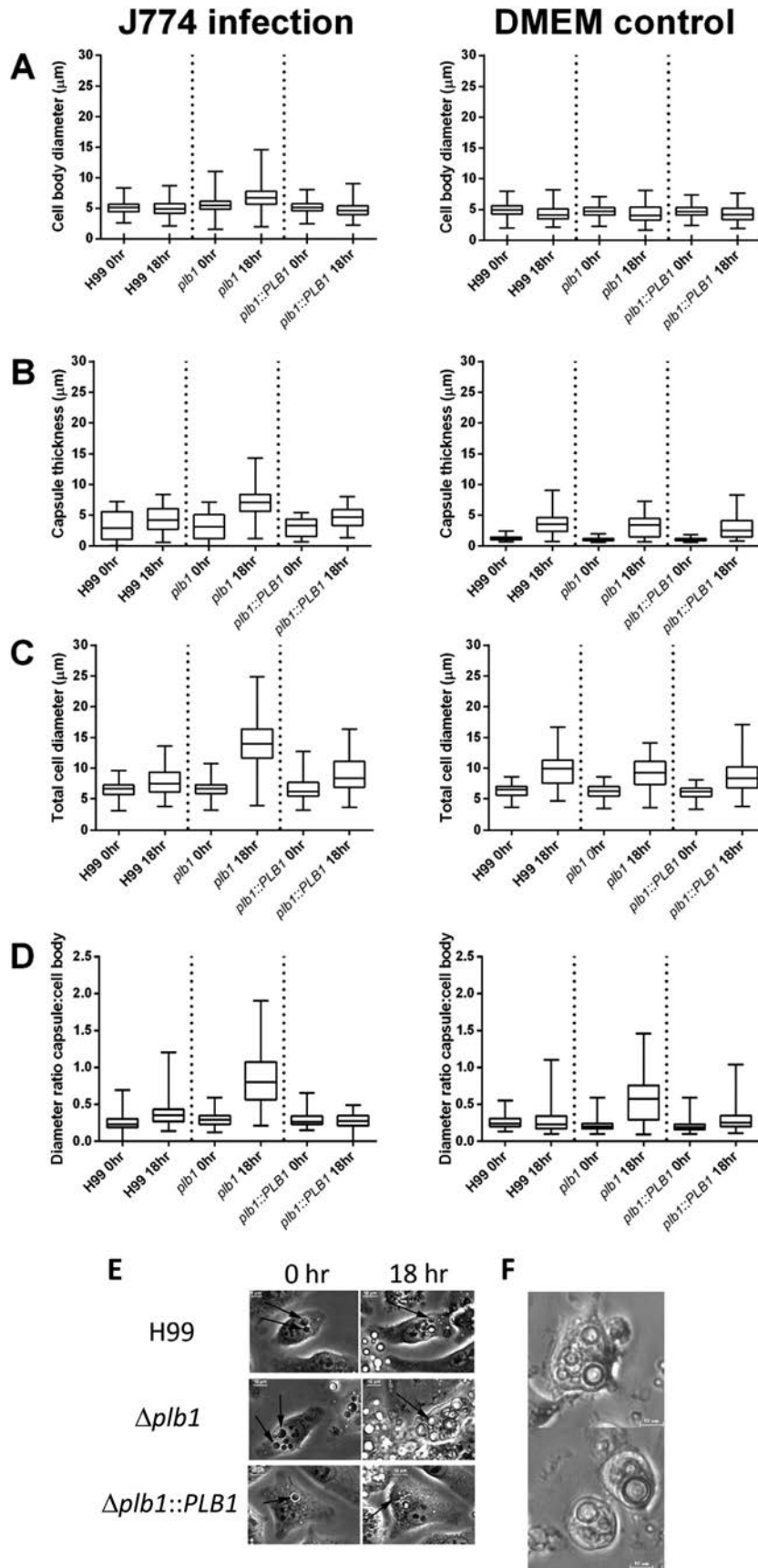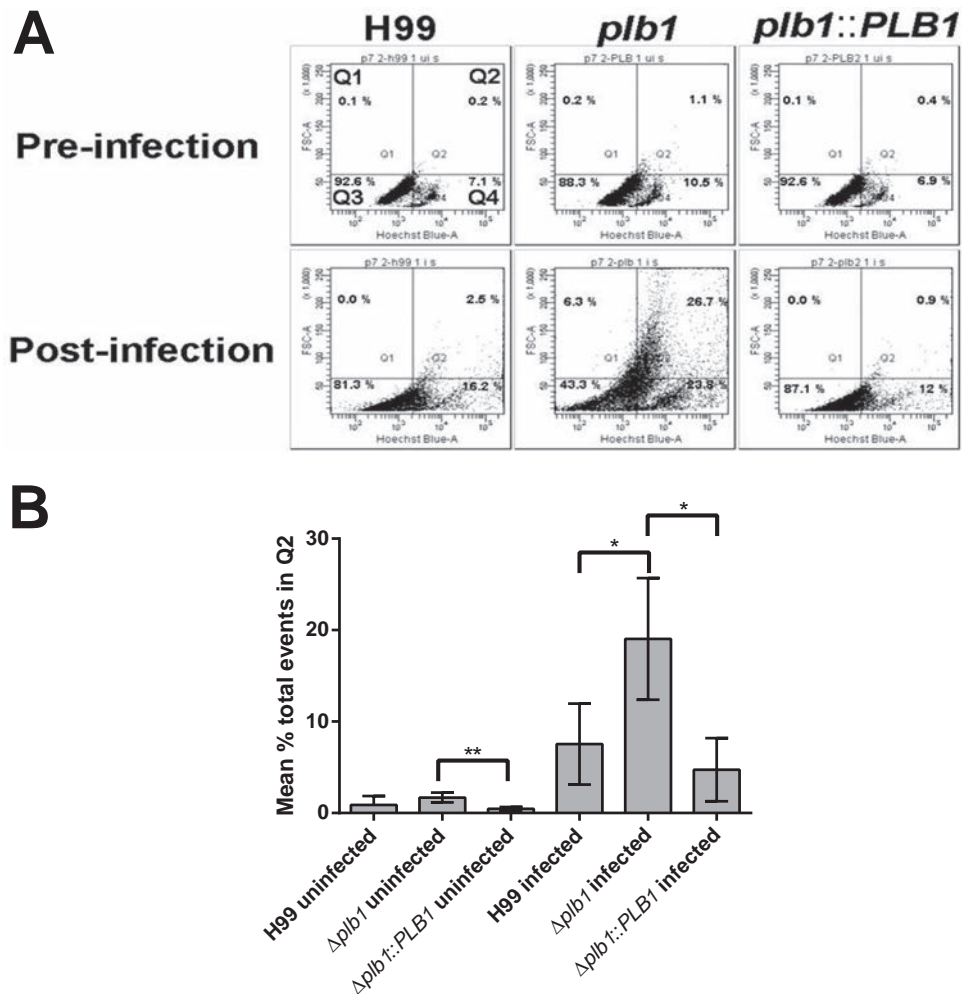
FIG 5 (A) Flow cytometric analysis of *C. neoformans* samples pre- and postincubation with J774 macrophages (18 h). Samples were stained with Hoechst to quantify DNA content; FSC-A (forward scatter area) indicates the relative cell size across the samples. Cells were gated based on size and nuclear content with cells in Q3 consistent with small cells in G_1, cells in Q4 indicative of small cells in G_2, and cells in Q2 indicative of polyploidy titan cells with both large size and increased DNA content. (B) Mean percentage of total events (10,000 collected) across 3 repeats occurring in the Q2 gate. A one-tailed *t* test was performed for H99 and Δ*plb1* strains as well as Δ*plb1*and Δ*plb1*::*PLB1* strains to determine if the increase in events within the Q2 gate observed was significant: *, H99-infected versus Δ*plb1* strain-infected cells, $P = 0.034$; *, Δ*plb1* strain-infected versus Δ*plb1*::*PLB1* strain-infected cells, $P = 0.015$; **, Δ*plb1* strain-uninfected versus Δ*plb1*::*PLB1* strain-uninfected cells, $P = 0.001$.

cells (cryptococci with a cell body diameter greater than 15 μm) than H99 or Δ*plb1*::*PLB1* cells (Fig. 6Ai). Flow cytometry of lavaged, Hoechst-stained Δ*plb1* titan cells indicated that these cells are polyploid, in agreement with previously published characterization of titan cells (15, 16) as well as our own *in vitro* observation of Δ*plb1* cells (Fig. 5A). Taken together, these findings suggest that the morphological changes that we observed in our Δ*plb1* cells are consistent with an increase in the production of titan cells by this strain both *in vitro* and *in vivo*.

In vivo Δ***plb1*** **titan cell formation is not associated with phagocytosed cells.** In addition to quantifying overall titan cell formation in BAL samples, we also counted the *Cryptococcus* cells within host phagocytes following BAL and measured the cell body diameter of each *Cryptococcus* cell within each lavaged host cell.

We found that there were significantly fewer lavaged host cells containing *Cryptococcus* for Δ*plb1* strain-infected mice than for mice infected with H99 or Δ*plb1*::*PLB1* strain (Fig. 6Aii, H99 versus Δ*plb1*, $P = 0.0001$; Δ*plb1* versus Δ*plb1*::*PLB1*, $P = 0.0018$).

FIG 4 (A to D) *C. neoformans* cells were measured after either 18 h inside J774 macrophages or 18 h in serum-free DMEM. The top and bottom of each box mark the 75th and 25th percentiles, respectively, the bisecting line in the box marks the median, and the two whiskers mark the maximum and minimum of the range. Mann-Whitney U tests were performed for each time point pair. Full statistical results are given in Tables S1 and S2 in the supplemental material. (B) Capsule thickness was calculated by subtracting cell body diameter from total diameter including capsule. (D) The ratio of cell body to capsule was calculated by dividing cell body diameter by capsule thickness. (E) Still bright-field images from live-cell microscopy following the same macrophage over 18 h for H99, Δ*plb1*, and Δ*plb1*::*PLB1* strains. Black arrows indicate the location of single *C. neoformans* cells within the macrophage. (F) Still bright-field images from live-cell microscopy following viable Δ*plb1* strain-infected macrophages. Images were taken at 40 h postinfection; bar, 10 μm.

A i

ii

iii

B

H99 (YPD)   **H99 (*In vivo*)**   **Δ*plb1* (*In vivo*)**
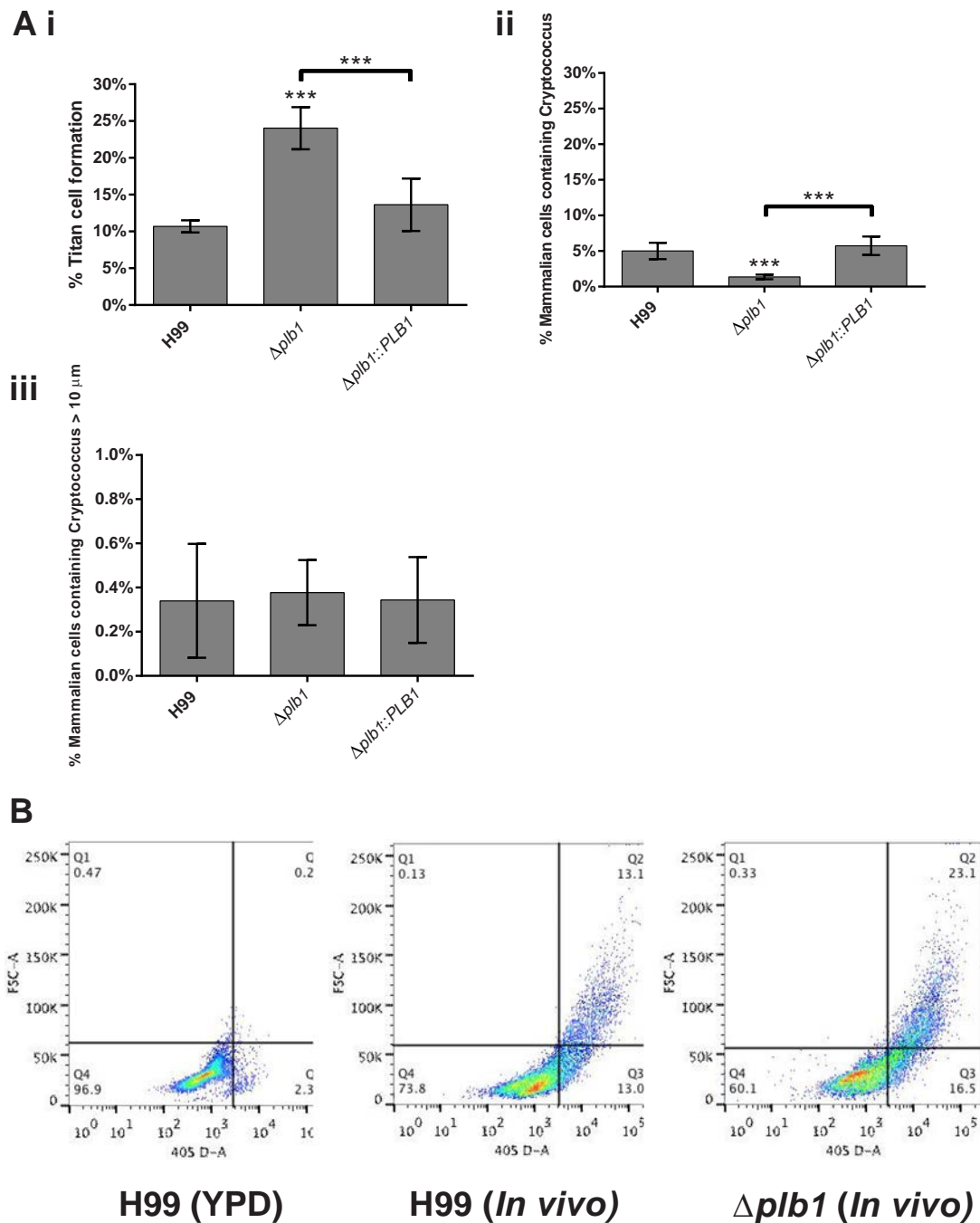
FIG 6 *In vivo* titan cell assay on *Cryptococcus* cells lavaged from mouse lungs 3 days postinfection. (Ai) A minimum of 500 cells per animal were analyzed to quantify cell body diameter, *Cryptococcus* cells >15 μm in diameter were considered titan cells (***, H99 versus Δ*plb1* strain, $P = 0.0001$; ***, Δ*plb1* versus Δ*plb1*::*PLB1* strains, $P = 0.0018$ [two-tailed unpaired *t* test]). (Aii) Host cells lavaged from the lungs were examined for phagocytosed *Cryptococcus* cells (***, H99 versus Δ*plb1* strain, $P = 0.0001$; ***, Δ*plb1* versus Δ*plb1*::*PLB1* strains, $P = 0.0001$ [two-tailed unpaired *t* test]). (Aiii) The cell body diameter of phagocytosed *Cryptococcus* cells within lavaged host macrophages was quantified, and data for phagocytosed cells >10 μm are given. (B) Bronchoalveolar lavage samples with *Cryptococcus* from H99 and Δ*plb1* strains were stained with Hoechst and analyzed for size and nuclear content. Cells were gated based on size and nuclear content with cells in Q3 consistent with small cells in G$_1$, Q4 indicative of small cells in G$_2$, and Q2 indicative of polyploidy titan cells with both large size and increased DNA content. (C) Bright-field images of lavaged cells from H99, Δ*plb1*, or Δ*plb1*::*PLB1* strain-infected lungs. Bar, 15 μm.

Very few of these internalized *Cryptococcus* cells were above 10 μm in diameter, and those that were above 10 μm could be found in similar numbers for H99, Δ*plb1*, and Δ*plb1*::*PLB1* cells (Fig. 6Aiii). No cells greater than 15 μm were found inside phagocytes in either the control or the Δ*plb1* strain infections (data not shown). This leads us to conclude that *in vivo* Δ*plb1* titan cell formation potentially occurs initially within host cells (as we observe *in vitro*) but these large cryptococci are released from host

DISCUSSION

During cryptococcal pathogenesis, *C. neoformans* interacts with professional phagocytes in the alveolar space (2), in the bloodstream, and in other tissues following dissemination. The outcome of this interaction appears to be vital for disease progression, as the macrophage provides a protective niche for replication (18) and a potential "Trojan horse" for dissemination to the central nervous system (22, 23). Together with previous studies, our findings strongly suggest that expression of Plb1 is critical in regulating cryptococcus-macrophage interactions.

First, we show that *PLB1* deletion leads to enhanced uptake by phagocytes *in vitro* (Fig. 1B). Since Plb1 is a GPI-linked, cell wall-associated protein (7), it is likely that loss of this enzyme affects the cryptococcal cell surface and, presumably, this change facilitates more-efficient binding of phagocyte receptors. Examination of different opsonization methods (see Fig. S1 in the supplemental material) suggests that increased uptake is due to a combination of antibody, complement, and nonopsonic ligands. Cryptococcal cell wall instability following *PLB1* deletion has been published previously (8), and thus this instability could lead to increased ligand exposure on the *Cryptococcus* cell surface. In light of these observations, a detailed chemical analysis of the cell surface composition in this strain would be of considerable future interest.

Following phagocytosis, we find that *C. neoformans* requires the expression of Plb1 to proliferate and survive normally within the macrophage (Fig. 2). This finding provides a mechanism to explain previous reports of reduced fungal burdens following infection with Δ*plb1* cells (9). Interestingly, however, the Δ*sec14-1* strain shows no such defect in intracellular proliferation. Since this strain shows strongly reduced Plb1 secretion (9), the most likely explanation is that the primary role of Plb1 in driving intracellular proliferation is in the metabolism of fungal phospholipids within the cryptococcal cell, rather than in acting directly upon host phospholipids. However, secreted Plb1 appears to have additional roles in virulence, since the Δ*sec14-1* strain is attenuated in animal models (9). It is tempting to speculate that the documented involvement of *SEC14* in regulating vomocytosis (9) may be one such role.

A striking morphological observation arising from our macrophage infection model was that Δ*plb1* cells showed a marked increase in both cell body diameter and capsule thickness during infection, with a maximum measured diameter (including capsule) of almost 25 μm (Fig. 4C). That this size change was not seen in the wild-type or Δ*plb1*::*PLB1* reconstituted strains suggests that this morphology results from the loss of Plb1. Previously reported titan cells grown *in vivo* range in diameter from 15 to 100 μm, excluding the capsule (15, 16). Therefore, the size increase that we observed is smaller than that of previously reported titan cells but significantly larger than the normal cryptococcal size range. Interestingly, previous reports of titan cells induced *in vitro* also noted that the cells tended to be smaller than those generated *in vivo* (16). Flow cytometry analysis of Δ*plb1* cells following macrophage infection (Fig. 5) indicates that the large cells show increased DNA content, consistent with the defining feature of titan cells (16). Thus, these cells may represent individual yeast cells that are "en route" to becoming Titan cells or have somehow been constrained by the macrophage, or it may

be that the *in vitro* conditions do not provide the necessary stimulus to produce the largest titan cells.

From our *in vitro* data, we conclude that the Δ*plb1* strain forms large cells within macrophages, which are similar to the titan cell morphology seen *in vivo*. Titan cell formation has previously been induced *in vitro* using macrophage-conditioned media (16); however, titan cell formation induced inside an infected macrophage has to our knowledge not previously been reported. Although we have not identified the trigger for this morphology, it is evidently linked to Plb1 deficiency. The development of this morphology within the macrophage may be a response to increased stress experienced by the Δ*plb1* strain, as indicated by the decreased viability of this strain within the phagosome. Although we did not detect any significant difference stress tolerance for Δ*plb1* organisms *in vitro*, other than the previously published susceptibility to SDS (9), growth within the phagosome exposes cryptococci to a diverse repertoire of additional stresses, and it is likely that these complex conditions limit the growth of this mutant. One possible source of stress within the phagosome, which links our observed phenotypes, is the observation that in wild-type cryptococci, Plb1 concentrates at the neck of newly forming buds (24). This suggests that Plb1 may have a role in bud development, and thus it is conceivable that modification of membrane phospholipids by Plb1 during budding could be required for membrane curvature at the newly formed bud site or release of the daughter cell. The inability of the Δ*plb1* strain to properly bud would explain the proliferation defect observed and could generate sufficient cellular stress to reduce cryptococcal viability and trigger the development of titan-like cells.

A strong link between our *in vitro* observations and previously published *in vivo* development of titan cells is supported by our finding that the Δ*plb1* strain forms greater numbers of "classical" titan cells (i.e., cell body diameter above 15 μm and high nuclear content indicative of polyploidy) *in vivo* than do the wild-type and reconstituted strains (Fig. 6Ai). These data suggest that Plb1 activity is involved in the repression of titan cell formation during infection. In addition, the fact that the Δ*sec14-1* strain does not manifest similar cell size increases during *in vitro* infection (our unpublished data) indicates that intracellular rather than extracellular Plb1 activity regulates the titan cell morphology. Interestingly, titan cell development may be linked to phospholipid availability (25), suggesting a potential link to Plb1 activity. Titan cell formation *in vivo* has been reported to increase the pathogenicity of *C. neoformans* (16, 17); our conclusion that the Δ*plb1* strain has increased titan cell formation therefore seems at odds with the *in vitro* data presented in Fig. 1 and 2 showing that the Δ*plb1* strain is attenuated in macrophages. It is therefore possible that the large Δ*plb1* cells may not exhibit all the features of titan cells (for instance, in conferring "cross-protection" on nontitan cells in the same host). Alternatively, it may be that full pathogenicity requires only a minor titan cell population and hence, the enhanced titan cell frequency seen in the Δ*plb1* strain actually reduces overall virulence.

In summary, our data indicate that Plb1 plays a key role both in intracellular survival within host phagocytes and in driving cryptococcal cell size changes both *in vitro* and *in vivo*.

REFERENCES

1. Park BJ, Wannemuehler KA, Marston BJ, Govender N, Pappas PG, Chiller TM. 2009. Estimation of the current global burden of cryptococcal
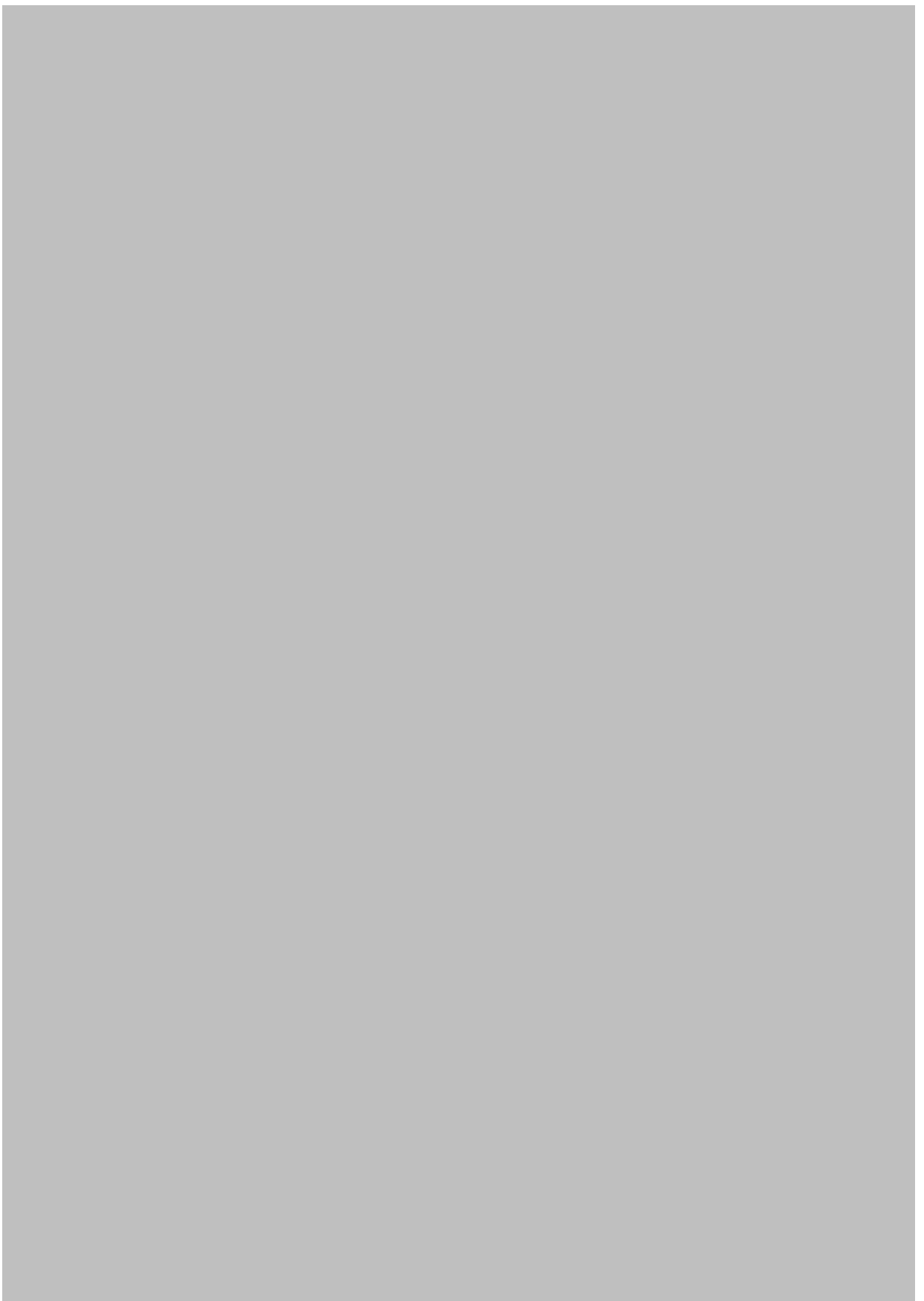
meningitis among persons living with HIV/AIDS. AIDS **23:**525–530. http://dx.doi.org/10.1097/QAD.0b013e328322ffac.

2. **Feldmesser M, Kress Y, Novikoff P, Casadevall A.** 2000. Cryptococcus neoformans is a facultative intracellular pathogen in murine pulmonary infection. Infect Immun **68:**4225–4237. http://dx.doi.org/10.1128/IAI.68.7.4225-4237.2000.

3. **Giles SS, Dagenais TR, Botts MR, Keller NP, Hull CM.** 2009. Elucidating the pathogenesis of spores from the human fungal pathogen Cryptococcus neoformans. Infect Immun **77:**3491–3500. http://dx.doi.org/10.1128/IAI.00334-09.

4. **Ma H, May RC.** 2009. Virulence in Cryptococcus species. Adv Appl Microbiol **67:**131–190. http://dx.doi.org/10.1016/S0065-2164(08)01005-8.

5. **Chen SC, Wright LC, Santangelo RT, Muller M, Moran VR, Kuchel PW, Sorrell TC.** 1997. Identification of extracellular phospholipase B, lysophospholipase, and acyltransferase produced by Cryptococcus neoformans. Infect Immun **65:**405–411.

6. **Wright LC, Chen SC, Wilson CF, Simpanya MF, Blackstock R, Cox GM, Murphy JW, Sorrell TC.** 2002. Strain-dependent effects of environmental signals on the production of extracellular phospholipase by Cryptococcus neoformans. FEMS Microbiol Lett **209:**175–181. http://dx.doi.org/10.1111/j.1574-6968.2002.tb11128.x.

7. **Djordjevic JT, Del Poeta M, Sorrell TC, Turner KM, Wright LC.** 2005. Secretion of cryptococcal phospholipase B1 (PLB1) is regulated by a glycosylphosphatidylinositol (GPI) anchor. Biochem J **389:**803–812. http://dx.doi.org/10.1042/BJ20050063.

8. **Siafakas AR, Sorrell TC, Wright LC, Wilson C, Larsen M, Boadle R, Williamson PR, Djordjevic JT.** 2007. Cell wall-linked cryptococcal phospholipase B1 is a source of secreted enzyme and a determinant of cell wall integrity. J Biol Chem **282:**37508–37514. http://dx.doi.org/10.1074/jbc.M707913200.

9. **Chayakulkeeree M, Johnston SA, Oei JB, Lev S, Williamson PR, Wilson CF, Zuo X, Leal AL, Vainstein MH, Meyer W, Sorrell TC, May RC, Djordjevic JT.** 2011. SEC14 is a specific requirement for secretion of phospholipase B1 and pathogenicity of Cryptococcus neoformans. Mol Microbiol **80:**1088–1101. http://dx.doi.org/10.1111/j.1365-2958.2011.07632.x.

10. **Chen SC, Wright LC, Golding JC, Sorrell TC.** 2000. Purification and characterization of secretory phospholipase B, lysophospholipase and lysophospholipase/transacylase from a virulent strain of the pathogenic fungus Cryptococcus neoformans. Biochem J **347:**431–439. http://dx.doi.org/10.1042/0264-6021:3470431.

11. **Cox GM, McDade HC, Chen SC, Tucker SC, Gottfredsson M, Wright LC, Sorrell TC, Leidich SD, Casadevall A, Ghannoum MA, Perfect JR.** 2001. Extracellular phospholipase activity is a virulence factor for Cryptococcus neoformans. Mol Microbiol **39:**166–175. http://dx.doi.org/10.1046/j.1365-2958.2001.02236.x.

12. **Santangelo R, Zoellner H, Sorrell T, Wilson C, Donald C, Djordjevic J, Shounan Y, Wright L.** 2004. Role of extracellular phospholipases and mononuclear phagocytes in dissemination of cryptococcosis in a murine model. Infect Immun **72:**2229–2239. http://dx.doi.org/10.1128/IAI.72.4.2229-2239.2004.

13. **Noverr MC, Cox GM, Perfect JR, Huffnagle GB.** 2003. Role of PLB1 in pulmonary inflammation and cryptococcal eicosanoid production. Infect Immun **71:**1538–1547. http://dx.doi.org/10.1128/IAI.71.3.1538-1547.2003.

14. **Maruvada R, Zhu L, Pearce D, Zheng Y, Perfect J, Kwon-Chung KJ, Kim KS.** 2012. Cryptococcus neoformans phospholipase B1 activates host cell Rac1 for traversal across the blood-brain barrier. Cell Microbiol **14:**1544–1553. http://dx.doi.org/10.1111/j.1462-5822.2012.01819.x.

15. **Zaragoza O, García Rodas R, Nosanchuk JD, Cuenca-Estrella M, Rodríguez Tudela JL, Casadevall A.** 2010. Fungal cell gigantism during mammalian infection. PLoS Pathog **6:**e1000945. http://dx.doi.org/10.1371/journal.ppat.1000945.

16. **Okagaki LH, Strain AK, Nielsen JN, Charlier C, Baltes NJ, Chrétien F, Heitman J, Dromer F, Nielsen K.** 2010. Cryptococcal cell morphology affects host cell interactions and pathogenicity. PLoS Pathog **6:**e1000953. http://dx.doi.org/10.1371/journal.ppat.1000953.

17. **Crabtree JN, Okagaki LH, Wiesner DL, Strain AK, Nielsen JN, Nielsen K.** 2012. Titan cell production enhances the virulence of Cryptococcus neoformans. Infect Immun **80:**3776–3785. http://dx.doi.org/10.1128/IAI.00507-12.

18. **Ma H, Hagen F, Stekel DJ, Johnston SA, Sionov E, Falk R, Polacheck I, Boekhout T, May RC.** 2009. The fatal fungal outbreak on Vancouver Island is characterized by enhanced intracellular parasitism driven by mitochondrial regulation. Proc Natl Acad Sci U S A **106:**12980–12985. http://dx.doi.org/10.1073/pnas.0902963106.

19. **Ma H.** 2009. Intracellular parasitism of macrophages by Cryptococcus Ph.D. thesis. University of Birmingham, Birmingham, United Kingdom.

20. **Guerra CR, Seabra SH, de Souza W, Rozental S.** 2014. Cryptococcus neoformans is internalized by receptor-mediated or 'triggered' phagocytosis, dependent on actin recruitment. PLoS One **9:**e89250. http://dx.doi.org/10.1371/journal.pone.0089250.

21. **Feldmesser M, Kress Y, Casadevall A.** 2001. Dynamic changes in the morphology of Cryptococcus neoformans during murine pulmonary infection. Microbiology **147:**2355–2365.

22. **Chrétien F, Lortholary O, Kansau I, Neuville S, Gray F, Dromer F.** 2002. Pathogenesis of cerebral Cryptococcus neoformans infection after fungemia. J Infect Dis **186:**522–530. http://dx.doi.org/10.1086/341564.

23. **Charlier C, Nielsen K, Daou S, Brigitte M, Chretien F, Dromer F.** 2009. Evidence of a role for monocytes in dissemination and brain invasion by Cryptococcus neoformans. Infect Immun **77:**120–127. http://dx.doi.org/10.1128/IAI.01065-08.

24. **Lev S, Crossett B, Cha SY, Desmarini D, Li C, Chayakulkeeree M, Wilson CF, Williamson PR, Sorrell TC, Djordjevic JT.** 2014. Identification of Aph1, a phosphate-regulated, secreted, and vacuolar acid phosphatase in Cryptococcus neoformans. mBio **5:**e01649-14. http://dx.doi.org/10.1128/mBio.01649-14.

25. **Chrisman CJ, Albuquerque P, Guimaraes AJ, Nieves E, Casadevall A.** 2011. Phospholipids trigger cryptococcus neoformans capsular enlargement during interactions with amoebae and macrophages. PLoS Pathog **7(5):**e1002047. http://dx.doi.org/10.1371/journal.ppat.1002047.

5 Macrophages in the Immune Response Against *Cryptococcus*

ROBERT J. EVANS[1], ROBIN C. MAY[1]

CONTENTS

List of References

Abadi, J. and Pirofski, L. (1999) Antibodies reactive with the cryptococcal capsular polysaccharide glucuronoxylomannan are present in sera from children with and without human immunodeficiency virus infection. **J Infect Dis,** 180 915-919.

Alanio, A., Desnos-Ollivier, M. and Dromer, F. (2011) Dynamics of Cryptococcus neoformans-macrophage interactions reveal that fungal background influences outcome during cryptococcal meningoencephalitis in humans. **mBio,** 2 (4): 10.1128/mBio.00158-11. Print 2011.

Alcouloumre, M.S., Ghannoum, M.A., Ibrahim, A.S., et al. (1993) Fungicidal properties of defensin NP-1 and activity against Cryptococcus neoformans in vitro. **Antimicrobial Agents and Chemotherapy,** 37 (12): 2628-2632.

Alvarez, M. and Casadevall, A. (2007) Cell-to-cell spread and massive vacuole formation after Cryptococcus neoformans infection of murine macrophages. **BMC immunology,** 8 16.

Alvarez, M. and Casadevall, A. (2006) Phagosome extrusion and host-cell survival after Cryptococcus neoformans phagocytosis by macrophages. **Curr Biol,** 16 2161-2165.

Amer, A.O. and Swanson, M.S. (2002) A phagosome of one's own: a microbial guide to life in the macrophage. **Current opinion in microbiology,** 5 (1): 56-61.

Aminnejad, M., Diaz, M., Arabatzis, M., et al. (2012) Identification of novel hybrids between Cryptococcus neoformans var. grubii VNI and Cryptococcus gattii VGII. **Mycopathologia,** 173 (5-6): 337-346.

Antinori, S. (2013) New Insights into HIV/AIDS-Associated Cryptococcosis. **Isrn Aids,** 2013 471363.

Baddley, J.W., Schain, D.C., Gupte, A.A., et al. (2011) Transmission of Cryptococcus neoformans by Organ Transplantation. **Clinical infectious diseases : an official publication of the Infectious Diseases Society of America,** 52 (4): e94-8.

Bain, J.M., Lewis, L.E., Okai, B., et al. (2012) Non-lytic expulsion/exocytosis of Candida albicans from macrophages. **Fungal genetics and biology : FG & B,** 49 (9): 677-678.

Ballabh, P., Braun, A. and Nedergaard, M. (2004) The blood-brain barrier: an overview: structure, regulation, and clinical implications. **Neurobiology of disease,** 16 (1): 1-13.

Barbosa, F.M., Fonseca, F.L., Holandino, C., et al. (2006) Glucuronoxylomannan-mediated interaction of Cryptococcus neoformans with human alveolar cells results in fungal internalization and host cell damage. **Microbes and infection / Institut Pasteur,** 8 (2): 493-502.

Bartlett, K.H., Cheng, P.Y., Duncan, C., et al. (2012) A decade of experience: Cryptococcus gattii in British Columbia. **Mycopathologia,** 173 (5-6): 311-319.

Bartlett, K.H., Kidd, S.E. and Kronstad, J.W. (2008) The emergence of Cryptococcus gattii in British Columbia and the Pacific Northwest. **Curr Infect Dis Rep,** 10 58-65.

Baughman, R.P. and Lower, E.E. (2005) Fungal infections as a complication of therapy for sarcoidosis. **QJM : monthly journal of the Association of Physicians,** 98 (6): 451-456.

Beale, M.A., Sabiiti, W., Robertson, E.J., et al. (2015) Genotypic Diversity Is Associated with Clinical Outcome and Phenotype in Cryptococcal Meningitis across Southern Africa. **PLoS neglected tropical diseases,** 9 (6): e0003847.

Bicanic, T., Harrison, T., Niepieklo, A., et al. (2006) Symptomatic relapse of HIV-associated cryptococcal meningitis after initial fluconazole monotherapy: the role of fluconazole resistance and immune reconstitution. **Clinical infectious diseases : an official publication of the Infectious Diseases Society of America,** 43 (8): 1069-1073.

Bicanic, T., Meintjes, G., Wood, R., et al. (2007) Fungal burden, early fungicidal activity, and outcome in cryptococcal meningitis in antiretroviral-naive or antiretroviral-experienced patients treated with amphotericin B or fluconazole. **Clinical infectious diseases : an official publication of the Infectious Diseases Society of America,** 45 (1): 76-80.

Bicanic, T., Wood, R., Meintjes, G., et al. (2008) High-dose amphotericin B with flucytosine for the treatment of cryptococcal meningitis in HIV-infected patients: a randomized trial. **Clinical infectious diseases : an official publication of the Infectious Diseases Society of America,** 47 (1): 123-130.

Billot, X., Chateauneuf, A., Chauret, N., et al. (2003) Discovery of a potent and selective agonist of the prostaglandin EP4 receptor. **Bioorganic & medicinal chemistry letters,** 13 (6): 1129-1132.

Bose, I., Reese, A.J., Ory, J.J., et al. (2003) PMC178345; A yeast under cover: the capsule of Cryptococcus neoformans. **Eukaryot Cell,** 2 655-663.

Botts, M.R., Giles, S.S., Gates, M.A., et al. (2009) Isolation and characterization of Cryptococcus neoformans spores reveal a critical role for capsule biosynthesis genes in spore biogenesis. **Eukaryotic cell,** 8 (4): 595-605.

Botts, M.R. and Hull, C.M. (2010) Dueling in the lung: how Cryptococcus spores race the host for survival. **Current opinion in microbiology,** 13 (4): 437-442.

Bovers, M., Hagen, F., Kuramae, E.E., et al. (2006) Unique hybrids between the fungal pathogens Cryptococcus neoformans and Cryptococcus gattii. **FEMS yeast research,** 6 (4): 599-607.

Bovers, M., Hagen, F., Kuramae, E.E., et al. (2008) AIDS patient death caused by novel Cryptococcus neoformans x C. gattii hybrid. **Emerging infectious diseases,** 14 (7): 1105-1108.

Brieland, J.K., Jones, M.L., Clarke, S.J., et al. (1992) Effect of acute inflammatory lung injury on the expression of monocyte chemoattractant protein-1 (MCP-1) in rat pulmonary alveolar macrophages. **American journal of respiratory cell and molecular biology,** 7 (2): 134-139.

Brown, G.D. and Gordon, S. (2003) Fungal beta-glucans and mammalian immunity. **Immunity,** 19 311-315.

Brown, G.D. and Gordon, S. (2001) Immune recognition. A new receptor for beta-glucans. **Nature,** 413 36-37.

Buchanan, K.L. and Murphy, J.W. (1998) PMC2627665; What makes Cryptococcus neoformans a pathogen? **Emerg Infect Dis,** 4 71-83.

Buchanan, K.L. and Doyle, H.A. (2000) Requirement for CD4+ T Lymphocytes in Host Resistance against Cryptococcus neoformans in the Central Nervous System of Immunized Mice. **Infection and immunity,** 68 (2): 456-462.

Byrnes, E.J., Bildfell, R.J., Frank, S.A., et al. (2009) PMC2715219; Molecular evidence that the range of the Vancouver Island outbreak of Cryptococcus gattii infection has expanded into the Pacific Northwest in the United States. **J Infect Dis,** 199 1081-1086.

Byrnes,Edmond J., I.,II, Li, W., Lewit, Y., et al. (2010) Emergence and Pathogenicity of Highly Virulent *Cryptococcus gattii* Genotypes in the Northwest United States. **PLoS Pathog,** 6 e1000850.

Casadevall, A. and Pirofski, L.A. (2007) Accidental virulence, cryptic pathogenesis, martians, lost hosts, and the pathogenicity of environmental microbes. **Eukaryotic cell,** 6 (12): 2169-2174.

Casadevall, A., Rosas, A.L. and Nosanchuk, J.D. (2000) Melanin and virulence in Cryptococcus neoformans. **Current opinion in microbiology,** 3 (4): 354-358.

Cauley, L.K. and Murphy, J.W. (1979) Response of congenitally athymic (nude) and phenotypically normal mice to Cryptococcus neoformans infection. **Infection and immunity,** 23 (3): 644-651.

Chang, Y.C. and Kwon-Chung, K. (1999) PMC94082; Isolation, characterization, and localization of a capsule-associated gene, CAP10, of Cryptococcus neoformans. **J Bacteriol,** 181 5636-5643.

Chang, Y.C. and Kwon-Chung, K. (1998) PMC108186; Isolation of the third capsule-associated gene, CAP60, required for virulence in Cryptococcus neoformans. **Infect Immun,** 66 2230-2236.

Chang, Y.C. and Kwon-Chung, K. (1994) PMC358863; Complementation of a capsule-deficient mutation of Cryptococcus neoformans restores its virulence. **Mol Cell Biol,** 14 4912-4919.

Chang, Y.C., Penoyer, L.A. and Kwon-Chung, K. (1996) PMC174025; The second capsule gene of cryptococcus neoformans, CAP64, is essential for virulence. **Infect Immun,** 64 1977-1983.

Chang, Y.C., Stins, M.F., McCaffery, M.J., et al. (2004) PMC517459; Cryptococcal yeast cells invade the central nervous system via transcellular penetration of the blood-brain barrier. **Infect Immun,** 72 4985-4995.

Chang, Z.L., Netski, D., Thorkildson, P., et al. (2006) Binding and internalization of glucuronoxylomannan, the major capsular polysaccharide of Cryptococcus neoformans, by murine peritoneal macrophages. **Infection and immunity,** 74 (1): 144-151.

Charlier, C., Nielsen, K., Daou, S., et al. (2009) PMC2612285; Evidence of a role for monocytes in dissemination and brain invasion by Cryptococcus neoformans. **Infect Immun,** 77 120-127.

Chatfield, M.W. and Richards-Zawacki, C.L. (2011) Elevated temperature as a treatment for Batrachochytrium dendrobatidis infection in captive frogs. **Diseases of aquatic organisms,** 94 (3): 235-238.

Chayakulkeeree, M., Johnston, S.A., Oei, J.B., et al. (2011) SEC14 is a specific requirement for secretion of phospholipase B1 and pathogenicity of Cryptococcus neoformans. **Mol Microbiol,** 80 1088-1101.

Chen, G.H., McNamara, D.A., Hernandez, Y., et al. (2008a) Inheritance of immune polarization patterns is linked to resistance versus susceptibility to Cryptococcus neoformans in a mouse model. **Infection and immunity,** 76 (6): 2379-2391.

Chen, J., Varma, A., Diaz, M.R., et al. (2008b) Cryptococcus neoformans strains and infection in apparently immunocompetent patients, China. **Emerging infectious diseases,** 14 (5): 755-762.

Chen, S.C., Muller, M., Zhou, J.Z., et al. (1997a) Phospholipase activity in Cryptococcus neoformans: a new virulence factor? **J Infect Dis,** 175 414-420.

Chen, S.C., Wright, L.C., Golding, J.C., et al. (2000) PMC1220975; Purification and characterization of secretory phospholipase B, lysophospholipase and lysophospholipase/transacylase from a virulent strain of the pathogenic fungus Cryptococcus neoformans. **Biochem J,** 347 431-439.

Chen, S.C., Wright, L.C., Santangelo, R.T., et al. (1997b) PMC174609; Identification of extracellular phospholipase B, lysophospholipase, and acyltransferase produced by Cryptococcus neoformans. **Infect Immun,** 65 405-411.

Chen, S.H., Stins, M.F., Huang, S.H., et al. (2003) Cryptococcus neoformans induces alterations in the cytoskeleton of human brain microvascular endothelial cells. **Journal of medical microbiology,** 52 (Pt 11): 961-970.

Chinen, J. and Buckley, R.H. (2010) Transplantation immunology: solid organ and bone marrow. **The Journal of allergy and clinical immunology,** 125 (2 Suppl 2): S324-35.

Chrétien, F., Lortholary, O., Kansau, I., et al. (2002) Pathogenesis of cerebral Cryptococcus neoformans infection after fungemia. **J Infect Dis,** 186 522-530.

Chrisman, C.J., Alvarez, M. and Casadevall, A. (2010) Phagocytosis of Cryptococcus neoformans by, and nonlytic exocytosis from, Acanthamoeba castellanii. **Applied and Environmental Microbiology,** 76 (18): 6056-6062.

Chrisman, C.J., Albuquerque, P., Guimaraes, A.J., et al. (2011) Phospholipids Trigger Cryptococcus neoformans Capsular Enlargement during Interactions with Amoebae and Macrophages. **Plos Pathogens,** 7(5):e1002047.

Chuck, S.L. and Sande, M.A. (1989) Infections with Cryptococcus neoformans in the acquired immunodeficiency syndrome. **The New England journal of medicine,** 321 (12): 794-799.

Chun, C.D., Brown, J.C. and Madhani, H.D. (2011) PMC3077425; A major role for capsule-independent phagocytosis-inhibitory mechanisms in mammalian infection by Cryptococcus neoformans. **Cell Host Microbe,** 9 243-251.

Classen, A., Lloberas, J. and Celada, A. (2009) Macrophage activation: classical versus alternative. **Methods in molecular biology (Clifton, N.J.),** 531 29-43.

Coe, J.G.S., Wilson, C.F., Sorrell, T.C., et al. (2003) Cloning of CnLYSO1, a novel extracellular lysophospholipase of the pathogenic fungus Cryptococcus neoformans. **Gene,** 316 67-78.

Cogliati, M. (2013) Global Molecular Epidemiology of Cryptococcus neoformans and Cryptococcus gattii: An Atlas of the Molecular Types. **Scientifica,** 2013 675213.

Cox, G.M., McDade, H.C., Chen, S.C., et al. (2001) Extracellular phospholipase activity is a virulence factor for Cryptococcus neoformans. **Mol Microbiol,** 39 166-175.

Crabtree, J.N., Okagaki, L.H., Wiesner, D.L., et al. (2012) Titan cell production enhances the virulence of Cryptococcus neoformans. **Infection and immunity,** 80 (11): 3776-3785.

Cross, C.E. and Bancroft, G.J. (1995) PMC173349; Ingestion of acapsular Cryptococcus neoformans occurs via mannose and beta-glucan receptors, resulting in cytokine production and increased phagocytosis of the encapsulated form. **Infect Immun,** 63 2604-2611.

Cruickshank, J.G., Cavill, R. and Jelbert, M. (1973) PMC380794; Cryptococcus neoformans of unusual morphology. **Appl Microbiol,** 25 309-312.

Del Poeta, M. (2004) Role of phagocytosis in the virulence of Cryptococcus neoformans. **Eukaryotic cell,** 3 (5): 1067-1075.

Del Poeta, M. and Casadevall, A. (2012) Ten challenges on Cryptococcus and cryptococcosis. **Mycopathologia,** 173 (5-6): 303-310.

Del Valle, L. and Pina-Oviedo, S. (2006) HIV disorders of the brain: pathology and pathogenesis. **Frontiers in bioscience : a journal and virtual library,** 11 718-732.

Deshaw, M. and Pirofski, L.A. (1995a) Antibodies to the Cryptococcus neoformans capsular glucuronoxylomannan are ubiquitous in serum from HIV+ and HIV- individuals. **Clinical and experimental immunology,** 99 (3): 425-432.

Deshaw, M. and Pirofski, L.A. (1995b) PMC1534191; Antibodies to the Cryptococcus neoformans capsular glucuronoxylomannan are ubiquitous in serum from HIV+ and HIV-individuals. **Clin Exp Immunol,** 99 425-432.

Deshmane, S.L., Kremlev, S., Amini, S., et al. (2009) Monocyte chemoattractant protein-1 (MCP-1): an overview. **Journal of interferon & cytokine research : the official journal of the International Society for Interferon and Cytokine Research,** 29 (6): 313-326.

Diamond, R.D. and Bennett, J.E. (1973) Growth of Cryptococcus neoformans within human macrophages in vitro. **Infection and immunity,** 7 (2): 231-236.

Diamond, R.D., May, J.E., Kane, M., et al. (1973) The role of late complement components and the alternate complement pathway in experimental cryptococcosis. **Proceedings of the Society for Experimental Biology and Medicine.Society for Experimental Biology and Medicine (New York, N.Y.),** 144 (1): 312-315.

Diamond, R.D., Root, R.K. and Bennett, J.E. (1972) Factors influencing killing of Cryptococcus neoformans by human leukocytes in vitro. **The Journal of infectious diseases,** 125 (4): 367-376.

Djordjevic, J.T. (2010) Role of phospholipases in fungal fitness, pathogenicity, and drug development - lessons from cryptococcus neoformans. **Frontiers in microbiology,** 1 125.

Djordjevic, J.T., Del Poeta, M., Sorrell, T.C., et al. (2005a) Secretion of cryptococcal phospholipase B1 (PLB1) is regulated by a glycosylphosphatidylinositol (GPI) anchor. **Biochem J,** 389 803-812.

Djordjevic, J.T., Del Poeta, M., Sorrell, T.C., et al. (2005b) Secretion of cryptococcal phospholipase B1 (PLB1) is regulated by a glycosylphosphatidylinositol (GPI) anchor. **The Biochemical journal,** 389 (Pt 3): 803-812.

Dromer, F., Mathoulin-Pelissier, S., Fontanet, A., et al. (2004) Epidemiology of HIV-associated cryptococcosis in France (1985-2001): comparison of the pre- and post-HAART eras. **AIDS (London, England),** 18 (3): 555-562.

Eng, R.H., Bishburg, E., Smith, S.M., et al. (1986) Cryptococcal infections in patients with acquired immune deficiency syndrome. **The American Journal of Medicine,** 81 (1): 19-23.

Erb-Downward, J.R. and Huffnagle, G.B. (2007) Cryptococcus neoformans produces authentic prostaglandin E2 without a cyclooxygenase. **Eukaryotic cell,** 6 (2): 346-350.

Erb-Downward, J.R., Noggle, R.M., Williamson, P.R., et al. (2008) The role of laccase in prostaglandin production by Cryptococcus neoformans. **Molecular microbiology,** 68 (6): 1428-1437.

Evans, R.J., Li, Z., Hughes, W.S., et al. (2015) Cryptococcal Phospholipase B1 (Plb1) is required for intracellular proliferation and control of titan cell morphology during macrophage infection. **Infection and immunity,** 83(4):1296-304.

Fan, W., Kraus, P.R., Boily, M.J., et al. (2005) Cryptococcus neoformans gene expression during murine macrophage infection. **Eukaryotic cell,** 4 (8): 1420-1433.

Feldmesser, M., Kress, Y. and Casadevall, A. (2001) Dynamic changes in the morphology of Cryptococcus neoformans during murine pulmonary infection. **Microbiology,** 147 2355-2365.

Feldmesser, M., Kress, Y., Novikoff, P., et al. (2000) PMC101732; Cryptococcus neoformans is a facultative intracellular pathogen in murine pulmonary infection. **Infect Immun,** 68 4225-4237.

Fox, M.P. and Rosen, S. (2010) Patient retention in antiretroviral therapy programs up to three years on treatment in sub-Saharan Africa, 2007-2009: systematic review. **Tropical medicine & international health : TM & IH,** 15 Suppl 1 1-15.

Frases, S., Nimrichter, L., Viana, N.B., et al. (2008) Cryptococcus neoformans capsular polysaccharide and exopolysaccharide fractions manifest physical, chemical, and antigenic differences. **Eukaryotic cell,** 7 (2): 319-327.

Fromtling, R.A., Shadomy, H.J. and Jacobson, E.S. (1982) Decreased virulence in stable, acapsular mutants of cryptococcus neoformans. **Mycopathologia,** 79 23-29.

Ganendren, R., Carter, E., Sorrell, T., et al. (2006) Phospholipase B activity enhances adhesion of Cryptococcus neoformans to a human lung epithelial cell line. **Microbes and infection / Institut Pasteur,** 8 (4): 1006-1015.

Ganendren, R., Widmer, F., Singhal, V., et al. (2004) In vitro antifungal activities of inhibitors of phospholipases from the fungal pathogen Cryptococcus neoformans. **Antimicrobial Agents and Chemotherapy,** 48 (5): 1561-1569.

Gantner, B.N., Simmons, R.M. and Underhill, D.M. (2005) PMC556398; Dectin-1 mediates macrophage recognition of Candida albicans yeast but not filaments. **EMBO J,** 24 1277-1286.

Ganz, T., Selsted, M.E., Szklarek, D., et al. (1985) Defensins. Natural peptide antibiotics of human neutrophils. **The Journal of clinical investigation,** 76 (4): 1427-1435.

Garcia-Barbazan, I., Trevijano-Contador, N., Rueda, C., et al. (2015) The formation of titan cells in Cryptococcus neoformans depends on the mouse strain and correlates with induction of Th2-type responses. **Cellular microbiology,** 18(1):111-24 .

Garcia-Hermoso, D., Janbon, G. and Dromer, F. (1999) PMC85528; Epidemiological evidence for dormant Cryptococcus neoformans infection. **J Clin Microbiol,** 37 3204-3209.

Garcia-Rodas, R., Gonzalez-Camacho, F., Rodriguez-Tudela, J.L., et al. (2011) The interaction between Candida krusei and murine macrophages results in multiple outcomes, including intracellular survival and escape from killing. **Infection and immunity,** 79 (6): 2136-2144.

Garcia-Rodas, R. and Zaragoza, O. (2012) Catch me if you can: phagocytosis and killing avoidance by Cryptococcus neoformans. **FEMS immunology and medical microbiology,** 64 (2): 147-161.

Gates, M.A. and Kozel, T.R. (2006) PMC1479286; Differential localization of complement component 3 within the capsular matrix of Cryptococcus neoformans. **Infect Immun,** 74 3096-3106.

Geunes-Boyer, S., Beers, M.F., Perfect, J.R., et al. (2012) Surfactant protein D facilitates Cryptococcus neoformans infection. **Infection and immunity,** 80 (7): 2444-2453.

Geunes-Boyer, S., Oliver, T.N., Janbon, G., et al. (2009) Surfactant protein D increases phagocytosis of hypocapsular Cryptococcus neoformans by murine macrophages and enhances fungal survival. **Infection and immunity,** 77 (7): 2783-2794.

Giaimis, J., Lombard, Y., Fonteneau, P., et al. (1993) Both mannose and beta-glucan receptors are involved in phagocytosis of unopsonized, heat-killed Saccharomyces cerevisiae by murine macrophages. **J Leukoc Biol,** 54 564-571.

Giles, S.S., Dagenais, T.R., Botts, M.R., et al. (2009) PMC2715683; Elucidating the pathogenesis of spores from the human fungal pathogen Cryptococcus neoformans. **Infect Immun,** 77 3491-3500.

Goldman, D.L., Khine, H., Abadi, J., et al. (2001) Serologic evidence for Cryptococcus neoformans infection in early childhood. **Pediatrics,** 107 E66.

Goldman, D.L., Lee, S.C., Mednick, A.J., et al. (2000a) Persistent Cryptococcus neoformans pulmonary infection in the rat is associated with intracellular parasitism, decreased inducible nitric oxide synthase expression, and altered antibody responsiveness to cryptococcal polysaccharide. **Infection and immunity,** 68 (2): 832-838.

Goldman, D.L., Lee, S.C., Mednick, A.J., et al. (2000b) PMC97212; Persistent Cryptococcus neoformans pulmonary infection in the rat is associated with intracellular parasitism, decreased inducible nitric oxide synthase expression, and altered antibody responsiveness to cryptococcal polysaccharide. **Infect Immun,** 68 832-838.

Granger, D.L., Perfect, J.R. and Durack, D.T. (1985) PMC423853; Virulence of Cryptococcus neoformans. Regulation of capsule synthesis by carbon dioxide. **J Clin Invest,** 76 508-516.

Grant, A.D., Djomand, G. and De Cock, K.M. (1997) Natural history and spectrum of disease in adults with HIV/AIDS in Africa. **AIDS (London, England),** 11 Suppl B S43-54.

Guerra, C.R., Seabra, S.H., de Souza, W., et al. (2014) Cryptococcus neoformans is internalized by receptor-mediated or 'triggered' phagocytosis, dependent on actin recruitment. **PloS one,** 9 (2): e89250.

Guimaraes, A.J., Frases, S., Cordero, R.J., et al. (2010) Cryptococcus neoformans responds to mannitol by increasing capsule size in vitro and in vivo. **Cellular microbiology,** 12 (6): 740-753.

Hagen, F., Khayhan, K., Theelen, B., et al. (2015) Recognition of seven species in the Cryptococcus gattii/Cryptococcus neoformans species complex. **Fungal Genetics and Biology,** 78 (0): 16-48.

Harizi, H., Corcuff, J.B. and Gualde, N. (2008) Arachidonic-acid-derived eicosanoids: roles in biology and immunopathology. **Trends Mol Med,** 14 461-469.

Harris, J., Lockhart, S. and Chiller, T. (2012) Cryptococcus gattii: where do we go from here? **Medical mycology,** 50 (2): 113-129.

Heiss, C., Klutts, J.S., Wang, Z., et al. (2009) The structure of Cryptococcus neoformans galactoxylomannan contains beta-D-glucuronic acid. **Carbohydrate research,** 344 (7): 915-920.

Hill, J.O. and Aguirre, K.M. (1994) CD4+ T cell-dependent acquired state of immunity that protects the brain against Cryptococcus neoformans. **Journal of immunology (Baltimore, Md.: 1950),** 152 (5): 2344-2350.

Himmelreich, U., Allen, C., Dowd, S., et al. (2003) Identification of metabolites of importance in the pathogenesis of pulmonary cryptococcoma using nuclear magnetic resonance spectroscopy. **Microbes and infection / Institut Pasteur,** 5 (4): 285-290.

Hoag, K.A., Lipscomb, M.F., Izzo, A.A., et al. (1997) IL-12 and IFN-gamma are required for initiating the protective Th1 response to pulmonary cryptococcosis in resistant C.B-17 mice. **Am J Respir Cell Mol Biol,** 17 733-739.

Hoang, L.M.N., Philips, P. and Galanis, E. (2011) Cryptococcus gattii: a Review of the Epidemiology, Clinical Presentation, Diagnosis, and Management of This Endemic Yeast in the Pacific Northwest. **Clinical Microbiology Newsletter,** 33 (24): 187-195.

Hole, C.R., Bui, H., Wormley, F.L.,Jr, et al. (2012) Mechanisms of dendritic cell lysosomal killing of Cryptococcus. **Scientific reports,** 2 739.

Holmer, S.M., Evans, K.S., Asfaw, Y.G., et al. (2014) Impact of surfactant protein D, interleukin-5, and eosinophilia on Cryptococcosis. **Infection and immunity,** 82 (2): 683-693.

Houpt, D.C., Pfrommer, G.S., Young, B.J., et al. (1994a) Occurrences, immunoglobulin classes, and biological activities of antibodies in normal human serum that are reactive with Cryptococcus neoformans glucuronoxylomannan. **Infection and immunity,** 62 (7): 2857-2864.

Houpt, D.C., Pfrommer, G.S., Young, B.J., et al. (1994b) PMC302892; Occurrences, immunoglobulin classes, and biological activities of antibodies in normal human serum that are reactive with Cryptococcus neoformans glucuronoxylomannan. **Infect Immun,** 62 2857-2864.

Huffnagle, G.B., Chen, G.H., Curtis, J.L., et al. (1995a) Down-regulation of the afferent phase of T cell-mediated pulmonary inflammation and immunity by a high melanin-producing strain of Cryptococcus neoformans. **Journal of immunology (Baltimore, Md.: 1950),** 155 (7): 3507-3516.

Huffnagle, G.B., Chen, G.H., Curtis, J.L., et al. (1995b) Down-regulation of the afferent phase of T cell-mediated pulmonary inflammation and immunity by a high melanin-producing strain of Cryptococcus neoformans. **Journal of immunology (Baltimore, Md.: 1950),** 155 (7): 3507-3516.

Huffnagle, G.B., Lipscomb, M.F., Lovchik, J.A., et al. (1994) The role of CD4+ and CD8+ T cells in the protective inflammatory response to a pulmonary cryptococcal infection. **Journal of leukocyte biology,** 55 (1): 35-42.

Huffnagle, G.B., Strieter, R.M., McNeil, L.K., et al. (1997) Macrophage inflammatory protein-1alpha (MIP-1alpha) is required for the efferent phase of pulmonary cell-mediated immunity to a Cryptococcus neoformans infection. **Journal of immunology (Baltimore, Md.: 1950),** 159 (1): 318-327.

Huffnagle, G.B., Strieter, R.M., Standiford, T.J., et al. (1995c) The role of monocyte chemotactic protein-1 (MCP-1) in the recruitment of monocytes and CD4+ T cells during a pulmonary Cryptococcus neoformans infection. **Journal of immunology (Baltimore, Md.: 1950),** 155 (10): 4790-4797.

Hussell, T. and Bell, T.J. (2014) Alveolar macrophages: plasticity in a tissue-specific context. **Nature reviews.Immunology,** 14 (2): 81-93.

Idnurm, A., Bahn, Y.S., Nielsen, K., et al. (2005) Deciphering the model pathogenic fungus Cryptococcus neoformans. **Nat Rev Microbiol,** 3 753-764.

Ikeda, R., Shinoda, T., Fukazawa, Y., et al. (1982) PMC272288; Antigenic characterization of Cryptococcus neoformans serotypes and its application to serotyping of clinical isolates. **J Clin Microbiol,** 16 22-29.

Jackson, A. and Hosseinipour, M.C. (2010) Management of cryptococcal meningitis in sub-saharan Africa. **Current HIV/AIDS reports,** 7 (3): 134-142.

Jarvis, J.N., Bicanic, T., Loyse, A., et al. (2014) Determinants of mortality in a combined cohort of 501 patients with HIV-associated Cryptococcal meningitis: implications for improving outcomes. **Clinical infectious diseases : an official publication of the Infectious Diseases Society of America,** 58 (5): 736-745.

Jarvis, J.N., Boulle, A., Loyse, A., et al. (2009) High ongoing burden of cryptococcal disease in Africa despite antiretroviral roll out. **AIDS (London, England),** 23 (9): 1182-1183.

Jarvis, J.N., Casazza, J.P., Stone, H.H., et al. (2013) The phenotype of the Cryptococcus-specific CD4+ memory T-cell response is associated with disease severity and outcome in HIV-associated cryptococcal meningitis. **The Journal of infectious diseases,** 207 (12): 1817-1828.

Johnston, S.A. and May, R.C. (2010) The Human Fungal Pathogen *Cryptococcus neoformans* Escapes Macrophages by a Phagosome Emptying Mechanism That Is Inhibited by Arp2/3 Complex-Mediated Actin Polymerisation. **PLoS Pathog,** 6 e1001041.

Jones, P.M., Turner, K.M., Djordjevic, J.T., et al. (2007) Role of conserved active site residues in catalysis by phospholipase B1 from Cryptococcus neoformans. **Biochemistry,** 46 (35): 10024-10032.

Jong, A., Wu, C.H., Chen, H.M., et al. (2007) Identification and characterization of CPS1 as a hyaluronic acid synthase contributing to the pathogenesis of Cryptococcus neoformans infection. **Eukaryotic cell,** 6 (8): 1486-1496.

Jong, A., Wu, C.H., Shackleford, G.M., et al. (2008) Involvement of human CD44 during Cryptococcus neoformans infection of brain microvascular endothelial cells. **Cellular microbiology,** 10 (6): 1313-1326.

Kambugu, A., Meya, D.B., Rhein, J., et al. (2008) Outcomes of cryptococcal meningitis in Uganda before and after the availability of highly active antiretroviral therapy. **Clinical infectious diseases : an official publication of the Infectious Diseases Society of America,** 46 (11): 1694-1701.

Kaplan, J.E., Hanson, D., Dworkin, M.S., et al. (2000) Epidemiology of human immunodeficiency virus-associated opportunistic infections in the United States in the era of highly active antiretroviral therapy. **Clinical infectious diseases : an official publication of the Infectious Diseases Society of America,** 30 Suppl 1 S5-14.

Kawakami, K., Kohno, S., Kadota, J., et al. (1995) T cell-dependent activation of macrophages and enhancement of their phagocytic activity in the lungs of mice inoculated with heat-killed Cryptococcus neoformans: involvement of IFN-gamma and its protective effect against cryptococcal infection. **Microbiology and immunology,** 39 (2): 135-143.

Kozel, T.R. and Gotschlich, E.C. (1982) The capsule of cryptococcus neoformans passively inhibits phagocytosis of the yeast by macrophages. **J Immunol,** 129 1675-1680.

Kronstad, J.W., Attarian, R., Cadieux, B., et al. (2011) Expanding fungal pathogenesis: Cryptococcus breaks out of the opportunistic box. **Nat Rev Microbiol,** 9 193-203.

Kwon-Chung, K. and Rhodes, J.C. (1986) PMC261090; Encapsulation and melanin formation as indicators of virulence in Cryptococcus neoformans. **Infect Immun,** 51 218-223.

Kwon-Chung, K.J. (1976a) Morphogenesis of Filobasidiella neoformans, the sexual state of Cryptococcus neoformans. **Mycologia,** 68 (4): 821-833.

Kwon-Chung, K.J. (1976b) A new species of Filobasidiella, the sexual state of Cryptococcus neoformans B and C serotypes. **Mycologia,** 68 (4): 943-946.

Kwon-Chung, K.J., Polacheck, I. and Popkin, T.J. (1982) Melanin-lacking mutants of Cryptococcus neoformans and their virulence for mice. **Journal of Bacteriology,** 150 (3): 1414-1421.

Kwon-Chung, K.J., Boekhout, T., Fell, J.W., et al. (2002) Proposal to Conserve the Name Cryptococcus gattii against C. hondurianus and C. bacillisporus (Basidiomycota, Hymenomycetes, Tremellomycetidae). **Taxon,** 51 (4): 804-806.

Kwon-Chung, K.J. and Varma, A. (2006) Do major species concepts support one, two or more species within Cryptococcus neoformans? **FEMS Yeast Research,** 6 (4): 574-587.

Latouche, G.N., Sorrell, T.C. and Meyer, W. (2002) Isolation and characterisation of the phospholipase B gene of Cryptococcus neoformans var. gattii. **FEMS yeast research,** 2 (4): 551-561.

Lee, K.S., Patton, J.L., Fido, M., et al. (1994) The Saccharomyces cerevisiae PLB1 gene encodes a protein required for lysophospholipase and phospholipase B activity. **The Journal of biological chemistry,** 269 (31): 19725-19730.

Lehrer, R.I. and Ladra, K.M. (1977) Fungicidal components of mammalian granulocytes active against Cryptococcus neoformans. **The Journal of infectious diseases,** 136 (1): 96-99.

Leidich, S.D., Ibrahim, A.S., Fu, Y., et al. (1998) Cloning and disruption of caPLB1, a phospholipase B gene involved in the pathogenicity of Candida albicans. **The Journal of biological chemistry,** 273 (40): 26078-26086.

Lengeler, K.B., Cox, G.M. and Heitman, J. (2001) PMC97862; Serotype AD strains of Cryptococcus neoformans are diploid or aneuploid and are heterozygous at the mating-type locus. **Infect Immun,** 69 115-122.

Lev, S., Crossett, B., Cha, S.Y., et al. (2014) Identification of Aph1, a phosphate-regulated, secreted, and vacuolar acid phosphatase in Cryptococcus neoformans. **mBio,** 5 (5): e01649-14.

Levitz, S.M., Nong, S.H., Seetoo, K.F., et al. (1999a) Cryptococcus neoformans resides in an acidic phagolysosome of human macrophages. **Infection and immunity,** 67 (2): 885-890.

Levitz, S.M., Nong, S.H., Seetoo, K.F., et al. (1999b) PMC96400; Cryptococcus neoformans resides in an acidic phagolysosome of human macrophages. **Infect Immun,** 67 885-890.

Lin, Y.Y., Shiau, S. and Fang, C.T. (2015) Risk factors for invasive Cryptococcus neoformans diseases: a case-control study. **PloS one,** 10 (3): e0119090.

Lindell, D.M., Ballinger, M.N., McDonald, R.A., et al. (2006) Diversity of the T-cell response to pulmonary Cryptococcus neoformans infection. **Infection and immunity,** 74 (8): 4538-4548.

Litvintseva, A.P., Thakur, R., Vilgalys, R., et al. (2006) Multilocus sequence typing reveals three genetic subpopulations of Cryptococcus neoformans var. grubii (serotype A), including a unique population in Botswana. **Genetics,** 172 (4): 2223-2238.

Liu, O.W., Chun, C.D., Chow, E.D., et al. (2008) PMC2628477; Systematic genetic analysis of virulence in the human fungal pathogen Cryptococcus neoformans. **Cell,** 135 174-188.

Liu, T.B., Kim, J.C., Wang, Y., et al. (2013) Brain inositol is a novel stimulator for promoting Cryptococcus penetration of the blood-brain barrier. **PLoS pathogens,** 9 (4): e1003247.

Loftus, B.J., Fung, E., Roncaglia, P., et al. (2005) The genome of the basidiomycetous yeast and human pathogen Cryptococcus neoformans. **Science (New York, N.Y.),** 307 (5713): 1321-1324.

Love, G.L., Boyd, G.D. and Greer, D.L. (1985) PMC271885; Large Cryptococcus neoformans isolated from brain abscess. **J Clin Microbiol,** 22 1068-1070.

Luberto, C., Martinez-MariÃ±o, B., Taraskiewicz, D., et al. (2003) PMC198528; Identification of App1 as a regulator of phagocytosis and virulence of Cryptococcus neoformans. **J Clin Invest,** 112 1080-1094.

Lupo, P., Chang, Y.C., Kelsall, B.L., et al. (2008) The presence of capsule in Cryptococcus neoformans influences the gene expression profile in dendritic cells during interaction with the fungus. **Infection and immunity,** 76 (4): 1581-1589.

Ma, H., Croudace, J.E., Lammas, D.A., et al. (2007) Direct cell-to-cell spread of a pathogenic yeast. **BMC immunology,** 8 15.

Ma, H., Croudace, J.E., Lammas, D.A., et al. (2006) Expulsion of live pathogenic yeast by macrophages. **Curr Biol,** 16 2156-2160.

Ma, H., Hagen, F., Stekel, D.J., et al. (2009) Pmc2722359; The fatal fungal outbreak on Vancouver Island is characterized by enhanced intracellular parasitism driven by mitochondrial regulation. **Proc Natl Acad Sci U S A,** 106 12980-12985.

Ma, H. (2009) **Intracellular parasitism of macrophages by Cryptococcus.** University of Birmingham.

Ma, H. and May, R.C. (2009) "Chapter 5 Virulence in Cryptococcus Species" In Allen I. Laskin,Sima Sariaslani and Geoffrey M.Gadd (ed.) Academic Press. pp. 131-190.

MacDougall, L., Kidd, S.E., Galanis, E., et al. (2007) PMC2725832; Spread of Cryptococcus gattii in British Columbia, Canada, and detection in the Pacific Northwest, USA. **Emerg Infect Dis,** 13 42-50.

Mak, S., Klinkenberg, B., Bartlett, K., et al. (2010) Ecological niche modeling of Cryptococcus gattii in British Columbia, Canada. **Environmental health perspectives,** 118 (5): 653-658.

Mambula, S.S., Simons, E.R., Hastey, R., et al. (2000) Human neutrophil-mediated nonoxidative antifungal activity against Cryptococcus neoformans. **Infection and immunity,** 68 (11): 6257-6264.

Mansour, M.K., Latz, E. and Levitz, S.M. (2006) Cryptococcus neoformans glycoantigens are captured by multiple lectin receptors and presented by dendritic cells. **Journal of immunology (Baltimore, Md.: 1950),** 176 (5): 3053-3061.

Mansour, M.K., Vyas, J.M. and Levitz, S.M. (2011) Dynamic virulence: real-time assessment of intracellular pathogenesis links Cryptococcus neoformans phenotype with clinical outcome. **mBio,** 2 (5): 10.1128/mBio.00217-11. Print 2011.

Martinez, F.O. and Gordon, S. (2014) The M1 and M2 paradigm of macrophage activation: time for reassessment. **F1000prime reports,** 6 13-13. eCollection 2014.

Maruvada, R., Zhu, L., Pearce, D., et al. (2012) Cryptococcus neoformans phospholipase B1 activates host cell Rac1 for traversal across the blood-brain barrier. **Cellular microbiology,** 14 (10): 1544-1553.

Mayanja-Kizza, H., Oishi, K., Mitarai, S., et al. (1998) Combination therapy with fluconazole and flucytosine for cryptococcal meningitis in Ugandan patients with AIDS. **Clinical infectious diseases : an official publication of the Infectious Diseases Society of America,** 26 (6): 1362-1366.

Milefchik, E., Leal, M.A., Haubrich, R., et al. (2008) Fluconazole alone or combined with flucytosine for the treatment of AIDS-associated cryptococcal meningitis. **Medical mycology,** 46 (4): 393-395.

Miller, G.P. and Kohl, S. (1983) Antibody-dependent leukocyte killing of Cryptococcus neoformans. **Journal of immunology (Baltimore, Md.: 1950),** 131 (3): 1455-1459.

Miller, M.F. and Mitchell, T.G. (1991) Killing of Cryptococcus neoformans strains by human neutrophils and monocytes. **Infection and immunity,** 59 (1): 24-28.

Mirza, S.A., Phelan, M., Rimland, D., et al. (2003) The changing epidemiology of cryptococcosis: an update from population-based active surveillance in 2 large metropolitan areas, 1992-2000. **Clinical infectious diseases : an official publication of the Infectious Diseases Society of America,** 36 (6): 789-794.

Mitchell, T.G. and Perfect, J.R. (1995) PMC172874; Cryptococcosis in the era of AIDS-- 100 years after the discovery of Cryptococcus neoformans. **Clin Microbiol Rev,** 8 515-548.

Monari, C., Bistoni, F., Casadevall, A., et al. (2005a) Glucuronoxylomannan, a microbial compound, regulates expression of costimulatory molecules and production of cytokines in macrophages. **The Journal of infectious diseases,** 191 (1): 127-137.

Monari, C., Bistoni, F. and Vecchiarelli, A. (2006) Glucuronoxylomannan exhibits potent immunosuppressive properties. **FEMS Yeast Res,** 6 537-542.

Monari, C., Pericolini, E., Bistoni, G., et al. (2005b) Cryptococcus neoformans capsular glucuronoxylomannan induces expression of fas ligand in macrophages. **Journal of immunology (Baltimore, Md.: 1950),** 174 (6): 3461-3468.

Monari, C., Retini, C., Casadevall, A., et al. (2003) Differences in outcome of the interaction between Cryptococcus neoformans glucuronoxylomannan and human monocytes and neutrophils. **European journal of immunology,** 33 (4): 1041-1051.

Mukherjee, S., Feldmesser, M. and Casadevall, A. (1996) J774 murine macrophage-like cell interactions with Cryptococcus neoformans in the presence and absence of opsonins. **J Infect Dis,** 173 1222-1231.

Murdoch, D.M., Venter, W.D., Van Rie, A., et al. (2007) Immune reconstitution inflammatory syndrome (IRIS): review of common infectious manifestations and treatment options. **AIDS research and therapy,** 4 9.

Mwaba, P., Mwansa, J., Chintu, C., et al. (2001) Clinical presentation, natural history, and cumulative death rates of 230 adults with primary cryptococcal meningitis in Zambian AIDS patients treated under local conditions. **Postgraduate medical journal,** 77 (914): 769-773.

Nicola, A.M., Robertson, E.J., Albuquerque, P., et al. (2011) Nonlytic exocytosis of Cryptococcus neoformans from macrophages occurs in vivo and is influenced by phagosomal pH. **mBio,** 2 (4): 10.1128/mBio.00167-11. Print 2011.

Nimmerjahn, F. and Ravetch, J.V. (2007) Fc-receptors as regulators of immunity. **Advances in Immunology,** 96 179-204.

Nosanchuk, J.D., Rosas, A.L. and Casadevall, A. (1998) The antibody response to fungal melanin in mice. **Journal of immunology (Baltimore, Md.: 1950),** 160 (12): 6026-6031.

Nosanchuk, J.D., Valadon, P., Feldmesser, M., et al. (1999) Melanization of Cryptococcus neoformans in murine infection. **Molecular and cellular biology,** 19 (1): 745-750.

Noverr, M.C., Cox, G.M., Perfect, J.R., et al. (2003a) PMC148814; Role of PLB1 in pulmonary inflammation and cryptococcal eicosanoid production. **Infect Immun,** 71 1538-1547.

Noverr, M.C., Erb-Downward, J.R. and Huffnagle, G.B. (2003b) Production of eicosanoids and other oxylipins by pathogenic eukaryotic microbes. **Clinical microbiology reviews,** 16 (3): 517-533.

Noverr, M.C., Phare, S.M., Toews, G.B., et al. (2001) Pathogenic yeasts Cryptococcus neoformans and Candida albicans produce immunomodulatory prostaglandins. **Infection and immunity,** 69 (5): 2957-2963.

Oishi, H., Tsuda, S., Watanabe, Y., et al. (1996) Purification and some properties of phospholipase B from Schizosaccharomyces pombe. **Bioscience, biotechnology, and biochemistry,** 60 (7): 1087-1092.

Okagaki, L.H. and Nielsen, K. (2012) PMC3370461; Titan cells confer protection from phagocytosis in Cryptococcus neoformans infections. **Eukaryot Cell,** 11 820-826.

Okagaki, L.H., Strain, A.K., Nielsen, J.N., et al. (2010) PMC2887476; Cryptococcal cell morphology affects host cell interactions and pathogenicity. **PLoS Pathog,** 6 e1000953.

Olszewski, M.A., Noverr, M.C., Chen, G.H., et al. (2004) Urease expression by Cryptococcus neoformans promotes microvascular sequestration, thereby enhancing central nervous system invasion. **The American journal of pathology,** 164 (5): 1761-1771.

Osterholzer, J.J., Chen, G.H., Olszewski, M.A., et al. (2009a) Accumulation of CD11b+ lung dendritic cells in response to fungal infection results from the CCR2-mediated recruitment and differentiation of Ly-6Chigh monocytes. **Journal of immunology (Baltimore, Md.: 1950),** 183 (12): 8044-8053.

Osterholzer, J.J., Chen, G.H., Olszewski, M.A., et al. (2011) Chemokine receptor 2-mediated accumulation of fungicidal exudate macrophages in mice that clear cryptococcal lung infection. **The American journal of pathology,** 178 (1): 198-211.

Osterholzer, J.J., Milam, J.E., Chen, G.H., et al. (2009b) Role of dendritic cells and alveolar macrophages in regulating early host defense against pulmonary infection with Cryptococcus neoformans. **Infection and immunity,** 77 (9): 3749-3758.

Osterholzer, J.J., Surana, R., Milam, J.E., et al. (2009c) Cryptococcal urease promotes the accumulation of immature dendritic cells and a non-protective T2 immune response within the lung. **The American journal of pathology,** 174 (3): 932-943.

Ou, X.T., Wu, J.Q., Zhu, L.P., et al. (2011) Genotypes coding for mannose-binding lectin deficiency correlated with cryptococcal meningitis in HIV-uninfected Chinese patients. **The Journal of infectious diseases,** 203 (11): 1686-1691.

Paralkar, V.M., Borovecki, F., Ke, H.Z., et al. (2003) An EP2 receptor-selective prostaglandin E2 agonist induces bone healing. **Proceedings of the National Academy of Sciences of the United States of America,** 100 (11): 6736-6740.

Parameswaran, N. and Patial, S. (2010) Tumor necrosis factor-alpha signaling in macrophages. **Critical reviews in eukaryotic gene expression,** 20 (2): 87-103.

Park, B.J., Wannemuehler, K.A., Marston, B.J., et al. (2009) Estimation of the current global burden of cryptococcal meningitis among persons living with HIV/AIDS. **AIDS,** 23 525-530.

Park, J.Y., Pillinger, M.H. and Abramson, S.B. (2006) Prostaglandin E2 synthesis and secretion: the role of PGE2 synthases. **Clinical immunology (Orlando, Fla.),** 119 (3): 229-240.

Patel, D., Desai, G.M., Frases, S., et al. (2013) Methamphetamine enhances Cryptococcus neoformans pulmonary infection and dissemination to the brain. **mBio,** 4 (4): 10.1128/mBio.00400-13.

Patel, R. and Paya, C.V. (1997) Infections in solid-organ transplant recipients. **Clinical microbiology reviews,** 10 (1): 86-124.

Perfect, J.R. (2012a) The impact of the host on fungal infections. **The American Journal of Medicine,** 125 (1 Suppl): S39-51.

Perfect, J.R. (2012b) The triple threat of cryptococcosis: it's the body site, the strain, and/or the host. **mBio,** 3 (4): 10.1128/mBio.00165-12. Print 2012.

Perfect, J.R. (2006) Cryptococcus neoformans: the yeast that likes it hot. **FEMS yeast research,** 6 (4): 463-468.

Perfect, J.R. and Bicanic, T. (2015) Cryptococcosis diagnosis and treatment: What do we know now. **Fungal genetics and biology : FG & B,** 78 49-54.

Perfect, J.R., Dismukes, W.E., Dromer, F., et al. (2010) Clinical practice guidelines for the management of cryptococcal disease: 2010 update by the infectious diseases society of america. **Clinical infectious diseases : an official publication of the Infectious Diseases Society of America,** 50 (3): 291-322.

Petzold, E.W., Himmelreich, U., Mylonakis, E., et al. (2006) PMC1594924; Characterization and regulation of the trehalose synthesis pathway and its importance in the pathogenicity of Cryptococcus neoformans. **Infect Immun,** 74 5877-5887.

Porcaro, I., Vidal, M., Jouvert, S., et al. (2003) Mannose receptor contribution to Candida albicans phagocytosis by murine E-clone J774 macrophages. **J Leukoc Biol,** 74 206-215.

Qureshi, A., Grey, A., Rose, K.L., et al. (2011) Cryptococcus neoformans modulates extracellular killing by neutrophils. **Frontiers in microbiology,** 2 193.

Qureshi, A., Subathra, M., Grey, A., et al. (2010) Role of sphingomyelin synthase in controlling the antimicrobial activity of neutrophils against Cryptococcus neoformans. **PloS one,** 5 (12): e15587.

Remijsen, Q., Kuijpers, T.W., Wirawan, E., et al. (2011) Dying for a cause: NETosis, mechanisms behind an antimicrobial cell death modality. **Cell death and differentiation,** 18 (4): 581-588.

Ricciotti, E. and FitzGerald, G.A. (2011) Prostaglandins and inflammation. **Arteriosclerosis, Thrombosis, and Vascular Biology,** 31 (5): 986-1000.

Rivera, J., Feldmesser, M., Cammer, M., et al. (1998) PMC108624; Organ-dependent variation of capsule thickness in Cryptococcus neoformans during experimental murine infection. **Infect Immun,** 66 5027-5030.

Rocha, J.D., Nascimento, M.T., Decote-Ricardo, D., et al. (2015) Capsular polysaccharides from Cryptococcus neoformans modulate production of neutrophil extracellular traps (NETs) by human neutrophils. **Scientific reports,** 5 8008.

Rosas, A.L., Nosanchuk, J.D., Feldmesser, M., et al. (2000) PMC97496; Synthesis of polymerized melanin by Cryptococcus neoformans in infected rodents. **Infect Immun,** 68 2845-2853.

Russell, D.G., Vanderven, B.C., Glennie, S., et al. (2009) The macrophage marches on its phagosome: dynamic assays of phagosome function. **Nature reviews.Immunology,** 9 (8): 594-600.

Sabiiti, W. and May, R.C. (2012) Mechanisms of infection by the human fungal pathogen Cryptococcus neoformans. **Future microbiology,** 7 (11): 1297-1313.

Sabiiti, W., Robertson, E., Beale, M.A., et al. (2014) Efficient phagocytosis and laccase activity affect the outcome of HIV-associated cryptococcosis. **Journal of Clinical Investigation,** 124 2000-2008.

Salas, S.D., Bennett, J.E., Kwon-Chung, K.J., et al. (1996) Effect of the laccase gene CNLAC1, on virulence of Cryptococcus neoformans. **The Journal of experimental medicine,** 184 (2): 377-386.

Santangelo, R., Zoellner, H., Sorrell, T., et al. (2004) PMC375158; Role of extracellular phospholipases and mononuclear phagocytes in dissemination of cryptococcosis in a murine model. **Infect Immun,** 72 2229-2239.

Santangelo, R.T., Chen, S.C., Sorrell, T.C., et al. (2005) Detection of antibodies to phospholipase B in patients infected with Cryptococcus neoformans by enzyme-linked immunosorbent assay (ELISA). **Med Mycol,** 43 335-341.

Santangelo, R.T., Nouri-Sorkhabi, M.H., Sorrell, T.C., et al. (1999) Biochemical and functional characterisation of secreted phospholipase activities from Cryptococcus neoformans in their naturally occurring state. **Journal of medical microbiology,** 48 (8): 731-740.

Sarma, J.V. and Ward, P.A. (2011) The complement system. **Cell and tissue research,** 343 (1): 227-235.

Savina, A. and Amigorena, S. (2007) Phagocytosis and antigen presentation in dendritic cells. **Immunological reviews,** 219 143-156.

Schoenborn, J.R. and Wilson, C.B. (2007) Regulation of interferon-gamma during innate and adaptive immune responses. **Advances in Immunology,** 96 41-101.

Segal, A.W. (2005) How neutrophils kill microbes. **Annual Review of Immunology,** 23 197-223.

Shao, X., Mednick, A., Alvarez, M., et al. (2005) An innate immune system cell is a major determinant of species-related susceptibility differences to fungal pneumonia. **Journal of immunology (Baltimore, Md.: 1950),** 175 (5): 3244-3251.

Shea, J.M., Henry, J.L. and Del Poeta, M. (2006) Lipid metabolism in Cryptococcus neoformans. **FEMS Yeast Res,** 6 469-479.

Shelburne, S.A.,3rd, Darcourt, J., White, A.C.,Jr, et al. (2005) The role of immune reconstitution inflammatory syndrome in AIDS-related Cryptococcus neoformans disease in the era of highly active antiretroviral therapy. **Clinical infectious diseases : an official publication of the Infectious Diseases Society of America,** 40 (7): 1049-1052.

Shen, D.K., Noodeh, A.D., Kazemi, A., et al. (2004) Characterisation and expression of phospholipases B from the opportunistic fungus Aspergillus fumigatus. **FEMS microbiology letters,** 239 (1): 87-93.

Shen, L. and Liu, Y. (2015) Prostaglandin E2 blockade enhances the pulmonary anti-Cryptococcus neoformans immune reaction via the induction of TLR-4. **International immunopharmacology,** 28 (1): 376-381.

Shi, M., Li, S.S., Zheng, C., et al. (2010a) PMC2860939; Real-time imaging of trapping and urease-dependent transmigration of Cryptococcus neoformans in mouse brain. **J Clin Invest,** 120 1683-1693.

Shi, M., Li, S.S., Zheng, C., et al. (2010b) Real-time imaging of trapping and urease-dependent transmigration of Cryptococcus neoformans in mouse brain. **The Journal of clinical investigation,** 120 (5): 1683-1693.

Shibuya, K., Hirata, A., Omuta, J., et al. (2005) Granuloma and cryptococcosis. **Journal of infection and chemotherapy : official journal of the Japan Society of Chemotherapy,** 11 (3): 115-122.

Shoham, S. and Marr, K.A. (2012) Invasive fungal infections in solid organ transplant recipients. **Future microbiology,** 7 (5): 639-655.

Siafakas, A.R., Sorrell, T.C., Wright, L.C., et al. (2007) Cell wall-linked cryptococcal phospholipase B1 is a source of secreted enzyme and a determinant of cell wall integrity. **J Biol Chem,** 282 37508-37514.

Siafakas, A.R., Wright, L.C., Sorrell, T.C., et al. (2006) Lipid rafts in Cryptococcus neoformans concentrate the virulence determinants phospholipase B1 and Cu/Zn superoxide dismutase. **Eukaryotic cell,** 5 (3): 488-498.

Simmons, D.L., Botting, R.M. and Hla, T. (2004) Cyclooxygenase isozymes: the biology of prostaglandin synthesis and inhibition. **Pharmacological reviews,** 56 (3): 387-437.

Singh, A., Panting, R.J., Varma, A., et al. (2013) Factors required for activation of urease as a virulence determinant in Cryptococcus neoformans. **mBio,** 4 (3): e00220-13.

Singh, N., Husain, S., De Vera, M., et al. (2004) Cryptococcus neoformans Infection in Patients With Cirrhosis, Including Liver Transplant Candidates. **Medicine,** 83 (3): 188-192.

Sionov, E., Chang, Y.C. and Kwon-Chung, K.J. (2013) Azole heteroresistance in Cryptococcus neoformans: emergence of resistant clones with chromosomal disomy in the mouse brain during fluconazole treatment. **Antimicrobial Agents and Chemotherapy,** 57 (10): 5127-5130.

Smith, K.D., Achan, B., Huppler Hullsiek, K., et al. (2015a) Increased Antifungal Drug Resistance in Ugandan Clinical Isolates of Cryptococcus neoformans. **Antimicrobial Agents and Chemotherapy,** 59(12):7197-204.

Smith, L.M., Dixon, E.F. and May, R.C. (2015b) The fungal pathogen Cryptococcus neoformans manipulates macrophage phagosome maturation. **Cellular microbiology,** 17 (5): 702-713.

Standiford, T.J., Kunkel, S.L., Phan, S.H., et al. (1991) Alveolar macrophage-derived cytokines induce monocyte chemoattractant protein-1 expression from human pulmonary type II-like epithelial cells. **The Journal of biological chemistry,** 266 (15): 9912-9918.

Steenbergen, J.N. and Casadevall, A. (2003) The origin and maintenance of virulence for the human pathogenic fungus Cryptococcus neoformans. **Microbes Infect,** 5 667-675.

Steenbergen, J.N., Shuman, H.A. and Casadevall, A. (2001) PMC65014; Cryptococcus neoformans interactions with amoebae suggest an explanation for its virulence and intracellular pathogenic strategy in macrophages. **Proc Natl Acad Sci U S A,** 98 15245-15250.

Stenson, W.F., Nickells, M.W. and Atkinson, J.P. (1981) Metabolism of exogenous arachidonic acid by murine macrophage-like tumor cell lines. **Prostaglandins,** 21 (5): 675-689.

Sugatani, J., Kawasaki, N. and Saito, K. (1978) Studies on a phospholipase B from Penicillium notatum. Substrate specificity. **Biochimica et biophysica acta,** 529 (1): 29-37.

Sugiyama, Y., Nakashima, S., Mirbod, F., et al. (1999) Molecular cloning of a second phospholipase B gene, caPLB2 from Candida albicans. **Medical mycology,** 37 (1): 61-67.

Taborda, C.P. and Casadevall, A. (2002) CR3 (CD11b/CD18) and CR4 (CD11c/CD18) are involved in complement-independent antibody-mediated phagocytosis of Cryptococcus neoformans. **Immunity,** 16 (6): 791-802.

Talloczy, Z., Martinez, J., Joset, D., et al. (2008) Methamphetamine inhibits antigen processing, presentation, and phagocytosis. **PLoS pathogens,** 4 (2): e28.

Traynor, T.R., Kuziel, W.A., Toews, G.B., et al. (2000) CCR2 expression determines T1 versus T2 polarization during pulmonary Cryptococcus neoformans infection. **Journal of immunology (Baltimore, Md.: 1950),** 164 (4): 2021-2027.

Tucker, S.C. and Casadevall, A. (2002) Replication of Cryptococcus neoformans in macrophages is accompanied by phagosomal permeabilization and accumulation of vesicles containing polysaccharide in the cytoplasm. **Proceedings of the National Academy of Sciences of the United States of America,** 99 (5): 3165-3170.

Turner, K.M., Wright, L.C., Sorrell, T.C., et al. (2006) N-linked glycosylation sites affect secretion of cryptococcal phospholipase B1, irrespective of glycosylphosphatidylinositol anchoring. **Biochimica et biophysica acta,** 1760 (10): 1569-1579.

Uicker, W.C., McCracken, J.P. and Buchanan, K.L. (2006) Role of CD4+ T cells in a protective immune response against Cryptococcus neoformans in the central nervous system. **Medical mycology,** 44 (1): 1-11.

van der Pouw Kraan, T.C., Boeije, L.C., Smeenk, R.J., et al. (1995) PMC2191857; Prostaglandin-E2 is a potent inhibitor of human interleukin 12 production. **J Exp Med,** 181 775-779.

van Meer, G., Voelker, D.R. and Feigenson, G.W. (2008) Membrane lipids: where they are and how they behave. **Nature reviews.Molecular cell biology,** 9 (2): 112-124.

Vartivarian, S.E., Anaissie, E.J., Cowart, R.E., et al. (1993) Regulation of cryptococcal capsular polysaccharide by iron. **The Journal of infectious diseases,** 167 (1): 186-190.

Vecchiarelli, A., Retini, C., Monari, C., et al. (1996) PMC174153; Purified capsular polysaccharide of Cryptococcus neoformans induces interleukin-10 secretion by human monocytes. **Infect Immun,** 64 2846-2849.

Velagapudi, R., Hsueh, Y.P., Geunes-Boyer, S., et al. (2009) Spores as infectious propagules of Cryptococcus neoformans. **Infection and immunity,** 77 (10): 4345-4355.

Villena, S.N., Pinheiro, R.O., Pinheiro, C.S., et al. (2008) Capsular polysaccharides galactoxylomannan and glucuronoxylomannan from Cryptococcus neoformans induce macrophage apoptosis mediated by Fas ligand. **Cellular microbiology,** 10 (6): 1274-1285.

Voelz, K., Johnston, S.A., Rutherford, J.C., et al. (2010) Automated analysis of cryptococcal macrophage parasitism using GFP-tagged cryptococci. **PloS one,** 5 (12): e15968.

Voelz, K., Lammas, D.A. and May, R.C. (2009) PMC2715691; Cytokine signaling regulates the outcome of intracellular macrophage parasitism by Cryptococcus neoformans. **Infect Immun,** 77 3450-3457.

Voelz, K. and May, R.C. (2010) Cryptococcal interactions with the host immune system. **Eukaryotic cell,** 9 (6): 835-846.

Wang, P., Cardenas, M.E., Cox, G.M., et al. (2001) Two cyclophilin A homologs with shared and distinct functions important for growth and virulence of Cryptococcus neoformans. **EMBO reports,** 2 (6): 511-518.

Wang, Y., Aisen, P. and Casadevall, A. (1995) PMC173427; Cryptococcus neoformans melanin and virulence: mechanism of action. **Infect Immun,** 63 3131-3136.

Warpeha, K.M., Park, Y.D. and Williamson, P.R. (2013) Susceptibility of intact germinating Arabidopsis thaliana to human fungal pathogens Cryptococcus neoformans and C. gattii. **Applied and Environmental Microbiology,** 79 (9): 2979-2988.

Watanabe, S., Sakatani, M., Kubota, K., et al. (1995) Primary pulmonary cryptococcosis with pleural effusion, and clinical studies of five cases. **Nihon Kyobu Shikkan Gakkai zasshi,** 33 (12): 1430-1435.

Wickes, B.L., Mayorga, M.E., Edman, U., et al. (1996) Dimorphism and haploid fruiting in Cryptococcus neoformans: association with the alpha-mating type. **Proceedings of the National Academy of Sciences of the United States of America,** 93 (14): 7327-7331.

Williamson, P.R., Wakamatsu, K. and Ito, S. (1998) Melanin biosynthesis in Cryptococcus neoformans. **Journal of Bacteriology,** 180 (6): 1570-1572.

World Health Organisation (2015) **WHO | HIV/AIDS.** [Online]. Available from: http://www.who.int/gho/hiv/en/ [Accessed 22.08.2015 2015].

Wormley, F.L., Perfect, J.R., Steele, C., et al. (2007) PMC1828544; Protection against cryptococcosis by using a murine gamma interferon-producing Cryptococcus neoformans strain. **Infect Immun,** 75 1453-1462.

Wozniak, K.L., Vyas, J.M. and Levitz, S.M. (2006) In vivo role of dendritic cells in a murine model of pulmonary cryptococcosis. **Infection and immunity,** 74 (7): 3817-3824.

Wozniak, K.L., Young, M.L. and Wormley, F.L.,Jr (2011) Protective immunity against experimental pulmonary cryptococcosis in T cell-depleted mice. **Clinical and vaccine immunology : CVI,** 18 (5): 717-723.

Wright, L.C., Chen, S.C., Wilson, C.F., et al. (2002) Strain-dependent effects of environmental signals on the production of extracellular phospholipase by Cryptococcus neoformans. **FEMS Microbiol Lett,** 209 175-181.

Wright, L.C., Payne, J., Santangelo, R.T., et al. (2004) Cryptococcal phospholipases: a novel lysophospholipase discovered in the pathogenic fungus Cryptococcus gattii. **The Biochemical journal,** 384 (Pt 2): 377-384.

Wright, L.C., Santangelo, R.M., Ganendren, R., et al. (2007) Cryptococcal lipid metabolism: phospholipase B1 is implicated in transcellular metabolism of macrophage-derived lipids. **Eukaryotic cell,** 6 (1): 37-47.

Yoshimura, T., Yuhki, N., Moore, S.K., et al. (1989) Human monocyte chemoattractant protein-1 (MCP-1). Full-length cDNA cloning, expression in mitogen-stimulated blood mononuclear leukocytes, and sequence similarity to mouse competence gene JE. **FEBS letters,** 244 (2): 487-493.

Yuchong, C., Fubin, C., Jianghan, C., et al. (2012) Cryptococcosis in China (1985-2010): review of cases from Chinese database. **Mycopathologia,** 173 (5-6): 329-335.

Zaragoza, O. and Casadevall, A. (2004) Experimental modulation of capsule size in Cryptococcus neoformans. **Biological Procedures Online,** 6 10-15.

Zaragoza, O., Fries, B.C. and Casadevall, A. (2003a) Induction of capsule growth in Cryptococcus neoformans by mammalian serum and $CO(2)$. **Infection and immunity,** 71 (11): 6155-6164.

Zaragoza, O., Garcia-Rodas, R., Nosanchuk, J.D., et al. (2010) PMC2887474; Fungal cell gigantism during mammalian infection. **PLoS Pathog,** 6 e1000945.

Zaragoza, O., Rodrigues, M.L., De Jesus, M., et al. (2009) The capsule of the fungal pathogen Cryptococcus neoformans. **Advances in Applied Microbiology,** 68 133-216.

Zaragoza, O., Taborda, C.P. and Casadevall, A. (2003b) The efficacy of complement-mediated phagocytosis of Cryptococcus neoformans is dependent on the location of C3 in the polysaccharide capsule and involves both direct and indirect C3-mediated interactions. **Eur J Immunol,** 33 1957-1967.

Zheng, C.F., Ma, L.L., Jones, G.J., et al. (2007) Cytotoxic CD4+ T cells use granulysin to kill Cryptococcus neoformans, and activation of this pathway is defective in HIV patients. **Blood,** 109 (5): 2049-2057.

Zhu, L.P., Wu, J.Q., Xu, B., et al. (2010) Cryptococcal meningitis in non-HIV-infected patients in a Chinese tertiary care hospital, 1997-2007. **Medical mycology,** 48 (4): 570-579.